Universidad del País Vasco Euskal Herriko Unibertsitatea

NAZIOARTEKO BIKAINTASUN CAMPUSA
CAMPUS DE EXCELENCIA INTERNACIONAL

Department of Zoology and Animal Cell Biology
PhD programme on Environmental Contamination and Toxicology

Impacts of graphene-family nanomaterials and nano and microplastics and associated pollutants in the marine environment using mussels *Mytilus galloprovincialis* as target organisms

International Ph.D. Thesis submitted by
Nagore González Soto

for the degree of
Philosophiae Doctor

May, 2022

Supervised by Prof. Miren P. Cajaraville and Dr. Eider Bilbao

FUNDING

This work has been funded by:

- University of the Basque Country UPV/EHU (VRI grant PLASTOX) and the EU project "Direct and indirect ecotoxicological impacts of microplastics on marine organisms-PLASTOX", JPI Oceans 005/2015.
- Basque Government through a grant to the Consolidated Research Group "Cell Biology in Environmental Toxicology", Refs IT1302-19 and IT1743-22, and through a predoctoral fellowship to Nagore González Soto.
- Spanish Ministry of Economy and Competitiveness MINECO through the project "Nanomaterials as carriers of persistent organic pollutants in the aquatic environment: development of tools for risk assessment based on alternative methods and model organisms NanoCarrierERA-NACE", Ref CTM2016-81130-R.
- European Commission though the project "Integrated oil spill response actions and environmental effects-GRACE", H2020-BG-2005-2, grant agreement number 679266.

ACKNOWLEDGEMENTS

I wish to thank all the people and institutions that helped me to carry out this Ph.D. research.

- Professor Miren P. Cajaraville and Dr. Eider Bilbao (University of the Basque Country), supervisors of this PhD thesis, for giving me the opportunity to perform this research work and sharing your great knowledge, time and science eagerness over these years.
- All past and current members involved in the "*Nano"* projects: Dr. Amaia Orbea, Dr. Alberto Katsumiti, Dr. Nerea Duroudier, Dr. Jose María Lacave, Dr. Ignacio Martínez Álvarez and Ada Esteban. Thank you for the helpful discussions and for your sharing your knowledge.
- Professor Lúcia Guilhermino for hosting me at the University of Porto and guiding me into the world of enzyme activities.
- Professor Jörg Schäfer (University of Bordeaux) for his collaboration and support with the chemical analyses.
- Professor Enrique Navarro (University of the Basque Country) for his collaboration to perform the physiological analyses.
- Dr. Mireia Irazola (University of the Basque Country) for always having a smile during the endless Raman analyses.
- Dr. Radmila Tomovska for her collaboration in supplying and characterizing the samples of graphene family nanomaterials used in the experiments.
- The staff of Driftslaboratoriet Mongstad, Equinor (former Statoil) for supplying the sample of crude oil used in the experiments.
- To all members of the Research Group "Cell Biology in Environmental Toxicology" (University of the Basque Country) for contributing to carry out this work.

TABLE OF CONTENTS

1. INTRODUCTION

1.1. Nanomaterials 3

1.2. Graphene-family nanomaterials 8

1.3. Nanoplastics and microplastics 23

1.4. Mussels as sentinels of nanomaterial toxicity 46

2. STATE OF THE ART, HYPOTHESIS AND OBJECTIVES 83

3. RESULTS AND DISCUSSION 91

CHAPTER 1. Impacts of dietary exposure to different sized polystyrene nano and microplastics alone and with sorbed benzo[a]pyrene on biomarkers and whole organism responses in mussels *Mytilus galloprovincialis* 93

Supplementary material to Chapter 1 145

CHAPTER 2. Effects of microplastics alone or with sorbed oil compounds from the water accommodated fraction of a North Sea crude oil on marine mussels *Mytilus galloprovincialis* 155

Supplementary material to Chapter 2 195

CHAPTER 3. Fate and effects of graphene oxide alone and with sorbed benzo(a)pyrene in mussels *Mytilus galloprovincialis* 205

Supplementary material to Chapter 3 249

CHAPTER 4. Fate and effects of a reduced graphene oxide-silver nanoparticle hybrid material on mussels *Mytilus galloprovincialis* 255

Supplementary material to Chapter 4 299

CHAPTER 5. Toxicity of graphene family nanomaterials alone and with associated benzo(a)pyrene on early embryo developmental stages of mussels *Mytilus galloprovincialis* 305

Supplementary material to Chapter 5 335

4. GENERAL DISCUSSION **338**

4.1. The Trojan Horse effect 341

4.2. Fate and impact of polystyrene NPs and MPs and GFNs in mussels 345

4.3. Comparison of responses measured in hemocytes *in vitro* versus *in vivo* responses 347

4.4. Comparison of embryo versus adult responses 348

5. CONCLUSIONS AND THESIS 353

1. INTRODUCTION

1. NANOMATERIALS

During the last decades, a *nano* boom has been experienced. Terms as *nano*-technology, *nano*-industry, *nano*-particle and *nano*-material have gone from exotic to usual. These terms have even crossed boundaries and they are not only used in research, but they are also part of our everyday life in marketing strategies and newspapers. The beginning of the *nano*-era is dated 1959, after Richard Feynman gave his speech "*There's plenty of room at the bottom"* in a Meeting of the American Physical Society at CalTech (Pacheco-Torgal & Jalali, 2011). Until then, less than 10 research papers were published each year with the "*nano*" term in their title but afterwards, the field grew exponentially, blooming in the late 1990's. In 2016 the barrier of 30k papers with the "*nano*" term in the title was crossed in the Scopus database and nowadays the field continues to grow (Figure 1). In concordance, the economic impact of *nano* related technology, industry and products is also raising and by the current year (2022), this market was estimated to reach 55 billion US dollars (Inshakova & Inshakov, 2017). Some countries are developing national nanotechnology plans (Soltani et al., 2011) such as the actual Horizon 2020 program, the largest EU research and innovation program, which allocated approximately 2 billion euros, nearly the 2% of the total budget for projects related to nanomaterials and nanotechnology (EUON, ECHA, 2022).

However, as a consequence of such a rapid development, a lack of agreement on definitions and terms can occur within the scientific community (Hannah & Thompson, 2007) as it occurred in 1981, when an expert group appointed by the European Commission was not able to agree on what *nano*-technology exactly meant (Glazel et al., 2003).

Nanomaterials (NMs) have been commonly defined as materials with at least one dimension in the nanoscale (< 100nm) (Nel et al., 2006). In 2011, the European Commission established the following definition for NMs: *"a natural, incidental or manufactured material containing particles, in an unbound state or as an aggregate or as an agglomerate and where, for 50 % or more of the particles in the number size distribution, one or more external dimensions is in the size range 1 nm - 100 nm" (2011/696/EU).*

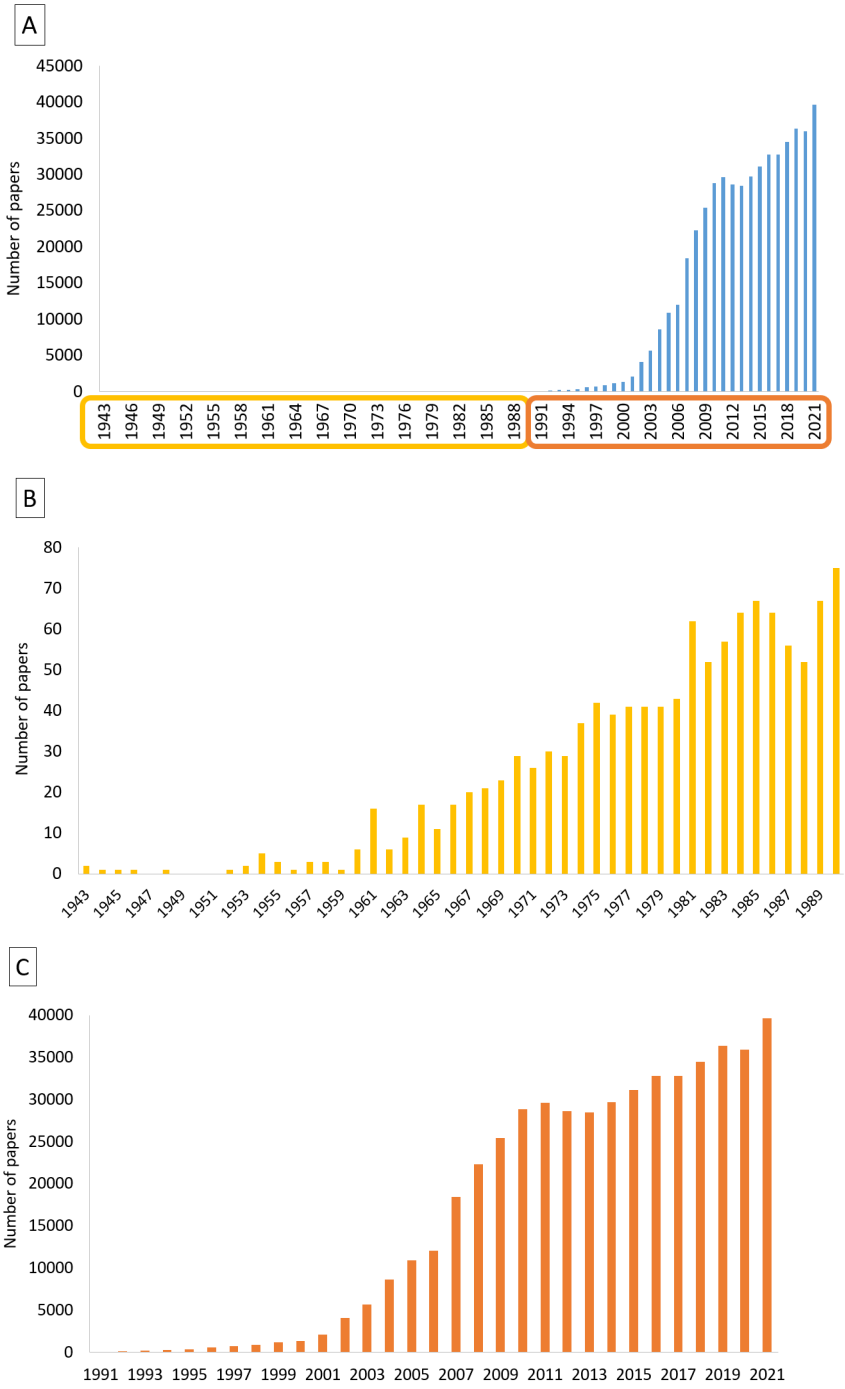

Figure 1. Number of papers published in the Scopus database per year with the term *"nano"* in the title. A) from the first appearance to 2021; B) from the first appearance to 1990; C) from 1991 to nowadays. Source Scopus (April, 2022).

NMs can be classified based on various criteria, such as the number of dimensions (Figure 2): 0D (spheres, ej: fullerenes and nanoparticles), 1D (tubes and threads, ej: carbon-nanotubes and gold nanothreads), 2D (plates and sheets, ej: graphene) and 3D (any 3D shape, ej: gold nanocubes and DNA tetrahedrons) (Prokropivny & Skorokhod, 2007; Quesada-González & Merkoçi, 2018). Based on their composition they can be

classified as follows (Figure 3): carbon-based NMs, metallic NMs, ceramic-based NMs, polymeric NMs and biomolecules derived NMs (Sajig, 2021).

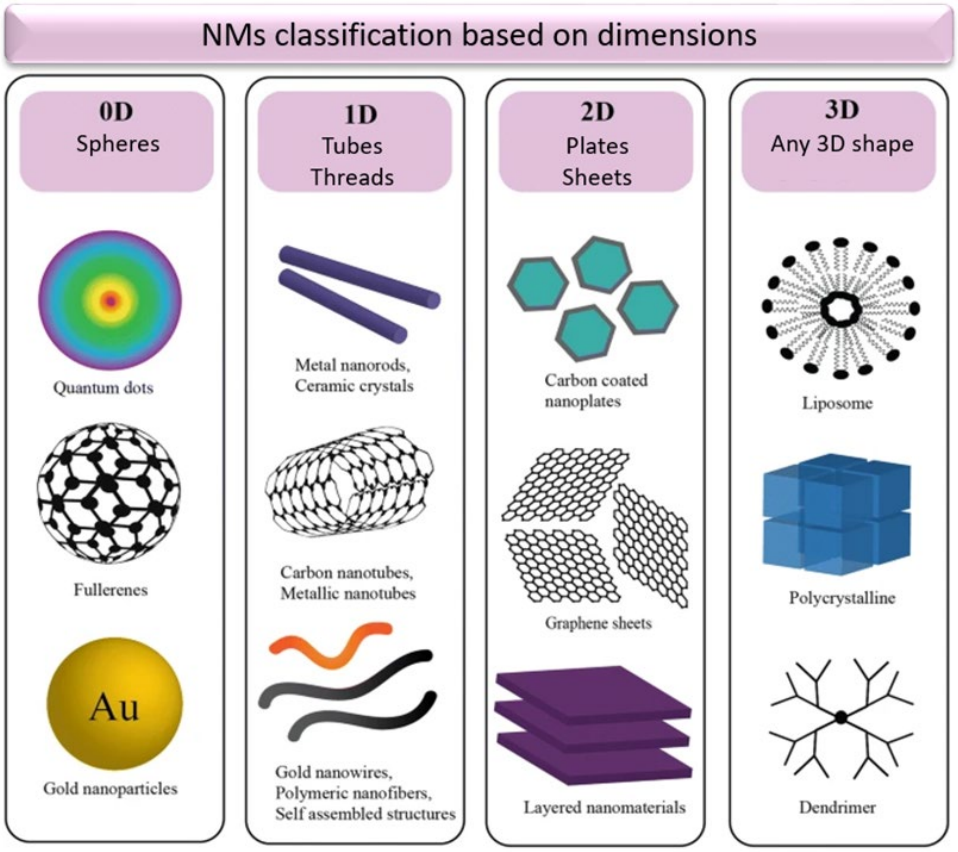

Figure 2. Examples of nanomaterials existing in zero (0D), one (1D), two (2D) and three (3D) dimensions. Modified from Poh et al. (2018).

In general, NMs can also be classified based on other physical and chemical properties that they present, including surface, shape, size, stabilization, presence of functional groups, charge, hydrophobicity or reactivity (Figure 4), which are key to determine their applications (Heinz et al., 2017).

In the last decades, the applications of NMs have reached almost all the industrial and technological fields including energy, electronic, aerospace, agriculture and biomedicine (Malakar et al., 2021; Liu et al., 2022). According to the Nanodatabase, nowadays there are more than 5000 consumer products containing NMs, twice as much as in 2016 (https://nanodb.dk/en/search-database).

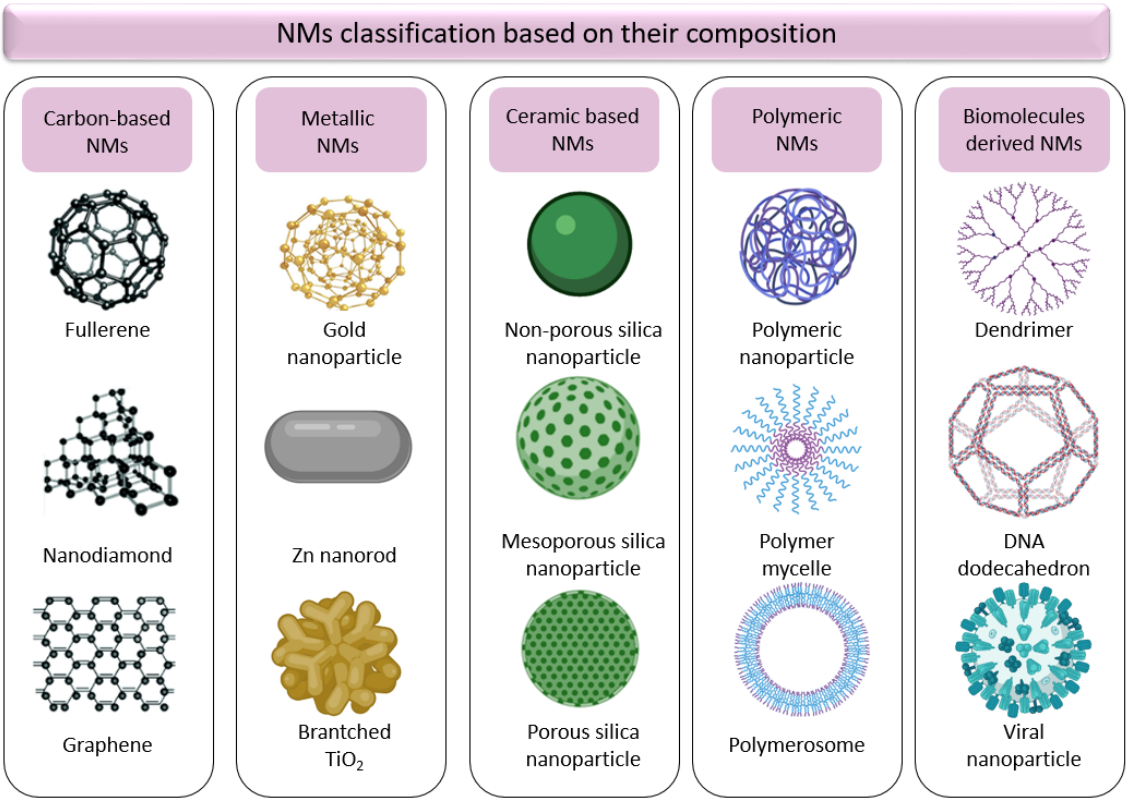

Figure 3. Classification of NMs based on their composition. Classification according to Sajig (2021).

The wide variety of technical and consumer applications of NMs would result, as for any other material, in their introduction the environment (Gottschalk & Nowack, 2011). NMs would enter into the environment during any step of their life cycle that includes production, transport, use and waste management (Caballero-Guzmán & Nowack, 2016; Bundschuh et al., 2018). The fact that some NMs are designed for environmental applications increases this possibility significantly.

NMs can enter into the aquatic environment, through direct release, via sewage, effluents or river influx and indirectly through aerial deposition or dumping and run-off (Rocha et al., 2015; de Marchi et al., 2019). Once in the aquatic environment they tend to sink, specially in seas and oceans (Selck et al., 2016) (Figure 5).

Environmental conditions (pH, temperature, ionic strength, organic matter, water currents…) play a role in the behavior and fate of NMs (Rocha et al., 2015; Avant et al., 2019), though intrinsic properties of NMs will also determine interactions with the media and their fate (Rocha et al., 2015). In addition, due to their small size and reactivity, NMs pose a potential threat to multiple type of organisms and the potential

ecotoxicological impact of NMs in aquatic, and especially in marine environments, is of concern for the scientific community. Thus, nowadays NMs are considered as emerging pollutants since they imply a perceived, potential or real threat to human health or the environment and there are no published health standards for NMs (EPA, 2010).

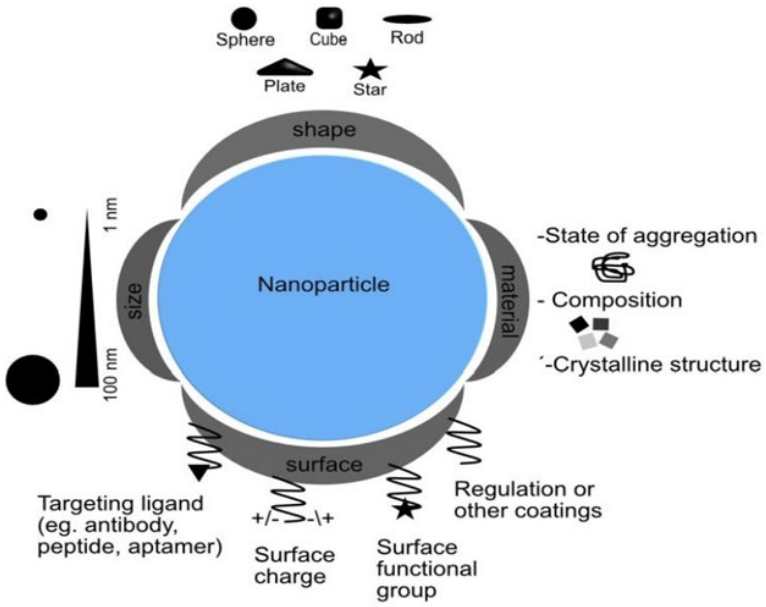

Figure 4: Main properties of nanomaterials. Taken from Auria-Soro et al. (2019).

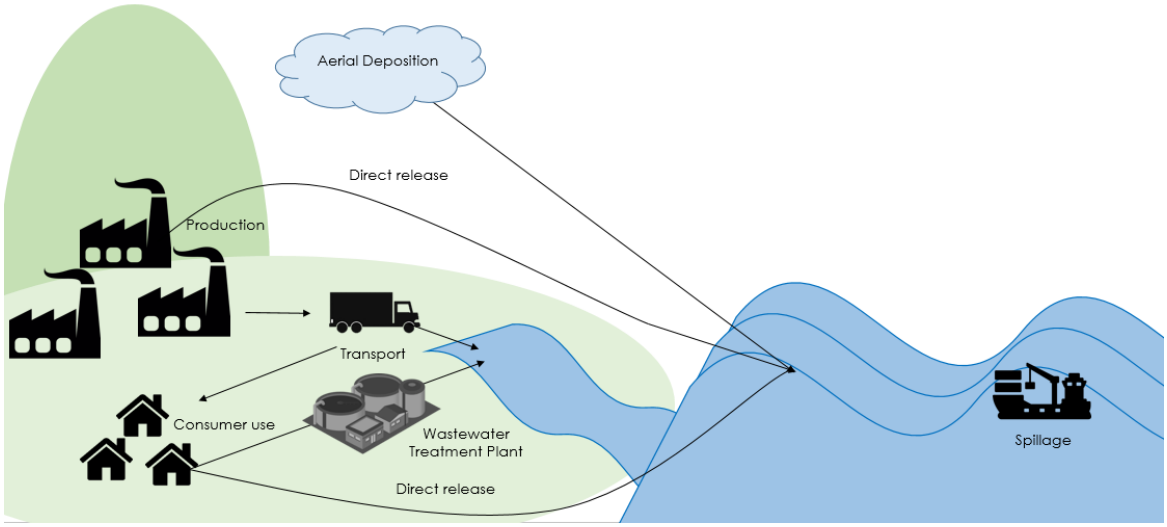

Figure 5. Schematic representation of the entrance of NMs into the marine environment.

2. GRAPHENE FAMILY NANOMATERIAL (GFNS)

Since the discovery of fullerenes in the middle 1980's, the capacity of carbon to form different allotropes, structurally different forms of the same element, has lead to a cascade of carbon-based NMs arraiving to our lives. In addition to fullerenes, other notable carbon-based NMs include carbon nanotubes, nanodiamonds, carbon-based quantum dots, black carbon and graphene and its derivatives (Dowling et al., 2004; Dinadayalane et al., 2010; Neto et al., 2011; Patel et al., 2019) (Figure 6).

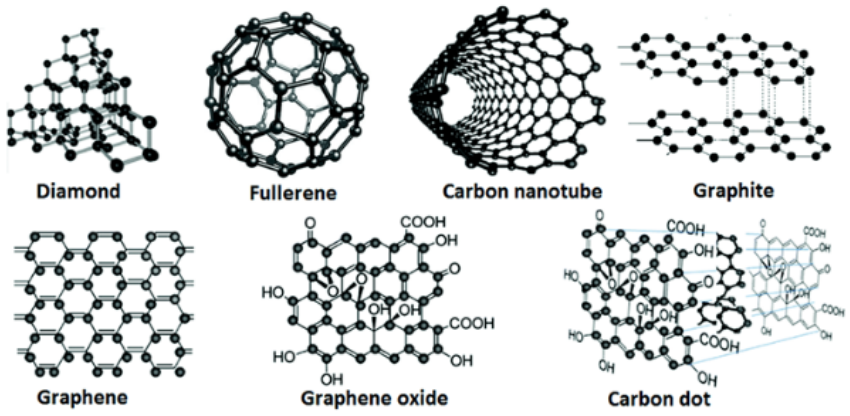

Figure 6. Representation of the chemical structure of some carbon-based nanomaterials. From Yan et al. (2016).

Among carbon-based NMs, graphene stands out for its unique properties and it has attracted the attention of researchers since its discovery in 2004. The discovery ofgraphene was worth the Nobel Prize to Novoselov and colleagues, for their original experiments in which they described graphene and its properties. In fact, graphene and its derivatives are expected to form the basis of a new generation of materials, the graphene family NMs (GFNs) and technologies (McWilliams, 2016).

Graphene is a one atom-thick sheet of sp^2 bounded carbon atoms arranged in a honeycomb-like structure (Figure 7) (Novoselov et al., 2012). GFNs can be classified according to their oxidation degree in pure graphene, graphene oxide (GO) and reduced graphene oxide (rGO) (Figure 7). In GO, the carbon atoms are covalently bounded to oxygen functional groups such as hydroxyl, epoxy, and carboxy containing sp^3 hybrid groups, which are displaced above or below the graphene plane. When some of these functional groups are removed by thermal, chemical or electrical treatment, the obtained material is rGO (Bianco et al., 2013).

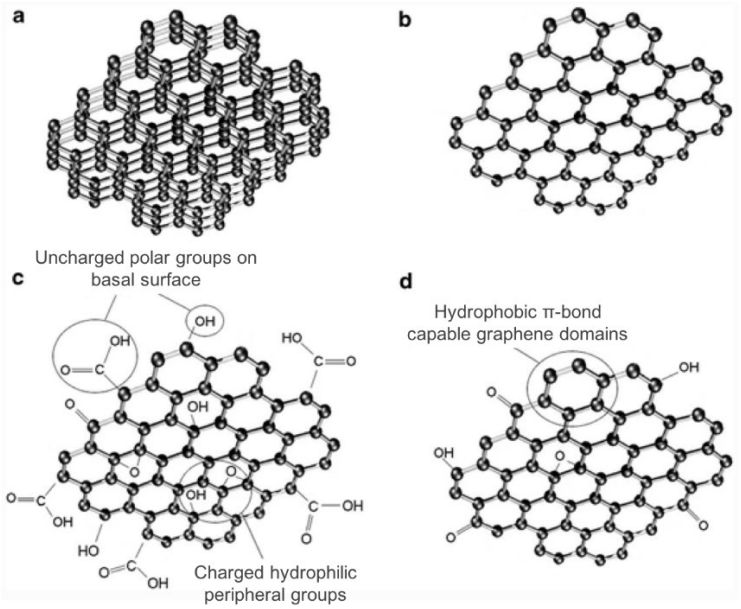

Figure 7. Structural models of some members of the graphene family materials (GFNs): (a) few-layered graphene, (b) graphene, (c) graphene oxide, and (d) reduced graphene. Taken from Jastrzębska et al. (2012).

Graphene is the strongest material known and it has been observed that its combination with several materials can increase its strength or lighten it, since it is necessary to use less quantity of material to achieve the same resistance. This has promising applications in aerospace, automobile and building industries, among others (Pacheco-Torgal & Labrincha, 2013; Ramon-Raygoza et al., 2016; Kausar et al., 2017). The high thermal conductivity of graphene in combination with the lightness of the material makes it suitable as heat sink in electronical devices (Lin et al., 2015). Its high surface makes graphene a promising material for batteries and supercapacitors (El-Kadi et al., 2016) as graphene may enable storage of more energy and charge faster. The impermeability of graphene makes it suitable for developing technologies that need from fluid-encasement, selective gas-permeation or nanopore diffusion, among others (Berri, 2013). Due to its stability at room temperature and its high conductivity graphene has been proposed for gas detection sensors (Wang et al., 2015). In addition, graphene and its derivatives are suitable for biomedical applications, such as formation of scaffolds for proliferation and differentiation of cells, drug delivery, and anticancer therapies (Tadyszak et al.,2018) and environmental applications in agricultural procedures (Kabiri et al., 2017), waste water treatments (Peng et al., 2020) and water desalination (Le et al., 2021), among others. For instance, GFNs exhibit characteristics that allow their use

as novel sorbents, as catalyst systems for degrading different compounds or even as sterilizers (Sun & Li, 2018; Facure et al., 2020). In addition, GFNs have been proposed as anticorrosion agents in the shipping industry (Yao et al., 2020; Ziat et al., 2020).

Due to all these unique properties of GFNs (large surface area, high electrical and thermal conductivity, unique optical properties, impermeability, high intrinsic electron mobility and physical strength, among others), the graphene related market is growing day-by-day (Ren & Chen, 2014). The global market for GFNs generated 87.5 million dollars in 2019 and it would achieve 876.8 millions in 2027 (Narune et al., 2022). Nowadays, there are more than 26000 patents including graphene related products (Scott, 2016) and this number is expected to increase as production methods become cheaper and more efficient (Lin et al., 2019). Therefore, graphene production is expected to reach 3800 tones in 2027 (Colins, 2021).

The direct use of GFNs in the environment has already started to raise the attention of the scientific community as their impact towards the biota is not clear and many voices have claim for preventive actions towards possible damages (Jastrebska & Olszyna, 2015). Moreover, the wide application of GFNs in industrial and consumer products will lead to their entry into the environment (de Marchi et al., 2018). For instance, the presence of GFNs has already been detected in the biomass obtained from wastewater treatment plants (Goodwin et al., 2018). However, nowadays, there is a lack of technology able to measure GFNs concentrations in the environment (Goodwin et al., 2018). This is mainly due to the fact that GFNs, as other carbon-based NMs, are difficult to be distinguished from natural carbon (Gottschalk et al., 2013). In addition, GFNs may suffer unknown transformations due to their interactions with the media and other environmental elements (Goodwin et al., 2018). Thus, until analytical techniques for measuring GFNs are improved, prediction models are required. However, prediction models are based on data about production and application, but these data are still in continus change for GFNs. Thus, prediction models are still pending. Since most of the applications are still under research and have not been commercialized yet (Ciriminna et al., 2015; Tiwari et al., 2020), some authors claimed that predicted environmental concentrations of other carbon based NMs can be used for GFNs due to their similar

physicochemical characteristics (de Marchi et al., 2018). These predicted concentrations fall mainly in the ng dimension, but in some cases, predictions achieve the μg and even the mg dimension (Table 1). Moreover, it is important to take into consideration that GFNs are being produced at a higher extent than any other carbon-based NM and many of their applications would result in direct release into the environment. Therefore, the real release of GFNs could overcome these expected concentrations.

Furthermore, most of the models do not distinguish different categories for each aquatic compartment (river, lake, sea…) and most of them are focused on the freshwater mass. However, once in the environment, GFNs would undoubtedly reach coastal and marine ecosystems (De Marchi et al., 2018) and interact with components of the natural system, which would alter their behavior, transport and fate (He et al., 2017).

One of the major environmental factors contributting to the alter physico-chemical properties of GFNs in the aqueous environment is light. As Zhao et al. (2021) reviewed, GO exposure to sunlight, UV, visible light or ultrafast laser caused different outcomes and, as Sun et al. (2021) reported, the colloidal stability of GO was altered by its phototransformation. Sunlight not only reduced the oxygen content of GO, enhancing its hydrophobicity and reducing its stability in the solution but it also reduced its capacity to absorb proteins present in the solution (Sun et al., 2021). Thus, transport and fate of GFNs would mainly depend on their stability in the suspension, which can be altered by environmental factors such as light, pH, salinity, organic matter concentration, oxidation status and ionic strength, among others (Gigault et al., 2012; Liu et al., 2012; Chang & Bouchar, 2016; Jiang et al., 2017; Ali et al., *in press*).

As mentioned, the colloidal stability of GFNs can be altered by environmental factors. In aquatic environments sedimentation is one of the most crucial processes affected by GFNs aggregation which, at the same time, depends on the concentration of GFNs and thus, it will be more likely to occur near places where GFNs are released (Zhao et al., 2014; Ali et al., *in press)*. Due to the expected low concentration of GFNs in the environment, heteroaggregation would be more prone to occur than homoaggregation (Zhao et al., 2014; Ali et al., *in press)*. Such aggregation phenomena with different

biomolecules will destabilize GO (Sun et al., 2021). Due to intrinsic hydrophobicity, pure graphene and rGO will always be unstable in water solutions but the presence of salts and electrolytes would enhance its unstability (Zhao et al., 2014). In general, large size

Table 1. Predicted environmental concentrations for carbon nanototubes, fullerenes and total carbon-based NMs in different environmental compartments.

Carbon natotubes			
Soil	0.43-3.83	ng/kg/year	Gottchalk et al. (2009)
Sludge treated soil	23.9-157	ng/kg/year	
Surface water	0.0003-0.025	ng/L	
Sewage treatment plant effluent	6.6-31.5	ng/L	
Sewage treatment plant sludge	0.047-0.147	mg/kg	
Sediment	40-1557	ng/kg/year	
Air	0.00096-0.07	ng/m^3	
surface water	0.23	ng/L	Sun et al. (2014)
Waste water treatment plant effluent	4	ng/L	
Natural and urban soil	5.1	ng/kg/year	
Air	1.5-2.3	ng/m^3	Mueller & Nowack (2008)
Water	0.0005-0.008	µg/L	
Soil	0.01-0.02	µg/kg	
Water	$2*10^{-5}$-1.89	ng/L	Zhao et al. (2020)
Sediment	10^{-4}- 2.66 $*10^{-2}$	mg/kg	
Fullerenes			
Soil	0.024-0.605	ng/kg/year	Gottchalk et al. (2009)
Sludge treated soil	1.0-22.2	ng/kg/year	
Surface water	0.0024-0.19	ng/L	
Sewage treatment plant effluent	3.69-32.66	ng/L	
Sewage treatment plant sludge	0.0088-0.068	mg/kg	
Sediment	1.05-787	ng/kg/year	
Air	<0.0005	ng/m^3	
Surface water	0.11	ng/L	Sun et al. (2014)
Waste water treatment plant effluent	1.7	ng/L	
Natural and urban soil	0.1	ng/kg/year	
Surface water	0.003	ng/L	Kunhikrishann et al. (2014)
Waste water treatment plant effluent	4	ng/L	
Total carbon based NMs			
Water column	0.0005-0.0008	µg/L	Koelmans et al. (2009)
Sediment	1.2-2000	µg/Kg	

aggregates of GFNs would favour sedimentation, but at the same time, they would avoid GFNs entry in the sediments and thus, aggregates will remain in the water column (Zaho et al., 2014; 2021). Accordingly, Avant et al. (2019) simulated the dynamics that both rGO and GO would suffer after a hypothetical leak in four different aquatic scenarios including a seepage river, a coastal plain river, a seepage lake and an unstratified wetland lake and observed that lakes would accumulate more rGO than GO, whereas the contrary would occur in rivers. In addition, the 99% of the NMs were predicted to accumulate downstream the river systems, which would lead to their entry into the oceans, where they could persist in the water column for a long time. Water chemistry such as the organic matter concentration or salinity (Zhao et al., 2014; Ali et al., *in press)* will also affect sedimentation.

Therefore, dynamics and fate of GFNs in marine environments would depend on the intrinsic properties of GFNs, including size, shape, surface charge, surface area, functional groups, polarity or morphology (de Marchi et al., 2019; Ali et al., *in press*) and the surrounding aqueous environment. Such expected dynamics could facilitate GFNs uptake by a large variety of organisms and it should be of primary concern (Han et al., 2019). Futhermore, the high persistence of GFNs in aquatic environments could result in their bioaccumulation and biomagnification along the food web (Peng et al., 2020), increasing the potential impact on marine ecosystems even when released concentrations are low (Arvidsson et al., 2013).

Due to the phiso-chemical properties of GFNs, especially the large surface to volume ratio and porosity, GFNs are prone to adsorb different compounds and therefore, the adsorption of pollutants present in the media are of special concern. GFNs are able to sorbe dyes (Liu et al., 2012; Sharma & Das, 2013; Robati et al., 2016), pharmaceuticals (Nam et al., 2015), metals (Janik et al., 2018; Wei et al., 2018; Wu et al., 2018) and persistent organic pollutants, such as polycyclic aromatic hydrocarbons (Apul et al., 2013; He et al., 2013; Ersan et al., 2017), among others. Therefore, GFNs have been proposed to be used in the remediation of water pollution (Yang et al., 2014; Li et al., 2020b; Younis et al., 2020). On the other hand, GFNs release could pose an additional risk to aquatic organisms as GFNs could alter the bioavailability of contaminants and

increase their toxicity. This phenomenon is commonly called as the Trojan horse effect. Originally, Limbach et al. (2007) introduced this concept to refer to the extended toxicity caused by metal nanoparticles in comparison to their soluble forms, due to the continuous release of metal ions in and out of cells. Later, this concept was extended to include environmental perspectives (Baun et al., 2008; Hartmann & Baun, 2010). However, as the use of the term became popular, its meaning started to become misleading (Naasz et al., 2018). In order to clarify it, many researchers tried to put together the current knowledge about this term in multiple reviews (Canesi et al., 2015; Deng et al., 2017; Freixa et al., 2018; Naasz et al., 2018). The reviews agreed in defining the Trojan horse effect as the possible threat of NMs due to their ability to adsorb and carry adsorbed compounds to organisms. This phenomenon is known to occur for many NMs and several metal or organic compounds (Canesi et al., 2015; Deng et al., 2017; Freixa et al., 2018; Naasz et al., 2018). However, the different works do not agree when defining the Trojan horse effect in terms of toxicity. Most of them considered to mimic co-exposure situations and the toxicity of the mixture is normally compared to the toxicity of the dissolved pollutant (Deng et al., 2017; Naasz et al., 2018) while the toxicity in comparison to the NM alone is frequently ignored, which could lead to an underestimation of the toxicity of the mixture (Deng et al., 2017).

Among pollutants, persistent organic pollutants (POPs) are especially worrying since they are carcinogenic, mutagenic, or steroidogenic and may have an effect on the endocrine system, among other effects. Thus, they are regulated in the European Union by various laws (E.U. 2008), especially since the 2001 Stockholm Convention. POPs are defined as organic compounds that are hardly degraded through chemical, biological and photolitic processes (Ritter et al., 2007). POPs include polycyclic aromatic hydrocarbons (PAHs), that are widely found in the sea, mainly due to the anthropogenic activity in land, maritime traffic, off-shore production of oil and gas, oil spills… (Meador et al., 1995; Abdel-Shafy et al., 2016). PAHs are the major contributors to the toxicity of petroleum oil mixtures. Among PAHs, benzo(a)pyrene (BaP) is one of the most studied (CCME, 2010). The toxicity profile of BaP is very broad: it is not only genotoxic, endocrine disruptor and mutagenic, it is also capable of causing oxidative stress and cancer. As a result, BaP is a priority pollutant for several international organizations and legislations

(Jinadasa et al., 2020). In addition, BaP can be usually found in marine environments and it is often used as a model PAH in environmental toxicology (Banni et al., 2017; Di et al., 2017).

In addition, since various GFNs have different properties, different toxicity is expected. However, there is no agreement about which GFNs is more toxic. Some works claimed that rGO should pose higher toxicity than GO due to the smaller thickness of the sheets, sharper edges and greater electrical conductivity (Akhavan & Ghaderi, 2010), while others pointed that GO could be more toxic due to its greater dispersability and higher surface functionality (Gurunathan et al., 2012). For instance, Katsumiti et al. (2017) observed that rGO nanoplatelets were internalized at higher extent in mussel hemocytes than GO nanoplatelets causing higher toxicity, whereas Martínez-Álvarez et al. (2021) reported a higher mortality of zebrafish embryos exposed to GO than to rGO.

At the cellular level, GFNs (Figure 8) can cause physical damage due to the sharp edges of platelets and then caused decrease in the integrity of the plasma membrane. Nanosheets may enter the cells by direct penetration but endocytosis has also been observed also (Zhao et al., 2014). *In vitro,* interaction of GFN sheets with the plasma membrane can produce invaginations or even perforations that may lead to the internalization of GFNs (Lammel et al., 2013; Katsumiti et al., 2017). Moreover, GFNs can cover cells and/or unicellular organisms, limiting exchange through the membrane, which can ultimately inhibit cell growth (Zhao et al., 2014). Additionally, the interaction of GFNs with different biomolecules may damage them, as observed for enzymes, lipids and even DNA (Tu et al., 2013; Wang et al., 2013; Hosende et al., 2020).

Disruption of the plasma membrane and internalization of GFNs can increase the production of reactive oxygen species (ROS) and lead to oxidative stress (Katsumiti et al., 2017). Consequent oxidative damage is considered the main mechanism of toxicity of NMs (Katsumiti & Cajaraville, 2019). ROS production can be caused by the presence of the NM itself (Chang et al., 2011) but interaction of the NM with cellular components such as mitochondria, peroxisomes and oxidases is the main mechanism (Begum & Fugetsu, 2013). Oxidative damage can lead to dysfunction of cell organelles and

decrease of cell viability (Katsumiti et al., 2017). In addition, oxidative damage can affect DNA leading to genotoxic effects (Wang et al., 2013). These altetations at the cellular level alterations could lead to the impact at higher biological levels including reduction of the metabolic activity (Peng et al., 2020; Britto et al., 2021), histopathological lesions (Souza et al., 2017; Khan et al., 2019a), alterations in behavior and locomotor functions (Audira et al., 2021) and impact in the reproduction capacity, growth and survival (Bortozollo et al., 2021).

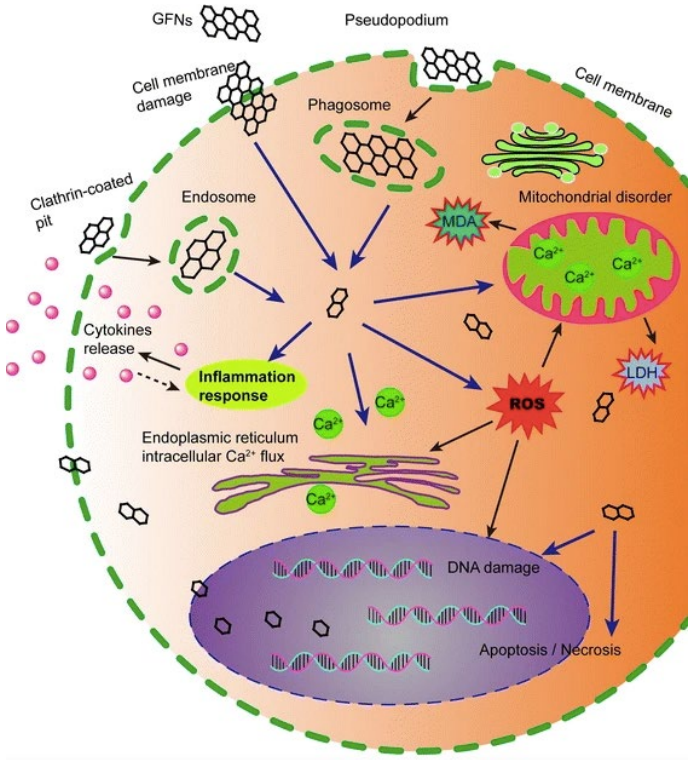

Figure 8. Schematic diagram showing the possible mechanisms of GFNs toxicity at the cellular level. ROS: reactive oxygen species. LDH: lactate dehydrogenase. MDA: malondialdehyde. Taken from Ou et al. (2016).

In aquatic animals, acute toxicity caused by GFNs could be achieved only by relatively high concentrations that are not expected in the environment. Bortolozzo et al. (2020) observed that the LC_{50} of GO for the nematode *Caenorhabditis elegans* was above 10 mg/L. Similarly, De Marchi et al. (2017) observed only a 20% mortality after the exposure of *Diopatra neapolitana* polychaete to 1 mg/L of GO. In crustaceans, controversial data have been published: Sanchis et al. (2016) reported that EC_{50} of GO was 20 mg/L in *Daphnia magna* whereas Liu et al. (2018) reported an EC_{50} of 150.75 mg/L for GO and 31.62 mg/L for graphene in the same species, both after 48 hours of exposure. Similarly,

in the case of *Artemia salina* Zhu et al. (2017) reported a LC_{50} between 368.18-387.68 mg/L of GO depending on the larvae stage, whereas Mesaric et al. (2015) did not observe mortality at concentrations as high as 600 mg/L. In bivalves lethal doses of GFNs have not been reported after *in vivo* exposures. However, *in vitro* exposures of mussel hemocytes revealed that the LC_{50} of rGO was between 29.902 and 33.94 mg/L depending on the source and between 49.84 and 54.51 mg/L for GO (Katsumiti et al., 2017). Malina et al. (2019) suggested that the toxicity of GO could be related more to small variations in the physico-chemical properties of the nanoplatelets, such as the oxygen content, than to the concentration. Regarding teleostei, no acute toxicity was observed in a number of studies that exposed zebrafish embryos to different GFNs (Chen et al., 2016; Soares et al., 2017), while in others, low mortality (<10%) was found (Mu et al., 2015; Martínez-Álvarez et al., 2021), though in one of the cases, only at high concentrations (100 mg/L) (Chen et al., 2020).

Concentrations close to those expected in aquatic and marine environments cause sublethal effects that could give rise to detrimental consequences on the health and wellbeing of organisms such as bivalve mollucs (Table 2). Aquatic animals can internalize GFNs, especially in organs related with food uptake and therefore, ocurrence of GFNs was observed in exposed oligochaetes (Mao et al., 2016), nematodes (Bortolozzo et al., 2020), polychaetes (Urban-Malinga et al., 2021), crustaceans (Guo et al., 2013; Pretti et al., 2014; Mesaric et al., 2015; Mao et al., 2016; Zhu et al., 2017; Lv et al., 2018; Souza et al., 2018; Zhang. et al., 2019; Josende et al., 2020) and fishes (Chen et al., 2015; Hu et al., 2017; Zhang et al.,2017; Martínez-Álvarez et al., 2021).

Internalization of GFNs in digestive organs may cause detrimental effects such as inflammatory reactions, alterations of enzyme activities related with digestion processes and loss of digestive tissue (Chen et al., 2016; Dziewiecka et al., 2017; Fernandes et al., 2017; Meng et al., 2019; Flasz et al., 2020; Alian et al., 2021; Martínez-Álvarez et al., 2021; Bi et al., 2022). Then, GFN nanoplatelets may translocate to other parts of the body such as gonads (Chatterjee et al., 2017) and even from exposed parentals to their offspring (Guo et al., 2013; Hu et al., 2017).

In addition to causing oxidative stress and oxidative damage as mentioned before, GFNs can asldo produce alterations in enzyme activities related with the biotransformation metabolism of pollutants and neurotoxic and genotoxic effects (Table 2) (Chen et al., 2015; 2016; Mesaric et al., 2015; Ren et al., 2016; Clemente et al., 2017; de Marchi et al., 2017; Fernandes et al., 2017; Soares et al., 2017; Soueza et al., 2017; Zhang et al., 2017; Zhu et al., 2017; Lv et al., 2018; Souza et al., 2018; Y. Zhang et al., 2018; Khan et al., 2019; Meng et al., 2019; Britto et al., 2020; Coppola et al., 2020; Josende et al., 2020; Urban-Malinga et al., 2021). Further, several immunological effects could be observed in animals exposed to GFNs (Diziewiecka et al., 2017; 2018; Meng et al., 2019; Flasz et al., 2020) as well as detrimental effects over oocytes (Diziewiecka et al., 2017; 2018; Bi et al., 2022).

As mentioned above environmental conditions could change the toxicity of GFNs. For instance, Zhang et al. (2019) reported that humic acid reduced both accumulation and toxic effects caused by GO in *Daphnia magna*. Similarly, decrease in GO toxicity towards *Daphnia magna* was observed when animals were exposed to GO previously incubated with microalgaes (Malina et al., 2019). Thus, in a complex scenario like the marine environment combination of GFNs with different chemicals must be studied. Among all the elements present in the media that could interact with GFNs, other pollutants are the highest concern. As mentioned above, due to their physicochemical characteristics GFNs are prone to adsorb a wide variety of compounds including classic and emerging pollutants.

Overall, there are few works that studied the toxicity caused by GFNs in combination with other pollutants in the aquatic environment, and most of them are with metals. Liu et al. (2018) reported that toxicity profiles of graphene and GO were different in combination with Cu or alone. Crustaceans exposed to graphene with Cu accumulated more Cu than animals exposed to Cu alone, whereas the contrary was observed in animals exposed to GO in combination with Cu. On the contrary, Lu et al. (2018) reported that GO displayed a synergistic effect with both Cd and phenanthrene in *Artemia salina,* while Josende et al. (2020) reported that GO alone was more toxic to *Litopenaeus vannamei* than with As. In bivalves, Meng et al. (2019) reported that

mussels co-exposed to graphene and triphenyl phosphate (TTP) accumulated more TTP than mussels exposed to TTP alone and enzyme activities were different in both cases. Similarly, Coppola et al. (2020) and (2021) reported a higher toxicity in mussels co-exposed to GO with polyethyleneimine (GO-PEI) with Hg than in those exposed to GO-PEI alone, as well as Bi et al (2022) reported a higher accumulation of perfluorooctanesulfonic acid (PFOs) and increased toxicity in Asian clams co-exposed to PFOs and GO. In fish, de Medeiros et al. (2020) observed that the metabolism of *Geophagus iporangensis* was differently altered when fish were co-exposed to GO and Zn or Cd. Regarding organic contaminants, Martínez-Álvarez et al. (2021) showed that sorption of PAHs onto GFNs did not impair survival of zebrafish fish embryos. Similarly, Yang et al. (2019) reported that bisphenol A bioavailability decreased when zebrafish embryos were co-exposed with GO. On the contrary, survival decreased and hatching was delayed when zebrafish embryos were exposed to irradiated graphene aerogel combined with naphthalene as reported by Liu et al. (2020). Similarly, when adult zebrafish were exposed to GO with sorbed BaP and with sorbed oil compounds derived from the water accommodated fraction of a crude oil, PAHs were accumulated in fish tissues and GST activity in gills increased in comparison to animals exposed to GO alone (Martínez-Álvarez et al., 2021).

In addition, as mention above variations in physico-chemical properties of GFNs would affect their toxicity. Mao et al. (2016) observed that bioaccumulation in the crustacean *Daphnia magna* of a few layer graphene was different depending on its coating and Mu et al. (2015) reported that coating GO with L-cysteine reduced its toxicity towards zebrafish embryos. In the last years production of nanocomposites formed by GFNs and other compounds is rising. GFNs are combined with different compounds to achieve a new generation of hybrid nanocomposites (Stankovich et al., 2006; Bai et al., 2011; Hassandoost et al., 2019; Mu et al., 2021). Among them, nanocomposites formed by GFNs and metal nanoparticles have been proposed for multiple applications (Hassandoost et al., 2019), especially those containing silver nanoparticles (Ag NPs) (Huang et al., 2014; Krishnaaj et al., 2022). GFN-Ag NP nanocomposites have shown promising applications in multiple fields, from electronics to biomedicine (De Moraes et al., 2015; Zhou et al., 2016; Sharma et al., 2017; Xu et al., 2017). In addition, many of

these applications are proposed to be directly used in the environment and especially in the marine environment (Chen et al., 2016; Koushick et al., 2016; Yee et al., 2016; Jin et al., 2021) which could lead to a direct release of both GFNs and Ag NPs into the marine environment. Ag NPs are known to be toxic for multiple aquatic and marine species (Cajaraville et al., 2021). Ag NPs are able to cause inhibition of microalgae growth, oxidative stress, genotoxicity, lysosomal damage and tissue alterations in bivalves, embryotoxicity in echinoderms and fishes, alterations in the development of polychaeta and mortality of crustaceans, among others (Cajaraville et al., 2021). Consequently, concerns are rising on the possible impact that nanocomposites such as those formed of GFNs and Ag NPs could pose on the marine environment. Thus, their toxicity should be investigated in a preventive way before they are released into the environment.

Table 2: Summary of studies reporting effects GFNs alone and with other pollutants in bivalves.

GFNs	Other contaminants	Exposure concentration	Exposure time	Other experimental conditions	Endpoints	Reference
Crassostrea virginica						
GO		1 and 10 mg/L	72 h		- LPO, GST, Total protein content - Histopathological analysis of gills	Khan et al. (2019a)
GO		2.5 and 5 mg/L	14 d		- LPO, GST, Total protein in gill and digestive gland	Khan et al. (2019b)
Corbicula fluminea						
GO	PFOS	0.2, 1, 5 mg/L GO alone or + 500 ng/L PFOS	28 d		- Concentration of PFOS in soft tissues, - Gene expression (*cyp30, cyp4, hsp60, hsp40, hsp22, gr, sod, and se-gpx*) - ROS, CAT, SOD, GR, GST,LPO - Histopathological analysis of gills and visceral mass - Filtration rate	Bi et al. (2022)
Mytilus galloprovincialis						
GO, GO-PVP, rGO-PVP		0.001, 0.01, 0.1, 1, 10, 25, 50 and 100 mg/L	24 h	*In vitro*	- Cell viability - Cell membrane integrity - ROS - TEM analysis	Katsumiti et al. (2017)
Graphene	TPP	0.5 mg/L graphene 0.5 mg/L TPP, 0.5 mg/L graphene + 0.5 mg/L TPP	7 days		- Concentration of TPP in soft tissues - Gene expression (*fkbp, hsp90, nfkb, myd88a, matrilin, dlc2, mhc1, pmyo, tmyo, cublin, mgc, cp450, vtg, hsd)* - GSH, GPx, SOD, CAT - Histopathological analysis of digestive gland	Meng et al., 2019
GO-PEI	Hg	10 mg/L GO-PEI 10 mg/L GO-PEI+ 50 µg/L Hg Remediated seawater	28 days	Remediated sweater of Hg	- Concentration of Hg in soft tissues - ETS in soft tissues - GLY content in soft tissues - Total protein content in soft tissues - SOD, CAT, GPx, GR, GSH/GSSG, LPO, GST, ACHE - Mortality	Coppola et al. (2020)

		50 µg/L Hg				
Graphene	TPP	5 mg/L graphene; 0.5 mg/L TPP; 0.5 mg/L TPP + 0.5 mg/L graphene	7d	All parameters measured in hemocytes	- Gene expression (*bl2, ras, nfkb, caspase 2, caspase 3, caspase8)* - Lysosomal membrane stability - Phagocytic activity - CAT, SOD, GSH, GST - Micronucleus frequency - TEM analysis	Meng et al 2020
GO-PEI	Hg	10 mg/L GO-PEI 10 mg/L GO-PEI+ 50 µg/L Hg Remediated seawater 50 µg/L Hg	28 days	17 and 22 degrees + remediated sweater of Hg	- Concentration of Hg in soft tissues - ETS in soft tissues - GLY content,Total protein content - SOD, CAT, GSH, LPO, ACHE - Histopathological analysis of digestive gland and gills	Coppola et al. (2021)
				Ruditapes philippinarum		
GO	Cu	GO: 0.1 mg/L GO; Cu: 0.025 mg/L Cu; (GO + Cu): 0.1 mg/L GO and 0.025 mg/L Cu	28 days	pH: 7.8 and 7.3	- ETS in soft tissues - GLY content, Total protein content - CAT, GSH, LPO, GST	Britto et al. (2020)
GO		0.01, 0.1 and 1 mg/L	28 days	With and without sediments	- Total protein content in soft tissues - CAT, SOD, GST, LPO, GSH	Britto et al. 2021

Abbreviations: GO: graphene oxide, GO-PVP: graphene oxide with polyvinylpyrrolidone, rGO-PVP: reduced graphene oxide with polyvinylpyrrolidone, GO-PEI: graphene oxide with polyethyleneimine, PFOS: perfluorooctanesulfonic acid, TTP: triphenyl phosphate, ACHE: acetylcholinesterase, CAT: catalase, SOD: superoxide dismutase, GR: glutathione reductase, LPO: lipid peroxidation, GSH: reduced glutathione, GSSG: glutathione disulfide, GPx: glutathione peroxidase, ETS: electron transport system, GLY: glycogen, GST: glutathione-S-transferases, ROS: reactive oxygen species, TEM: Transmission Electron Microscopy.

3. NANOPLASTICS AND MICROPLASTICS

The scientific community has discussed the problem of plastic pollution for decades. The durability of plastic has gone from being one of its strengths to being one of the biggest causes of environmental problems (Kuhn et al., 2015). Today it is considered that all natural spaces are contaminated by plastic polymers. Presence of plastics has been found in soils, air, seas, freshwater bodies and sediments (Galgani et al., 2015). Among them, the marine environment is considered as the most impacted environmental compartment (Browne et al., 2011; Horton & Dixon, 2018). Plastic waste has been found in all the seas and oceans in the world, from the Arctic to the Atlantic (Auta et al., 2017), and thus, plastic waste is currently considered an ubiquitous pollutant, with the potential to provoke serious consequences in the marine environment (UNEP, 2011). Even so, due to the characteristics of the marine environment, especially its wide extension and currents, accounting for plastic waste in seas and oceans is a challenge today (Rylan et al., 2009; Cole et al 2011; Doyle et al., 2011). Due to limitations of the current analytical methods, this problem is aggravated as the size of the plastic particles is reduced (Gaylarde et al., 2021).

In recent years, plastics smaller than 5 mm, called microplastics (MPs), have been identified as particularly worrying (Andrady, 2011; Cole et al., 2011). MPs are mostly derived from the mechanical, chemical and biological fragmentation of larger plastic waste that takes place in the environment (secondary MPs), though MPs can also enter directly into the marine environment (primary MPs). The main sources are the microspheres used in many cosmetic products, such as scrubs and toothpastes, and the synthetic fibers of fabrics such as polyester (Cole et al., 2011). These type of products are in contact with water, which makes them highly susceptible to release plastic particles into the effluents that flow into the sea (Cole et al., 2011). In addition, in industrial techniques such as sandblasting, sand has been replaced by plastic microspheres, and the possibility of a spill during their transport, which is usually done in the form of microbeads or powders, increases the possible routes of entry of MPs into the environment (Cole et al., 2011).

The scientific literature on MPs has grown exponentially in recent years and articles showing that MPs are just as ubiquitous as their macroscopic counterparts (Besseling et al., 2018). Once MPs enter the ocean, their fate largely depends on the density of their main polymer. It is calculated that 46% of the plastic polymers could remain on the surface because they have a lower density than water. The rest would have a neutral or negative buoyancy (Lattin et al., 2004). Thus, they would be concentrated in the water column and could settle on the seabed. Thus, marine sediments are considered the largest recipient of MPs at in the environment (Woodall et al., 2014), beig fibers the dominant MP type (Harris, 2020).

MP concentrations in the water column range from 2 x 10^{-7} particles/m^3 in the Bearing Sea (Day et al., 1990) to 102,000 particles/m^3 off the coast of Sweden (Norén & Naustvoll 2010), with intermediate values of 9180 particles/m^3 in the Northwest Pacific Ocean (Deforges et al., 2014), 6000 particles/m^3 in South Korea (Song et al., 2014); 4137.3 particles/m^3 in China (Zhao et al., 2014) and less than 1 particle/m^3 in the Baltic (Bagaev et al., 2018). These differences are not only due to geographical differences; they also vary depending on the distance from the coast to the collection point and depth of sampling. In the northwestern Atlantic Ocean, particles per km^2 in the open ocean were 1000 times higher than near the coast (Colton et al., 1974) while in a campaign carried out in the Mediterranean sea, an average of 69,161.3 particles/km^2 was collected on the surface and only 0.26 particles/km^2 in the depths of the water column (Baini et al., 2018). These variations have also been found in sediments where the range of particle numbers can vary from 0.21 to more than 770,000 per m^3 (Hidalgo-Ruz et al., 2012). In general, contrary to water samples, in sediments, the highest MP concentrations are found near the coast, especially in industrialized areas (Lusher, 2015). Oceanic gyres are site of MP accumulation (Lusher, 2015), 26,989 items/km^2 being found in the subtropical gyre of the South Pacific Ocean (Eriksen et al., 2013). Currently there are no standardized methods to determine MP concentration in the environment and, given the difficulties to collect and identify the smallest particles, all data could be underestimated (Lusher, 2015). Most of the field studies only sample MPs above 300 µm, whereas most of the MPs are below this range. Based on this Van Cauwenbergue et al. (2016) calculated that the concentration of MPs (<5 mm) in coastal and marine environments, based on the

plastics production data in 2015, should be between 4.7 *10^{-4} and 3.5 * 10^{3} particles/L, and with the current growth of annual plastic production the expected concentration in 2100 could be between 0.01 and 2.2 * 10^{5} particles/L. In addition, the differences between sampling strategies and units to show data, make comparisons and determination of places that show the greatest contamination very complicated (Vandermeersch et al., 2015). Besseling et al. (2018) reviewed particle concentrations reported in the literature in several aquatic compartments and found differences of orders of magnitude.

The need to standardize methods for MP determination has been systematically repeated not only by scientist experts in the field, but also by international organizations such as the International Council for the Exploration of the Sea (ICES, 2015; Li et al., 2019). Futhermore, in the recent years a debate has been opened about what should be the size classification concerning the smallest plastics (Hartmann et al. 2019). For instance, the term nanoplastic is still under debate and works that set its upper limit at 100 and 1000 nm can be found (Gigault et al., 2018). In order to avoid this ambiguity some authors have claimed that plastic debris should be categorized according to International System of Units. Therefore Hartmann et al. (2019) proposed the following categories: nanoplastics from 1 nm to 1 µm, microplastics from 1 µm to 1 mm, mesoplastics from 1 to 10 mm and macroplastics for plastics larger to 1 cm.

Relatively little information is available nowadays regarding abundance and distribution of nanoplastics in the environment, although this fraction of plastic pollution could have a great ecological relevance. Particles below 10 µm are not quantified in environmental samplings and there are not suitable quantitative analytical techniques to assess the concentration of nanoplastics in the environment (Gaylarde et al., 2021). However, first steps have been made and nanoplastics have been detected in samples collected from the influent and effluents of wastewater treatment plants (Zkai & Aris, 2022). It is expected that the concentration of nanoplastics in the environment may exceed by 10^{14} times the concentrations that are currently being reported for MPs (Gaylarde et al., 2021).

On the other hand, the impact of visible plastics is well studied, especially as it has a great impact on popular animals such as cetaceans and sea turtles. However, the problems that MPs can cause on aquatic biota are still unclear. Despite the lack of consensus among studies, the range of possible negative effects attributed to MPs is very wide (Akdogan & Guven, 2019). In marine animals, damage has been observed at all levels of biological organization, from the molecular to the population level. Among the most common effects caused by MPs, oxidative damage, genotoxicity, neurotoxicity, inmunotoxicity, damage at the histological level and effects at the physiological level, both in digestive and reproductive systems could be highlighted (Alimba & Faggio, 2009; Pirsaheb et al., 2020). MPs can also transferred from exposed parentals to their offspring, causing toxic effects on gametes and embryos that may lead to population level consequences (Yin et al., 2021).

More than 220 marine species have been reported to ingest MPs, which raises concerns about their possible negative impact (Lusher et al., 2017). Affected organisms include cnidarians, annelids, molluscs, echinoderms, crustaceans, fish and seabirds (Hoss & Settle, 1990; Jumars et al., 1993; Thompson et al., 2004; Ward & Shumway; 2004; van Franeker et al., 2011; Hall et al., 2015). Among them, those that feed by filtration and detritivores are especially sensitive to the ingestion of MPs since they could feed directly on MPs and actively select them (Graham & Thompson, 2009). In addition, biomagnification of MPs may occur through the food chain, especially in filter-feeders and dentritevores that of various ecosystems (Farrell & Nelson, 2013; Batel et al., 2016).

Furthermore, MPs can carry toxic chemicals to organisms (Rochman et al., 2013; Browne et al., 2013; Avio et al., 2015; Sendra et al., 2021) in a process that can occur either by leaching of compounds added during their industrial production, such as plasticizers, or through the adsorption and desorption of pollutants that can be adsorbed on the surface of MPs (Lusher et al., 2015). Due to the small size of MPs, they have a high surface-to-volume ratio, which combined with their hydrophobic nature, makes them candidates to adsorb organic compounds (Cole et al., 2011; Avio et al., 2015; Wang et al., 2017). Thus, they pose an additional threat the marine environment (Frias et al., 2010; Bakir et al., 2014; Klein et al., 2015). The ability of MPs to adsorb and desorb many

environmental pollutants has been characterized (Huang et al., 2021). For instance, PAHs have been detected in MP pellets from different parts of the world (Ahmed et al., 2021).

Several authors have shown that this process depends, on the polymer type, the organic compound and the incubation or co-exposure time (Koelmans, 2015; Bakir et al., 2016), which underlines the need for studying a wide variety of plastic polymer-pollutant combinations that can be found in the environment, especially focusing on the factors that can alter bioavailability of both compounds (Koelmans, 2015). Among them, MP size, surface texture and chemical composition can be highlighted; as well asfactors that can be altered through aging processes and formation of biofilms once MPs are in the environment (Ziccardi et al., 2016). As the size of plastics decrease, not only does the surface area to volume ratio increase, but the diffusion pathways decrease. Therefore, the smaller the size of a plastic particle, the greater its ability to adsorb contaminants, at higher concentrations, and to participate in adsorption and desorption interactions in the environment (Velzeboer et al., 2014). Most of the adsorption studies have been carried out under laboratory conditions that are not environmentally relevant and, thus, they are difficult to extrapolate to realistic situations in the marine environment. In addition, the vast majority of these studies lack information on whether once a compound is adsorbed by MPs it remains stably attached to it or not. As mentioned before for GFNs, the hypothesis known as the Trojan horse effect supposes that MPs that have adsorbed contaminants could act as vectors and release contaminants once they are in contact with organisms, especially if animals ingest MPs, due to the physico-chemical characteristics of the digestive process (Boncel et al 2015, Sanchis et al., 2016). Two of the most relevant variables that could influence desorption of chemical compounds in organisms and their possible toxic consequences, are the time that these particles spend in the organism and their capacity to migrate throughout it (Bakir et al., 2016).

Transfer of various chemical compounds via MPs has been demonstrated in controlled laboratory experiments in annelids, molluscs, crustaceans and fish (Oliveira et al., 2013; Rochman et al., 2013b; Batel et al., 2016; Devrieseet al. 2014; Besselling et al., 2013;

Avio et al., 2015; Paul-Pont et al., 2016). However, the possible negative effects of this exposure route are not fully elucidated yet, especially since the toxicity of MPs alone is also not clear. For instance, similar detrimental effects were found on the nervous system of the common gudgeon (*Pomatoschistus microps*) exposed to polyethylene MPs alone or with adsorbed pyrene (Oliveira et al., 2013) but liver damage in Japanese medaka exposed to MPs with adsorbed organic contaminants was significantly greater compared to those exposed to MPs alone (Rochman et al., 2013).

As mentioned previously, transmission through the food chain could lead to a biomagnification process, which is especially relevant since, in general, animals that are at the base of the food chain feed in a non-selective way. Among them, bivalves have been widely studied for MPs toxicity in recent years (Table 3).

When Ding et al. (2020) studied the digestive system of 4 different bivalve species they found MPs in 80% of the animals. However, differences among species were found in MPs content, related to their feeding strategy (Ding et al., 2020). Von Moos et al. (2012) indicated that the main route for MP internalization in bivalves would be ingestion. Plastic particles would randomly contact with the surface of the gills, where they would adhere to the surface, which is rich in mucous-like sustances. Subsequently, these particles would be conducted through the movement of the gill channels to the mouth for ingestion, as if they were any other food particle. This hypothesis has been especially supported by the evidence that MPs are mainly located in the digestive tract of bivalves (Avio et al., 2015). However, since bivalves have historically dealt with inorganic particles such as sand and the rests of diatoms, they are capable of actively separating particles that are considered ingestable, discarding those that will not be ingested as pseudofeces. In addition, the retention efficiency of particles smaller than 1 µm in gills is calculated to be less than 15% (Ward and Shumway, 2004). This indicates that there might be other routes for the internalization of MPs such contact adsorption or adherence, as particles smaller than this size have been observed inside the animals (Kolandhasamay et al., 2018; Li et al., 2021). Li et al. (2021) proposed that during the processes of particle excretion via feces or pseudofeces, MPs may be trapped in

different organs of the animals, but MP size and shape will play a decisive role in this type of accumulation.

Several works have pointed out the importance of the size of MPs for their assimilation by mussels (Browne et al., 2008; Van Cauwenberghe et al., 2015; Kolandhasamay et al., 2018; Qu et al., 2018; Li et al., 2018; Li et al., 2019). Browne et al. (2008) found that the occurrence of MPs in mussel hemolymph was 60% higher in mussels exposed to 3 µm particles compared to those exposed to 9 µm particles. Von Hellfeld et al. (2022) observed that after 1 day of exposure 45 µm MPs were mostly found in lumen of stomach and ducts of mussels, while 4.5 µm MPs showed higher presence lumen of digestive tubules and gills. Since mussels have an open circulatory system, the fact that MPs can be found in hemolymph supports the idea that toxic effects would be extended throughout the body. For instance, 3 routes have been proposed for MPs elimination: first, through the exhalant siphon, second, directly from the digestive tract to feces and the last through different cells and tissues after MPs translocate from digestive tract to hemolymph (Sendra et al., 2021). Katsumiti et al. (2021) observed that after an *in vitro* exposure mussels hemocytes internalized nanoplastics and MPs of 0.05, 0.5 and 4.5 µm.

Bivalves exposed to MPs show changes in the transcription of genes (Avio et al., 2015), neurotoxicity, oxidative stress and oxidative damage (Paul-Pont et al., 2016), reduced lysosomal membrane stability (Von Moos et al., 2012) and histopathological lesions (Von Moos et al., 2012; Paul-Pont et al., 2016). At organismal level, reduced food intake and increase production of pseudofeces have been observed (Wegner et al., 2012). In addition, different effects have been reported in mussels exposed to MPs alone or in those exposed to MPs with adsorbed contaminants. Avio et al. (2015) observed greater DNA damage and neurotoxicity when mussels were exposed to polystyrene (PS) and polyethylene (PE) MPs with pyrene in comparison to MPs alone. In other studies, for some biomarkers, including oxidative stress, MPs alone had a greater negative impact than MPs containing fluoranthene (Paul Pont et al., 2016). DNA damage is one of the most controversial effects in the literature. Although Avio et al. (2015) reported increased DNA damage in mussels exposed to PS and PE MPs with pyrene compared to those exposed to MPs alone. In some studies (Paul-Pont et al., 2016; Pittura et al., 2018)

no DNA damage was observed in any of the conditions. In contrast, DNA damage was observed when mussels were exposed to nanoplastics of 110 nm (Brandts et al., 2018). Overall, toxicity of MPs and nanoplastics towards bivalves has been observed at all biological levels. However, the inconsistencies found in the literature highlights the necessity of further work to clarify the effects of MPs and nanoplastics alone or in combination with other pollutants towards marine bivalves.

Table 4: Summary of studies performed with MPs (<1 mm) and nanoplastics (<1 µm) alone and with associated pollutants in bivalves. Adults and embryos are considered separately and works dealing with hemocytes are also included.

MPs			Other contaminants	Exposure concentration	Exposure time	Other experimental conditions	Endpoints	Reference
Polymer	**Shape**	**Sizes**						
	Atactode striala							
PS	Granules	63-250 µm		10,1000 MPs/L	10 d		- Internalization and depuration of MPs - Presence of MPs in faeces and pseudofaeces - Clearance rate - Absorption efficiency - Respiration rate	Xu et al. (2017)
	Choromytilus chorus							
PS	Spheres	8.1–12 µm		-100 MPs/L - 1000 MPs/L	40 d		- Histological analysis - MPs Ingestion rate - Clearance rate - Absorption Efficiency - Ammonia excretion - Oxygen uptake - SFG - Growth rate	Opitz et al. (2021)
	Corbicula fluminea							
Proprietary polymer	Spheres	1-5 µm	FLO	-0.2 mg/L ($MP_{L)}$ -0.7 mg/L ($MP_{H)}$ -1.8 mg/L (FLO_L) -7.1 mg/L (FLO_H) -MP_L + FLO_L -MP_H+FLO_L	96 h		- Concentration of FLO in soft tissues - Internalization of MPs - CAT, GR, GPx, LPO, GST, ACHE - IDH, ODH - Histological analysis	Guilhermino et al. (2018)

				-MP_L+FLO_H MP_H+FLO_H		- Feeding inhibition	
Fluorescent polymer	Spheres	1-5 µm	Hg	-0.13 mg/L MP -30 mg/L Hg - MIX	8 d exposure + 6 d depuration	- Internalization of MPs - Concentration of Hg in soft tissues - CAT, GR, GPx, LPO, GST, ACHE - IDH, ODH - Filtration rate	Oliveira et al. (2018)
Fluorescent PS	Particles	80 nm		-0.1 mg/L -1 mg/L -5 mg/L	96h	- GOT, GPT, DAO - CAT, SOD, GSH, GPx, GR, LPO - GST, ACHE - Histological observation	Li et al. (2020)
	Crassostrea brasiliana						
PE	Spheres	150–250 µm	TCS	250 mg/L MPs	72 h 7 days	- EROD,DBF - GST, GSH, GPx, ACHE, LPO - NRRT - DNA damage	Nobre et al. (2020)
	Crassostrea gigas						
PS	Beads	2,6 µm		2 µm: 2,062 ± 170 MPs/mL 6 µm: 118 ± 15 MPs/ mL	8 weeks	- Internalization of MPs - Histological analysis - Algae consumption - Proteomic analysis - Gene expression (microarray) - Dynamic energy budget - Gamete quality - Embryo development	Sussarellu et al. (2015)
PS	Beads	50 nm & 3 µm		*In vitro:* 10 and 100 ppb *In vivo:* 50 ppb	*In vitro:* 4h *In vivo:* 48h	- Lysosomal destabilization - Internalization of MPs and NPs	Gaspar et al. (2018)

PS	Beads	6 µm	-10^4 MPs /L -10^5 MPs /L -10^6 MPs /L	80 d		- Internalization of MPs - LMS - Histological analysis - Shell length - Weight - Condition index	Thomas et al. (2020)
	Dreissena polymorpha						
PS	Beads	1, 10 µm	-1×10^6 MPs/L - 4×10^6 MPs/L	6 d		- Internalization of MPS - Confocal microscopy analyses - CAT, SOD, GPx, GST, LPO - PCC, DOP, SER	Magni et al. (2018)
Land collected MPs	Not specified	>63 µm	A non specified batch of MPs	7 d		- Internalization of MPs - CAT, SOD, GPx, GST, ROS - PCC - MN	Binelli et al. (2020)
PS	Fragments	<63 µm	-6.4 MPs/mL -160 MPs/mL -4000 MPs/mL -100,000 MPs/mL + Extra group of 100,000 diatomites/mL	14 d	At 14, 23, 17 °C	- Energy content: protein, glycogen and total lipid content in digestive gland - LPO in digestive gland - Phagocytic activity - Clearance rate	Weber et al. (2020)
	Geukensia demissa						
PS, PE	Spheres	5 µm PS 250-300 µm PE	-PS 0.167 g/L -PE 3.3. g/L	2h	Collected 4 and 12 h post exposure	- MPs Ingestion rate - MPs Rejection rate	Khan & Prezant (2018)
	Mactra veneriformis						

PS	Beads	17 µm 150 µm	Phe	-1 mg/L PS -20 µg/L Phe - 50 µg/L Phe	8 d exposure 3 d depuration		- Concentration of Phe in soft tissues - SOD, GST, LPO	Zhang et al. (2021)
	Mytilus coruscus							
PS	Spheres	2 µm		-10 MPs/L -10^4 MPs/L -10^6 MPs/L	14 d exposure + 7 d depuration	pH: 7.7 and 8.1	- CAT, SOD, GSH, GPx, - PES,TRS, AMS - LPS, LZM	Wang et al. (2020)
	Mytilus edulis							
PS	Spheres	3, 9.6 µm		42 MPs/L	3h - 48d		- MPs ingestion, translocation, accumulation	Browne et al. (2008)
PS	Beads	30 nm		-0.1 g/L -0.2 g/L -0.3 g/L	8 h		- Production of pseudofeces and feces - Filtering activity	Wegner et al. (2012)
PS	Spheres	10, 30, 90 µm		110 MPs/mL	14 d-24 h clearance		- Protein content - Carbohydrate content - Lipid content - ETS - Cellular Energy Allocation	Van Cauwenbergh e et al. (2015)
HDPE	Powder	0-80 µm		2.5 g/L	96 h		- MPs uptake - LMS - Lipofuscin - Neutral lipids - Histological analysis - Condition index	Von Moos et al. (2012)
PLA, HDPE	Particles	0.48-363 µm		-2.5 µg/L -25 µg/L	50 d		- Filtration rate	Green et al. (2017)

Not specified	Fibers	Manually produced		2000 MPs /L	48h exposure 48h depuration	-	Accumulation of MPs and NPs	Kolandhasamy et al. (2018)
PE	Powder	10–90 µm	Fluoranthene	-106 MPs /L -Fluoranthene: 100 µg/L	96h	- -	Concentration of fluoranthene in soft tissues GSH, GSSG, SOD, CAT, GPx	Magara et al. (2018)
HDPE, PLA	Fragments	HDPE: 102, 6 µm PLA 65.6 µm		-25 µg/L HDPE -800 µg/L PLA	52 d	- - -	Number of byssal threads Attachment strength Hemolymph proteome	Green et al. (2019)
PE, PHB	Beads	10–90 µm	Fluoranthene	-1000 MPs /mL -Fluoranthene: 100 µg/L	96 h	-	GSH, GR, SOD, CAT, GPx, GST	Magara et al. (2019)
	M. galloprovincialis							
PS, PE	Powders	<100 µm	Pyrene (sorbed)	-1.5 g/L MPs -Pyrene:50 µg/L	7 d	- - - - - - - - - - - - -	Concentration of pyrene in soft tissues MPs presence Gene expression (microarray) Granulocytes/hyalinocytes ratio Phagocytosis activity in hemocytes LMS in hemocytes NRRT in hemocytes; ACHE, AOX, CAT, GST, GPx, TOSC, LPO Lipofuscin in digestive gland Neutral lipids in digestive gland Comet assay in hemocytes MN and NA in in hemocytes	Avio et al. (2015)

HDPE	Beads	1-50 µm		-1.5* 10 ^{7}MPs/L	24 h	- Gene expression (*pk, id, sd, tlr, pgrp, myticin a, myticin b p53, caspase 3/7, FADD, catalase, sod, αtubulin)*	Détrée & Gallardo-Escárate (2017)
PS	Beads	100 nm	Cbz	-0.05-50 mg/L PS alone -6.3 µg/L Cbz	96 h	- gene expression (*act, 18s, tub, cyp11, cyp32, gst, pgp, gaadd45a, p53, hsp70, cat, lys* - TOC, TAC - ACHE - AST, ALT - GLU, EA,LPO - DNA damage in hemolymph	Brandts et al. (2018)
PE	Fragments	50-590 µm		0.01 mg/mL	21 d	- MPs ingestion - MN - Histological analysis - Condition index	Bråte et al. (2018)
LDPE	Particles	20-25 µm	BaP	-2.34×10^{7} MPs/L -BaP: 150 ng/L	28 d	- Concentration of BaP in soft tissues - Presence of MPs in soft tissues - Gene expression (*cat, Se-gpx, gstpi, aox1, hsp70*) - Granolocytes/hyalinocytes ratio - Phagocytosis activity in hemocytes - LMS in hemocytes - NRRT in hemocytes; - ACHE, AOX, CAT, GST,GPx, TOSC, LPO - Lipofuscin in digestive gland - Neutral lipids in digestive gland	Pittura et al. (2018)

						- Comet assay in hemocytes - MN in hemocytes	
HDPE	Not mentioned	2-4; 4-6; 6-8: 8-10 µm		-2 -4 mm^3/L	4 h exposure 144 h depuration	- Uptake of MPs - Elimination of MPs - MPs quantification in biodeposits and digestive glands	Fernandez & Albentosa (2019)
PS	Spheres	2,5,6,10 µm		A&B)6µm+10µm: 1000 MPs/mL C) 2µm+6µm+10µm: 10 and 1000 MPs/mL D)5µm+10µm: 1000 MPs/mL	A) 90 min B) 20 min C) 48 h D) 21 d exposure + 7 d depuration	- Internalization of MPs - Histological analysis - GST in digestive gland and gills - LPO in digestive gland and gills	Gonçalves et al. (2019)
PS	Spheres	0.5, 4.5 µm	BaP (sorbed)	0.058 mg/L = 1000 particles/mL 4.5 µm 7.44 × 105 particles/ mL 0.5 µm	26 D	- Concentration of BaP in soft tissues - Presence of MPs in soft tissues - Hemocyte viability - Comet assay - CAT - Cell composition, quantitative structure of mussel digestive gland - Histopathological analysis - Clearance rate, respiration rate, absorption efficiency, SFG - CI	Gonzalez-Soto et al. (2019)
PS	Spheres	1, 10, 90 µm		$75*10^6$ MPs/L	4 h exposure	- Internalization of MPs - Gut retention time	Kinjo et al. (2019)

					40 d depuration			
PS, PA	Spheres Fragments Fibers	Microspheres 10 µm, fragments and fibers < 5 mm		1000 MPs/L	3 d exposure		- Internalization of MPs	Li et al. (2019)
PE	Spheres	108-212 µm		10 mg/L = 2000 MPs/L	1 h exposure 24 h depuration	Presence and absence of algae during exposure	- Internalization and elimination of MPs	Chae & An (2020)
PS	Spheres	50, 10 nm 1 µm		10 mg/L	A) *In vivo* 24 h B&C) *In vitro* 3 h	C) MPs + *V. splendidus*	- Histological analysis - Uptake pathway of MPs into hemocytes - Gene expression - (*irg1, mytilin d and myticin c, duox, ucp2)* - Motility of hemocytes - -Effects of *Vibrio splendidus* on hemocytes exposure	Sendra et al. (2020)
HDPE, PS	Not mentioned	90-110 µm		50 µg/mL	96 h exposure 144 h depuration		- Internalization of MPs - Elimination of MPs - Histological analysis - SOD, CAT - Total protein content - Metabolomic analysis	Wei et al. (2021)
PS	Spheres	4.5,45 µm	BaP Cd	1, 100 and 1000 particles/mL = 0.05, 5 and	1 d expodure + 3 d depuration		- Presence of MPs in soft tissues - Concentration of BaP and Cd in soft tissues	von Hellfeld et al. (2022)

				50 mg/L 45 µm and 0.05, 5 and 50 µg/L for 4.5 µm MPs 1000 particles/mL 4.5 µm or + 1 µM Cd / BaP (sorbed)	3 d exposure		- Tissue Metal Distribution and Accumulation - CAT, SOD, AOX - LMS - Cell composition, quantitative structure of mussel digestive gland -	
	***Mytilus* spp.**							
PS	Beads	2,6 µm	Fluoranthene	-32 µg/L/=2000 MPs/mL Fluoranthene:30 µg/L	7 d exposure 7 d depuration	MPs given with algae	- Fluoranthene concentration in algae - Fluoranthene concentration in soft tissues - Hemocyte mortality - Granulocytes / hyalinocytes - Phagocytosis activity - Phagocytosis capacity - ROS production - Gene expression (*cat, sod, gpx, cyp11, cyp32, ωgst, µgst, δgst, αadd45α, amylase, pk, idp, gapdh, hk, p53, pgp, lys, casp37-3*) - SOD, CAT, GR, GST, LPO - Histological observation	Paul-Pont et al. (2016)
PS PVC polyster	A)Beads, fragments and fibers	Beads: 0.01 Fragments 0.02-0.5		-100 MPs/L -1000 MPs/L	5 d	Water change every day	- Internalization of MPs	Qu et al. (2018)

	B)Field samples	Fiber 0.1-3.5 mm					
PE, PP	Not mentioned	<400 µm		-0.008 µg/L -10 µg/L -100 µg/L	10 d exposure + 10 d depuration	- Internalization of MPs - Gene expression (*cat, gpx, sod)* - CAT, SOD, GST - ROS Production - Comet assay - Histological analysis - Clerance rate - Condition index	Revel et al. (2019)
PS	Spheres	40 µm ± 10 µm		-15 -1500 -15000 -150000 -1500000 MPs/individual/ week	42 weeks	- SOD, LPO - Byssus production - Clearance rate - Growth - Condition index	Hamm & Lenz (2021)
	Pecten maximus						
14C-radio-labeled PS	Spheres	24 and 250 nm		<15 µg/L	6 h exposure 48 d depuration	- Internalization of NPs	Al-Sid-Cheikh et al. (2018)
	Perna canaliculus						
PE	Beads	38–45 µm,	TCS	-0.5 g/L MPs -0.36 mg/g TCS	48 h	- Concentration of TCS in water - Concentration of TCS in soft tissues - Internalization of MPs - LPO, SOD, GST	Webb et al. (2020)

						- Byssus production - Clearance rate - Respiration rate	
	Perna perna						
PVC	Powder	0.1-1 µm		0.125 g/L =1.115×10^{10} MPs/L	90 d	- NRRT - LPO - DNA damage - Clearance rate - Absorption efficiency - Growth rate - Condition index	Santana et al. (2018)
	Ruditapes philippinarum						
PS	Beads	100, 250, 500 µm		60 MPs/L 1:1:1 proportion	24 h exposure 72 h depuration	- Internalization of MPs - -Depuration of MPs	Graham et al. (2019)
PE	Beads	10-45 µm	Hg	-MP: 25 µg/L = 144 ±27 MPs/mL -Hg: 10 µg/L	7 d	- Concentration of Hg in soft tissues - Internalization of MPs - Filtration rate - Histological analysis - Hemocyte viability - LMS in hemocytes - CAT, GSH, LPO	Skidokur et al. (2020)
	Scrobicularia plana						
PS	Beads	20 µm		1 mg/L	14 d exposure 7 d depuration	- Internalization of MPs - CAT, SOD, GPx, GST, LPO, ACHE - Comet assay in hemocytes - Condition index	Ribeiro et al. (2017)

LDPE	Particles	11-13 µm	BaP PFOS (sorbed)	-LDPE 1 mg/L -BaP 16.8 ± 0.22 µg/g -PFOS 70.22 ± 12.41 µg/g	14 d	- Concentration of BaP in soft tissues - SOD, CAT, GPx, GST, LPO, ACHE - Total protein content - Comet assay in hemocytes - Condition index	O'Donovan et al. (2018)
	Tegillarca granosa						
PS	Not mentioned	500 nm	OTC FLO	-0.26 mg/L MPs -OTC 270 ng/L, -FLO 42 ng/L	14 d	- Total hemocyte number - % of hemocyte type - Phagocytosis activity - ROS in hemocytes - LPO in hemocytes - Viability of hemocytes - Comet assay in hemocytes - Lectin content in hemolymph - Gene expression in gills (*nfkb, ikkα, mapk, caspase3, gst, cyp1)*	Zhou et al. (2021)
				EMBRYOS			
	Crassostrea gigas						
PS	Beads	50, 500 nm & 2 µm		-0.1 µg/mL -1 µg/mL -10 µg/mL -25 µg/mL	48 h	- Embryo development	Tallec et al. (2018)
HDPE	Beads	4-6 µm 11-13 µm 20-25 µm		1 mg/L -1 mg/L -10 mg/L	24 h	- Embryo development - Swimming activity	Bringer et al. (2020)
	Mytilus edulis						

PS	Beads	2 µm 100 nm		A&B) -1.40 -1.05 - 0.7 mg/L C) -Low:100 nm: 0.77 *10^6/mL; 2 µm: 96/mL -Medium: 100 nm: 5.1 *10^7/mL; 2 µm 6398/mL -High: 100 nm: 5.1 *10^8/mL; 2 µm 63980/mL	A) 4 h exposure, 16 h depuration B) 48 h exposure C) 15 d	A&B) 12 d old larvae C) 7 d old larvae	- Ingestion - Egestion - -Larval growth	Rist et al. (2019)
	M. galloprovincialis							
PS-NH_2	Particles	50 nm		A)0.001 mg/L -0.01 mg/L -0.05 mg/L -0.1 mg/L -0.25 mg/L -0.5 mg/L -1 mg/L -2.5 mg/L -5 mg/L -10 mg/L -20 mg/L B)0.150 mg/L	48 h		- Embryo development - Polarized light microscopy - SEM - Gene expression (*cs, ca, ep, 5-htr, cat,sod, gst, abcb, mtor, p53, tlr i, lyso*)	Balbi et al. (2017)
LDPE	Spheres	1-4 µm 4-6 µm	BP-3	A) -20 mg/L MPs	48 h	A) all sizes	- Internalization of MPs - Embryo development	Beiras et al. (2018)

		6-8.5 µm 11-13 µm <63 µm	-50 mg/L MPs 100 mg/L MPs B) -1 mg/L MPs -10 mg/L MPs +0.2 µg/L BP-3 - 20 µg/L BP-3	B) 4-6 and 11-13 µm		
PS	Spheres	3 µm	50-1×10^4 MPs/mL	24 h-192 h	- Internalization of MPs - Microalgae consumption - Embryo development - Gene expression (*mytc, lys, mytlb, gusb, hex, ctsl, 5-ht1, meer1, meer2, ep, ca, cs, mt10, mt20*)	Capolupo et al. (2018)
	Perna perna					
PP	Pellets	various	2 ml in 10 ml water	48 h	- Embryo development	Gandara e Silva et al. (2016)
			HEMOCYTES			
	M. galloprovincialis					
PS-NH_2	Particles	50 nm	-1 µg /mL -5 µg /mL -50 µg /mL	4 h	- NRRT - Lysozyme activity - ROS production - NO_2 production - Phagocytosis - Apoptosis - Confocal microscopy	Canesi et al. (2015)
PS-NH_2	Particles	50 nm	-1 µg /mL -5 µg /mL -50 µg /mL	The influence of hemolymph serum was investigated.	- NRRT time - ROS - Phagocytosis - TEM	Canesi et al. (2016)

						- p38mapk protein expression - PKC protein expression	
PS	Spheres	0.05 µm 0.5 µm 4.5 µm	BaP	- 0.05 µm: $10^{2,}$ 10^{3}, 10^{5}, 10^{6}, 10^{8}, 10^{9}, 10^{12} alone and + 1µM BaP (coexposure) - 0.5 µm: $10^{2,}$ 10^{3}, 10^{5}, 10^{6}, 10^{8}, 10^{9} alone and + 1µM BaP (sorbed) - 4.5 µm: $10^{2,}$ 10^{3}, 10^{5}, 10^{6}, 10^{8} alone and + 1µM BaP (sorbed)	24 h	- TEM - Confocal microscopy - Cell viability - Plasma membrane integrity - Phagocytic activity - Lysosomal acid phosphatase - ROS - Comet Assay	Katsumiti et al. (2021)

Abbreviations: ACHE: acetylcholinesterase, ALT: alanine transaminase; AST: aspartate aminotransferase; BaP: benzo(a)pyrene, BP-3: benzophenone3; CAT: catalase, Cbz: carbazepine; D.Lac: D lactate; DAO: diamine oxidase; DBF: Dibenzylfuorescein Dealkylase; DOP: dopamine concentration; EA: Esterase activity; EROD: Ethoxyresorufn-O-Deethylase; ETS: electron transport system, FLO: florfenicol; GLU: glucose content; GLY: glycogen, GOT: aspartate aminotransferase; GPT: alanine aminotransferase; GPx: glutathione perodixase, GR: glutathione reductase, GSH: reduced , GSSG: glutathione disulfide, GST: glutathione-S-transferases, HDPE: high-density polyethylene; IDH: isocytrate deshydrogenase; LDPE: low-density polyethylene; LMS: lysosomal membrane stability; LPO: lipid peroxidation, MN: micronuclei assay; NA: nuclear abnormalities, NRRT: neutral red retention time; ODH: octopine deshydrogenase; OTC: oxytetracycline; PA: polyamide; PCC: protein carbonylation content; PE: polyethylene; PFOS: perfluorooctanesulfonic acid; PHB: Polyhydroxybutyrate; Phe: phenanthrene; PLA: polylactic acid; PP: polypropylene; PS: polystyrene; PVC: polyvinyl chloride; ROS: reactive oxygen species, SER: serotonine concentration; SOD: superoxide dismutase, TAC: total antioxidant capacity; TCS: triclosan; TEM: Transmission Electron Microscopy; TOSC: total oxidant status.

4. MUSSELS AS SENTINELS OF NANOMATERIAL, NANOPLASTICS AND MICROPLASTIC TOXICITY

Mytilus spp. mussels are often used as model organisms to study the accumulation of pollutants and their effects in the marine environment (Viarengo et al., 2007). Among the characteristics that make mussels so useful as sentinels of pollution the following can be highlighted: **1.** ubiquity, mussels can be found in the coasts all over the world; **2.** they are part of many trophic chains; **3.** they form a group of high economic interest since they are consumed by humans; **4.** they are sessile, which makes them good indicators of pollution; **5.** due to their feeding strategy, they are constantly filtering large volumes of water and due to their low capacity to metabolize xenobiotics, contaminants from the environment tend to accumulate in their tissues; **6.** they are capable of withstanding high levels of pollution but at the same time, they are sensitive to low levels of pollution, which allows determination of response mechanisms (Cajaraville et al., 2000). Therefore, mussels are used in various biomonitoring programs, both as bioindicators and as sentinel organisms, in order to determine bioavailability of contaminants and the response of organisms to such contaminants, eg: Mussel Watch program, MEDPOL-UNEP/RAMOGE, OSPAR joint monitoring programme (Goldberg, 1976; Vethaack et al., 2017). In recent years, due to the high filtration capacity of mussels and their developed endolysosomal system, they also have been proposed as model organisms to study the toxicity of NMs, MPs and nanoplastics and their associated contaminants (Moore, 2006; Canesi et al., 2012; Matranga & Corsi, 2012; Rocha et al., 2015; Li et al., 2019; Katsumiti & Cajaraville, 2019).

The first contact for micro and nano scale materials in mussels are the gills (Corsi et al., 2014; Rocha et al., 2015; Sendra et al., 2021), where depending on the size of the particles, two mechanisms have been proposed to internalization, directly through the gill surface or by transport to the mouth (Sendra et al., 2021). Particles that are ingested will be transported to the digestive gland which in mussels is one of the main targets for contaminants and where micro and nano scale materials will mostly accumulate (Cajaraville et al., 2000; Canesi et al., 2012; Rocha et al., 2015; Canesi & Corsi 2016;

Cajaraville et al., 2021; Sendra et al., 2021). At the subcellular level, the well developed endolysosomal system of mussels, which plays a key role in intracellular digestion, is considered one of the targets for micro and nano scale pollutants (Cajaraville et al., 1995; Robledo et al., 1997; Moore, 2006; Canesi et al, 2012; Katsumiti et al., 2014; Rocha et al., 2015). Moreover, since the pH of digestive processes can stimulate desorption of adsorbed pollutants, the digestion process could contribute to the Trojan horse *effect*.

Micro and nano scale materials can translocate from the digestive system to the hemolymph or to gonads (Sendra et al., 2021). Therefore, the impact of NMs, nanoplastics and MPs could be expected to occur at whole organism, exerting a wide variety of biological effects.

Biomarkers are commonly defined as quantifiable measurements that can indicate that an organism has being exposed to a pollutant (biomarkers of exposure) or the magnitude of the response (stress biomarkers) (Cajaraville et al., 2000). They are early warning responses measured at low levels of biological complexity that allow prediction of consequences of an exposure. However, biomarkers can be influenced by physiological parameters such as sex, developmental stage or age and by environmental factors such as temperature, salinity and food availability. Generally, the use of a battery of biomarkers that belong to different biological organization levels as well as homogeneous experimental conditions are recommended to asses biological effects of pollutants. Thus, in order to decipher the impact of GFNs and micro and nanoplastics alone or in combination with other pollutants on mussels, a whole battery biological responses considering different biological organization levels, from molecular level to organism level, should be assessed. This would help to establish the adverse outcome pathway (AOP) of each pollutant. Each AOP is initiated with a molecular-cellular event that leads effects at higher levels of biological organization with direct relevance for risk assessments (e.g. survival, development, reproduction…) (Ankley et al., 2010). Thus, the study of AOPs would help in early identification of hazards linked to GFNs, MPs and nanoplastics.

Gene and protein expression are sensitive indicators of environmental changes, including exposure to pollutants, even at low doses and short exposures (Denslow et al., 2007). At short time of exposure, these changes are normally adaptative responses which aim to protect the organism (Denslow et al., 2007). Changes in gene expression have been recorded after exposure to micro and nanoscale particles in bivalves, including GFNs, MPs and nanoplastics (Tables 2 and 3).

At both gene and enzyme levels, the biotransformation metabolism is one of the main biological pathway explored after exposure to pollutants. Biotransformation is commonly defined as the biological processes in which a substance is changed (Timbrell, 2009) usually in order to convert lipophilic substances into more polar compounds that could be more easily excreted from the organism. The process is ussually divided into 3 separated phases: phase I, phase II and phase III metabolism. Phase I is governed by oxidative, hydrolytic or reductive processes that add reactive functional groups (such as –OH, NH2, SH, COOH..) to the target compound while the aim of Phase II is to conjugate the metabolite with water soluble compounds naturally present in cells (Livingstone, 1991; Timbrell, 2009). Glutathione-S-transferases (GST) are the most studied phase II enzymes. GSTs form a family of multiple isoforms that can be found mostly in the cytosol and in the endoplasmic reticulum of cells of most mussel tissues, especially in the digestive gland and gills (Listowsky et al., 1988; Sheehan et al., 2001). Alterations of GST activity after exposure to micro and nanoscale particles in bivalves, including GFNs, MPs and nanoplastics has been observed in several works (Tables 2 and 3).

Phase II reactions can be considered biosynthetic reactions that require energy (Livingstone, 1991) and thus, when organisms are exposed to pollutants the energy metabolism may be modulated. Pollutants can also affect the energy metabolism directly, so regulation of the energy metabolism is a key aspect that should be taken into account during response to stress (Solokova et al., 2012). Since intertidal mussels have to adapt to low tides, mussels can close their valves and adapt the aerobic metabolism to the anaerobic one. Hence, both the aerobic and anaerobic metabolisms should be taken into consideration to evaluate the energetic metabolism of mussels. Isocitrate dehydrogenase is involved in the Krebs cycle for regeneration of cellular NADPH and

octopine dehydrogenase is one of the major contributors to the pyruvate degradation during anaerobic glycolysis. Both enzymes have been studied in several biomonitoring and laboratory works (Lima et al., 2007), and their alterations have been recorded after exposure to micro and nanoscale particles in bivalves, including GFNs, MPs and nanoplastics (Tables 2 and 3).

Alteration of the balance between the aerobic and anaerobic metabolisms can also be part of the defense mechanism of organisms towards oxidative stress. Oxygen reactive species (ROS) including superoxide anion (O_2^-), hydroxyl radical (OH^-) and hydrogen peroxide (H_2O_2) are naturally formed during the aerobic metabolism (Halliwell & Gutteridge, 2007) and under normal conditions they will be eliminated by different molecular weight scavengers and antioxidant enzymes. Antioxidant enzymes form a group of enzymes responsible for the transformation of ROS into stable and less reactive molecular structures. The three main antioxidant enzymes are: superoxide dismutases (SOD), glutathione peroxidases (GPx) and catalase (Cat) (Saez & Están-Capell, 2017). SODs are responsible for the dismutation of superoxide ion into hydrogen peroxide. Afterwards, both Cat and GPx can catalize the, break down of hydrogen peroxide into water and oxygen molecules or catalyzing the reduction of hydroperoxides to alcoholic groups and water using reduced glutathione (GSH) as co-substrate, respectively (Saez & Están-Capell, 2017). Exposure to micro and nanoscale particles is known to cause alterations in the oxidative defences of bivalves, including GFNs, MPs and nanoplastics (Tables 2 and 3).

Exposure to pollutants can increase ROS production and lead cells to an oxidative imbalance, known as oxidative stress. This imbalance is normally compensated by the modulation of the antioxidant system. However, under highly toxic or prolonged situations of oxidative stress the antioxidant system can be overwhelmed and be unable to compensate the production of ROS, leading to a detrimental imbalance. Intracellular ROS can react with different macromolecules and cause damage (Sies, 1991; Halliwell & Whiteman, 2004). ROS can react with lipids, especially fatty acids and cause lipid peroxidation which can alter cell membranes or even break them (Halliwell, 1992). The loss in cell membrane integrity can lead to cytotoxicity and affect other cellular

compartments. In addition, ROS and compounds derived from lipid peroxidation can also interact with proteins and nucleic acids. DNA is one of the most susceptible cell components towards oxidative damage and interactions could cause alterations in gene expression, DNA strand breaks or chromosomal fragmentation (Singht et al., 2009). Changes in gene expression or DNA strand breaks can be transitory whereas other alterations such as chromosomal fragmentation are irreversible. A combination of assays including comet assay for reversible DNA strand breaks and the micronuclei test for chromosomal damage can be applied to assess pollutants genotoxicity (Bolognesi & Fenech, 2012; Canesi et al., 2014; Rocha et al., 2014). Oxidative damage and DNA damage have been widely described after exposure to micro and nanoscale particles in bivalves, including GFNs, MPs and nanoplastics (Tables 2 and 3).

Some pollutants including micro and nanoscale particles show neurotoxic effects which can be assessed measuring the activity of Acetycholinesterase (AChE) (Tables 2 and 3). AChE is an enzyme involved in the correct transmission of the nervous signal across cholinergic synapses, by converting the presynaptic electrical signal into a chemical signal (acetycholine) (Bocquené & Galgani, 1998). AChE activity has been reported in a variety of tissues of mussels including the adductor muscle (Frasco et al., 2010). Alterations in AChE activity can interrupt the transmission of nervous signals, damage sensory and muscular systems (Murphy, 1986) and cause death (Britt, 2015). Many chemical compounds/pollutants alter AChE activity in a transitory or irreversible way and thus, AChE has been proposed as biomarker for environmental pollution (Bocquene & Galgani 1990; Guilhermino et al., 1998; ICES, 2012).

Micro and nano scale materials are also able to interact with cellular membranes directly and cause perforations (Katsumiti et al., 2017) that would decrease cell viability. In mussels, micro and nano scale materials can alter viability of hemocytes and thus cause immunotoxicity. Viability of hemocytes can be assessed by the neutral red uptake test (Gómez-Mendikute et al., 2002) which is based on the fact that the dye will be only incorporated into lysosomes of living cells (Borenfreund & Puerner, 1984). Alterations of immunological status of bivalves after exposure to micro and nanoscale particles,

including GFNs, MPs and nanoplastics, have already been described in the literature (Tables 2 and 3).

The digestive gland of mussels is a plastic organ that can respond to multiple environmental stressors (Winsted, 1995). However, exposure to pollutants may lead to the loss of digestive cells and then, the digestive epithelium can undergo from thinning to atrophy (Cajaraville et al., 1990; Garmendia et al., 2010; ICES 2012). The digestive tubules of mussels are formed by a single and dynamic epithelium, comprised by two cell types: digestive cells and basophilic cells. Under normal physiological conditions, basophilic cells are less abundant than digestive cells, but this is reversed under stress conditions by the hypertrophy of basophilic cells and the loss of digestive cells (Zaldibar et al., 2007), probably due to the degeneration of digestive cells caused by the exposure to pollutants (Cajaraville et al., 1990; ICES 2012). This alteration in the composition of cell types of the digestive epithelium may affect food digestion (Marigómez et al., 1998). Changes in the cell composition of the digestive epithelium and in the structure of digestive tubules can be measured in terms of volume density of basophilic cells (VvBAS) and mean epithelial thickness to mean diverticular radius (MET/MDR) and mean luminal radius to mean epithelial thickness (MLR/MET), respectively (Bignell et al., 2012; De los Ríos et al., 2013). These parameters are commonly used biomarkers in ecosystem health assessment, as they significantly reflect changes in the general health status of mussels (Marigómez et al., 2006; Zorita et al., 2006; Garmendia et al., 2011; De los Ríos et al., 2013). In addition, histopathology of the digestive gland or other tissues is a reliable tool to determine the toxicity profile of a pollutant as it can help to dissociate markers of underlying health or disease condition from those associated with an exposure (Bignell et al., 2012). Alterations such as occurrence of parasites, fibrosis in the connective tissue, necrosis of digestive tubule epithelium, focal and diffuse hemocytic infiltrations, presence of brown cells in connective tissue and brown aggregates in epithelium of the digestive tract are usually recorded (Garmendia et al., 2011; Bignell et al., 2012; Ruiz et al., 2014).

On the other hand, histopathology of the gonad incorporates measures of reproductive and metabolic condition of organisms (Bignell et al., 2012) and thus, it is a useful tool to

evaluate the reproductive status and condition of the gonad (Hines et al., 2007). The gonad index can be calculated based on proportions of gamete developmental stages of the gonad (Seed 1969; Kim et al., 2006) and oocyte atresia and oocyte necrosis (Ortiz-Zarragoitia and Cajaraville, 2006, 2010; Kim et al., 2006; Ruiz et al., 2014) are also usually assessed. The seasonal reproductive cycle of bivalves is dependent on environmental conditions (Seed & Suchanek, 1992; Villalba 1995; Ortiz-Zarragoitia et al., 2011; Gosling, 2015) and pollutants can have a great impact over the sex ratio and reproductive cycle (Ortiz-Zarragoitia et al., 2011). In addition, the mantle is also the main site for nutrient storage in mussels. Once mussels have released gametes, reserves are accumulated, usually during summer in temperate latitudes, for their use in autumn and winter. This seasonal developmental cycle of the gonad has an impact in the metabolism and physiology of mussels (Gosling, 2004). Several histological alterations of different organs of bivalves have already been described after exposure to micro and nanoscale particles, including GFNs, MPs and nanoplastics (Table 2 and 3).

It is also importat to dtermine the impact of pollutants at whole organism level and at higher biological organization levels (Tsangaris et al., 2008). Energy balance and growth capacity of animals can be indirectly obtained by measuring respiration, feeding, digestion and excretion rates and integrating them in physiological energetic parameters such as Scope for growth (Widdows, 1985; Widdows & Johnson, 1988). Similarly, the condition index, calculated as the ratio between animals mass and length, can be altered during the gametogenic cycle or due to environmental factors including exposure to pollutants (Widdows & Johnson, 1988). The impact over the gonad can lead to detrimental effects at individual level but also at population level (Canesi & Corsi, 2016).

Finally, embryos and larval stages are more susceptible to changes in their environment than adult stages (Pörtner et al., 1998; Ringwood et al., 2009; Fabbri et al., 2014). Several studies have demonstrated that the early stages of mussel's development, are sensitive to NM exposure (Balbi et al., 2017; Auguste et al., 2018) and even that arrested development and malformed larvae can be observed after parental exposures to Ag NPs (Duroudier et al., 2019). In mussels, after external oocyte fertilization, embryos undergo

fast cell divisions that lead into their segmentation and differentiation into motile forms: first, a trocophore at 24 hours post-fertilization and then, various shelled forms (D-larvae), starting from 48 hours post-fertilization (Rusk, 2012) (Figure 9). The study of effects on such early developmental stages by using embryo toxicity tests is a useful approach to determine the biological impact of NMs in marine invertebrates (Fabbri et al., 2014; Balbi et al., 2014).

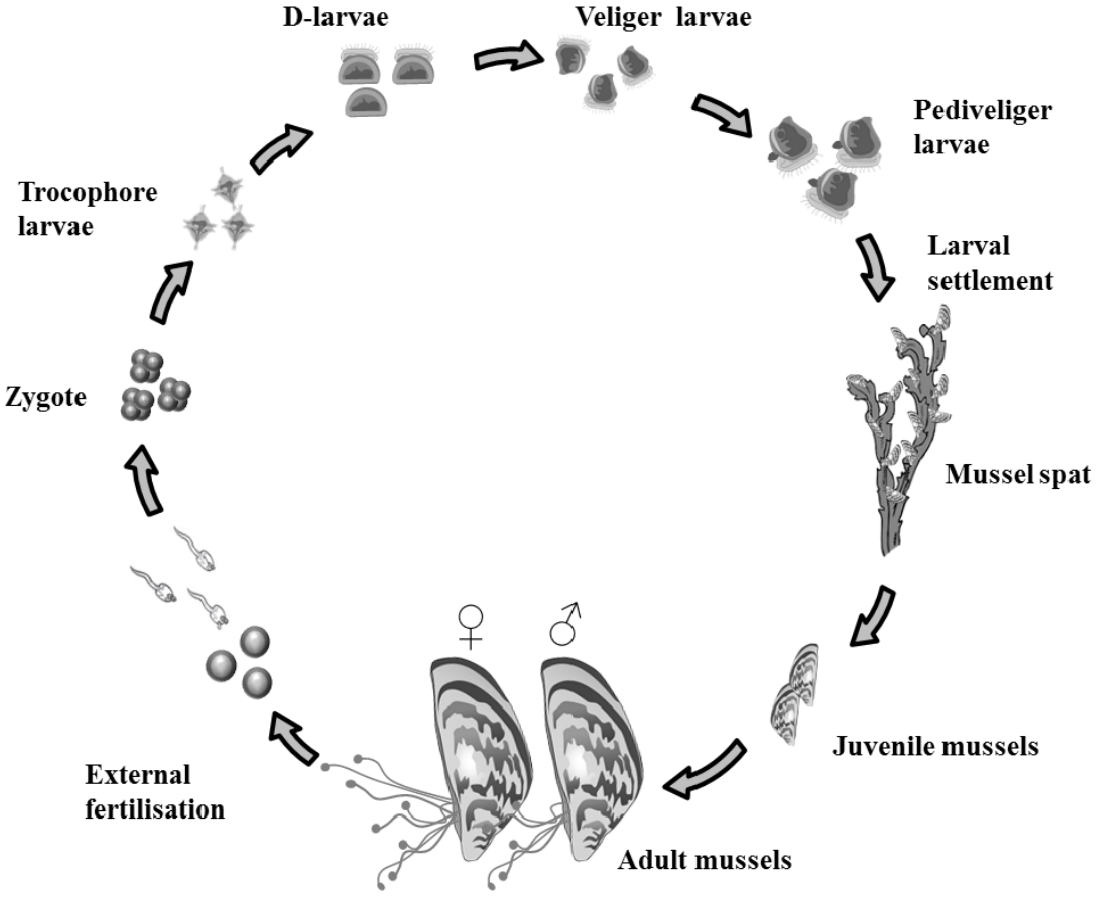

Figure 9: Life cycle of a mussel. Taken from Rusk, 2012.

REFERENCES

Abdel-Shafy, H.I., Mansour, M.S.M. 2016. A review on polycyclic aromatic hydrocarbons: Source, environmental impact, effect on human health and remediation. Egyptian Journal of Petrolium 25, 107-123.

Adeola, A. O., & Forbes, P. B. C. (2021). Influence of natural organic matter fractions on PAH sorption by stream sediments and a synthetic graphene wool adsorbent. *Environmental Technology and Innovation*, *21*, 101202.

Ahmad, S. Z. N., Wan Salleh, W. N., Ismail, A. F., Yusof, N., Mohd Yusop, M. Z., & Aziz, F. (2020). Adsorptive removal of heavy metal ions using graphene-based nanomaterials: Toxicity, roles of functional groups and mechanisms. *Chemosphere*, *248*, 126008.

Ale, A., Liberatori, G., Vannuccini, M. L., Bergami, E., Ancora, S., Mariotti, G., Bianchi, N., Galdopórpora, J. M., Desimone, M. F., Cazenave, J., & Corsi, I. (2019). Exposure to a nanosilver-enabled consumer product results in similar accumulation and toxicity of silver nanoparticles in the marine mussel Mytilus galloprovincialis. *Aquatic Toxicology*, *211*(December 2018), 46–56.

Ali, J., Li, Y., Shang, E., Wang, X., Zhao, J., Mohiuddin, M., & Xia, X. (2022). Aggregation of graphene oxide and its environmental implications in the aquatic environment. *Chinese Chemical Letters*. https://doi.org/10.1016/j.cclet.2022.03.050

Al-Sid-Cheikh M., Rowland S.J., Stevenson K., Rouleau C., Henry T.B., Thompson R.C. 2018. Uptake, whole-body distribution, and depuration of nanoplastics by Scallop Pecten maximus at environmentally realistic concentrations. Envrionmental Science & Tecnology 52, 14480-14486.

Andrady, A. L., (2011). Microplastics in the marine environment. Marine pollution bulletin, 62(8), 1596–605.

Apul, O.G., Wang, Q., Zhou, Y., Karanfil, T., 2013. Adsorption of aromatic organic contaminants by graphene nanosheets: Comparison with carbon nanotubes and activated carbon. Water Res. 47, 1648-1654.

Arnot, J. A., & Gobas, F. A. P. C. (2006). A review of bioconcentration factor (BCF) and bioaccumulation factor (BAF) assessments for organic chemicals in aquatic organisms. *Environmental Reviews*, *14*(4), 257–297.

Audira, G., Lee, J. S., Siregar, P., Malhotra, N., Rolden, M. J. M., Huang, J. C., Chen, K. H. C., Hsu, H. S., Hsu, Y., Ger, T. R., & Hsiao, C. Der. (2021). Comparison of the chronic toxicities of graphene and graphene oxide toward adult zebrafish by using biochemical and phenomic approaches. *Environmental Pollution*, *278*, 116907.

Auría-Soro, C., Nesma, T., Juanes-Velasco, P., Landeira-Viñuela, A., Fidalgo-Gomez, H., Acebes-Fernandez, V., Gongora, R., Parra, M. J. A., Manzano-Roman, R., & Fuentes, M. (2019). Interactions of nanoparticles and biosystems: Microenvironment of nanoparticles and biomolecules in nanomedicine. *Nanomaterials*, *9*(10).

Avant, B., Bouchard, D., Chang, X., Hsieh, H. S., Acrey, B., Han, Y., Spear, J., Zepp, R., & Knightes, C. D. (2019). Environmental fate of multiwalled carbon nanotubes and graphene oxide across different aquatic ecosystems. *NanoImpact*, *13*(September 2018), 1–12. https://doi.org/10.1016/j.impact.2018.11.001

Avio C.G., Gorbi S., Milan M., Benedetti M., Fattorini D., d'Errico G., Pauletto M., Bargelloni L., Regoli F., 2015. Pollutants bioavailability and toxicological risk from microplastics to marine mussels. Environmental Pollution 198, 211-222.

Baig, N., Ihsanullah, Sajid, M., & Saleh, T. A. (2019). Graphene-based adsorbents for the removal of toxic organic pollutants: A review. *Journal of Environmental Management*, *244*(October 2018), 370–382. https://doi.org/10.1016/j.jenvman.2019.05.047

Bakir, A., Rowland, S. J., & Thompson, R. C. (2014). Enhanced desorption of persistent organic pollutants from microplastics under simulated physiological conditions. Environmental Pollution, 185, 16-23.

Balbi T., Camisassi G., Montagna M., Fabbri R., Franzellitti S., Carbone C., Dawson K., Canesi L. 2017. Impact of cationic polystyrene nanoparticles (PS-NH2) on early embryo development of Mytilus galloprovincialis: Effects on shell formation. Chemosphere 186, 1-9.

Banni, M., Sforzini, S., Arlt, V.M., Barranger, A., Dallas, L.J., Oliveri, C., Aminot, Y., Pacchioni, B., Milino, C., Lanfranchi, G., Readman, J.W., Moore, M.N., Viarengo, A., Jha, A.N. 2017. Assessing the impact of benzo[a]pyrene on marine mussels: application of a novel targeted low density microarray complementing classical biomarker responses. PloS one 12, e0178460

Barranger, A., Langan, L. M., Sharma, V., Rance, G. A., Aminot, Y., Weston, N. J., Akcha, F., Moore, M. N., Arlt, V. M., Khlobystov, A. N., Readman, J. W., & Jha, A. N. (2019). Antagonistic interactions between benzo[a]pyrene and fullerene (C60) in toxicological response of marine mussels. *Nanomaterials*, *9*(7). https://doi.org/10.3390/nano9070987

Barrick, A., Manier, N., Lonchambon, P., Flahaut, E., Jrad, N., Mouneyrac, C., & Châtel, A. (2019). Investigating a transcriptomic approach on marine mussel hemocytes exposed to carbon nanofibers: An in vitro/in vivo comparison. *Aquatic Toxicology*, *207*(November 2018), 19–28. https://doi.org/10.1016/j.aquatox.2018.11.020

Batel, A., Linti, F., Scherer, M., Erdinger, L., Braunbeck, T., (2016). The transfer of benzo[a]pyrene from microplastics to Artemia nauplii and further to zebrafish via a trophic

food web experiment– CYP1A induction and visual tracking of persistent organic pollutants. Environ.Toxicol. Chem.35,:1656-66.

Begum, P., Fugetsu, B. 2013. Induction of cell death by graphene in Arabidopsis thaliana (Columbia ecotype) T87 cell suspensions. Journal of hazardous materials 260, 1032-1041.

Beiras R., Bellas J., Cachot J., Comier B., Cousin X., Engwall M., Gambardella C., Garaventa F., Keiter S., Le Bhanic F., López-Ibañez S., Piazza V., Rial D., Tato T., Vidal-Liñan L. 2018. Ingestion and contact with polyethylene microplastics does not cause acute toxicity on marine zooplankton. Journal of Hazardous Materials 360, 452-460.

Benali, I., Boutiba, Z., Merabet, A., & Chèvre, N. (2015). Integrated use of biomarkers and condition indices in mussels (Mytilus galloprovincialis) for monitoring pollution and development of biomarker index to assess the potential toxic of coastal sites. *Marine Pollution Bulletin*, *95*(1), 385–394. https://doi.org/10.1016/j.marpolbul.2015.03.041

Berry, V. (2013). Impermeability of graphene and its applications. *Carbon*, *62*, 1–10. https://doi.org/10.1016/j.carbon.2013.05.052

Bi, C., Junaid, M., Liu, Y., Guo, W., Jiang, X., Pan, B., Li, Z., & Xu, N. (2022). Graphene oxide chronic exposure enhanced perfluorooctane sulfonate mediated toxicity through oxidative stress generation in freshwater clam Corbicula fluminea. *Chemosphere*, *297*(February), 134242. https://doi.org/10.1016/j.chemosphere.2022.134242

Bi, C., Junaid, M., Liu, Y., Guo, W., Jiang, X., Pan, B., Li, Z., & Xu, N. (2022). Graphene oxide chronic exposure enhanced perfluorooctane sulfonate mediated toxicity through oxidative stress generation in freshwater clam Corbicula fluminea. Chemosphere, 297(February), 134242. https://doi.org/10.1016/j.chemosphere.2022.134242

Bianco, A., Cheng, H.-M., Enoki, T., Gogotsi, Y., Hurt, R.H., Koratkar, N., Kyotani, T., Monthioux, M., Park, C.R., Tascon, J.M.D., Zhang, J., 2013. All in the graphene family – a recommended nomenclature for two-dimensional carbon materials. Carbon 65, 1–6.

Bignell J., Cajaraville M.P., Marigómez I. 2012. Background document: histopathology of mussels (*Mytilus spp*.) for health assessment in biological effects monitoring. Integrated monitoring of chemicals and their effects. IM DAVIES, AD VETHAAK (eds.). ICES Cooperative Research Report N. 315, Copenhagen, Denmark pages, 111-120.

Binelli A., Pietrelli L., Di Vito S., Coscia L., Sighicelli M., Della Torre C., Parenti C.C., Magni S. 2020. Hazard evaluation of plastic mixtures from four Italian subalpine great laked on the basis of laboratory exposure of zebra mussels. Science of Total Environment 699, 134366.

Bitounis, D., Ali-Boucetta, H., Hong, B. H., Min, D. H., & Kostarelos, K. (2013). Prospects and challenges of graphene in biomedical applications. *Advanced Materials*, *25*(16), 2258–2268. https://doi.org/10.1002/adma.201203700

Boncel, S., Kyziol-Komosińska, J., Krzyzewska, I., & Czupiol, J. (2015). Interactions of carbon nanotubes with aqueous/aquatic media containing organic/inorganic contaminants and selected organisms of aquatic ecosystems - A review. *Chemosphere*, *136*, 211–221. https://doi.org/10.1016/j.chemosphere.2015.04.095

Bortolozzo, L. S., Côa, F., Khan, L. U., Medeiros, A. M. Z., Da Silva, G. H., Delite, F. S., Strauss, M., & Martinez, D. S. T. (2021). Mitigation of graphene oxide toxicity in C. elegans after chemical degradation with sodium hypochlorite. *Chemosphere*, *278*. https://doi.org/10.1016/j.chemosphere.2021.130421

Bråte I.L.N., Blázquez M., Brooks S.J., Thomas K.V., 2018. Weathering impacts the uptake of polyethylene microparticles from toothpaste in Mediterranean mussels (M. galloprovincialis). Science of Total Environment 626, 1310-1318.

Bringer A., Thomas H., Prunier G., Dubillot E., Bossut N., Churlaud C., Clérandeau C., Le Bihanic F-. Cachot J. 2020. High density polyethylene (HDPE) microplastics impair development and swimming activity of Pacific oyster D-larvae, Crassostrea gigas, depending on particle size. Environmental Pollution 26, 113978.

Britto, R. S., Nascimento, J. P., Serode, T., Santos, A. P., Soares, A. M. V. M., Figueira, E., Furtado, C., Lima-Ventura, J., Monserrat, J. M., & Freitas, R. (2020). The effects of co-exposure of graphene oxide and copper under different pH conditions in Manila clam Ruditapes philippinarum. *Environmental Science and Pollution Research*, *27*(25), 30945–30956. https://doi.org/10.1007/s11356-019-06643-4

Britto, R. S., Nascimento, J. P., Serodre, T., Santos, A. P., Soares, A. M. V. M., Furtado, C., Ventura-Lima, J., Monserrat, J. M., & Freitas, R. (2021). Oxidative stress in Ruditapes philippinarum after exposure to different graphene oxide concentrations in the presence and absence of sediment. *Comparative Biochemistry and Physiology Part - C: Toxicology and Pharmacology*, *240*(October 2020). https://doi.org/10.1016/j.cbpc.2020.108922

Browne M.A., Dissanayake A., Galloway T.S., Lowe D.M., Thompson R.C., 2008. Ingested microscopic plastic translocates to the circulatory system of the mussel, Mytilus edulis (L.). Envrionmental Science & Tecnology 42, 5026-5031.

Browne, M.A., Crump, P., Niven, S. J., Teuten, E., Tonkin, A., Galloway, T., & Thompson, R. (2011). Accumulation of microplastic on shorelines worldwide: sources and sinks. Environmental science technology, 45(21), 9175–9

Caballero-Guzmán A., Nowack B. 2016. A critical review of engineered nanomaterial release. Environmental Pollution 213, 502-517.

Cajaraville M.P., Bebianno M.J., Blasco J., Porte C., Sarasquete C., Viarengo A. 2000. The use of biomarkers to assess the impact of pollution in coastal environments of the Iberian Peninsula: a practical approach. The Science of the Total Environment 247: 295-311.

Cajaraville M.P., Pal S.G. 1995. Morphofunctional study of the haemocytes of the bivalve mollusc Mytilus galloprovincialis with emphasis on the endolysosomal compartment. Cell Struct Funct 20, 355-67

Cajaraville M.P., Robledo Y., Etxebarria M., Marigómez I. 1995. Cellular biomarkers as useful tools in the biological monitoring of environmental pollution: molluscan digestive lysosomes. In: Cell Biology in Environmental Toxicology. Cajaraville M.P. (Ed.), University of the Basque Country Press Service, Bilbao, pp. 29-55.

Cajaraville, M. P., Duroudier, N., & Bilbao, E. (2021). Mechanisms of toxicity of engineered nanoparticles: adverse outcome pathway for dietary silver nanoparticles in mussels. In *Health and Environmental Safety of Nanomaterials*. LTD. https://doi.org/10.1016/b978-0-12-820505-1.00002-x

Cancio I., Ibabe A., Cajaraville M.P. 1999. Seasonal variation of peroxisomal enzyme activities and peroxisomal structure in mussels Mytilus galloprovincialis and its relationship with the lipid content. Comparative Biochemistry and Physiology, Part C 123: 135-144.

Canesi L., Ciacci C., Bergami E., Monopoli M.P., Dawson K.A., Papa S., Canonico B., Corsi I. 2015. Evidence for immunomodulation and apoptotic processes induced by cationic polystyrene nanoparticles in the hemocytes of the marine bivalve Mytilus. Marine Environmental Research 111, 34-40.

Canesi L., Ciacci C., Fabbri R., Balbi T., Salis A., Damonte G., Cortese K., Caratto V., Monopoli M.P., Dawson K., Bergami E., Corsi I. 2016. Interactions of cationic polystyrene nanoparticles with marine bivalve hemocytes in a physiological environment: Role of soluble hemolymph proteins. Environmental Research 150, 73–81.

Canesi, L., & Corsi, I. (2015). Effects of nanomaterials on marine invertebrates. *Science of the Total Environment*, *565*, 933–940. https://doi.org/10.1016/j.scitotenv.2016.01.085

Canesi, L., Ciacci, C., & Balbi, T. (2015). Interactive effects of nanoparticles with other contaminants in aquatic organisms: Friend or foe? *Marine Environmental Research*, *111*, 128–134. https://doi.org/10.1016/j.marenvres.2015.03.010

Capolupo M., Franzellitti S., Valbonesi P., Lanzas C.S., Fabbri E. 2018. Uptake and transcriptional effects of polystyrene microplastics in larval stages of the Mediterranean mussel Mytilus galloprovincialis. Environmental Pollution 241, 1038-1047.

Carls, M.G., Meador, J.P. 2009. A perspective on the toxicity of petrogenic PAHs to developing fish embryos related to environmental chemistry. Human and Ecological Risk Assessment 15,1084–1098.

Carlsson, P., Crosse, J.D., Halsall, C., Evenset, A., Heimstad, E.S., HARJU M. 2016. Perfluoroalkylated substances (PFASs) and legacy persistent organic pollutants (POPs) in halibut and shrimp from coastal areas in the far north of Norway: Small survey of important dietary foodstuffs for coastal communities. Marine Pollution Bulletin 105, 81-7.

Carroccio, S. C., Scarfato, P., Bruno, E., Aprea, P., Dintcheva, N. T., & Filippone, G. (2022). Impact of nanoparticles on the environmental sustainability of polymer nanocomposites based on bioplastics or recycled plastics – A review of life-cycle assessment studies. *Journal of Cleaner Production*, *335*(April 2021), 130322. https://doi.org/10.1016/j.jclepro.2021.130322

Carusi, A., Wittwehr, C., & Whelan, M. (2022). *Addressing evidence needs in chemicals policy and regulation*. https://doi.org/10.2760/9130

CCME (Canadian Council of Ministers of the Environment). Canadian soil quality guidelines for potentially carcinogenic and other PAHs: scientific criteria document. CCME: Winnipeg: 2010.

Chan Y., An Y.J. 2020. Effect of food presence on micorplastic ingestion and egestion in Mytilus galloprovincialis. Chemosphere 240, 124855.

Chang, X.J., Bouchard, D.C., 2016. Surfactant-wrapped multiwalled carbon nanotubes in aquatic systems: surfactant displacement in the presence of humic acid. Environ. Sci. Technol. 50 (17), 9214–9222.

Chang, Y., Yang, S. T., Liu, J. H., Dong, E., Wang, Y., Cao, A., Liu, Y., Wang, H. 2011. In vitro toxicity evaluation of graphene oxide on A549 cells. Toxicology letters 200, 201-210.

Chapman, P. M. (2010). Learned discourses: Timely scientific opinions. *Integrated Environmental Assessment and Management*, *6*(2), 308–308. https://doi.org/10.1002/ieam.44

Chatterjee, N., Kim, Y., Yang, J., Roca, C. P., Joo, S. W., & Choi, J. (2017). A systems toxicology approach reveals the Wnt-MAPK crosstalk pathway mediated reproductive failure in Caenorhabditis elegans exposed to graphene oxide (GO) but not to reduced graphene oxide (rGO). In *Nanotoxicology* (Vol. 11, Issue 1). Taylor & Francis. https://doi.org/10.1080/17435390.2016.1267273

Chen, M., Yin, J., Liang, Y., Yuan, S., Wang, F., Song, M., & Wang, H. (2016). Oxidative stress and immunotoxicity induced by graphene oxide in zebrafish. *Aquatic Toxicology*, *174*, 54–60. https://doi.org/10.1016/j.aquatox.2016.02.015

Chen, Y., Li, J., Zhou, Q., Liu, Z., & Li, Q. (2021). Hexavalent chromium amplifies the developmental toxicity of graphene oxide during zebrafish embryogenesis. *Ecotoxicology and Environmental Safety*, *208*, 111487. https://doi.org/10.1016/j.ecoenv.2020.111487

Chen, Z., Yu, C., Khan, I. A., Tang, Y., Liu, S., & Yang, M. (2020). Toxic effects of different-sized graphene oxide particles on zebrafish embryonic development. *Ecotoxicology and Environmental Safety*, *197*(February). https://doi.org/10.1016/j.ecoenv.2020.110608

Ciriminna, R., Zhang, N., Yang, M., Meneguzzo, F., Xu, Y., Pagliaro, M., 2016. Commercialization of graphene-based technologies: a critical insight. Chem. Comm. 51, 7090-7095

Clemente, Z., Castro, V. L. S. S., Franqui, L. S., Silva, C. A., & Martinez, D. S. T. (2017). Nanotoxicity of graphene oxide: Assessing the influence of oxidation debris in the presence of humic acid. *Environmental Pollution*, *225*, 118–128. https://doi.org/10.1016/j.envpol.2017.03.033

Cole, M., Lindeque, P., Halsband, C., & Galloway, T. S. (2011). Microplastics as contaminants in the marine environment: a review. Marine Pollution Bulletin, 62(12), 2588–97.

Commission Recommendation of 18 October 2011 on the definition of nanomaterial Text with EEA relevance 20.10.2011, p. 38–40; http://data.europa.eu/eli/reco/2011/696/oj

Coppola, F., Bessa, A., Henriques, B., Russo, T., Soares, A. M. V. M., Figueira, E., Marques, P. A. A. P., Polese, G., Di Cosmo, A., Pereira, E., & Freitas, R. (2020). Oxidative stress, metabolic and histopathological alterations in mussels exposed to remediated seawater by GO-PEI after contamination with mercury. *Comparative Biochemistry and Physiology -Part A : Molecular and Integrative Physiology*, *243*(February), 110674. https://doi.org/10.1016/j.cbpa.2020.110674

Coppola, F., Jiang, W., Soares, A. M. V. M., Marques, P. A. A. P., Polese, G., Pereira, M. E., Jiang, Z., & Freitas, R. (2021). How efficient is graphene-based nanocomposite to adsorb Hg from seawater. A laboratory assay to assess the toxicological impacts induced by remediated water towards marine bivalves. *Chemosphere*, *277*, 130160. https://doi.org/10.1016/j.chemosphere.2021.130160

Corso, B., Magistrale, L., Marina, B., Correlatore, B., & Upv, B. C. (2017). *In vitro toxicity profiling of the effects of oil and of oil remediation strategies on mussel Mytilus galloprovincialis hemocytes*.

Cossutta, M., Vretenar, V., Centeno, T. A., Kotrusz, P., McKechnie, J., & Pickering, S. J. (2020). A comparative life cycle assessment of graphene and activated carbon in a supercapacitor application. *Journal of Cleaner Production*, *242*, 118468. https://doi.org/10.1016/j.jclepro.2019.118468

Cruces, E., Barrios, A. C., Cahue, Y. P., Januszewski, B., Gilbertson, L. M., & Perreault, F. (2021). Similar toxicity mechanisms between graphene oxide and oxidized multi-walled carbon nanotubes in Microcystis aeruginosa. *Chemosphere*, *265*, 129137. https://doi.org/10.1016/j.chemosphere.2020.129137

De los Ríos A., Perez L., Ortiz-Zarragoitia M., Serrano T., Barbero M.C., Echavarri-Erasun B., Juanes J.A., Orbea A., Cajaraville M.P. 2013. Assessing the effects of treated and untreated urban discharges to estuarine and coastal waters applying selected biomarkers on caged mussels. Marine Pollution Bulletin 77, 251-265.

De Marchi, L., Coppola, F., Soares, A. M. V. M., Pretti, C., Monserrat, J. M., Torre, C. della, & Freitas, R. (2019). Engineered nanomaterials: From their properties and applications, to their toxicity towards marine bivalves in a changing environment. *Environmental Research*, *178*(July), 108683. https://doi.org/10.1016/j.envres.2019.108683

De Marchi, L., Neto, V., Pretti, C., Figueira, E., Brambilla, L., Rodriguez-Douton, M. J., Rossella, F., Tommasini, M., Furtado, C., Soares, A. M. V. M., & Freitas, R. (2017). Physiological and biochemical impacts of graphene oxide in polychaetes: The case of Diopatra neapolitana. *Comparative Biochemistry and Physiology Part - C: Toxicology and Pharmacology*, *193*(January), 50–60. https://doi.org/10.1016/j.cbpc.2017.01.005

De Marchi, L., Pretti, C., Chiellini, F., Morelli, A., Neto, V., Soares, A. M. V. M., Figueira, E., & Freitas, R. (2019). The influence of simulated global ocean acidification on the toxic effects of carbon nanoparticles on polychaetes. *Science of the Total Environment*, *666*, 1178–1187. https://doi.org/10.1016/j.scitotenv.2019.02.109

De Marchi, L., Pretti, C., Gabriel, B., Marques, P. A. A. P., Freitas, R., & Neto, V. (2018). An overview of graphene materials: Properties, applications and toxicity on aquatic environments. *Science of the Total Environment*, *631–632*, 1440–1456. https://doi.org/10.1016/j.scitotenv.2018.03.132

de Medeiros, A. M. Z., Khan, L. U., da Silva, G. H., Ospina, C. A., Alves, O. L., de Castro, V. L., & Martinez, D. S. T. (2021). Graphene oxide-silver nanoparticle hybrid material: an integrated nanosafety study in zebrafish embryos. Ecotoxicology and Environmental Safety, 209. https://doi.org/10.1016/j.ecoenv.2020.111776

Deng, R., Lin, D., Zhu, L., Majumdar, S., White, J. C., Gardea-Torresdey, J. L., & Xing, B. (2017). Nanoparticle interactions with co-existing contaminants: joint toxicity, bioaccumulation and risk. *Nanotoxicology*, *11*(5), 591–612. https://doi.org/10.1080/17435390.2017.1343404

Détrée C., Gallardo-Escárate C. 2017. Polyethylene microbeads induce transcriptional responses with tissue-dependent patterns in the mussel Mytilus galloprovincialis. Journal of Molluscan Studies 83, 220-225.

Di, Y., Aminot, Y., Schroeder, D.C., Readman, J.W., Jha, A.N. 2017 Integrated biological responses and tissue-specific expression of p53 and ras genes in marine mussels following exposure to benzo(α)pyrene and C60 fullerenes, either alone or in combination. Mutagenesis 32, 77-90.

Dinadayalane, T.C., Leszczynski, J. 2010. Remarkable diversity of carbon-carbon bonds: structures and properties of fullerenes, carbon nanotubes, and graphene. Structural Chemistry 21, 1155–1169.

Ding, G., Zhang, N., Wang, C., Li, X., Zhang, J., Li, W., Li, R., & Yang, Z. (2018). Effect of the size on the aggregation and sedimentation of graphene oxide in seawaters with different salinities. *Journal of Nanoparticle Research*, *20*(11), 1–10. https://doi.org/10.1007/s11051-018-4421-1

Ding, X., Pu, Y., Tang, M., & Zhang, T. (2022). Environmental and health effects of graphene-family nanomaterials: Potential release pathways, transformation, environmental fate and health risks. *Nano Today*, *42*, 101379. https://doi.org/10.1016/j.nantod.2022.101379

Dong, S., Xia, T., Yang, Y., Lin, S., & Mao, L. (2018). Bioaccumulation of 14C-Labeled Graphene in an Aquatic Food Chain through Direct Uptake or Trophic Transfer. *Environmental Science and Technology*, *52*(2), 541–549. https://doi.org/10.1021/acs.est.7b04339

Dowling, A., Clift, R., Grobert, N., Hutton, D., Oliver, R., O'neill, O., Pethica J., Pidgeon, N., Porritt, J., Ryan, J. 2004. Nanoscience and nanotechnologies: opportunities and uncertainties. London The Royal Society of Royal Academy of Engineering 46, 6-18.

Du, S., Zhang, P., Zhang, R., Lu, Q., Liu, L., Bao, X., & Liu, H. (2016). Reduced graphene oxide induces cytotoxicity and inhibits photosynthetic performance of the green alga Scenedesmus obliquus. *Chemosphere*, *164*, 499–507. https://doi.org/10.1016/j.chemosphere.2016.08.138

Dziewięcka, M., Karpeta-Kaczmarek, J., Augustyniak, M., & Rost-Roszkowska, M. (2017). Short-term in vivo exposure to graphene oxide can cause damage to the gut and testis. *Journal of Hazardous Materials*, *328*, 80–89. https://doi.org/10.1016/j.jhazmat.2017.01.012

Dziewięcka, M., Witas, P., Karpeta-Kaczmarek, J., Kwaśniewska, J., Flasz, B., Balin, K., & Augustyniak, M. (2018). Reduced fecundity and cellular changes in Acheta domesticus after multigenerational exposure to graphene oxide nanoparticles in food. *Science of the Total Environment*, *635*, 947–955. https://doi.org/10.1016/j.scitotenv.2018.04.207

El-Kady M.E., Shao Y., KAner R.B. 2016. Graphene for batteries, supercapacitors and beyond. Nature Review Material 1, 16033.

Ema, M., Gamo, M., & Honda, K. (2017). A review of toxicity studies on graphene-based nanomaterials in laboratory animals. *Regulatory Toxicology and Pharmacology*, *85*, 7–24. https://doi.org/10.1016/j.yrtph.2017.01.011

Ersan, G., Apul, O. G., Perreault, F., & Karanfil, T. (2017). Adsorption of organic contaminants by graphene nanosheets: A review. *Water Research*, *126*, 385–398. https://doi.org/10.1016/j.watres.2017.08.010

Ervidsson, R., Molander, S., Sandén, B. A. 2013. Review of potential environmental and health risks of the nanomaterial graphene. Human and Ecological Risk Assessment: An International Journal 19, 873-887.

EUON/ECHA, 2022: https://euon.echa.europa.eu/eu-research-projects)

Evariste, L., Mottier, A., Lagier, L., Cadarsi, S., Barret, M., Sarrieu, C., Soula, B., Mouchet, F., Flahaut, E., Pinelli, E., & Gauthier, L. (2020). Assessment of graphene oxide ecotoxicity at several trophic levels using aquatic microcosms. *Carbon*, *156*, 261–271. https://doi.org/10.1016/j.carbon.2019.09.051

Facure, M. H. M., Schneider, R., Mercante, L. A., & Correa, D. S. (2020). A review on graphene quantum dots and their nanocomposites: From laboratory synthesis towards agricultural and environmental applications. *Environmental Science: Nano*, *7*(12), 3710–3734. https://doi.org/10.1039/d0en00787k

Fadeel, B., & Garcia-Bennett, A. E. (2010). Better safe than sorry: Understanding the toxicological properties of inorganic nanoparticles manufactured for biomedical applications. *Advanced Drug Delivery Reviews*, *62*(3), 362–374. https://doi.org/10.1016/j.addr.2009.11.008

Farrell, P., Nelson, K., 2013. Trophic level transfer of microplastic: Mytilus edulis (L.) to Carcinus maenas (L.). Environ. Pollut. 177, 1–3.

Fernádez B., Albentosa M. 2019. Insights into the uptake, elimination and accumulation of microplastics in mussel. Environmental Pollution 249, 321-329.

Fernandes, A. L., Josende, M. E., Nascimento, J. P., Santos, A. P., Sahoo, S. K., Da Silva, F. M. R., Romano, L. A., Furtado, C. A., Wasielesky, W., Monserrat, J. M., & Ventura-Lima, J. (2017). Exposure to few-layer graphene through diet induces oxidative stress and histological changes in the marine shrimp: Litopenaeus vannamei. *Toxicology Research*, *6*(2), 205–214. https://doi.org/10.1039/c6tx00380j

Fernandes, A. L., Nascimento, J. P., Santos, A. P., Furtado, C. A., Romano, L. A., Eduardo da Rosa, C., Monserrat, J. M., & Ventura-Lima, J. (2018). Assessment of the effects of graphene exposure in Danio rerio: A molecular, biochemical and histological approach to investigating

mechanisms of toxicity. *Chemosphere*, *210*, 458–466. https://doi.org/10.1016/j.chemosphere.2018.06.183

Flasz, B., Dziewięcka, M., Kędziorski, A., Tarnawska, M., & Augustyniak, M. (2020). Vitellogenin expression, DNA damage, health status of cells and catalase activity in Acheta domesticus selected according to their longevity after graphene oxide treatment. *Science of the Total Environment*, *737*. https://doi.org/10.1016/j.scitotenv.2020.140274

Freixa, A., Acuña, V., Sanchís, J., Farré, M., Barceló, D., & Sabater, S. (2018). Ecotoxicological effects of carbon based nanomaterials in aquatic organisms. *Science of the Total Environment*, *619–620*, 328–337. https://doi.org/10.1016/j.scitotenv.2017.11.095

Gandara e Silva P.P., Nobre C.R., Resaffe P., Pereira C.D.S., Gusmão F., 2016. Leachate from microplastics impairs larval development in brown mussels. Water Research 106, 364-370.

Gao, Y., Zeng, X., Zhang, W., Zhou, L., Xue, W., Tang, M., & Sun, S. (2022). The aggregation behaviour and mechanism of commercial graphene oxide in surface aquatic environments. *Science of the Total Environment*, *806*, 150942. https://doi.org/10.1016/j.scitotenv.2021.150942

Gaspar T.M., Chi R.J., Parrow M.W., Ringwood. 2018. Cellular Bioreactivity of Micro- and Nano-Plastic Particles in Oysters. Frontiers in Marine Science 5:345.

Gigault, J., Grassl, B., Lespes, G., 2012. Size characterization of the associations between carbon nanotubes and humic acids in aqueous media by asymmetrical flow field-flow fractionation combined with multi-angle light scattering. Chemosphere 86 (2), 177–182.

Glanzel W et al. Nanotechnology. Analysis of an emerging domain of scientific and technological endeavour. Steunpunt O&O Statistieken, Leuven; 2003.

Gonçalves C., Martins M., Sobral P., Costa P.M:, Costa M.H. 2019. An assessment of the ability to ingest an excrete microplastics by filter feeders: A case study with the Mediterranean mussel. Environmental Pollution 245, 600-606.

Goodwin, D. G., Adeleye, A. S., Sung, L., Ho, K. T., Burgess, R. M., & Petersen, E. J. (2018). Detection and Quantification of Graphene-Family Nanomaterials in the Environment. *Environmental Science and Technology*, *52*(8), 4491–4513. https://doi.org/10.1021/acs.est.7b04938

Gottschalk, F., & Nowack, B. (2011). The release of engineered nanomaterials to the environment. *Journal of Environmental Monitoring*, *13*(5), 1145–1155. https://doi.org/10.1039/c0em00547a

Gottschalk, F., Nowack, B. 2011. The release of engineered nanomaterials to the environment. Journal of Environmental Monitoring 13, 1145-1155.

Gottschalk, F., Ort, C., Scholz, R.W., Nowack, B., 2011. Engineered nanomaterials in rivers - exposure scenarios for Switzerland at high spatial and temporal resolution. Environ. Pollut. 159 (12), 3439–3445.

Gottschalk, F., Sun, T.Y., Nowack, B., 2013. Environmental concentrations of engineered nanomaterials: review of modeling and analytical studies. Environ. Pollut. 181, 287–300.

Graham P., Palazzo L., Andrea de Lucia G., Telfer T.C. Baroli M., Carboni S. 2019. Microplastics uptake and egestion dynamic in Pacific oyter Magallana gigas (Thunberg, 1793), under controlled conditions. Environmental Pollution 252, 742-748.

Graham P., Palazzo L., Andrea de Lucia G., Telfer T.C. Baroli M., Carboni S. 2019. Microplastics uptake and egestion dynamic in Pacific oyter Magallana gigas (Thunberg, 1793), under controlled conditions. Environmental Pollution 252, 742-748.

Graham, E. R., & Thompson, J. T. (2009). Deposit- and suspension-feeding sea cucumbers (Echinodermata) ingest plastic fragments. Journal of Experimental Marine Biology and Ecology, 368(1), 22–29.

Green D.S., Boots B., O'Connor N.E., Thompson R. 2017. Microplastics affect the ecological functioning of an important biogenic habitat. Environment Science & Tecnology 51, 68-77.

Green D.S., Colgan T.J., Thompson R.C., Carolan J.C. 2019. Exposure to microplastics reduces attachment stregth and alters the haemolumph proteome of blu mussels (Mytilus edulis). Environmental Pollution 246, 423-434.

Guilhermino L., Vieira L.R., Ribeiro D., Tavares A.S., Cardoso V., Alves A., Almeida J.M. 2018. Uptake and effects of the antimicrobial florfenicol, microplastics and their mixtures on freshwater exotic invasive bivalve Corbicula fluminea. Science of the Total Environment 622–623, 1131–1142.

Guo, X., & Mei, N. (2014). Assessment of the toxic potential of graphene family nanomaterials. *Journal of Food and Drug Analysis*, *22*(1), 105–115. https://doi.org/10.1016/j.jfda.2014.01.009

Guo, X., Dong, S., Petersen, E. J., Gao, S., Huang, Q., & Mao, L. (2013). Biological uptake and depuration of radio-labeled graphene by Daphnia magna. *Environmental Science and Technology*, *47*(21), 12524–12531. https://doi.org/10.1021/es403230u

Gurunathan, S., Han, J. W., Dayem, A. A., Eppakayala, V., Kim, J. H. 2012. Oxidative stress-mediated antibacterial activity of graphene oxide and reduced graphene oxide in Pseudomonas aeruginosa. International Journal of Nanomedicine 7, 5901−5914.

Hall, N. M., Berry, K. L. E., Rintoul, L., & Hoogenboom, M. O. (2015). Microplastic ingestion by scleractinian corals. Marine Biology, 162(3), 725-732.

Han, Y., Knightes, C. D., Bouchard, D., Zepp, R., Avant, B., Hsieh, H. S., Chang, X., Acrey, B.,

Henderson, W. M., Spear, J. 2019. Simulating graphene oxide nanomaterial phototransformation and transport in surface water. Environmental Science: Nano 6, 180-194.

Hannah, W., & Thompson, P. B. (2008). Nanotechnology, risk and the environment: A review. *Journal of Environmental Monitoring*, *10*(3), 291–300. https://doi.org/10.1039/b718127m

Hartmann, N. B., Hüffer, T., Thompson, R. C., Hassellöv, M., Verschoor, A., Daugaard, A. E., Rist, S., Karlsson, T., Brennholt, N., Cole, M., Herrling, M. P., Hess, M. C., Ivleva, N. P., Lusher, A. L., & Wagner, M. (2019). Are We Speaking the Same Language? Recommendations for a Definition and Categorization Framework for Plastic Debris. *Environmental Science and Technology*, *53*(3), 1039–1047. https://doi.org/10.1021/acs.est.8b05297

Hartmann, N. B., Hüffer, T., Thompson, R. C., Hassellöv, M., Verschoor, A., Daugaard, A. E., Rist, S., Karlsson, T., Brennholt, N., Cole, M., Herrling, M. P., Hess, M. C., Ivleva, N. P., Lusher, A. L., & Wagner, M. (2019). Are We Speaking the Same Language? Recommendations for a Definition and Categorization Framework for Plastic Debris. Environmental Science and Technology, 53(3), 1039–1047. https://doi.org/10.1021/acs.est.8b05297

Havan, O., Ghaderi, E. 2010. Toxicity of graphene and graphene oxide nanowalls against bacteria. ACS Nano 4, 5731−5736.

He, K., Chen, G., Zeng, G., Peng, M., Huang, Z., Shi, J., Huang, T. 2017. Stability, transport and ecosystem effects of graphene in water and soil environments. Nanoscale 9, 5370-5388.

He, Y., Liu, Y., Wu, T., Ma, J., Wang, X., Gong, Q., Kong., W., Xing, F., Liu, Y., Gao, J. 2013. An environmentally friendly method for the fabrication of reduced graphene oxide foam with a super oil absorption capacity. Journal of hazardous materials 260, 796-805.

Heinz, H., Pramanik C., Heinz O., Ding Y., Mishra R.K., Marchon D., Flatt, R.J., Lopis, I.E., Llop, J., Moya, S., Ziolo, R.F. 2017. Nanoparticle decoration with surfactants: molecular interactions, assembly, and applications. Surface Science Reports 72, 1–58.

Herrera, G., Peña-Bahamonde, J., Paudel, S., & Rodrigues, D. F. (2021). The role of nanomaterials and antibiotics in microbial resistance and environmental impact: an overview. *Current Opinion in Chemical Engineering*, *33*. https://doi.org/10.1016/j.coche.2021.100707

Hoss D.E., Settle L.R. (1990) Ingestion of plastics by teleost fishes. In: Shomura RS, Godfrey ML (eds) Proceedings of the second international conference on marine debris. US Department of Commerce, NOAA Technical Memo, Honolulu, HI, p 693–709.

Hsu, H., Kuo, C., Jehng, J., Wei, C., Wen, C., Chen, J., & Chen, L. (2019). Application of Graphene Oxide Aerogel to the Adsorption of Polycyclic Aromatic Hydrocarbons Emitted from the

Diesel Vehicular Exhaust. *Journal of Environmental Chemical Engineering*, *7*(6), 103414. https://doi.org/10.1016/j.jece.2019.103414

Hu, X., Wei, Z., & Mu, L. (2017). Graphene oxide nanosheets at trace concentrations elicit neurotoxicity in the offspring of zebrafish. *Carbon*, *117*, 182–191. https://doi.org/10.1016/j.carbon.2017.02.092

Huang, D., Xu, B., Wu, J., Brookes, P. C., & Xu, J. (2019). Adsorption and desorption of phenanthrene by magnetic graphene nanomaterials from water: Roles of pH, heavy metal ions and natural organic matter. *Chemical Engineering Journal*, *368*(January), 390–399. https://doi.org/10.1016/j.cej.2019.02.152

Hussain, I., Hussain, A., Ahmad, A., Rahman, H., Alajmi, M. F., Ahmed, F., & Amir, S. (2019). New generation graphene oxide for removal of polycyclic aromatic hydrocarbons. In *Graphene-Based Nanotechnologies for Energy and Environment*. Elsevier Inc. https://doi.org/10.1016/b978-0-12-815811-1.00014-4

Inshakova, E., & Inshakov, O. (2017). World market for nanomaterials: Structure and trends. *MATEC Web of Conferences*, *129*(2017), 1–5. https://doi.org/10.1051/matecconf/201712902013

Janik, P., Zawisza, B., Talik, E., Sitko, R. 2018. Selective adsorption and determination of hexavalent chromium ions using graphene oxide modified with amino silanes. Microchimica Acta 185, 117.

Jastrzębska, A.M., Olszyna, A.R., 2015. The ecotoxicity of graphene family materials: current status, knowledge gaps and future needs. J. Nanopart. Res. 17 (1), 40.

Jiang, Y., Raliya, R., Liao, P., Biswas, P., Fortner, J. D. 2017. Graphene oxides in water: assessing stability as a function of material and natural organic matter properties. Environmental Science: Nano 4, 1484-1493.

Josende, M. E., Nunes, S. M., de Oliveira Lobato, R., González-Durruthy, M., Kist, L. W., Bogo, M. R., Wasielesky, W., Sahoo, S., Nascimento, J. P., Furtado, C. A., Fattorini, D., Regoli, F., Machado, K., Werhli, A. V., Monserrat, J. M., & Ventura-Lima, J. (2020). Graphene oxide and GST-omega enzyme: An interaction that affects arsenic metabolism in the shrimp Litopenaeus vannamei. *Science of the Total Environment*, *716*(January), 136893. https://doi.org/10.1016/j.scitotenv.2020.136893

Jumars, P.A. (1993). Gourmands of mud: Diet selection in marine deposit feeders. pp. 124-156 in R.N. Hughes, Ed. Mechanisms of Diet Choice, Blackwell Scientific Publishers, Oxford.

Kalman, J., Merino, C., Fernández-Cruz, M. L., & Navas, J. M. (2019). Usefulness of fish cell lines for the initial characterization of toxicity and cellular fate of graphene-related materials

(carbon nanofibers and graphene oxide). *Chemosphere*, *218*, 347–358. https://doi.org/10.1016/j.chemosphere.2018.11.130

Katsumiti, A., Cajaraville, M. P. 2019. In Vitro Testing: In Vitro Toxicity Testing with Bivalve Mollusc and Fish Cells for the Risk Assessment of Nanoparticles in the Aquatic Environment. In Ecotoxicology of Nanoparticles in Aquatic Systems (pp. 62-98). CRC Press.

Katsumiti, A., Tomovska, R., & Cajaraville, M. P. (2017). Intracellular localization and toxicity of graphene oxide and reduced graphene oxide nanoplatelets to mussel hemocytes in vitro. *Aquatic Toxicology*, *188*(April), 138–147. https://doi.org/10.1016/j.aquatox.2017.04.016

Katsumiti, A., Tomovska, R., Cajaraville, M. 2017. Intracellular localization and toxicity of Graphene oxide and reduced Graphene oxide nanoplatelets to mussel hemocytes in vitro. Aquatic Toxicology 188, 138-147.

Khan M.B. Prezant R.S. 2018. Microplastic abundances in a mussel bed and ingestion by the ribbed marsh mussel *Geukensia demissa*. Marine Pollution Bulletin 130, 67-75.

Khan, B., Adeleye, A. S., Burgess, R. M., Russo, S. M., & Ho, K. T. (2019). Effects of graphene oxide nanomaterial exposures on the marine bivalve, Crassostrea virginica. *Aquatic Toxicology*, *216*(April), 105297. https://doi.org/10.1016/j.aquatox.2019.105297

Khan, B., Adeleye, A. S., Burgess, R. M., Smolowitz, R., Russo, S. M., & Ho, K. T. (2019). A 72-h exposure study with eastern oysters (Crassostrea virginica) and the nanomaterial graphene oxide. *Environmental Toxicology and Chemistry*, *38*(4), 820–830. https://doi.org/10.1002/etc.4367

Khosravi-Katuli, K., Prato, E., Lofrano, G., Guida, M., Vale, G., Libralato, G. 2017. Effects of nanoparticles in species of aquaculture interest. Environmental Science and Pollution Research 24, 17326-17346.

Kim Y., Ashton-Alcox A., Powell E.N. 2006. Histological techniques for marine bivalve molluscs: update NOAA technical memorandum NOS NCCOS 27, 76 pp.

Kinjo A., Mizukawa K., Takada H., Inoue K. 2019. Size-dependent elimination of ingested microplastics in the mediterranean mussel Mytilus galloprovincialis. Marine Pollution Bulletin 149, 110512.

Koelmans AA. 2015. Modeling the role of microplastics in bioaccumulation of organic chemicals to marine aquatic organisms. A critical review. See Bergmann et al. 2015, pp. 309–24.

Kolandhasamy P., Su L:, Li J., Qu X., Jabeen K., Shi H. 2018. Adherence of microplastics to soft tissue of mussels: A novel way yo uptake microplastics beyond ingestion. Science of Total Environment 610-611, 635-640.

Krishnaraj, C., Kaliannagounder, V. K., Rajan, R., Ramesh, T., Kim, C. S., Park, C. H., Liu, B., & Yun, S. Il. (2022). Silver nanoparticles decorated reduced graphene oxide: Eco-friendly synthesis, characterization, biological activities and embryo toxicity studies. Environmental Research, 210(January), 112864. https://doi.org/10.1016/j.envres.2022.112864

Kühn, S., Rebolledo, E. L. B., & van Franeker, J. A. (2015). Deleterious effects of litter on marine Life. In Marine anthropogenic litter (pp. 75-116). Springer International Publishing.

Lalwani, G., D'Agati, M., Khan, A. M., & Sitharaman, B. (2016). Toxicology of graphene-based nanomaterials. *Advanced Drug Delivery Reviews*, *105*, 109–144. https://doi.org/10.1016/j.addr.2016.04.028

Lammel, T., Boisseaux, P., Fernández-Cruz, M. L., Navas, J. M. 2013. Internalization and cytotoxicity of graphene oxide and carboxyl graphene nanoplatelets in the human hepatocellular carcinoma cell line Hep G2. Particle and fibre toxicology 10, 27.

Lapresta-Fernández, A., Fernández, A., & Blasco, J. (2012). Nanoecotoxicity effects of engineered silver and gold nanoparticles in aquatic organisms. *TrAC - Trends in Analytical Chemistry*, *32*(797), 40–59. https://doi.org/10.1016/j.trac.2011.09.007

Lattin, G. L., Moore, C. J., Zellers, a F., Moore, S. L., & Weisberg, S. B. (2004). A comparison of neustonic plastic and zooplankton at different depths near the southern California shore. Marine pollution bulletin, 49(4), 291–4.

Le, V. T., Almomani, F., Vasseghian, Y., Vilas–Boas, J. A., & Dragoi, E. N. (2021). Graphene-based nanomaterial for desalination of water: A systematic review and meta-analysis. *Food and Chemical Toxicology*, *148*(December 2020), 1–8. https://doi.org/10.1016/j.fct.2020.111964

Li Q., Sun C., Wang Y., Cai H., Li L., Li J., Shi H. 2019. Fuxion of microplastics into the mussels byssus. Environmental Pollution 252, 420-426.

Li Z., Feng C., Wu Y., Guo X. 2020. Impacts of nanoplastics on bivalve: fluorescence tracing of organ accumulation, oxidative stress and damage. Journal of Hazardous Materials 3922, 122418.

Li, F., Chen, J., Hu, X., He, F., Bean, E., Tsang, D.C.W., Ok, Y.S., Gao, B., 2020b. Applications of carbonaceous adsorbents in the remediation of polycyclic aromatic hydrocarbon-contaminated sediments: A review. J. Clean. Prod. 255, 120263.

Limbach, L. K., Wick, P., Manser, P., Grass, R. N., Bruinink, A., & Stark, W. J. (2007). Exposure of engineered nanoparticles to human lung epithelial cells: Influence of chemical composition and catalytic activity on oxidative stress. *Environmental Science and Technology*, *41*(11), 4158–4163. https://doi.org/10.1021/es062629t

Lin, L., Peng, H., & Liu, Z. (2019). Synthesis challenges for graphene industry. *Nature Materials*, *18*(6), 520–524. https://doi.org/10.1038/s41563-019-0341-4

Lin, Y. F., Hsieh, C. Te, & Wai, R. J. (2015). Facile synthesis of graphene sheets for heat sink application. *Solid State Sciences*, *43*, 22–27. https://doi.org/10.1016/j.solidstatesciences.2015.03.010

Liu, F., Chung, S., Oh, G., Seo, T.S. 2012. Three-dimensional graphene oxide nanostructure for fast and efficient water-soluble dye removal. ACS Applied Materials & Interfaces 4, 922–927.

Liu, J.F., Legros, S., Ma, G.B., Veinot, J.G.C., von der Kammer, F., Hofmann, T., 2012. Influence of surface functionalization and particle size on the aggregation kinetics of engineered nanoparticles. Chemosphere 87 (8), 918–924.

Liu, S., Ge, H., Wang, C., Zou, Y., & Liu, J. (2018). Agricultural waste/graphene oxide 3D bio-adsorbent for highly efficient removal of methylene blue from water pollution. *Science of the Total Environment*, *628–629*, 959–968. https://doi.org/10.1016/j.scitotenv.2018.02.134

Liu, X.T., Mu, X.Y., Wu, X.L., Meng, L.X., Guan, W.B., Ma, Y.Q., Sun, H., Wang, C.J., Li, X.F., 2014. Toxicity of multi-walled carbon nanotubes, graphene oxide, and reduced graphene oxide to zebrafish embryos. Biomed. Environ. Sci. 27, 676-683.

Liu, Y., Fan, W., Xu, Z., Peng, W., & Luo, S. (2018). Comparative effects of graphene and graphene oxide on copper toxicity to Daphnia magna: Role of surface oxygenic functional groups. *Environmental Pollution*, *236*(2017), 962–970. https://doi.org/10.1016/j.envpol.2017.10.082

Liu, Y., Zhu, S., Gu, Z., Chen, C., & Zhao, Y. (2022). Toxicity of manufactured nanomaterials. *Particuology*, *69*, 31–48. https://doi.org/10.1016/j.partic.2021.11.007

Lu, J., Zhu, X., Tian, S., Lv, X., Chen, Z., Jiang, Y., Liao, X., Cai, Z., & Chen, B. (2018). Graphene oxide in the marine environment: Toxicity to Artemia salina with and without the presence of Phe and Cd2+. *Chemosphere*, *211*, 390–396. https://doi.org/10.1016/j.chemosphere.2018.07.140

Lusher, A. (2015). Microplastics in the marine environment: Distribution, interactions and effects. In M. Bergmann, L. Gutow & M. Klages (Eds.), Marine anthropogenic litter (pp. 245–308). Berlin: Springer.

Lusher, A. L., Welden, N. A., Sobral, P., & Cole, M. (2017). Sampling, isolating and identifying microplastics ingested by fish and invertebrates. Analytical Methods, 9(9), 1346-1360.

Lv, X., Yang, Y., Tao, Y., Jiang, Y., Chen, B., Zhu, X., Cai, Z., & Li, B. (2018). A mechanism study on toxicity of graphene oxide to Daphnia magna: Direct link between bioaccumulation and oxidative stress. *Environmental Pollution*, *234*, 953–959. https://doi.org/10.1016/j.envpol.2017.12.034

Ma, S., Si, Y., Wang, F., Su, L., Xia, C. C., Yao, J., Chen, H., & Liu, X. (2017). Interaction processes of ciprofloxacin with graphene oxide and reduced graphene oxide in the presence of montmorillonite in simulated gastrointestinal fluids. *Scientific Reports*, *7*(1), 1–11. https://doi.org/10.1038/s41598-017-02620-4

Magni S., Gagné F., André C., Della Torre C., Auclair J., Hanana H., Parenti C.C., Bonasoro F., Binelli A. 2018. Evaluation of uptake and chronic toxicity of virgin polystyrene microbeads in freshwater zebra mussel Dreissena polymorpha (Mollusca: Bivalvia). Science of Total Environment 631, 778-788.

Malakar, A., Kanel, S. R., Ray, C., Snow, D. D., & Nadagouda, M. N. (2021). Nanomaterials in the environment, human exposure pathway, and health effects: A review. *Science of the Total Environment*, *759*, 143470. https://doi.org/10.1016/j.scitotenv.2020.143470

Malina, T., Maršálková, E., Holá, K., Tuček, J., Scheibe, M., Zbořil, R., & Maršálek, B. (2019). Toxicity of graphene oxide against algae and cyanobacteria: Nanoblade-morphology-induced mechanical injury and self-protection mechanism. *Carbon*, *155*, 386–396. https://doi.org/10.1016/j.carbon.2019.08.086

Malina, T., Maršálková, E., Holá, K., Zbořil, R., & Maršálek, B. (2020). The environmental fate of graphene oxide in aquatic environment—Complete mitigation of its acute toxicity to planktonic and benthic crustaceans by algae. *Journal of Hazardous Materials*, *399*(January), 123027. https://doi.org/10.1016/j.jhazmat.2020.123027

Manjunatha, B., Park, S. H., Kim, K., Kundapur, R. R., & Lee, S. J. (2018). Pristine graphene induces cardiovascular defects in zebrafish (Danio rerio) embryogenesis. *Environmental Pollution*, *243*, 246–254. https://doi.org/10.1016/j.envpol.2018.08.058

Mao, L., Liu, C., Lu, K., Su, Y., Gu, C., Huang, Q., & Petersen, E. J. (2016). Exposure of few layer graphene to Limnodrilus hoffmeisteri modifies the graphene and changes its bioaccumulation by other organisms. *Carbon*, *109*, 566–574. https://doi.org/10.1016/j.carbon.2016.08.037

Martínez-Álvarez, I., Le Menach, K., Devier, M. H., Barbarin, I., Tomovska, R., Cajaraville, M. P., Budzinski, H., & Orbea, A. (2021). Uptake and effects of graphene oxide nanomaterials alone and in combination with polycyclic aromatic hydrocarbons in zebrafish. Science of the Total Environment, 775. https://doi.org/10.1016/j.scitotenv.2021.145669.

Mazari, S. A., Ali, E., Abro, R., Khan, F. S. A., Ahmed, I., Ahmed, M., Nizamuddin, S., Siddiqui, T. H., Hossain, N., Mubarak, N. M., & Shah, A. (2021). Nanomaterials: Applications, waste-handling, environmental toxicities, and future challenges - A review. *Journal of Environmental Chemical Engineering*, *9*(2), 105028. https://doi.org/10.1016/j.jece.2021.105028

Meador, J.P., Stein, J.E., Reichert, W.L., Varanasi, U. 1995. Bioaccumulation of polycyclic aromatic hydrocarbons by marine organisms. Reviews of Environmental Contamination and Toxicology 143,79-165.

Meng, X., Li, F., Wang, X., Liu, J., Ji, C., & Wu, H. (2019). Combinatorial immune and stress response, cytoskeleton and signal transduction effects of graphene and triphenyl phosphate (TPP) in mussel Mytilus galloprovincialis. *Journal of Hazardous Materials*, *378*(January), 120778. https://doi.org/10.1016/j.jhazmat.2019.120778

Meng, X., Li, F., Wang, X., Liu, J., Ji, C., & Wu, H. (2020). Toxicological effects of graphene on mussel Mytilus galloprovincialis hemocytes after individual and combined exposure with triphenyl phosphate. *Marine Pollution Bulletin*, *151*(August 2019), 110838. https://doi.org/10.1016/j.marpolbul.2019.110838

Mesarič, T., Sepčić, K., Drobne, D., Makovec, D., Faimali, M., Morgana, S., Falugi, C., & Gambardella, C. (2015). Sperm exposure to carbon-based nanomaterials causes abnormalities in early development of purple sea urchin (Paracentrotus lividus). *Aquatic Toxicology*, *163*, 158–166. https://doi.org/10.1016/j.aquatox.2015.04.012

mollusc Mytilus galloprovincialis with emphasis on the endolysosomal compartment. Cell Structure and Function 20: 355-367

Moore, M. N., Sforzini, S., Viarengo, A., Barranger, A., Aminot, Y., Readman, J. W., Khlobystov, A. N., Arlt, V. M., Banni, M., & Jha, A. N. (2021). Antagonistic cytoprotective effects of C60 fullerene nanoparticles in simultaneous exposure to benzo[a]pyrene in a molluscan animal model. *Science of the Total Environment*, *755*, 142355. https://doi.org/10.1016/j.scitotenv.2020.142355

Mu, L., Gao, Y., & Hu, X. (2015). L-Cysteine: A biocompatible, breathable and beneficial coating for graphene oxide. *Biomaterials*, *52*(1), 301–311. https://doi.org/10.1016/j.biomaterials.2015.02.046

Mullick Chowdhury, S., Dasgupta, S., Mcelroy, A. E., & Sitharaman, B. (2014). Structural disruption increases toxicity of graphene nanoribbons. *Journal of Applied Toxicology*, *34*(11), 1235–1246. https://doi.org/10.1002/jat.3066

Naasz, S., Altenburger, R., & Kühnel, D. (2018). Environmental mixtures of nanomaterials and chemicals: The Trojan-horse phenomenon and its relevance for ecotoxicity. *Science of the Total Environment*, *635*, 1170–1181. https://doi.org/10.1016/j.scitotenv.2018.04.180

Nam, S.W., Jung, C., Li, H., Yu, M., Flora, J.R.V., Boateng, L.K., Her, N., Zoh, K.D., Yoon, Y. 2015. Adsorption characteristics of diclofenac and sulfamethoxazole to graphene oxide in aqueous solution. Chemosphere 136, 20–26.

Nanodatabase: https://nanodb.dk/en/search-database

Narune A, Danekar R., Prasad E. 2021. Graphene market by type (mono layer and bi layer graphene, few layer graphene, graphene oxide, groahene nano platelets), by application (RFID, composites, sensors, research and development, energy storage, functional ink, polymer additives, tire, coatings, others) and region: global opportunity analysis and industry forecast, 2020-2030. Advanced Materials A00361, 1-273.

Nel, A., Xia, T., Mädler, L., & Li, N. (2006). Toxic potential of materials at the nanolevel. *Science*, *311*(5761), 622–627. https://doi.org/10.1126/science.1114397

Neto, V.F., Vaz, R., Ali, N., Oliveira, M.S.A. Grácio, J. 2008. Performance of sub-micron diamond films coated on mould inserts for plastic injection moulding. Journal of Materials Science 43, 3392–3399.

Nogueira, P. F. M., Nakabayashi, D., & Zucolotto, V. (2015). The effects of graphene oxide on green algae Raphidocelis subcapitata. *Aquatic Toxicology*, *166*, 29–35. https://doi.org/10.1016/j.aquatox.2015.07.001

Novoselov, K. S., Fal, V. I., Colombo, L., Gellert, P. R., Schwab, M. G., Kim, K. 2012. A roadmap for graphene. Nature 490, 192-200.

O'Donovan S., Mestre N.C., Abel S., Fonseca T.G., Carteny C.C., Cormier B., Keiter S.H., Bebianno M.J. 2018. Ecotoxicological Effects of chemical contaminants adsorbed to microplastics in the clam Scrobicularia plana. Frontiers in Marine Science 5,143.

Odabasi, M., Dumanoglu, Y., Ozgunerge, E., TUNA, G. 2016. Investigation of spatial distributions and sources of persistent organic pollutants (POPs) in a heavily polluted industrial region using tree components. Chemosphere 160, 114–125.

Oliveira P., Barboza L.G.A., Branco V., Figueiredo N., Carvalho C., Guilhermino L. 2018. Effects of microplastics and mercury in the freshwater bivalve Corbicula fluminea (Müller, 1774): filtration rate, biochemical biomarkers and mercury bioconcentration. Ecotoxicology and Environmental Safety 164, 155-163.

Oliveira P., Barboza L.G.A., Branco V., Figueiredo N., Carvalho C., Guilhermino L. 2018. Effects of microplastics and mercury in the freshwater bivalve Corbicula fluminea (Müller, 1774): filtration rate, biochemical biomarkers and mercury bioconcentration. Ecotoxicology and Environmental Safety 164, 155-163.

Ortiz-Zarragoitia M., Cajaraville M.P. 2006. Biomarkers of exposure and reproduction-related effects in mussels exposed to endocrine disruptors. Archives of Environmental Contamination and Toxicology 50, 361-369.

Ortiz-Zarragoitia M., Cajaraville M.P. 2010. Intersex and oocyte atresia in a mussel population from the Biosphere's Reserve of Urdaibai (Bay of Biscay). Ecotoxicology and Environmental Safety 73, 693-701.

Ou, L., Song, B., Liang, H., Liu, J., Feng, X., Deng, B., Sun, T., Shao, L. 2016. Toxicity of graphene-family nanoparticles: a general review of the origins and mechanisms. Particle and fibre toxicology 13, 57.

Pacheco-Torgal, F., & Jalali, S. (2011). Nanotechnology: Advantages and drawbacks in the field of construction and building materials. *Construction and Building Materials*, *25*(2), 582–590. https://doi.org/10.1016/j.conbuildmat.2010.07.009

Pacheco-Torgal, F., & Labrincha, J. A. (2013). The future of construction materials research and the seventh un Millennium Development Goal: A few insights. *Construction and Building Materials*, *40*, 729–737. https://doi.org/10.1016/j.conbuildmat.2012.11.007

Patel, K. D., Singh, R. K., & Kim, H. W. (2019). Carbon-based nanomaterials as an emerging platform for theranostics. *Materials Horizons*, *6*(3), 434–469. https://doi.org/10.1039/c8mh00966j

Paul-Pont I., Lacroix C., Fernández C.G., Hégaret H., Lambert C., Le Goïc N., Frère L., Cassone A.L., Sussarellu R., Fabioux C., Guyomarch J. 2016. Exposure of marine mussels Mytilus spp. to polystyrene microplastics: Toxicity and influence on fluoranthene bioaccumulation. Environmental Pollution 216, 724-737.

Peng, Z., Liu, X., Zhang, W., Zeng, Z., Liu, Z., Zhang, C., Liu, Y., Shao, B., Liang, Q., Tang, W., & Yuan, X. (2020). Advances in the application, toxicity and degradation of carbon nanomaterials in environment: A review. *Environment International*, *134*(November 2019), 105298. https://doi.org/10.1016/j.envint.2019.105298

Pittura L., Avio C.G., Giuliani M.E., d'Errico G., Keiter S., Cormier B., Gorbi S., Regoli F. 2018. Microplastics as vehicles of environmental PAHs to marine organisms: combined chemical and physical hazards to the mediterranean mussels, Mytilus galloprovincialis. Frontiers in Marine Science 5,103.

Pokropivny, V.V., Skorokhod, V.V. 2007. Classification of nanostructures by dimensionality and concept of surface forms engineering in nanomaterial science. Materials Science and Engineering: C 27,990-993.

Press Release: Graphene, 2D Materials and Carbon Nanotubes: Markets, Technologies and Opportunities 2017−2027. In IDTechEx.

Pretti, C., Oliva, M., Pietro, R. Di, Monni, G., Cevasco, G., Chiellini, F., Pomelli, C., & Chiappe, C. (2014). Ecotoxicity of pristine graphene to marine organisms. *Ecotoxicology and Environmental Safety*, *101*(1), 138–145. https://doi.org/10.1016/j.ecoenv.2013.11.008

Qu X., Su L., Li H., Liang M., Shi H. 2018. Assessing the relationship between the abundance and properties of microplastics in water and in mussels. Science of the Total Environment 621, 679–686.

Quesada-González, D., Merkoçi, A. 2018. Nanomaterial-based devices for point-of-care diagnostic applications. Chemical Society Reviews 47, 4697–4709

Ramón-Raygoza, E. D., Rivera-Solorio, C. I., Giménez-Torres, E., Maldonado-Cortés, D., Cardenas-Alemán, E., & Cué-Sampedro, R. (2016). Development of nanolubricant based on impregnated multilayer graphene for automotive applications: Analysis of tribological properties. *Powder Technology*, *302*, 363–371. https://doi.org/10.1016/j.powtec.2016.08.072

Ranjan, S., Dasgupta, N., & Lichtfouse, E. (2016). *Nanoscience in Food and Agriculture 3* (Vol. 23). https://doi.org/10.1007/978-3-319-48009-1

Ren, C., Hu, X., Li, X., & Zhou, Q. (2016). Ultra-trace graphene oxide in a water environment triggers Parkinson's disease-like symptoms and metabolic disturbance in zebrafish larvae. *Biomaterials*, *93*, 83–94. https://doi.org/10.1016/j.biomaterials.2016.03.036

Ren, W., & Cheng, H. M. (2014). The global growth of graphene. *Nature Nanotechnology*, *9*(10), 726–730. https://doi.org/10.1038/nnano.2014.229

Revel M., Lagarde F., Perrein-Ettajani H., Bruneau M., Akcha F., Sussarellu R., Rouxel J., Costil K., Decottignies P., Cognie B., Châtel A., Mouneyrac C. 2019. Tissue-Specific biomarker responses in the blue mussel Mytilus spp. Exposed to a mixture of microplastics at environmentally relevant concentrations. Frontiers in Environmental Science 7:33.

Ribeiro F., Garcia A.R., Pereira B.P., Fonseca M., Mestre N.C., Fonseca T.G., Ilharco L.M., Bebianno M.J. 2017. Microplastics effects in Scrobicularia plana. Marine Pollution Bulletin 122, 379-391.

Rist S., Baun A., Almeda R., Hartmann N.B. 2019. Ingestion and effects of micro- and nanoplastics in blue mussel (Mytilus edulis) larvae. Marine Pollution Bulletin 140, 423-430.

Ritter, L., Solomon, Kr., Forget, J., Stemeroff, M., O'leary, C. 2007. "Persistent organic pollutants". United Nations Environment Programme. Retrieved 2007-09-16 (4).

ROBATI, D., MIRZA, B., RAJABI, M., MORADI, O., TYAGI, I., AGARWAL, S., GUPTA, V.K. 2016. Removal of hazardous dyes-BR 12 and methyl orange using graphene oxide as an adsorbent from aqueous phase. Chemical Engineering Journal 284, 687–697.

Rocha, T. L., Gomes, T., Sousa, V. S., Mestre, N. C., & Bebianno, M. J. (2015). Ecotoxicological impact of engineered nanomaterials in bivalve molluscs: An overview. *Marine Environmental Research*, *111*, 74–88. https://doi.org/10.1016/j.marenvres.2015.06.013

Rowan, S., & Taylor, A. (2018). The role of microbiota in retinal disease. *Advances in Experimental Medicine and Biology*, *1074*, 429–435. https://doi.org/10.1007/978-3-319-75402-4_53

Ruiz P., Ortiz-Zarragoitia M., Orbea A., Vingen S., Hjelle A., Baussant T., Cajaraville M.P. 2014. Short- and long-term responses and recovery of mussels *Mytilus edulis* exposed to heavy fuel oil no. 6 and styrene. Ecotoxicology 23, 861-879

Sajid, M. (2022). Nanomaterials: types, properties, recent advances, and toxicity concerns. *Current Opinion in Environmental Science and Health*, *25*, 100319. https://doi.org/10.1016/j.coesh.2021.100319

Sajid, M. (2022). Nanomaterials: types, properties, recent advances, and toxicity concerns. *Current Opinion in Environmental Science and Health*, *25*, 100319. https://doi.org/10.1016/j.coesh.2021.100319

Saleh, T. A. (2020). Trends in the sample preparation and analysis of nanomaterials as environmental contaminants. *Trends in Environmental Analytical Chemistry*, *28*, 1–10. https://doi.org/10.1016/j.teac.2020.e00101

Sanchís, J., Olmos, M., Vincent, P., Farré, M., & Barceló, D. (2016). New Insights on the Influence of Organic Co-Contaminants on the Aquatic Toxicology of Carbon Nanomaterials. *Environmental Science and Technology*, *50*(2), 961–969. https://doi.org/10.1021/acs.est.5b03966

Santana M.F., Moreira, F.T., Pereira, C.D., Abessa, D.M., Turra, A. 2018. Continuous exposure to microplastics does not cause physiological effects in the cultivated mussel Perna perna. Archives of Environmental Contamination and Toxicology 74, 594-604.

Scott, A. Graphene's Global Race to Market (citing an IDTechEx market report). Chem. Eng. News, Vol. 94, pp 28−33.

Seifi, T., & Kamali, A. R. (2021). Anti-pathogenic activity of graphene nanomaterials: A review. *Colloids and Surfaces B: Biointerfaces*, *199*(November 2020), 111509. https://doi.org/10.1016/j.colsurfb.2020.111509

Selck, H., Handy, R.D., Fernandes, T.F., Klaine, S.J., Petersen, E.J., 2016. Nanomaterials in the aquatic environment: a European Union-United States perspective on the status of ecotoxicity testing, research priorities, and challenges ahead. Environ. Toxicol. Chem. 35 (5), 1055–1067.

Sendra M., Saco A., Yeste M.P., Romero A., Novoa B., Figueras A. 2020. Nanoplastics: From tissue accumulation to cell translocation into Mytilus galloprovincialis hemocytes. Resilence of immune cells exposed to nanoplastics and nanoplastics plus Vibrio splendidus combination. Journal of Hazardous Materials 388, 121788.

Sendra, M., Sparaventi, E., Novoa, B., & Figueras, A. (2021). An overview of the internalization and effects of microplastics and nanoplastics as pollutants of emerging concern in bivalves.

Science of the Total Environment, 753, 142024. https://doi.org/10.1016/j.scitotenv.2020.142024

Sharma, P., Das, M.R. 2013. Removal of a cationic dye from aqueous solution using graphene oxide nanosheets: investigation of adsorption parameters. Journal of Chemical & Engineering Data 58, 151–158.

Sikdokur E., Belivermis M., Sezer N., Pekmez M., Bulan O.K., Kiliç., O. 2020. Effects of microplastics and mercury on manila clam Ruditapen philippinarum: Feeding rate, immunomodulation, histopathology and oxidative stress. Environmental Pollution 262, 114247.

Singh, H., Bhardwaj, N., Arya, S. K., & Khatri, M. (2020). Environmental impacts of oil spills and their remediation by magnetic nanomaterials. *Environmental Nanotechnology, Monitoring and Management*, *14*(May), 100305. https://doi.org/10.1016/j.enmm.2020.100305

Smaradhana, D. F., Prabowo, A. R., & Ganda, A. N. F. (2021). Exploring the potential of graphene materials in marine and shipping industries – A technical review for prospective application on ship operation and material-structure aspects. *Journal of Ocean Engineering and Science*, *6*(3), 299–316. https://doi.org/10.1016/j.joes.2021.02.004

Soares, J. C., Pereira, T. C. B., Costa, K. M., Maraschin, T., Basso, N. R., & Bogo, M. R. (2017). Developmental neurotoxic effects of graphene oxide exposure in zebrafish larvae (Danio rerio). *Colloids and Surfaces B: Biointerfaces*, *157*, 335–346. https://doi.org/10.1016/j.colsurfb.2017.05.078

Soltani, A. M., Tabatabaeian, S. H., Hanafizadeh, P., & Soofi, J. B. (2011). An evaluation scheme for nanotechnology policies. *Journal of Nanoparticle Research*, *13*(12), 7303–7312. https://doi.org/10.1007/s11051-011-0584-8

Song, T., Tian, W., Qiao, K., Zhao, J., Chu, M., Du, Z., Wang, L., & Xie, W. (2021). Adsorption Behaviors of Polycyclic Aromatic Hydrocarbons and Oxygen Derivatives in Wastewater on N-Doped Reduced Graphene Oxide. *Separation and Purification Technology*, *254*(July 2020), 117565. https://doi.org/10.1016/j.seppur.2020.117565

Song, Y. K., Hong, S. H., Kang, J. H., Kwon, O. Y., Jang, M., Han, G. M., et al. (2014). Large accumulation of micro-sized synthetic polymer particles in the sea surface microlayer. Environmental Science & Technology, 48(16), 9014–9021.

Souza, J. P., Baretta, J. F., Santos, F., Paino, I. M. M., & Zucolotto, V. (2017). Toxicological effects of graphene oxide on adult zebrafish (Danio rerio). *Aquatic Toxicology*, *186*, 11–18. https://doi.org/10.1016/j.aquatox.2017.02.017

Souza, J. P., Venturini, F. P., Santos, F., & Zucolotto, V. (2018). Chronic toxicity in Ceriodaphnia dubia induced by graphene oxide. *Chemosphere*, *190*, 218–224. https://doi.org/10.1016/j.chemosphere.2017.10.018

Suhendra, E., Chang, C. H., Hou, W. C., & Hsieh, Y. C. (2020). A review on the environmental fate models for predicting the distribution of engineered nanomaterials in surface waters. *International Journal of Molecular Sciences*, *21*(12), 1–19. https://doi.org/10.3390/ijms21124554

Sun, B., Zhang, Y., Li, R., Wang, K., Xiao, B., Yang, Y., Wang, J., & Zhu, L. (2021). New insights into the colloidal stability of graphene oxide in aquatic environment: Interplays of photoaging and proteins. *Water Research*, *200*, 117213. https://doi.org/10.1016/j.watres.2021.117213

Sun, M., & Li, J. (2018). Graphene oxide membranes: Functional structures, preparation and environmental applications. *Nano Today*, *20*, 121–137. https://doi.org/10.1016/j.nantod.2018.04.007

Sundukov, Y. N. (2006). First record of the ground beetle Trechoblemus postilenatus (Coleoptera, Carabidae) in Primorskii krai. *Far Eastern Entomologist*, *165*(April), 16. https://doi.org/10.1002/tox

Sussarellu R., Suquet M., Thomas Y., Lambert C., Fabioux C., Pernet M.E.J., Le Goïc N.L., Quillien V., Mingant C., Epelboin Y., Corporeau C., Guyomarch J., Robbens J., Paul-Pont I., Soudant P., Huvet A. 2015. Oyster reproduction is affected by exposure to polystyrene microplastics. PNAS 113, 2430-2435.

Tadyszak, K., Wychowaniec, J. K., & Litowczenko, J. (2018). Biomedical applications of graphene-based structures. *Nanomaterials*, *8*(11), 1–20. https://doi.org/10.3390/nano8110944

Tallec K., Huvet A., Di Poi C., González-Fernández C., Kambert C., Petton B., Le Goïc N., Berchel M., Soudan P., Paul-Pont I. 2018. Nanoplastics impaired oyster free living stages, gametes and embryos. Environmental Pollution 242, 1226-135.

Thang Y., Rong J., guan X., Zha S., Shi W., Han Y., Du X., Wu F., Huang W., Liu G. 2020. Immunotoxicity of microplastics and two persistent organic pollutants alone or in combination to a bivalve species. Environmental Pollution 258, 113845.

Thiagarajan, V., Alex, S. A., Seenivasan, R., Chandrasekaran, N., & Mukherjee, A. (2021). Interactive effects of micro/nanoplastics and nanomaterials/pharmaceuticals: Their ecotoxicological consequences in the aquatic systems. *Aquatic Toxicology*, *232*(December 2020), 105747. https://doi.org/10.1016/j.aquatox.2021.105747

Thomas M., Jon B., Craig S., Edward R., Ruth H., John B., Dick V.A., Heather L.A., Matthew S. 2020. The world is your oyster: low-dose, long-term microplastic exposure of juvenile oysters. Heliyon 6, e03103.

Thompson, R. C., Olsen, Y., Mitchell, R. P., Davis, A., Rowland, S. J., John, A. W. & Russell, A. E. (2004). Lost at sea: where is all the plastic?. Science, 304(5672), 838-838.

Tiwari, S.K., Sahoo, S., Wang, N., Huczko, A., 2020. Graphene research and their outputs: Status and prospect. J. Sci. Adv. Mater. Dev. 5, 10-29.

Trestail C., Walpitagama M., Miranda A., Nugegoda D., Shimeta J. 2021. Microplastics altes digestive enzyme activities in the marine bivalve, Mytilus galloprovincialis. Science of the Total Environment 779, 146418.

Tu, Y., Lv, M., Xiu, P., Huynh, T., Zhang, M., Castelli, M., Liu, Z., Huang, Q., Fan, C., Fang, H., Zhou, R. 2013. Destructive extraction of phospholipids from Escherichia coli membranes by graphene nanosheets. Nature nanotechnology 8, 594-601.

U. S. EPA, 2014. IRIS Toxicological Review of Benzo[a]pyrene (External Review Draft). U.S. Environmental Protection Agency, Washington, DC EPA/635/R-14/312.

U.E. Water Framework Directive, 2008. Environmental Quality Standards Directive (EQSD). 105/EC. http://ec.europa.eu/environment/water/water-framework/priority_ substances.htm.

U.S. EPA, 2010. Emerging contamiants-nanomaterials.

UNEP (2011). UNEP year book: Emerging issues in our global environment (79 p). Nairobi: United Nations Environmental Programme.

UNEP/RAMOGE, (1999). Manual on the biomarkers recommended for the MED POL biomonitoring programme. UNEP, Athens, Greece

Urban-Malinga, B., Jakubowska, M., Hallmann, A., & Dąbrowska, A. (2021). Do the graphene nanoflakes pose a potential threat to the polychaete Hediste diversicolor? *Chemosphere*, *269*(xxxx). https://doi.org/10.1016/j.chemosphere.2020.128685

Van Cauwenberghe L., Claessens M., Vandegehuchte M.B., Janssen C.R. 2015. Microplastics are taken up by mussels (Mytilus edulis) and lugworms (Arenicola marina) living in natural habitats. Environmental Pollution 199, 10-17.

van Franeker, J.A., Blaize, C., Danielsen, J., Fairclough, K., Gollan, J., Guse, N., Hansen,P.-L., Heubeck, M., Jensen, J.-K., Le Guillou, G., Olsen, B., Olsen, K.-O., Pedersen, J., Stienen, E.W.M., Turner, D.M., (2011). Monitoring plastic ingestion by the northern fulmar Fulmarus glacialis in the North Sea. Environmental Pollution, 159, 2609–2615

Velzeboer, I., Kwadijk, C.J.A.F. & Koelmans, A.A., (2014). Strong Sorption of PCBs to Nanoplastics, Microplastics, Carbon Nanotubes, and Fullerenes. Envionmental Science and Technology, 48, pp. 4869–4876.

Von Moos N., Burkhardt-Holm P., Köhler A. 2012. Uptake and effects of microplastics on cells and tissue of the blue mussel Mytilus edulis L. after an experimental exposure. Environmental Science and Technology 46, 11327-11335.

Wagner S. 2018. Nanoparticles in the environment: where do we come from, where do we go

Wang X. Huang W., Wei S., Shang Y., Gu H., Wu F., Lan Z., Hu M., Shi H., Wang Y. 2020. Microplastics impair digestive performance but show little effects on antioxidant activity in mussels under low pH conditions. Environmental Pollution 258, 113691.

Wang, A., Pu, K., Dong, B., Liu, Y., Zhang, L., Zhang, Z., Duan, D., Zhu, Y. 2013. Role of surface charge and oxidative stress in cytotoxicity and genotoxicity of graphene oxide towards human lung fibroblast cells. Journal of Applied Toxicology 33, 1156-1164.

Wang, J., Chen, Z., Chen, B. 2014. Adsorption of polycyclic aromatic hydrocarbons by graphene and graphene oxide nanosheets. Environmental Science & Technology 48, 4817–4825.

Wang, J., Zhang, J., Han, L., Wang, J., Zhu, L., & Zeng, H. (2021). Graphene-based materials for adsorptive removal of pollutants from water and underlying interaction mechanism. *Advances in Colloid and Interface Science*, *289*, 102360. https://doi.org/10.1016/j.cis.2021.102360

Wang, T., Huang, D., Yang, Z., Xu, S., He, G., Li, X., Hu, N., Yin, G., He, D., & Zhang, L. (2016). A Review on Graphene-Based Gas/Vapor Sensors with Unique Properties and Potential Applications. *Nano-Micro Letters*, *8*(2), 95–119. https://doi.org/10.1007/s40820-015-0073-1

Ward, J.E., Shumway, S.E., (2004). Separating the grain from the chaff: particle selection in suspension- and deposit-feeding bivalves. J. Exp. Mar. Biol. Ecol. 300, 83e130

Weber A., Jeckel N., Wagner M. 2020. Combined effects of polystyrene microplastics and thermal stress on the freshwater mussel Dreissena polymorpha. Science of Total Environment 718, 137253.

Wegner A., Besseling E., Foekema E.M., Kamermans P., Koelmans A.A. 2012. Effects of nanopolystyrene on the feeding behavior of the blue mussel (Mytilus edulis L.). Environmental Toxicology and Chemistry 31, 2490-2497.

Wei, M., Chai, H., Cao, Y., Jia, D. 2018. Sulfonated graphene oxide as an adsorbent for removal of Pb2+ and methylene blue. Journal of Colloid and Interface Science 524, 297–305.

Woodall, L. C., Sanchez-Vidal, A., Canals, M., Paterson, G. L., Coppock, R., Sleight, V., & Thompson, R. C. (2014). The deep sea is a major sink for microplastic debris. Royal Society Open Science, 1(4), 140317.

Wu, L.K., Wu, H., Zhang, H.-B., Cao, H.-Z., Hou, G.Y., Tang, Y.P., Zheng, G.Q. 2018. Graphene oxide/CuFe2O4 foam as an efficient absorbent for arsenic removal from water. Chemical Engineering Journal 334, 1808–1819.

Xu X.Y., Lee W.T., Chan A.K.Y., Lo H.S., Shin P.K.S., Cheung S.G. 2017. Microplastic ingestion reduces energy intake in the clam Atactodea striata. Marine Pollution Buletin 124, 798-802.

Yan, Qi-Long, et al. "Highly energetic compositions based on functionalized carbon nanomaterials." Nanoscale 8.9 (2016): 4799-4851. Lin, Jing, Xiaoyuan Chen, and Peng Huang. "Graphene-based nanomaterials for bioimaging." Advanced drug delivery reviews (2016).

Yang, J., Zhong, W., Chen, P., Zhang, Y., Sun, B., Liu, M., Zhu, Y., Zhu, L., 2019. Graphene oxide mitigates endocrine disruption effects of bisphenol A on zebrafish at an early development stage. Sci. Total. Environ. 697, 134158.

Yang, K., Gong, H., Shi, X., Wan, J., Zhang, Y., & Liu, Z. (2013). In vivo biodistribution and toxicology of functionalized nano-graphene oxide in mice after oral and intraperitoneal administration. *Biomaterials*, *34*(11), 2787–2795. https://doi.org/10.1016/j.biomaterials.2013.01.001

Yang, K., Wang, J., Chen, B., 2014. Facile fabrication of stable monolayer and few-layer graphene nanosheets as superior sorbents for persistent aromatic pollutant management in water. J. Mater. Chem. 2, 18219.

Yao, W., Zhou, S., Wang, Z., Lu, Z., & Hou, C. (2020). Antioxidant behaviors of graphene in marine environment: A first-principles simulation. *Applied Surface Science*, *499*(May 2019), 143962. https://doi.org/10.1016/j.apsusc.2019.143962

Yee, M. S. L., Khiew, P. S., Chiu, W. S., Tan, Y. F., Kok, Y. Y., & Leong, C. O. (2016). Green synthesis of graphene-silver nanocomposites and its application as a potent marine antifouling agent. Colloids and Surfaces B: Biointerfaces, 148, 392–401. https://doi.org/10.1016/j.colsurfb.2016.09.011

Yin, J., Fan, W., Du, J., Feng, W., Dong, Z., Liu, Y., & Zhou, T. (2020). The toxicity of graphene oxide affected by algal physiological characteristics: A comparative study in cyanobacterial, green algae, diatom. *Environmental Pollution*, *260*, 113847. https://doi.org/10.1016/j.envpol.2019.113847

Younis, S.A., Maitlo, H.A., Lee, J., Kim, K-H., 2020. Nanotechnology-based sorption and membrane technologies for the treatment of petroleum-based pollutants in natural ecosystems and wastewater streams. Adv. Colloid Interface Sci. 275, 102701.

Zhang, D., Zhang, Z., Wu, Y., Fu, K., Chen, Y., Li, W., & Chu, M. (2019). Systematic evaluation of graphene quantum dot toxicity to male mouse sexual behaviors, reproductive and offspring health. Biomaterials, 194(December 2018), 215–232. https://doi.org/10.1016/j.biomaterials.2018.12.001

Zhang, H., Vidonish, J., Lv, W., Wang, X., & Alvarez, P. (2020). Differential histological, cellular and organism-wide response of earthworms exposed to multi-layer graphenes with different morphologies and hydrophobicity. *Environmental Pollution*, *263*, 114468. https://doi.org/10.1016/j.envpol.2020.114468

Zhang, P., Selck, H., Tangaa, S. R., Pang, C., & Zhao, B. (2017). Bioaccumulation and effects of sediment-associated gold- and graphene oxide nanoparticles on Tubifex tubifex. Journal of Environmental Sciences (China), 51, 138–145. https://doi.org/10.1016/j.jes.2016.08.015

Zhang, Y., Duan, X., Bai, L., & Quan, X. (2020). Effects of nanomaterials on metal toxicity: Case study of graphene family on Cd. Ecotoxicology and Environmental Safety, 194(November 2019). https://doi.org/10.1016/j.ecoenv.2020.110448

Zhang, Y., Meng, T., Guo, X., Yang, R., Si, X., & Zhou, J. (2018). Humic acid alleviates the ecotoxicity of graphene-family materials on the freshwater microalgae Scenedesmus obliquus. In Chemosphere (Vol. 197). Elsevier Ltd. https://doi.org/10.1016/j.chemosphere.2018.01.051

Zhang, Y., Meng, T., Shi, L., Guo, X., Si, X., Yang, R., & Quan, X. (2019). The effects of humic acid on the toxicity of graphene oxide to Scenedesmus obliquus and Daphnia magna. Science of the Total Environment, 649, 163–171. https://doi.org/10.1016/j.scitotenv.2018.08.280

Zhang, Y., Tang, Y., Li, S., & Yu, S. (2013). Sorption and removal of tetrabromobisphenol A from solution by graphene oxide. Chemical Engineering Journal, 222, 94–100. https://doi.org/10.1016/j.cej.2013.02.027

Zhao, J., Cao, X., Wang, Z., Dai, Y., & Xing, B. (2017). Mechanistic understanding toward the toxicity of graphene-family materials to freshwater algae. Water Research, 111, 18–27. https://doi.org/10.1016/j.watres.2016.12.037

Zhao, J., Ning, F., Cao, X., Yao, H., Wang, Z., & Xing, B. (2020). Photo-transformation of graphene oxide in the presence of co-existing metal ions regulated its toxicity to freshwater algae. Water Research, 176, 115735. https://doi.org/10.1016/j.watres.2020.115735

Zhao, J., Wang, Z., White, J. C., & Xing, B. (2014). Graphene in the aquatic environment: Adsorption, dispersion, toxicity and transformation. Environmental Science and Technology, 48(17), 9995–10009. https://doi.org/10.1021/es5022679

Zhao, S., Wang, Y., & Duo, L. (2021). Biochemical toxicity, lysosomal membrane stability and DNA damage induced by graphene oxide in earthworms. Environmental Pollution, 269, 116225. https://doi.org/10.1016/j.envpol.2020.116225

Zhao, Y., Liu, Y., Zhang, X., & Liao, W. (2021). Environmental transformation of graphene oxide in the aquatic environment. Chemosphere, 262(26), 127885. https://doi.org/10.1016/j.chemosphere.2020.127885

Zhu, S., Luo, F., Chen, W., Zhu, B., & Wang, G. (2017). Toxicity evaluation of graphene oxide on cysts and three larval stages of Artemia salina. *Science of the Total Environment*, *595*, 101–109. https://doi.org/10.1016/j.scitotenv.2017.03.224

Zhu, Y., Liu, X., Hu, Y., Wang, R., Chen, M., Wu, J., Wang, Y., Kang, S., Sun, Y., & Zhu, M. (2019). Behavior, remediation effect and toxicity of nanomaterials in water environments. *Environmental Research*, *174*(April), 54–60. https://doi.org/10.1016/j.envres.2019.04.014

Ziat, Y., Hammi, M., Zarhri, Z., & Laghlimi, C. (2020). Epoxy coating modified with graphene: A promising composite against corrosion behavior of copper surface in marine media. *Journal of Alloys and Compounds*, *820*, 153380. https://doi.org/10.1016/j.jallcom.2019.153380

Ziccardi, L. M., Edgington, A., Hentz, K., Kulacki, K. J., & Kane Driscoll, S. (2016). Microplastics as vectors for bioaccumulation of hydrophobic organic chemicals in the marine environment: A state-ofthe- science review. Environmental toxicology and chemistry, 35(7), 1667-1676.

2. STATE OF THE ART, HYPOTHESIS AND OBJECTIVES

2.1. STATE OF THE ART

Nanomaterials (NMs) are a diverse class of materials with at least one dimension at the nanoscale (<100 nm) that possess unique properties due to their higher surface area to volume ratio compared to bulk materials, which results in a higher chemical reactivity. The rapid development of nanotechnology and nanoindustry has led to a growing concern about the entry and possible impacts of these NMs in the environment. The marine environment merits special consideration because NMs tend to end up in waterways and finally in the oceans. Therefore, studies on the uptake and potential bioaccumulation and toxicity of NMs to marine organisms are urgently needed. In contrast with the growing knowledge on the toxicity of metal-bearing nanoparticles (NPs) in marine organisms, information on the impact of carbon-based nanomaterials such as graphene family nanomaterials (GFNs) is scarce, even though graphene and its derivatives have become one of the main research interest in nanotechnology due to the vast array of applications in diverse fields. On the other hand, plastic litter in the ocean is recognized as a global problem of growing concern. Little is known about the fate and effects of the smallest fraction of plastic litter in the marine environment, the nanoplastics (NPs, <1 μm) and microplastics (MPs, <1 mm). These NPs and MPs should be of increasing interest due to their size-specific properties, which make them the most hazardous type of marine litter. Moreover, pollutants do not appear alone in the marine environment. Thousands of organic compounds, including persistent organic pollutants (POPs) such as polycyclic aromatic hydrocarbons, are released into water bodies derived from natural, but mostly from anthropogenic sources, such as oil spills. GFNs have shown a great ability to adsorb organic pollutants and thus, their potential use in water pollution remediation is being extensively studied. However, the ability of both GFNs and NPs and MPs to adsorb POPs could cause an additional threat to marine organisms because GFNs, NPs and MPs could act as vehicles or carriers of pollutants to marine organisms, increasing their bioavailability and toxicity through the so-called Trojan horse effect. Therefore, a realistic assessment of the hazards of nano and micro scale particulate pollutants requires considering also their interactions with other pollutants available in the marine environment. Bivalve molluscs such as mussels (*Mytilus sp.*) are used worldwide as sentinels of environmental pollution. Due to their filter-feeding activity and well-developed endo-lysosomal system, mussels have been considered an

important target for NMs in the marine environment and thus, they represent a key species to evaluate the toxicity of nano and micro scale particulate pollutants. In view of the complex responses that could be triggered in mussels by a diverse range of NMs, a holistic approach involving the use of a wide battery of biomarkers and biological responses at different levels of biological organization in both embryo and adult stages of mussels is required in order to determine the potential impact of GFNs and NPs and MPs alone and in combination with adsorbed POPs in the marine environment.

2.2. HYPOTHESIS AND OBJECTIVES

The **hypothesis** of this PhD thesis is that nanoplastics (NPs), microplastics (MPs) and graphene family nanomaterials (GFNs) can act as carriers of persistent organic pollutants (POPs), such as polycyclic aromatic hydrocarbons (PAHs), and can enhance their toxicity at different levels of biological organization, including molecular, cellular, tissue and organism levels, to marine mussels *Mytilus galloprovincialis* through the so-called Trojan horse effect.

Thus, the **general objective** of this PhD thesis is to assess the potential hazards for the marine environment posed by GFNs and NPs and MPs and associated PAHs, contributing to our understanding of the role of GFNs and NPs and MPs as carriers of PAHs to mussels *M. galloprovincialis* and to gain knowledge on their toxicity at molecular, cellular, tissue and organism levels.

This general objective has been divided into five **specific objectives** described below which are addressed in the different chapters of the Results and Discussion section:

1.- To examine the effects of long-term (26 day) dietary exposure of polystyrene (PS) NPs (0.5 μm) and MPs (4.5 μm) alone and with sorbed benzo(a)pyrene (BaP) in mussels *M. galloprovincialis* in order to elucidate the influence of size and the presence of sorbed BaP on the organism at different levels of biological organization, along with bioaccumulation of BaP in mussel tissues and tissue distribution of MPs alone and with sorbed BaP.

2.- To determine the impact of dietary exposure of mussels *M. galloprovincialis* to PS MPs of 4.5 µm alone or with sorbed oil compounds from the WAF of a naphthenic crude oil in two dilutions (25% and 100%), using a battery of biological responses at molecular, cellular, tissue and organism levels, compared to the impact of exposure to a 25% dilution of WAF.

3.- To investigate the fate and effects of graphene oxide (GO), alone or with sorbed BaP, in adult marine mussels *M. galloprovincialis* using Raman spectroscopy and a battery of biological responses, contributing to understand the Trojan horse effect of GFNs towards BaP in mussels.

4.- To assess the toxicity of a reduced graphene oxide (rGO)-silver nanoparticle (Ag NP) hybrid material (rGO-Ag) at different levels of biological organization in mussels *M. galloprovincialis* and to compare its toxicity with that produced by rGO and Ag NPs separately, at concentrations equivalent to those in the hybrid material.

5.- To assess the impact of different GFNs alone or in combination with sorbed BaP on embryos of mussels *M. galloprovincialis.*

Finally, all the results obtained are integrated in the General Discussion section of the thesis.

3. RESULTS AND DISCUSSION

CHAPTER 1

Impacts of dietary exposure to polystyrene nano and microplastics alone and with sorbed benzo[a]pyrene on biomarkers and whole organism responses in mussels *Mytilus galloprovincialis*

This chapter has been published in:

GONZÁLEZ-SOTO, N; HATFIELD, J; KATSUMITI, A; DUROUDIER, N; LACAVE, JM; BILBAO, E; ORBEA, A; NAVARRO, E; CAJARAVILLE, MP. Impacts of dietary exposure to different sized polystyrene microplastics alone and with sorbed benzo[a]pyrene on biomarkers and whole organism responses in mussels *Mytilus galloprovincialis*. *Science of the Total Environment*, 684: 548-566 (2019).

This chapter has been presented at:

28th ANNUAL MEETING OF THE SOCIETY OF ENVIRONMENTAL TOXICOLOGY AND CHEMISTRY (SETAC)-EUROPE, Rome, 13-17 May 2018. HATFIELD, J; GONZÁLEZ-SOTO, N; KATSUMITI, A; DUROUDIER, N; LACAVE, JM; ORBEA, A; NAVARRO, E; CAJARAVILLE, MP. Impacts of exposure to microplastics alone and with adsorbed benzo(a)pyrene on biomarkers and scope for growth in marine mussels *M. galloprovincialis.* Poster.

11th IBERIAN and 8th IBERO-AMERICAN CONGRESS ON ENVIRONMENTAL CONTAMINATION AND TOXICOLOGY, Madrid, 11-13 July 2018. CAJARAVILLE, MP; MARTÍNEZ-ÁLVAREZ, I; HATFIELD, J; NICOLUSSI, G; GONZÁLEZ-SOTO, N; KATSUMITI, A; BILBAO, E; NAVARRO, E; TOMOVSKA, R; BUDZINSKI, H; ORBEA, A. Nanomaterials and microplastics as carriers of persistent organic pollutants in the aquatic environment: development of tools for risk assessment based on alternative methods and model organisms. Platform (MP Cajaraville).

MICRO 2018- International Conference on Fate and Impact of Microplastics: Knowledge, Actions and Solutions. Lanzarote, 19-23 November 2018. HATFIELD, J; GONZÁLEZ-SOTO, N; KATSUMITI, A; DUROUDIER, N; LACAVE, JM; ORBEA, A; NAVARRO, E; **CAJARAVILLE, MP**. Effects of exposure to microplastics alone and with adsorbed benzo(a)pyrene on marine mussels *M. galloprovincialis* at cell, tissue and physiological levels. Platform (MP Cajaraville).

ABSTRACT

Due to their hydrophobicity and relatively large surface area, nano (NPs) and microplastics (MPs) can act as carriers of hydrophobic pollutants in the ocean and may facilitate their transfer to organisms. This study examined effects of dietary exposure to polystyrene of 0.5 µm NPs and 4.5 µm MPs alone and with sorbed benzo[a]pyrene (BaP) on mussels *Mytilus galloprovincialis* in order to elucidate the effects of plastic size and the presence of sorbed BaP on the organism. NPs and MPs were provided daily, mixed with algae, during 26 days at equivalent mass (0.058 mg/L), corresponding to 1000 particles/mL for 4.5 µm MPs and to $7.44x10^5$ particles/mL for 0.5 µm NPs. Effects were determined on early cellular biomarkers in hemocytes, structure and cell type composition of digestive tubules (DTs), histopathology and whole organism responses (condition index (CI), clearance rate (CR), food absorption efficiency (AE), respiration rate (RR) and scope for growth (SFG)) . BaP concentrations in mussels increased with time, in particular when sorbed to 0.5 µm NPs. 4.5 µm MPs were abundant in the lumen of stomach and DTs, but were also occasionally found within epithelial cells. Effects in all treatments increased with exposure time. NPs and MPs with sorbed BaP were more toxic than NPs and MPs alone according to hemocyte viability and catalase activity and to the quantitative structure of DT epithelium. Higher toxicity of NPs compared to MPS was recorded for DNA damage and cell composition of DTs. At tissue level a slight increase in prevalence of inflammatory responses occurred in all exposed groups. At whole organism level a compensatory effect was observed on absorption efficiency across treatments at day 26, resulting in increased SFG in mussels exposed to NPs with sorbed BaP. This could be related to an increased energy need to deal with stress observed in biomarkers. Further work is required to understand the Trojan horse effect of a variety of plastic type, size, shape combinations together with a wide variety of pollutants.

1. INTRODUCTION

Plastic debris is now internationally recognized as an ubiquitous pollutant with potentially serious consequences in the marine environment (UNEP, 2011). Whilst the impacts of large plastic debris are well studied, it was only in recent years that interest developed in understanding and quantifying the abundance, distribution and effects of microplastics (MPs) and nanoplastics (NPs), defined as plastic particles <1 mm and <1 µm, respectively (Hartmann et al., 2019). MPs and NPs are largely derived from the *in situ* mechanical, chemical and biological breakdown of larger plastics. MPs and NPs may also enter the marine environment directly. Plastic microbeads used in exfoliating scrubs and synthetic fibres from clothes, such as polyester, are washed into the sea via effluent. Furthermore, industrial sandblasting now utilizes plastic microbeads rather than sand, and accidental industrial spills of pre-manufacture polymer powders and resin beads may occur (Cole et al., 2011). The scientific literature on MPs has grown exponentially and there are now a wealth of papers demonstrating that like large plastics, MPs are an ubiquitous if unevenly distributed pollutant in the oceans (Browne et al., 2011; Cole et al., 2011). Particle concentrations in the water column range from 2 x 10^{-7} particles/m^3 in the Bearing Sea (Day et al., 1990) to 102,000 particles/m^3 in coastal waters of Sweden (Norén & Naustvoll, 2010) or 9,180 particles/m^3 in the North East Pacific Ocean (Desforges et al., 2014), depending on distance from coast and depth (Desforges et al., 2014; Baini et al., 2018). In sediments particle concentrations may vary from 0.21 to >77,000 particles/m^3 (Hidalgo-Ruz et al., 2012). In general, concentrations are highest in coastal sediments particularly around heavily industrialized areas and in oceanic gyres but reported figures may be much higher due to sampling difficulties for smaller MPs (Lusher, 2015). Variations in sampling and quantification methods make it hard to compare MP concentrations in different works (Vandermeersch et al., 2015), highlighting the necessity for standardized methods (ICES, 2015; Li et al., 2019).

Marine organisms have been reported to ingest MPs in nature and the potential for negative effects on organisms after ingestion is a prominent environmental concern (Lusher et al., 2017). Affected organisms include molluscs, echinoderms, cnidarians, polychaete annelids, seabirds, fish and crustaceans (Hoss and Settle, 1990; Jumars et al., 1993; Thompson et al., 2004; Ward and Shumway; 2004; van Franeker et al., 2011; Hall et al., 2015). The investigation of the effects of MP ingestion in marine organisms is therefore a high priority for environmental science.

Filter feeders and deposit feeders are particularly vulnerable to MP ingestion in the wild as they are able to feed directly on MPs and may even selectively ingest them (Graham & Thompson, 2009). Mussels *Mytilus spp.* have been extensively used as model organisms to study the distribution and impact of marine pollutants (Cajaraville et al., 2000; Viarengo et al., 2007), and in recent years have been identified as an useful model organism for the study of MPs and their co-contaminants. The uptake of MPs (<80 µm) by mussels has been demonstrated both through the gill surface and via transfer of the MPs along gill channels to the mouth and into the digestive gland where translocation into cells could occur (Von Moos et al., 2012). MPs have been shown to appear in the intestinal lumen and epithelium, in digestive tubules (Avio et al., 2015; Paul-Pont et al., 2016) and within the lysosomal compartment (Von Moos et al., 2012). Polystyrene (PS) microspheres of 3 and 9.6 µm have been shown to translocate to the hemolymph were they persisted for up to 48 days, and even entered hemocytes (Browne et al., 2008). Browne et al. (2008) also showed that MP size plays a significant role in the transport and fate of MPs in mussels, as they found that abundance of 3 µm particles in the hemolymph increased by 60% as compared to the 9.6 µm particles. Mussels have an open circulatory system, therefore smaller particles can be seen to pose a greater threat than larger particles due to their enhanced ability to interact with cells throughout the organism (Browne et al., 2008). Toxic effects of virgin MPs in mussels at tissue level or below include changes in transcriptional profiles involving a number of indicators of toxicity, neurotoxicity (Avio et al., 2015), oxidative stress and damage (Paul-Pont et al., 2016), decrease in lysosomal membrane stability, alterations in immune parameters (Pittura et al., 2018) and increases in the formation of granulocytomas (Von Moos et al., 2012), and total histopathological lesions (Paul-Pont et al., 2016; Brate et al., 2018). At organism level, mussels chronically exposed to 30 nm PS nanoplastics showed reduced feeding activity and increased production of pseudofaeces which indicates reduced feeding efficiency (Wegner et al., 2012). However, integrated physiological responses to the impacts of MPs as represented by Scope For Growth (SFG) have yet to be characterized in mussels.

In addition to the effects of MPs on organisms that have initially ingested them, the accumulation of MPs (either absorbed into internal tissues or within the gut lumen) can lead to the trophic transfer of these particles within food chains. The biotransfer of MPs from mussels to crabs and puffer fish has been shown (Farrell & Nelson, 2013; Santana et al., 2017) and field studies have found MPs in mussels grown for aquaculture and in consumer products (van Cauwenberghe & Janssen, 2014; Li et al., 2018) thereby demonstrating the real world significance of this issue. Furthermore, the ingestion of MPs can facilitate the transport of harmful chemicals to organisms (Browne et al., 2013;

Rochman et al., 2013a; 2013b; Lusher, 2015; Ma et al., 2016). This may occur via leaching of chemicals added to plastics during manufacture, such as plasticizers, or via the release of persistent organic pollutants (POPs) which accumulate in MPs in seawater (e.g. polycyclic aromatic hydrocarbons, PAHs) (Lusher, 2015).

Sorption capacity of plastics and desorption rates of pollutants have been characterized for a number of prominent environmental contaminants across a number of polymer types and appear to be highly polymer and pollutant specific (Bakir et al., 2016) making it important to investigate the bioavailability and effects of a wide range of plastic-pollutant combinations. The transfer of chemicals to the body via MPs will ultimately depend on the concentration of the sorbed chemicals relative to the body burden of the contaminant in question derived from other sources (e.g. dietary). However, a number of other factors may also influence MP co-contaminant bioavailability (Koelmans, 2015). These include MP size, surface texture and chemistry all of which may be altered continuously due to the weathering process in nature; the formation of biofilms may also alter the MP surface chemistry (Ziccardi et al., 2016). Indeed size has been identified as a key factor influencing both sorption capacity and sorption/desorption rates of chemicals to and from plastics. Smaller plastics not only have a larger surface area to volume ratio but also have a shorter diffusion pathway; hence smaller plastics can sorb higher contaminant concentrations and exchange these more rapidly with the environment (Velzeboer et al., 2014). Once ingested, gut retention time and fate within the body will influence time available for desorption of chemicals into tissues and the sites of toxic action (Bakir et al., 2016). Again smaller MPs have been highlighted as potentially more dangerous due to their enhanced ability to translocate and increased retention times in mussels and crabs (>48 days and up to 21 days, respectively) (Browne et al., 2008; Farrell & Nelson, 2013; Watts et al., 2014).

The transfer of sorbed chemical pollutants via MPs has been demonstrated in fish, crustaceans, annelids and bivalve molluscs (Besseling et al., 2013; Oliveira et al., 2013; Rochman et al., 2013a; Avio et al., 2015; Batel et al., 2016; 2018; Paul-Pont et al., 2016; Guilhermino et al., 2018; Pittura et al., 2018). However, the extent to which these co-contaminants cause harmful effects beyond those of the MPs alone is less clear. The common goby (*Pomatoschistus microps*) showed a significant decrease in the activity of acetylcholinesterase (AchE), when exposed to polyethylene (PE) both with and without pyrene (Oliveira et al., 2013), indicating no additional effects of the sorbed pyrene. However, in Japanese medaka (*Oryzias latipes)* a higher level of hepatic stress was induced in fish exposed to PS MPs with sorbed mixed environmental POPs compared to fish exposed to PS alone

(Rochman et al., 2013a). Meanwhile, pyrene contaminated PS and PE particles (<100 µm) increased the frequency of micronuclei and inhibited the activity of AchE relative to plastics alone in *M. galloprovincialis* (Avio et al., 2015). Paul-Pont et al. (2016) observed mixed effects in *Mytilus spp*. whereby PS microspheres alone had greater effects than PS with sorbed fluoranthene for certain biomarkers, whilst the reverse was true for other biomarkers. Mixed effects on different biomarkers in *M. galloprovincialis* exposed to low density polyethylene (LDPE) and LDPE with sorbed BaP were also reported by Pittura et al. (2018) but, overall, using the integrative weight of evidence model, LDPE with sorbed BaP was classified as exerting greater hazard than LDPE MPs.

Clearly further work is required to elucidate the effects of a variety of contaminant-plastic combinations in a variety of species using a wide range of plastic sizes. Benzo(a)pyrene (BaP) is a priority pollutant (US EPA 2014, UE 2008) and has been widely used as a model PAH in ecotoxicology (Banni et al., 2017); it is both genotoxic and carcinogenic and can be found throughout the marine environment (Di et al., 2017). BaP has been reported to cause peroxisome proliferation, oxidative stress, endocrine disruption and genotoxic effects in mussels (Venier et al., 1997; Cancio et al., 1998; Gómez-Mendikute et al., 2002; Orbea et al., 2002; Banni et al., 2017). Because of its highly lipophilic nature BaP has been shown to strongly sorb to MPs and to be transferred via MPs to Artemia and then transfer up the food chain from Artemia to zebrafish (Batel et al., 2016).

This study aimed to examine the effects of long-term (26 day) dietary exposure of two different sized PS microspheres (4.5 µm and 0.5 µm) alone and with sorbed BaP in mussels *M. galloprovincialis* in order to elucidate the influence of MP size and the presence of sorbed BaP on the organism at different levels of biological organization. An increasing number of studies have used a variety of biomarkers to investigate the effects of MPs and their co-contaminants at cell and molecular levels. Biomarkers are generally used to predict changes at higher levels of biological organization and have been defined as “short-term indicators of long-term biological effects” (Cajaraville et al., 2000). However, in the case of emerging pollutants such as MPs it is important to evidence links between effects at cellular or subcellular levels such as oxidative stress and effects at a whole organism level such as effects on growth, reproduction or survival (Tsangaris et al., 2008). Hence this study adopted a battery of biomarkers approach and assessed effects using biomarkers for cell viability, oxidative stress, genotoxicity and structure and cell type composition of digestive tubules, together with histopathological analysis and measurement of effects on overall organism health (SFG and condition index). Bioaccumulation of BaP in mussel tissues and tissue distribution of MPs alone and

with sorbed BaP were also investigated.

2. MATERIALS AND METHODS

2.1. Sampling and maintenance of mussels

Roughly 600 mussels Mytilus galloprovincialis of 3.5-4.5 cm shell length were collected on the 1st of February 2017 from Plentzia, Bay of Biscay (43°24´N, 2°56´W), a relatively clean area (Orbea & Cajaraville, 2006; Bellas et al., 2011; 2014,) and maintained in aquarium facilities at the Plentzia Marine Station (PiE) of the University of the Basque Country (UPV/EHU). According to Ortiz-Zarragoitia et al. (2011) mussels from the sampling area are at advanced gametogenesis in February and spawning starts in March, with a peak in April. Thus, the experimental period was selected to avoid the cold temperature period where mussels remain metabolically less active (Cajaraville et al., 1995; Cancio et al., 1999) while at the same time avoiding spawning and post-spawning stress (Bayne, 1976).

Seawater from Plentzia was naturally filtered by sand in the uptake wells aided with a pump that sent the water to the Marine Station. Seawater gas balance was controlled in the Station and then passed through a decantation/inertial tank and filtered (particle size ≤3 μm). Mussels were fed with microalgae *Isochrysis galbana* (T-Iso clone) grown in 2 x 40 L plastic culture bags, in a room with controlled temperature at 20°C under white fluorescent light (GRO-LUX 36W) with constant aeration. Commercial F2 algae medium (Fritz Aquatics, USA) was supplied to algae cultures according to manufacturer´s instructions. Under these conditions, sufficient cells were produced to allow for 10 L of pure culture (cell density ~ $8x10^6$ algae cells/mL) to be used each day to feed mussels.

After collection mussels were placed in a single 600 L recirculating seawater system for 6 days without feeding. Then, 110 mussels were distributed in each of 5 static glass aquaria with 40 L seawater and maintained for a further 15 days (light regime 12L/12D, temperature: 13°C). Water was changed daily. Feeding conditions during both the acclimation period and subsequent exposure period were set to provide mussels with food around the maintenance ration (1.5% of soft body weight per day in mussels *Mytilus* of the size used in this study; Bayne et al., 1976). Assuming feeding (clearance) rates of 3 L/h per individual mussel, this was achieved by dosing the concentrated stock

of the pure phytoplankton culture by means of a multi-channel peristaltic pump (Ismatec, Glattbrugg, Switzerland), at rates set to produce a stable particle concentration of 2500 algal cells/mL in the tanks. Mussels were fed this ration over a period of 22 hours/day. Actual tank cell concentration during the acclimation period, recorded with a Coulter Counter Z1 (Beckman, Indianapolis, USA) in water samples taken twice a day (immediately before and 2 hours after the water change), ranged from 2500 to 5000 cells/mL, which represents 1 to 2 times the maintenance ration.

During both the acclimation and exposure period all tanks were rinsed with 10 L of seawater during the water change each day in order to prevent the buildup of mussel faeces at the bottom of tanks. Additionally all mussels were checked to ensure that they had closed their valves when exposed to air and post water change all tanks were checked to ensure that mussels had reopened their valves. Water quality parameters were checked daily during the fed portion of the acclimation period in all tanks and in the control tank throughout exposure. Salinity remained stable throughout the experiment and acclimation period at 33 PSU (±0.2) as did pH 8.00 (±0.05), dissolved oxygen >80% and 6.66-8.05 mg/L and NH_4 and NH_3 levels, which were below the threshold for chronic toxicity.

2.2. MPs source and preparation of MPs alone and with sorbed BaP

The plastics chosen for this experiment were unlabeled polystyrene microspheres (Polyscience Inc.; Badener, Germany density 1.05 g/cm^3) of two sizes: 4.5 µm (LMP) and 0.5 µm (SMP). MPs and NPs with sorbed BaP (LMPB and SMPB, respectively) were prepared according to Batel et al. (2016) with adaptations described below. 24 hours prior to the start of each exposure, 89.2 µL of LMP stock (4.9 x 10^8 particles/mL) was added to each of two aluminum foil wrapped glass vials containing 10 mL of Milli-Q water in order to create the particle suspensions for the LMP and LMPB treatments. This process was then repeated with the SMP stock (3.64 x 10^{11} particles/mL) for the SMP and SMPB treatments. 10 µL of 1 mM BaP (Sigma, St. Louis, Missouri) was then added to each the LMPB and SMPB vials to get a final concentration of 1 µM (252 µg/L) BaP solution containing 0.01% dimethyl sulfoxide (DMSO, purity >99% Sigma, St. Louis, Missouri). All vials were then incubated for 24 hours at 300 rpm in an orbital shaker at 18ºC in darkness. These suspensions were then syringe filtered using sterile 0.45 µm and 0.2 µm pore sized filters (Merck Millipore, Darmstadt, Germany) for the LMPB and SMPB treatments, respectively. The plastics were then resuspended in 40 mL of Milli-Q water and added to the algae feed for each respective mussel treatment. This procedure was repeated every day during the 26 day exposure experiment to ensure reproducible dosing of freshly

contaminated MPs and NPs to mussels. Non-contaminated pristine MPs and NPs were incubated, filtered and resuspended in the same way but in Milli-Q water alone. All solutions containing BaP were stored in glass vials wrapped in aluminum foil.

The sorption capacity of the PS microspheres used in this study for BaP has been reported in a separate study (Martínez-Álvarez et al., 2018). According to the Langmuir model, the maximum adsorption capacity (Q_{max}) ranged from 144.99 to 242.89 μg/g and from 30.5 to 67.65 μg/g for 0.5 μm NPs and 4.5 μm MPs, respectively.

2.3. Mussel exposure experiment

After acclimation, mussels were exposed to MPs and NPs alone and with sorbed BaP according to the following experimental groups: Control, 4.5 μm MPs alone (LMP), 0.5 μm NPs alone (SMP), 4.5 μm MPs with BaP (LMPB) and 0.5 μm NPs with BaP (SMPB). MPs and NPs were provided daily, mixed with algae, at equivalent mass of 0.058 mg/L, corresponding to 1000 particles/mL for 4.5 μm MPs and to $7.44x10^5$ particles/mL for 0.5 μm NPs) during 26 days. Selected concentrations are environmentally relevant according to Eriksen et al. (2013) and Lechner et al. (2014).

During exposure mussels were fed continuously with *I. galbana*, at the same rations administered during the acclimation period. Mussels were exposed to plastics together with algae and a daily water change was performed. The control aquaria received pure algae whereas the exposure aquaria received algae mixed with plastics (with/without BaP). Aeration was used to keep both plastics and algae in suspension. During the experiment, mortality recorded in each exposure group was 3 mussels in the LMP group, 4 in the SMPs, 1 in the LMPB and 3 in the SMPB. No mortality was recorded in control mussels.

Mussel sampling and dissection took place after 7 and 26 days exposure. 15 individuals were taken per experimental group and frozen whole at -40°C for analysis of BaP burden in tissues by GC-MS. Hemolymph was withdrawn from the posterior adductor muscle of 8 mussels per experimental group and used to measure neutral red (NR) uptake, catalase activity (CAT) and DNA damage (Comet assay). Another 10 mussels per experimental group were dissected and half of their digestive gland, gills and gonad preserved in formalin and processed for paraffin histology. The other halves of digestive glands were frozen in liquid nitrogen for cryostat histology. Finally, 7 individuals were taken

per experimental group for the analysis of SFG. Following sampling on day 7 dosing of algae was recalculated in order for maintenance rations to remain the same for the reduced number of mussels present in the tanks.

2.4. Bioaccumulation of BaP in mussel soft tissues

Whole mussels for chemical analysis (15 per experimental group) were stored at -40°C and analyzed at the General Services SGiker of UPV/EHU for BaP determination using GC-MS (SIM mode). The lyophilized tissues were homogenized and then extracted using a MARX microwave (CEM, Mathews, NC, USA) and cleaned through solid phase extraction (SPE Vacuum Manifold System, Millipore). The extracts obtained were concentrated through evaporation with nitrogen flow, filtered and encapsulated in chromatographic vials. Concentration of BaP was measured in an Agilent (6890) Gas Chromatograph with Mass Detector (Agilent 5975C) (Navarro et al., 2008) and given in ng/g dry weight. Calibration standards were obtained from Dr. Ehrenstorfer GmbH (Augsburg, Germany) and regression coefficients obtained for the calibration curves were always above 0.995. Limit of quantification for BaP was 1 ppb.

2.5. Tissue distribution of MPs in mussels

Digestive gland, gills and mantle tissue of 10 mussels per experimental group were dissected out. Half of the digestive gland, half of the gills and whole mantle were fixed in 4% formalin in individual cassettes and processed using an alternative tissue dehydration protocol which utilizes N-butyl alcohol (Stiles, 1934) in order to prevent the degradation of the PS microspheres by the organic solvents used in the standard histology tissue processing procedure. Then, samples were embedded in paraffin and sections of 5 µm thickness were cut in a Leitz 1512 microtome (Leica Instruments, Wetzlar, Germany). For staining, slides were placed in a heater at 130°C for 10 minutes and then immersed in N-butyl alcohol at 60°C for another 10 minutes to remove the paraffin. Then, slides were re-hydrated in a series of decreasing alcohol concentrations and stained with hematoxylin/eosin (Gamble & Wilson, 2002). Sections were observed under a BX51 light microscope (Olympus, Tokyo, Japan) and the prevalences of mussels showing MPs in the digestive gland, gills and gonad were calculated as percentages. For the quantification of the number of MPs in the digestive gland, one section containing the digestive tract was selected per mussel.

2.6. Cellular biomarkers in mussel hemocytes

On each sampling day, the hemolymph of 8 mussels per treatment was withdrawn from the

posterior adductor muscle and immediately cell viability, catalase activity and DNA damage were measured in hemocytes of individual mussels.

Neutral red (NR) uptake was assessed in hemocytes according to Borenfreund & Puerner (1985) with modifications as explained below. The assay is based on the incorporation of a cationic neutral red dye into the lysosomes of live cells. Hemolymph of 8 animals per group was collected and seeded into 4 replicates in a 96-well flat bottom microplate. Cells were kept at 18 °C in a FRIOCELL incubator (MMM group, Planegg, Germany) for 30 minutes in order to allow cell attachment. Afterwards, cells were incubated with NR solution (0.04% in PBS, pH 7.3–7.4) for 1 hour in the same incubator, and washed several times with PBS to eliminate non-incorporated dye. Then, NR was extracted from intact cells using an acetic acid (0.5%) ethanol (50%) solution and absorbance was measured at 550 nm in a Biotek EON microplate reader (Winooski, USA). Cell concentration was determined in the hemolymph of each animal using a Bright-Line™ Hemacytometer (Sigma Aldrich, St. Louis, USA) and used to normalize absorbance data.

Catalase activity (CAT) was assessed according to Aebi et al. (1984) with modifications as explained below. The method is based on the conversion of H_2O_2 into H_2O and O_2 by catalase. Hemolymph of 8 animals per group was centrifuged at 300 *g* for 10 minutes at 4°C, and pellets were resuspended and homogenized in TVBE buffer (1 mM sodium bicarbonate, 1 mM EDTA, 0.1% ethanol and 0.01% Triton X-100, pH 7.4) and stored at -80°C for further analysis. Then, samples of each animal were added into 4 replicates in a UV/VIS 96-well microplate and consumption of H_2O_2 (20 mM H_2O_2 in 50 mM phosphate buffer pH 7) was measured every 22 seconds during 4 minutes at 240 nm in a Bio-tek EL 312 microplate reader (Winooski, USA). Protein concentration was measured in each sample following Lowry et al. (1951) and used to normalize absorbance data. CAT activity was expressed as ΔAbs. mg protein^{-1}.

The Comet assay was performed on mussel hemocytes following Raisuddin & Jha (2004) with modifications, as described in Katsumiti et al. (2015). Briefly, hemolymph of 8 animals per group was centrifuged at 300 *g* for 10 minutes at 4ºC and pellets were resuspended in 0.5% low melting point agarose and placed on slides coated with 1% normal agarose. Slides were kept at 4°C for 10 minutes in order to allow agarose solidification. Slides were then immersed in chilled lysis solution (2.5 M NaCl, 100 mM EDTA, 10 mM Tris base, 1% N-lauroyl-sarcosine, 1% Triton X-100, 10% DMSO; pH 10)

for 1 hour at 4°C in the dark to remove cellular proteins. Afterwards, slides were washed with distilled water and transferred to a tank containing a chilled electrophoresis solution (1 N NaOH and 200 mM EDTA; pH 13) and kept for 20 minutes to allow alkaline DNA unwinding. Electrophoresis was carried out at 300 mA, 25V for 30 minutes in the same electrophoresis solution. Then, slides were incubated with neutralization buffer (0.4 M Tris-HCl; pH 7.5) and fixed with chilled methanol for 3 minutes. For analysis, slides (2 per animal) were stained with ethidium bromide (10 μg/L) and 50 randomly selected cells per slide were analyzed under an Olympus BX61 fluorescence microscope (Hamburg, Germany) and scored using the Komet 5.5 imaging software (Andor Bioimaging, Liverpool, UK). DNA strand breaks were determined as percentage of DNA in the comet tail.

2.7. Lysosomal enzyme histochemistry in mussel digestive gland

Samples of digestive gland for lysosomal enzyme histochemistry were frozen in liquid nitrogen and stored at -80°C. The 10 digestive gland samples per experimental group were frozen together in two plastic chucks, each containing 5 half digestive glands attached to the chuck with cryoMbed. Eight 10 μm sections were cut using a Leica CM 3050 S cryostat (Leica Instruments, Wetzlar, Germany), frozen and stored at -80°C. The obtained sections were then stained for lysosomal β-hexosaminidase activity according to UNEP-RAMOGE (1999). Additional serial sections from control mussels at day 7 were stained in the same way but without the substrate β-N-acetylhexosaminide and also stained for lipofuscins using the Schmorl´s reaction according to Pearse (1972).

2.8. Cell composition, quantitative structure and histopathology of mussel digestive gland

For these analyses, digestive gland paraffin sections stained with hematoxylin/eosin described in section 2.5 were used. Cell composition of digestive tubules was measured in terms of volume density of basophilic cells (VvBAS, given as $\mu m^3/\mu m^3$) and the structure of digestive tubules was quantified as mean epithelial thickness to mean diverticular radius (MET/MDR, μm/μm) and mean luminal radius to MET (MLR/MET, μm/μm) by using a stereological method (Bignell et al., 2012; De los Ríos et al., 2013). Hits on basophilic cells, digestive cells and lumen of digestive tubules were recorded using a modified Weibel graticule (multipurpose test system M-168) with a drawing-tube attached to a Leitz Laborlux S microscope (Stuttgart, Germany) using a 40x magnification in 3 fields per section in 10 mussels per experimental group. Then, the different parameters were calculated as described in Bignell et al. (2012).

Prevalences of general histopathological alterations were recorded for the same 10 mussels per

experimental group and given as percentages. The following alterations were recorded: occurrence of parasites, fibrosis in the connective tissue, necrosis of digestive tubule epithelium, focal and diffuse hemocytic infiltrations, presence of brown cells in connective tissue and brown aggregates in epithelium of the digestive tract (Garmendia et al., 2011; Bignell et al., 2012; Ruiz et al., 2014).

2.9. Gamete development, gonad index and histopathology of mussel gonad

For this, mantle paraffin sections stained with hematoxylin/eosin described in section 2.5 were used. Six gamete developmental stages were distinguished according to Seed (1969) and a gonad index value was assigned to each mussel following Kim et al. (2006) in one section per mussel and 10 mussels per experimental group. The gonad index ranged from 0 (resting gonad) to 5 (mature gonad), showing increasing GI values (0 to 5) during gametogenesis phases and decreasing GI values (5 to 1) at spawning and post-spawning phases.

Prevalences of general histopathological alterations were recorded for the same 10 mussels per experimental group and given as percentages. The following alterations were recorded: occurrence of parasites, fibrosis in the connective tissue, focal and diffuse hemocytic infiltrations and oocyte atresia (Ortiz-Zarragoitia & Cajaraville, 2006; 2010; Ruiz et al., 2014). For oocyte atresia, the following semiquantitative scale was used: 0 normal gonad, 1 less than half the follicles are affected, 2 about half the follicles are affected, 3 more than half the follicles are affected and 4 all follicles affected (Kim et al., 2006).

2.10. Whole organism responses

On each sampling day, 7 mussels from each treatment were collected to measure the physiological parameters and condition index. To this end, mussels from each treatment were placed in separate 20 L aerated static tanks filled with clean seawater. To allow for individual collection of biodeposits, each mussel was placed inside a 250 mL chamber, completely submerged. Feeding conditions prior (12 h) and during physiological measurements (2 days) were set to allow for rates of fecal production to be compatible with measurements of absorption efficiency (AE) based on gravimetric determinations. On the other hand, ashed silt particles (<30 μm) were added to *I. galbana* cultures to fulfill the requirements for an inorganic tracer in measurements of AE with the Conover method. This mixed diet (~70% organic content) was dosed to the feeding tanks by means of a multi-channel peristaltic pump (Ismatec, Glattbrugg, Switzerland), at a rate set to provide for particle concentrations of 15,000 particles/mL. Feeding conditions were maintained stable by frequent

checking of particle concentration using a Coulter Counter Coulter Z1 (mean of 3 replicates) and adjustment of pumping rates. Actual concentrations across all experiments ranged between 10,000 and 30,000 particles/mL, above the threshold to produce sufficient faeces and below the threshold for pseudofaeces production (Navarro et al., 1996).

Clearance rate (CR: L/h) was measured as volume of water cleared of particles per animal per hour according to Coughlan's (1969) method, based on recording the exponential decrease of particle concentration over the time in a static system. For each treatment, 8 beakers filled with 2.5 L seawater provided with gentle aeration were used: i.e. 7 replicates each containing 1 mussel and 1 control for sedimentation. Each replicate was sampled for particle concentration (Coulter Counter Z1) at least 6 times at 10-20 minute intervals. Respiration rate (RR: J/h) was used as a proxy for metabolic rate and was estimated from rates of O_2 consumption according to Gnaiger (1983). Individual mussels (n = 7) were placed in sealed 250 mL chambers, fitted with O_2xyDot®Sensor and filled with seawater. O_2 concentration was recorded using an Oxygen Analizer (OxySense 5250i, New Castle, UK), every 10 minutes for at least 7 times and the mean average of two O_2 measurements from each sampling point was used. One control (chamber without animal) was used with each treatment for checking O_2 concentration stability. Absorption efficiency (AE: fraction) was measured according to Conover's (1966) method based on the ratio of organic contents in food and faeces. To characterize food suspensions, duplicate water samples (0.8 to 2.5 L) taken from the feeding tanks were filtered onto ashed, pre-weighted Whatman® GF/C glass-fiber filters (Sigma-Aldrich, St. Louis, Missouri, USA), which were subsequently processed to determine concentrations of total particulate matter (TPM: mg/L) and inorganic and organic particulate matter (PIM and POM: mg/L). Salts retained in the filters were rinsed out with a solution of isotonic ammonium formate, then filters were dried at 110°C, weighed, ashed at 450°C and weighed again. TPM and PIM were estimated, respectively, as the dry and ash weight increment of the filters and POM as the weight loss of this filtered material on ashing. Organic content (OC) was estimated as POM/TPM. For faeces collection mussels were allowed to acclimate to the stable particle concentrations in each treatment for at least 12 hours before individual chambers were cleared of any solid material. Mussels were then left to feed and faeces produced collected by pipette. Faeces were then filtered onto ashed, pre-weighted GF/C glass-fiber filters and processed for organic content determination as indicated for food suspensions. Absorption rate (AR J/h) was computed as the product of CR (L/h), POM (mg/L), AE (fraction) and the energy content of food (= 18.75 J/mg POM for *I. galbana* cells; Whyte, 1987). Scope for growth (SFG: J/h) was then calculated as AR – RR (Navarro et al., 1991).

After physiological determinations soft tissues of each animal were excised from the shells, dried at 80°C for 24 hours and weighted. Physiological rates were then standardized to the mean dry weight of mussel´s tissue (0.2646 g) using size-scaling b values of 0.67 and 0.75 for CR and RR, respectively (Navarro et al., 1991). Mussel shell lengths were also recorded with vernier caliper and a condition index calculated as: tissue dry weight (g)/[shell length (cm)] ^{3}.

2.11. Data analysis

All data were tested for normality and homogeneity of variance using the Ryan-Joiner and Levene's tests, respectively. Normally distributed data which met the assumptions of homogeneity of variances were assessed via two-way ANOVAs with treatment and sampling day as factors and treatment x day as an interaction. Where differences were found at a $p<0.05$ significance level, Tukey's HSD post hoc test was used to find the source of any differences observed. Data which did not met the above assumptions were analyzed by separate one-way Kruskal-Wallis tests to look for differences between treatments within days, and by Mann-Whitney U-tests to look for differences between days within treatments. Where differences were found at a $p < 0.05$ significance level in the Kruskal-Wallis test, Dunn's post hoc tests were used to determine the source of the observed differences. Parametric tests were analyzed in Minitab 17 (Minitab Inc) and non-parametric tests were analyzed in SPSS 24 (IBM Analytics, Armonk, NY).

3. RESULTS

3.1. Bioaccumulation of BaP in mussel soft tissues

BaP concentrations were very low approaching detection limits in all control and plastic alone treatments (all <2.2 ng/g dry weight) across both sampling days (Table 1). At day 7 BaP concentrations increased in mussels exposed to plastics with sorbed BaP, values ranging from 17.3 to 66.7 ng/g dry weight (Table 1) thereby demonstrating the transfer of BaP from NPS and MPs to mussel tissues. BaP tissue concentrations were notably higher in both NPs and MP with sorbed BaP treated groups at day 26 compared to day 7 (96.1-306 ng/g dry weight) indicating the bioaccumulation of BaP in mussel tissues (Table 1). These differences amounted to an approximate 2.5 to 10 fold increase across days in BaP tissue burden in LMPB samples and a roughly 4 to 6 fold increase in SMPB samples. In addition, mussels in the SMPB treatment had considerably higher BaP

tissue burdens compared to LMPB treated mussels across both days. This difference remained roughly the same at day 26 compared to day 7, with SMPB treated mussels having roughly 2-4 fold greater BaP tissue burden compared to LMPB mussels at day 7 and a 2-3 fold greater BaP tissue burden at day 26.

Table 1. Bioaccumulation of benzo[a]pyrene (BaP) in mussel soft tissues (ng/g dry weight) in control mussels and in mussels dietarily exposed for 7 and 26 days to 4.5 µm MPs (LMP), 0.5 µm NPs (SMP), LMP with sorbed BaP (LMPB) and SMP with sorbed BaP (SMPB). Data are given for 15 mussels per experimental group in 2 replicates.

	CONTROL		**LMP**		**SMP**		**LMPB**		**SMPB**	
	1	**2**	**1**	**2**	**1**	**2**	**1**	**2**	**1**	**2**
7 d	<1	1.3	2.2	1.1	1	<1	37	17.3	54	66.7
26 d	2	<1	<1	2.1	1.3	1.4	96.1	163.7	306.7	277.4

3.2. Tissue distribution of MPs in mussels

4.5 µm MPs were localized and quantified in different tissues of mussels exposed to LMP and LMPB (Table 2). At least 80% of treated mussels presented MPs in the digestive gland in both treated groups. Only 10 to 40% of treated mussels showed MPs in gill tissues and these were only occasionally observed in gonad tissues (Table 2).

Table 2. Prevalence of mussels showing MPs in different tissues of control mussels and of mussels dietarily exposed to 4.5 µm MPs (LMP) and to LMP with sorbed BaP (LMPB) along 7 and 26 days. Data are shown as percentages of 8-10 mussels per experimental group (one section per mussel). Not observed, n.o.

	LOCALIZATION	**CONTROL**	**LMP**	**LMPB**
7 d	Digestive gland	n.o.	80	90
	Gills	n.o.	40	20
	Gonad	n.o.	10	20
26 d	Digestive gland	n.o.	90	100
	Gills	n.o.	20	10
	Gonad	n.o.	12.5	n.o.

In sections of the digestive gland, MPs were very abundant in the lumen of the stomach mixed with stomach contents (Figure 1A, Table 3). MPs were also found in the lumen of digestive tubules, associated to cell debris (Figure 1B) but at lower amounts than in the lumen of the stomach (Table 3). Occasionally individual MPs were observed within epithelial cells of the digestive tract (Figure 1C), ducts (Figure 1D) and digestive tubules (Table 3). Few MPs were also found isolated in the connective tissue (Figure 1D). In the gills, MPs were found interspersed between gill filaments (Figure 1E) but never within gill epithelial cells. In mantle sections, MPs were found in the connective tissue surrounding gonad follicles but not within the follicles. Overall, there was a high variability in numbers of MPs among different individuals in each exposure group (Table S1 of Supplementary material). The highest amount of MPs (120.60 ± 53.28) was found in mussels exposed to LMP for 7 days and the number of MPs decreased at 26 days in this group to 17 ± 10.57 particles (Table 3). Conversely, mussels exposed to LMPB treatment showed lower amounts of MPs at day 7 (11.70 ± 3.60) compared to the LMP group but numbers increased with exposure time up to 69 ± 41.91 particles (Table 3).

0.5 µm NPs were hardly seen in the histological sections of mussels exposed to SMP and SMPB. Only in few individuals large numbers of particle aggregates were observed in the lumen of the stomach, mixed with stomach contents.

Table 3. Tissue distribution of MPs in the digestive gland of mussels dietarily exposed to 4.5 µm MPs (LMP) and to LMP with sorbed BaP (LMPB) along 7 and 26 days. Data are shown as means and standard errors of the number of MPs in sections of the digestive gland of 10 mussels per experimental group (one section per mussel). Not observed, n.o.

	LOCALIZATION		**LMP**	**LMPB**
7 d	Stomach	Lumen food	126.78 ± 55.08	3.80 ± 1.78
		Lumen mucus	0.56 ± 0.36	0.20 ± 0.20
		Epithelium	1.67 ± 0.69	1.10 ± 0.53
	Ducts	Lumen	0.20 ± 0.13	0.40 ± 0.27
		Epithelium	0.10 ± 0.10	0.50 ± 0.31
	Digestive tubules	Lumen	0.80 ± 0.61	3.90 ± 3.11
		Epithelium	0.30 ± 0.21	0.10 ± 0.10
	Connective tissue		3.10 ± 1.16	1.70 ± 0.58
	Total MPs		**120.60 ± 53.28**	**11.70 ± 3.60**
	Total MPs within epithelial cells		**1.90 ± 0.84**	**1.70 ± 0.58**
26 d	Stomach	Lumen food	12.78 ± 11.06	56.90 ± 35.20
		Lumen mucus	0.78 ± 0.49	2.30 ± 1.99
		Epithelium	0.89 ± 0.42	2.30 ± 0.75
	Ducts	Lumen	2.40 ± 1.67	4.50 ± 4.50
		Epithelium	n.o.	0.30 ± 0.30
	Digestive tubules	Lumen	n.o.	0.80 ± 0.14
		Epithelium	n.o.	n.o.
	Connective tissue		1.16 ± 0.96	2.30 ± 1.11
	Total MPs		**17 ± 10.57**	**69 ± 41.91**
	Total MPs within epithelial cells		**0.80 ± 0.42**	**2.60 ± 0.91**

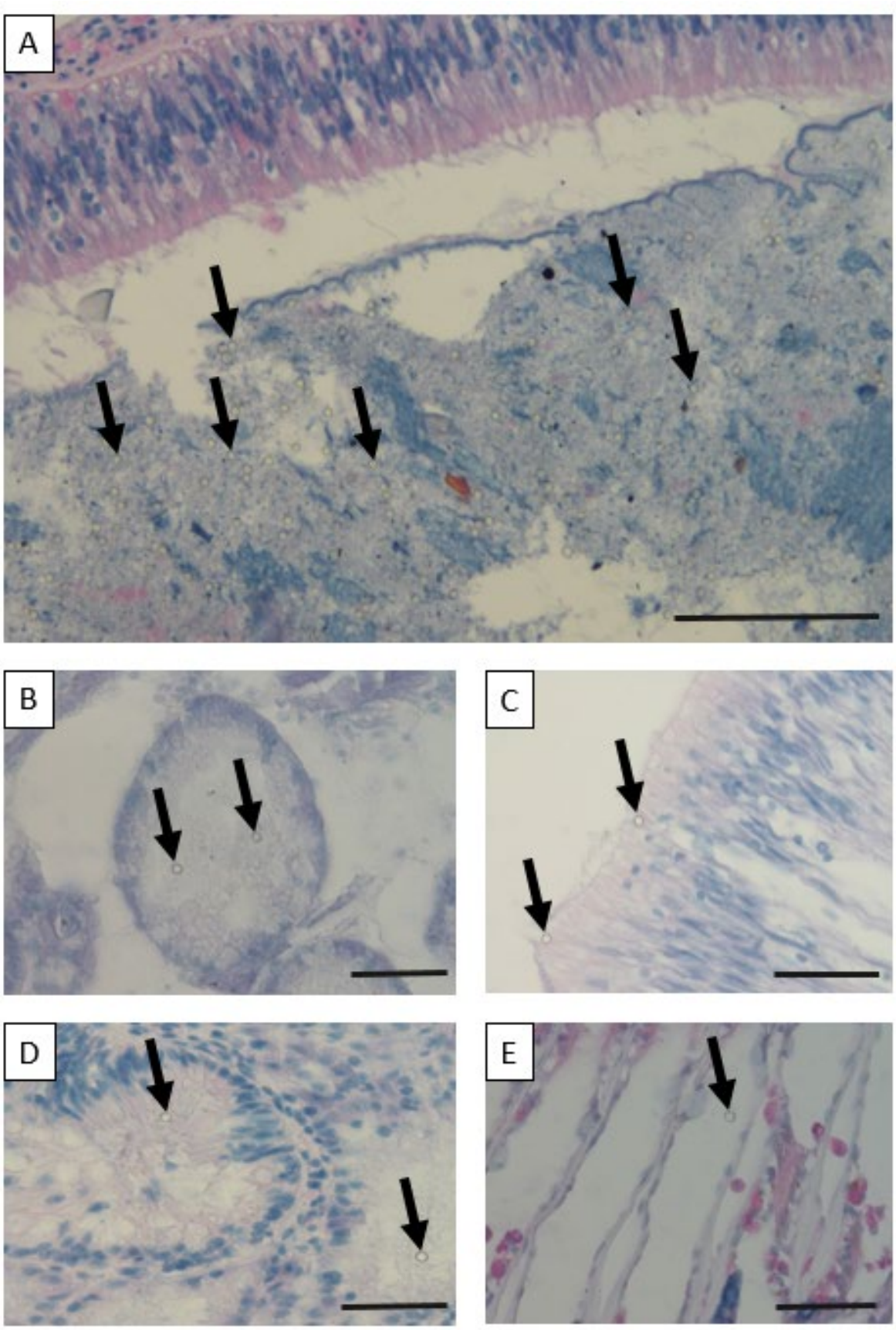

Figure 1. Bright field micrographs of mussel paraffin sections showing the presence of 4.5 µm MPs (black arrows) in: A) Stomach lumen of a mussel exposed to LMP for 7 days; B) Lumen of digestive tubule of a mussel exposed to LMPB for 7 days; C) Stomach epithelium of a mussel exposed to LMP for 7 days; D) Digestive duct and connective tissue of a mussel exposed to LMPB for 7 days; E) Gills of a mussel exposed to LMP for 7 days. Scale bars: A: 100 µm; B-E: 50 µm.

3.3. Cellular biomarkers in mussel hemocytes

There was no significant effect of any treatment on NR uptake at day 7. At day 26 hemocytes from mussels from both LMPB and SMPB groups showed a decrease in NR compared to controls, thereby indicating a decrease in cell viability in hemocytes from these treatments (Figure 2A). LMPB and SMPB treatments also showed a significant decrease in NR compared to their respective day 7 values. The reduced uptake of NR in the LMPB and SMPB groups can also clearly be observed in the micrographs in Figure 2B-F. Further, hemocytes from mussels in LMPB and SMPB groups showed altered morphology, cells becoming rounded and detaching from the substrate (Figs. 2E-F).

At day 7 there was a significant increase in CAT in hemocytes of both LMPB and SMPB mussels compared to the control (Figure 2G). However at day 26 this pattern was reversed, with hemocytes of mussels exposed to LMPB and SMPB showing a significant decrease in CAT compared to the control. LMPB and SMPB mussel hemocytes also showed significantly reduced CAT compared to their respective day 7 values (Figure 2G).

Background levels of DNA damage were observed in the control groups at mean values of 27.67%± SE 0.78 and 25.28% ± SE 0.76% tail DNA for days 7 and 26, respectively, and showed no significant change between days (Figure 3A). At day 7 the LMPB treatment displayed a significantly higher level of DNA damage as compared to the control and LMP treatment. At day 26 all treatments showed significantly higher levels of DNA strand breaks compared to the control except for LMPB which had higher than but not significantly different levels of DNA damage from the control. Highest levels of DNA damage were observed in the SMP treatment (mean 40.12% ± SE 0.72% tail DNA) which were also significantly higher than in the LMP treatment (mean 35.67% ± SE 0.71% tail DNA). There was no significant difference in DNA damage levels between SMP and SMPB mussels whereas levels in LMPB were significantly lower than in LMP mussels. DNA strand breaks increased significantly in LMP, SMP and SMPB treatments between day 7 and day 26. However in LMPB mussels DNA strand breaks decreased significantly from day 7 to day 26 (Figure 3A). Results shown in Figure 3A are illustrated in the fluorescence micrographs in Figs. 3B-F.

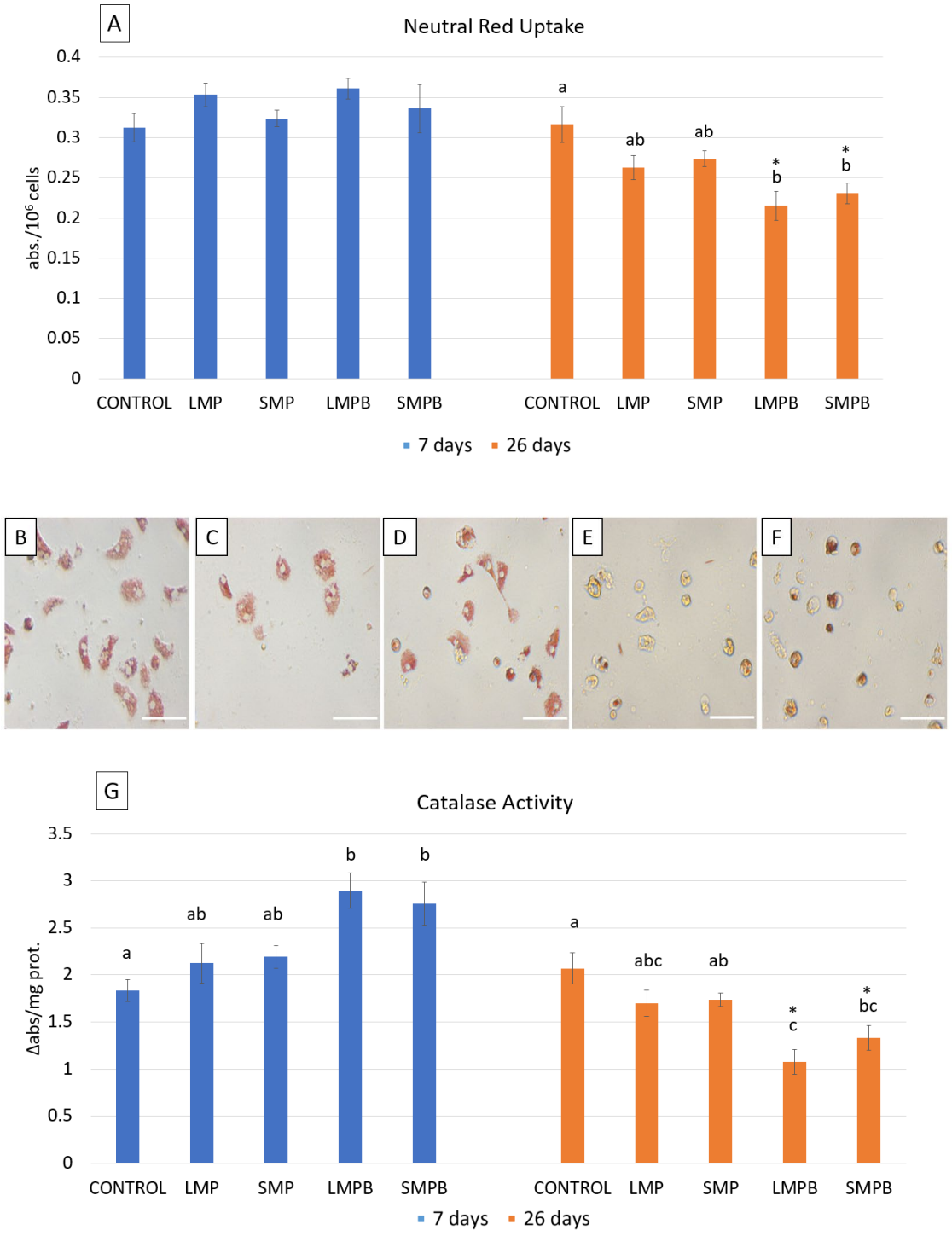

Figure 2: A: Neutral red uptake (given as absorbance/ 10^6 cells) and G: Catalase activity (given as absorbance difference/mg protein) in hemocytes of control mussels and in mussels dietarily exposed for 7 and 26 days to 4.5 µm MPs (LMP), 0.5 µm NPs (SMP), LMP with sorbed BaP (LMPB) and SMP with sorbed BaP (SMPB). Data are given as mean values and standard errors (8 mussels per experimental group, 4 replicates per mussel). Letters indicate significant differences among treatments within the same day (Kruskal-Wallis H test followed by Dunn's post hoc test, $p<0.05$). Asterisks indicate a significant difference between days within the same treatment (Mann-Whitney U test, $p<0.05$). B-F: Bright field micrographs of mussel hemocytes during the NR assay for hemocytes from control (B), LMP (C), SMP (D), LMPB (E), and SMPB (F) treatments at day 26. Scale bars: 50 µm.

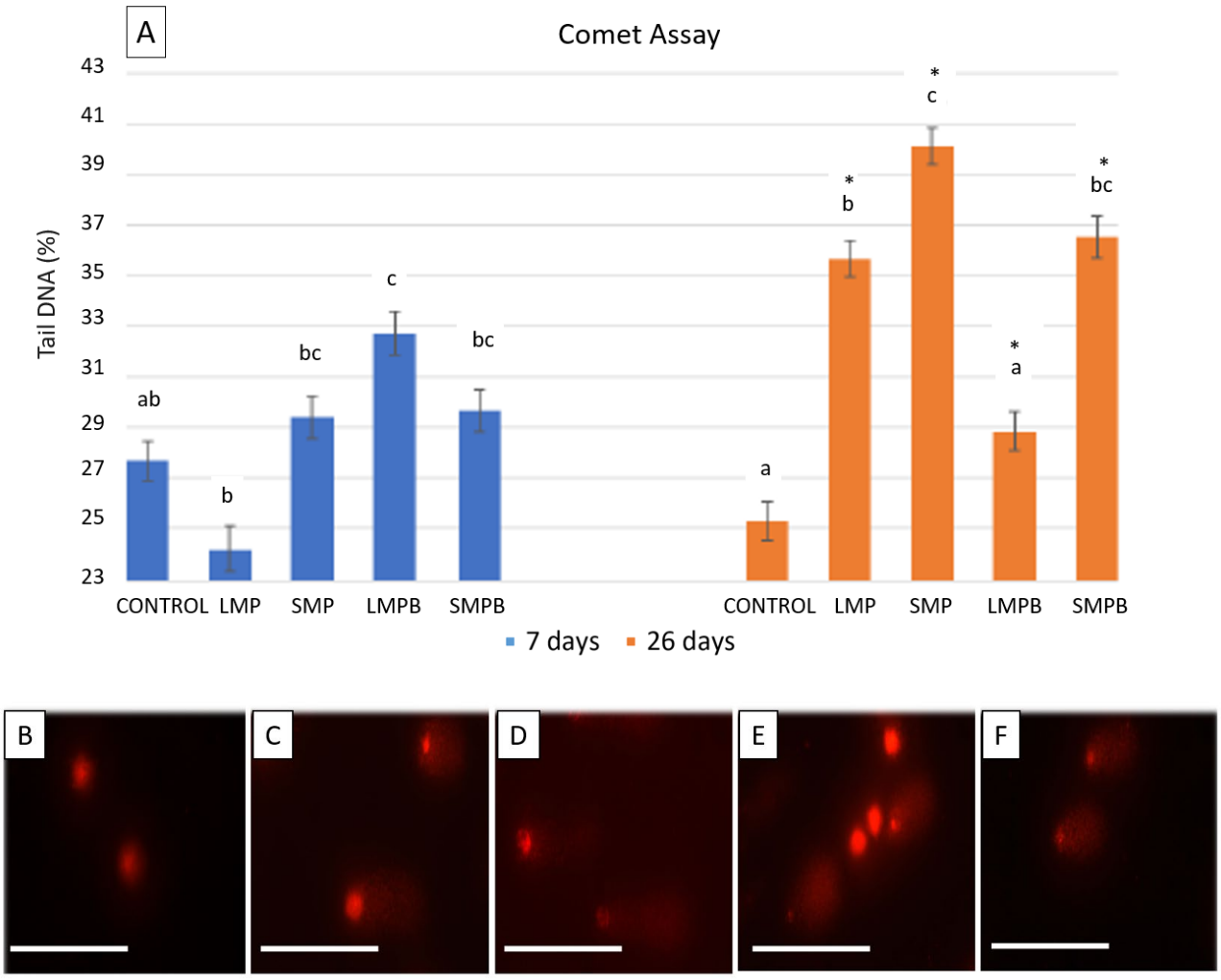

Figure 3: A: DNA strand breaks (given as % tail DNA) in hemocytes of control mussels and in mussels dietarily exposed for 7 and 26 days to 4.5 µm MPs (LMP), 0.5 µm NPs (SMP), LMP with sorbed BaP (LMPB) and SMP with sorbed BaP (SMPB). Data are given as mean values and standard errors (8 mussels per experimental group, 50 cells in 2 slides per mussel). Letters indicate significant differences among treatments within the same day (Kruskal-Wallis H test followed by Dunn's post hoc test, $p<0.05$). Asterisks indicate a significant difference between days within the same treatment (Mann-Whitney U test, $p<0.05$). B-F: Comet assay fluorescence micrographs displaying typical levels of DNA strand breaks for hemocytes from control (B), LMP (C), SMP (D), LMPB (E), and SMPB (F) treatments at day 26. Scale bars: 100 µm.

3.4. Lysosomal enzyme histochemistry in mussel digestive gland

Although the staining procedure for the lysosomal membrane stability test worked and lysosomes containing hexominidase activity could clearly be seen (Figs.4 A,B), a very strong yellow-brown background staining was present in digestive tubule cells in all treatments. The level of this staining was too high to be able to clearly distinguish staining level of lysosomes and hence determine lysosomal membrane labilization period. Background staining was also high in serial cryostat sections of 5 control digestive glands from day 7 stained for hexominidase activity but without the substrate β-N-acetylhexosaminide (Figs. 4C,D). This, along with the observation of unstained sections within the same series (Figs. 4E,F), confirmed that the staining observed was not an artefact and appeared to correspond to lipofuscin-like pigments, which can accumulate in lysosomes as the indigestible end product of intracellular digestion and have a yellow-brown coloration. This was confirmed by the Schmorl's reaction and lipofuscin like pigments were clearly seen as the indigo stained inclusions within the epithelial cells of the digestive tubules (Figs. 4G,H). Lipofuscin levels in the digestive gland of control mussels were too high to clearly distinguish differences in lipofuscin accumulation between treatments.

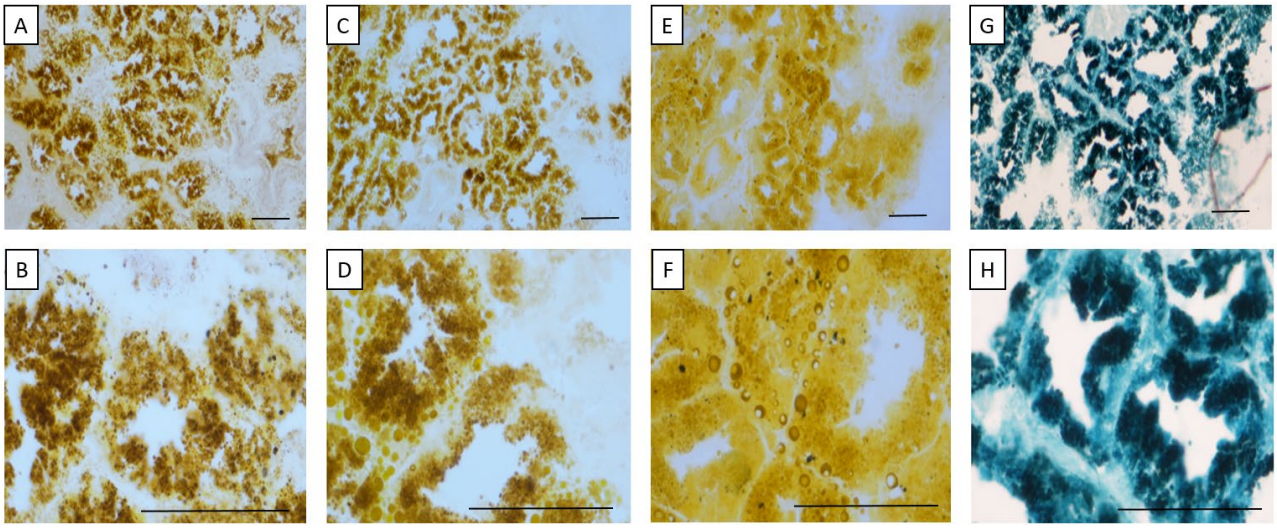

Figure 4: Bright field micrographs of serial cryostat sections of the digestive gland of control mussels from day 7 with different stains to illustrate high degree of background staining and presence of lipofuscins: A,B) histochemical detection of lysosomal β-hexosaminidase activity; C,D) same as A, B but omitting incubation with the substrate; E,F) unstained; and G,H) Schmorl´s reaction for lipofuscins. Scale bars: 100 µm.

3.5. Cell composition, quantitative structure and histopathology of mussel digestive gland

In general, in both control and treatment groups, the appearance of digestive tubules indicated a high digestive activity. In many tubules, cells in digestive epithelia were very high and contained a great number of large vesicles that obliterated the lumen (Figs. 5A,B,C). In other tubules, the digestive epithelium was thin and the large lumen appeared full of cell debris (including entire digestive cells). Tubules with totally disorganized necrotic areas were also observed (Figure 5B) in a single mussel each in treatments LMP at 7 days and LMP and SMP at 26 days (Table 4). Low prevalences of inflammatory responses such as fibrosis (Figure 5C), hemocytic infiltration (Figure 5D) and accumulation of brown cells in the connective tissue (Figure 5E) and in the epithelium of the digestive tract (Figure 5F) were observed in mussels exposed to MPs and NPs alone or with sorbed BaP in both sampling times (Table 4). The parasite *Mytilicola intestinalis* was observed in the digestive tract of a relevant number of individuals but there were no clear trends of parasite prevalence with treatments or along the exposure time (Table 4).

At day 7 of exposure, the volume density of basophilic cells (VvBAS) was significantly higher in mussels exposed to SMP and SMPB compared to the controls and to mussels exposed to LMP (Figure 6A). No significant differences were observed at day 26 of exposure with respect to controls, but a significantly higher VvBAS was recorded in mussels exposed to SMP in comparison to mussels exposed to LMP. No significant differences in VvBAS were recorded along the exposure within each treatment (Figure 6A).

Regarding the two parameters indicative of the structural integrity of the digestive tubules, mean epithelial thickness to mean diverticular radius (MET/MDR) and mean luminal radius to mean epithelial thickness (MLR/MET), no differences among treatments were observed at day 7 of exposure (Figs. 6B,C). At day 26 of exposure, mussels exposed to SMPB displayed significantly lower MET/MDR and higher MLR/MET than mussels treated with SMP. Values of MET/MDR decreased significantly between days 7 and 26 in LMP and SMPB mussels whereas MLR/MET increased significantly with time in SMPB (Figs. 6B,C).

Table 4. Prevalence of histopathological alterations in digestive gland of control mussels and of mussels dietarily exposed for 7 and 26 days to 4.5 µm MPs (LMP), 0.5 µm NPs (SMP), LMP with sorbed BaP (LMPB) and SMP with sorbed BaP (SMPB). Data are shown in percentages of 10 mussels per experimental group (one section per mussel). Not observed, n.o.

		CONTROL	LMP	LMPB	SMP	SMPB
7 d	Fibrosis	n.o.	10	10	n.o.	30
	Hemocytic infiltration Local	n.o.	n.o.	10	20	10
	Hemocytic infiltration Diffuse	n.o.	n.o.	n.o.	10	10
	Brown cells in connective tissue	n.o.	n.o.	10	10	n.o.
	Brown aggregates in epithelium of digestive tract	n.o.	n.o.	n.o.	10	10
	Necrosis	n.o.	10	n.o.	n.o.	n.o.
	Parasites	20	50	n.o.	20	20
26 d	Fibrosis	n.o.	n.o.	10	n.o.	n.o.
	Hemocytic infiltration Local	n.o	n.o	10	10	10
	Hemocytic infiltration Diffuse	n.o.	10	n.o.	n.o.	n.o.
	Brown cells in connective tissue	n.o.	10	n.o.	n.o.	10
	Brown aggregates in epithelium of digestive tract	n.o.	n.o.	n.o.	n.o.	20
	Necrosis	n.o.	10	n.o.	10	n.o.
	Parasites	20	40	20	20	10

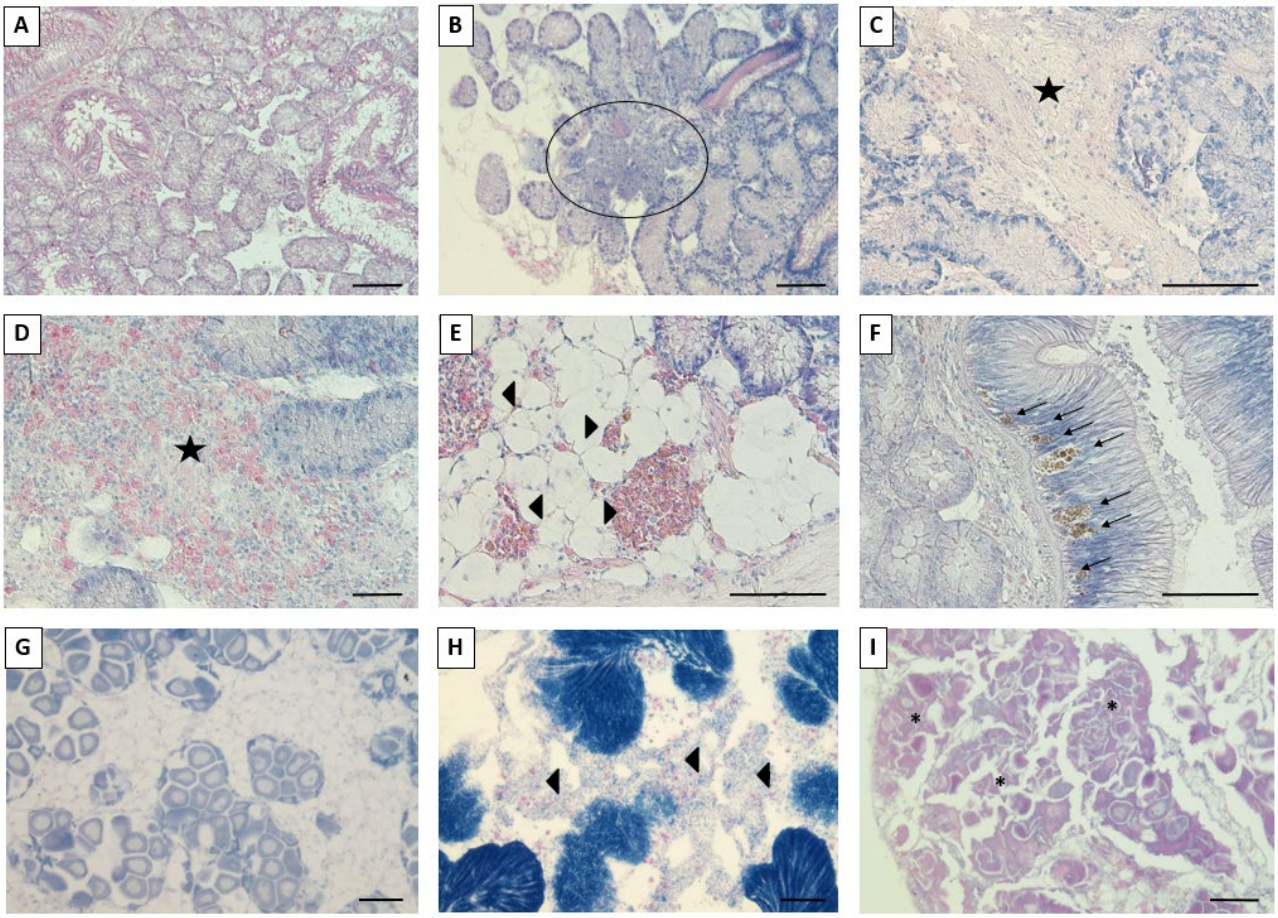

Figure 5: Bright field micrographs of mussel paraffin sections showing histopathological alterations in mussels digestive glands and gonads: A) control mussel at day 7; B) mussel after 7 days of exposure to LMP showing a necrotic area (encircled) in digestive tubules; C) mussel after 7 days of exposure to LMP showing fibrosis in the connective tissue (star); D) mussel after 7 days of exposure to SMP showing hemocytic infiltration (star); E) mussel after 7 days of exposure to LMPB showing accumulation of brown cells in connective tissue (arrow heads); F) mussel after 26 days of exposure to SMPB showing brown cell aggregations in the epithelium of digestive tract; G) Control female at day 7; H) male mussel after 7 days of exposure to SMP showing hemocytic infiltration (arrow heads); I) female mussel after 7 days of exposure to SMPB showing oocyte atresia (asterisks). Scale bars: 100 µm.

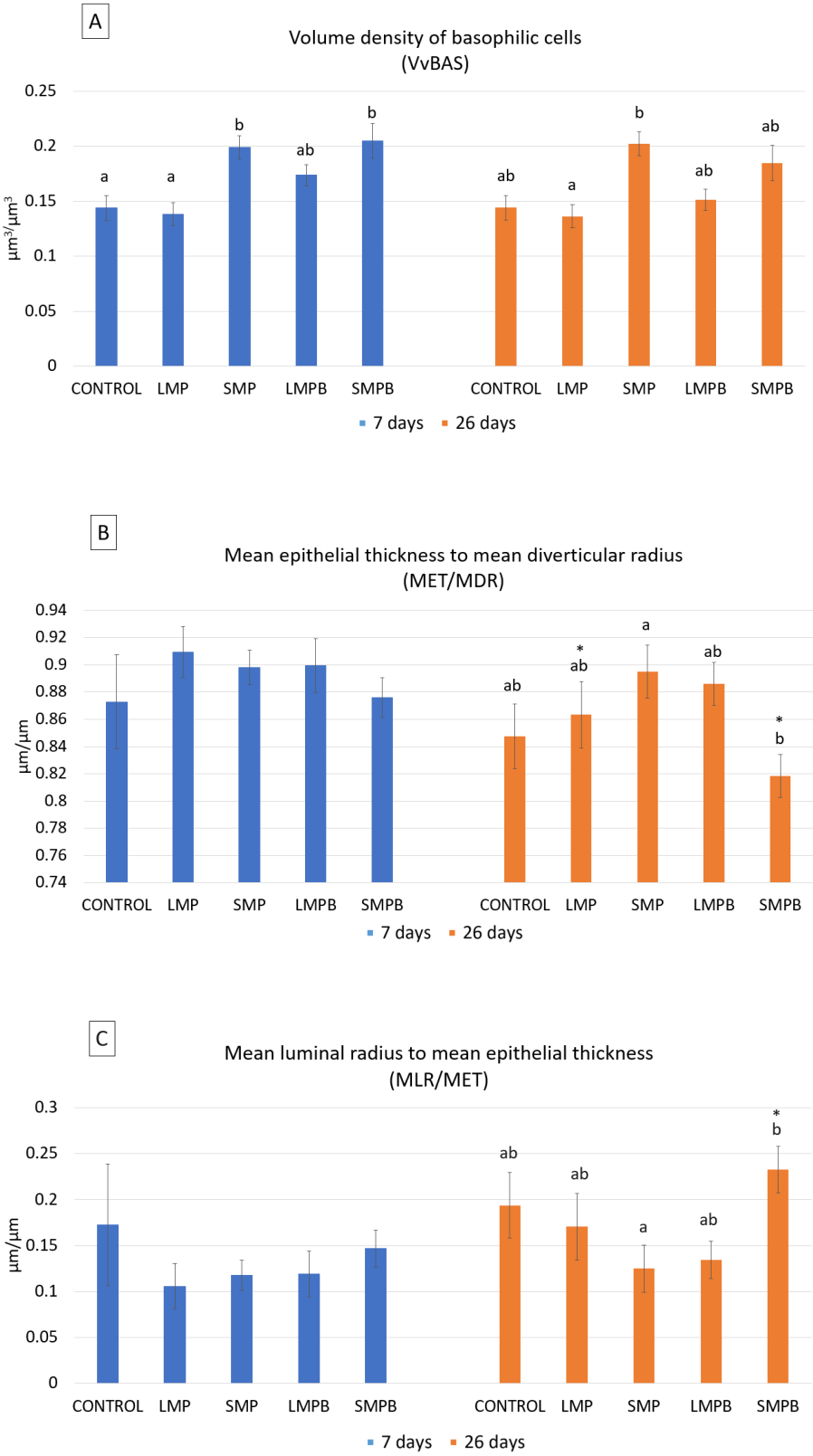

Figure 6: A: Volume density of basophilic cells (µm³/µm³), B: Mean epithelial thickness to mean diverticular radius (MET/MDR, µm/µm) and C: mean luminal radius to mean epithelial thickness (MLR/MET, µm/µm) in control mussels and in mussels dietarily exposed for 7 and 26 days to 4.5 µm MPs (LMP), 0.5 µm NPs (SMP), LMP with sorbed BaP (LMPB) and SMP with sorbed BaP (SMPB). Data are given as mean values and standard errors of 10 mussels per experimental group. Letters indicate significant differences among treatments within the same day (Kruskal-Wallis H test followed by Dunn's post hoc test, $p<0.05$). Asterisks indicate a significant difference between days within the same treatment (Mann-Whitney U test, $p<0.05$).

3.6. Gamete development, gonad index and histopathology of mussel gonad

Percentages of gametogenic stages were similar in all the different experimental groups, both controls and treated (Figure S1 of Supplementary Material). Mature gonad was the predominant stage in all mussels at day 7. Meanwhile at day 26 of exposure, the number of individuals with spawning gonad increased. The mean value for gonad index was around 4 for all experimental groups in both sampling days (Figure S1 of Supplementary Material).

In general, no significant histopathological alterations were observed in mussel gonads (Figure 5G). Fibrosis was recorded at low prevalences in mussels exposed to LMP, LMPB and SMPB at 7 days of exposure and in mussels exposed to LMPB at 26 days of exposure. Hemocytic infiltration (Figure 5H) and oocyte atresia (Figure 5I) were observed at low prevalences in both controls and in treated mussels at both sampling times (Table S2 of Supplementary Material). Oocyte atresia was found mostly at stage 1, with less than half the follicles being affected. A digenean trematode parasite was found in one mussel of the LMP treatment at day 26.

3.7. Whole organism responses

Mussels appeared in good health throughout the experimental period and were observed to close their valves tightly during the emersion of the daily water change and reopen their valves almost immediately following reimmersion. All physiological data met the assumptions to be analyzed by parametric tests. Two way ANOVAs revealed significant effects of treatment for all parameters tested except CR (Table 5). Effect of exposure time was significant for CR and RR, whereas significant effects of the interaction between treatment and time were found for all parameters except AE (Table 5).
For CI, post-hoc testing revealed no significant differences between mean values at day 7 (Figure S2 of Supplementary Material). Whilst by day 26 mussels exposed to SMP increased significantly their condition index compared to mussels from day 7 and presented higher values than the rest of treatments except SMPB (Figure S2 of Supplementary Material).

For CR, the results displayed an overall high degree of variability amongst treatments throughout the study which reduced from day 7 to day 26 (Figure S3 of Supplementary Material). No significant effect of treatments on CR was noticed (Table 5). except for SMP at day 7 that was significantly higher than LMP and SMPB. Maximum value achieved with SMP treatment in the short-term response (3.77 L/h) declined significantly after 26 days (1.82 L/h) (Figure S3 of Supplementary Material).

Similar to CR, there were no significant differences in RR compared to control values for any treatment in either sampling day, and no significant differences in control respiration rates between days (Figure S4 of Supplementary Material). Post hoc analysis revealed that, at day 7, SMPB mussels had a significantly lower RR than the rest of groups except the control, and the RR of LMP mussels decreased significantly from day 7 to day 26 (Figure S4 of Supplementary Material).

There were no significant differences in AE among treatments at day 7 and no significant difference between days by treatment. In contrast, at day 26, all treatments showed an increased AE as compared to the control, this increase being significant for SMP, LMPB and SMPB (Figure7A).

Differences in SFG among treatments reflected mainly the behavior of clearance rates: At day 7 SMP mussels exhibited significantly higher SFG values than the rest of groups, except LMPB (Figure7B). Whilst at day 26 all treatments had a higher SFG compared to the control, an effect which was only significant for the difference between the control and SMPB. In addition, SMP mussels displayed significantly lower SFG at day 26 compared to day 7 (Figure7B).

Table 5. Summary of two-way ANOVAs to analyze the effects of treatment, sampling time and their interaction on the studied parameters: Condition Index (CI), Clearance Rate (CR), Respiration Rate (RR), Absorption Efficiency (AE) and Scope for Growth (SFG). Characters in bold indicate significant differences ($p<0.05$). df: degrees of freedom; F: Fisher's F-ratio; p: probability of F.

PARAMETER	FACTOR	df	F	SIGNIFICANCE
CI	TREATMENT	4	3.06	**p=0.023**
	DAY	1	3.09	p=0.084
	TREATMENT x DAY	4	4.31	**p=0.004**
CR	TREATMENT	4	1.96	p=0.113
	DAY	1	9.67	**p=0.003**
	TREATMENT x DAY	4	11.67	**p<0.001**
RR	TREATMENT	4	4.24	**p=0.004**
	DAY	1	6.81	**p=0.012**
	TREATMENT x DAY	4	4.64	**p=0.003**
AE	TREATMENT	4	4.90	**p=0.002**
	DAY	1	0.18	p=0.675
	TREATMENT x DAY	4	2.17	p=0.085
SFG	TREATMENT	4	5.20	**p=0.001**
	DAY	1	3.67	p=0.061
	TREATMENT x DAY	4	7.14	**p<0.001**

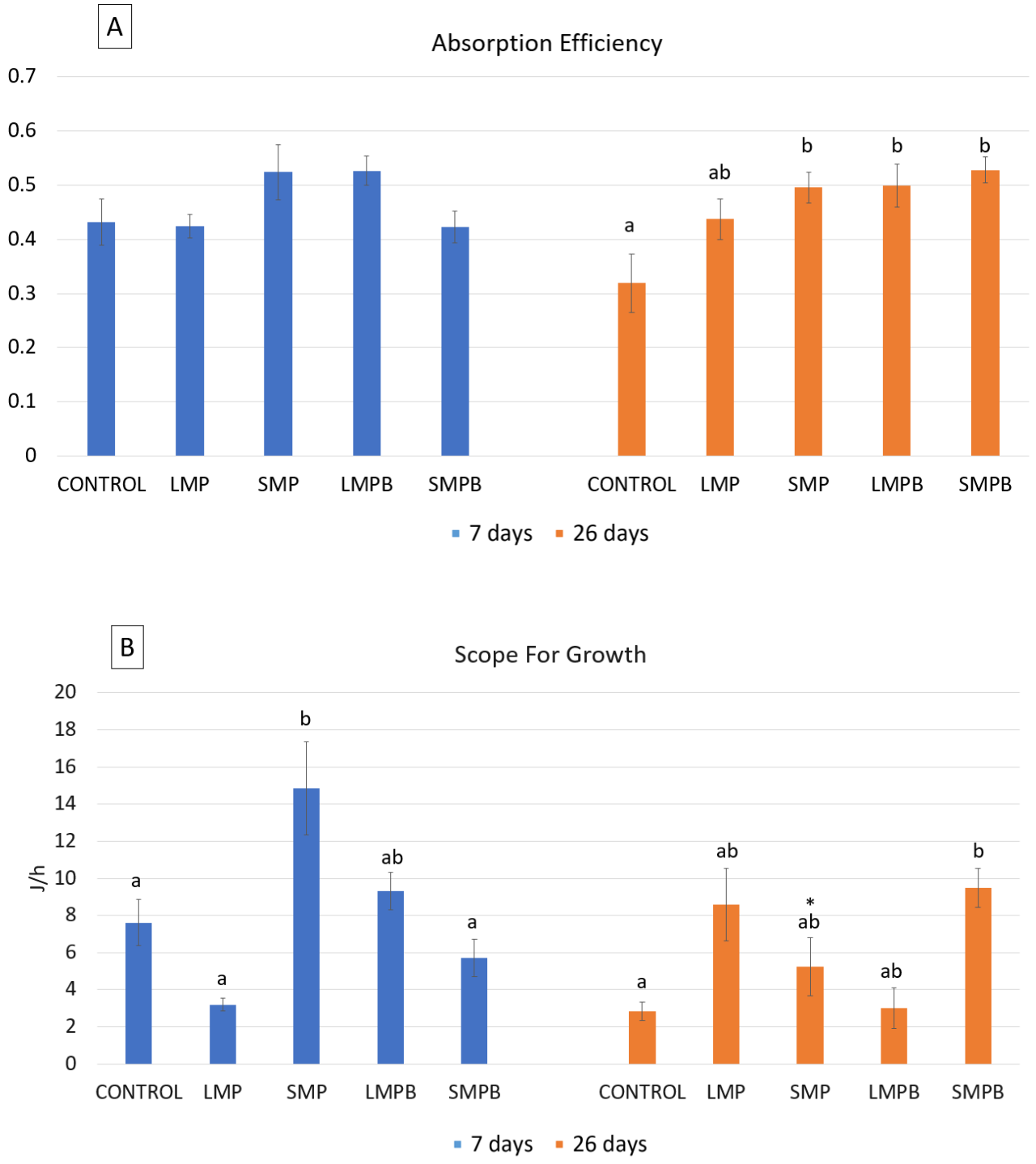

Figure 7: A: Absorption efficiency (fraction) and B: Scope for Growth (J/h) in control mussels and in mussels dietarily exposed for 7 and 26 days to 4.5 µm MPs (LMP), 0.5 µm NPs (SMP), LMP with sorbed BaP (LMPB) and SMP with sorbed BaP (SMPB). Data are given as mean values and standard errors of 7 mussels per experimental group. Letters indicate significant differences among treatments within the same day and asterisks indicate a significant difference between days within the same treatment (2-way ANOVA followed by Tukey's post hoc test, $p<0.05$).

4. DISCUSSION

4.1. Bioaccumulation of BaP in mussel soft tissues

The present study investigated the effects of long-term (26 days) dietary exposure of two different sized PS microspheres (4.5 µm MPs and 0.5 µm NPs) alone and with sorbed BaP in mussels in order to elucidate the influence of plastic size and the presence of sorbed BaP on the organism at different levels of biological organization. Results on BaP accumulation in mussel whole tissues clearly indicate that BaP was not present in significant amounts as a background contaminant; that BaP was transferred from the plastics to the mussels, and that BaP bioaccumulated in the mussel tissue of the BaP treated groups, an effect which increased with exposure time. Furthermore, as hypothesized, notably larger amounts of BaP were transferred to the mussel tissue in the SMPB treatment as compared to the larger plastics likely due to their larger surface to volume ratio which facilitates both the adsorption to and the desorption of PAHs from the plastic surface (Koelmans, 2015). In addition, concentrations of plastic particles administered were equivalent by weight, but not by number of particles, therefore the SMPB treated mussels were exposed to much higher plastic particle numbers compared to the LMPB treated mussels. Again this indicates that the SMPB treatment represented a much higher surface area for the adsorption and desorption of BaP. The fact that the differences in BaP tissue burden between LMPB and SMPB mussels remained the same between days suggests that, although NPs transfer larger amounts of BaP to mussels than MPs, degree of bioaccumulation over time was not increased with decreasing plastic size.

Avio et al. (2015) investigated the transfer of the PAH pyrene via MPs to *M. galloprovincialis*. After 7 days exposure there was a 13 fold increase in tissue concentrations in exposed mussels compared to the controls. Accumulation in the present study was markedly greater with up to a 37 fold increase in BaP tissue burdens in mussels exposed to LMPB and a 66 fold increase in mussels exposed to SMPB relative to the control at day 7. Whilst at day 26 the difference in BaP tissue burdens between controls and mussels exposed to plastics with sorbed BaP were even greater with up to a 150 fold increase in SMPB vs control and a roughly 80 fold increase in LMPB vs the control. Avio et al. (2015) used heterogeneously sized (1 to 100 µm) PS or PE MPs. As such, it is likely that the majority of the particles used in their study were significantly larger than the two particle sizes used in this study which may explain the differences seen. In addition, different MP polymers and concentrations were used in the two studies. Similarly, a lower bioaccumulation than in the present work was observed by Pittura et al. (2018) after exposure of *M. galloprovincialis* to 20-25 µm LDPE MPs with sorbed BaP,

equivalent to a waterborne exposure of 150 ng/L BaP for 28 days. Further, in the present study, in contrast to the majority of MP studies, mussels were fed continuously with microalgae. Okay et al. (2006) found that *Mytilus spp.* accumulated higher amounts of pyrene with increased algal feed concentration, hence this could be another reason why BaP bioaccumulation in the present study was higher than that documented previously (Avio et al., 2015; Pittura et al., 2018). Various studies have noted the increased sorption capacities and sorption/desorption rates with decreased MP size (Koelmans, 2015), however to the authors' knowledge this is the first study to demonstrate an increased transfer of an organic pollutant to tissues of a marine organism as a consequence of decreased MP size, in line with findings in freshwater organisms *Daphnia magna* (Ma et al., 2016) and *Danio rerio* (Chen et al., 2017).

The fact that plastics were found in mussel tissues, especially in the lumen of the gastrointestinal tract, suggests that BaP transferred from MPs to mussels via MP ingestion. This agrees with the higher accumulation of PAHs found in the digestive gland compared to gills in mussels exposed to MPs with PAHs (Paul-Pont et al., 2016; Pittura et al., 2018). But it may be that the plastics used were not the only transfer path. Many studies have shown that when MPs with sorbed PAHs are added to clean seawater the PAHs immediately begin to desorb in order to reach equilibrium concentrations with the surrounding seawater (Bakir et al., 2016; Ziccardi et al., 2016). Desorption dynamics depend on MP size, surface chemistry and texture, degree of weathering and fouling and also seawater temperature, pH and background PAH concentrations (Koelmans, 2015). Therefore, it is likely that the seawater represented an additional path for the transfer of BaP to the mussels in this study. In addition, the plastics with the sorbed BaP were added to a mixture of clean algae and seawater which was gradually and continuously administered to the mussel tanks over a period of 22 hours daily. Therefore, there was a long period for potential desorption of BaP from the MPs and potential sorption onto algae. *I. galbana* has a high lipid content (24%, Creswell, 2010) and would therefore likely have a higher affinity for BaP than seawater. This idea is supported by the results of Paul-Pont et al. (2016) who investigated the partitioning of the PAH fluoranthene in mixtures of algae and seawater, and of algae, PS microspheres (2 µm and 6 µm) and seawater. They found that when fluoranthene was added to algae and seawater without MPs, the PAH was largely associated with the algae (89%) with a fraction of only 11% remaining in water. However, when MPs were added, the fraction of dissolved fluoranthene remained similar (12%) whilst the fraction associated with the algae decreased to 67%. The remaining fraction (21%) was associated to the MPs (Paul-Pont et al., 2016). PS microspheres of 2 µm have also been observed to attach to microalgae aggregates in

laboratory studies (Long et al., 2015; 2017). This factor may have therefore affected the partitioning of BaP between MPs, algae and seawater by providing a direct pathway between MPs and algae.

4.2. Tissue distribution of MPs in mussels

Tissue distribution of 4.5 µm MPs in mussels was in agreement with previous works (Browne et al., 2008; Von Moos et al., 2012; Avio et al., 2015; Paul-Pont et al., 2016; Magni et al., 2018; Pittura et al., 2018). Thus, plastics in mussels dietarily exposed to LMP and LMPB were abundant in the lumen of stomach, mixed with stomach contents, and in the lumen of digestive tubules, associated to cell debris, although there was a marked interindividual variability that could be associated to heterogeneous distribution of MPs along the digestive tract. Occasionally MPs were found within epithelial cells of the stomach, ducts and digestive tubules and in the connective tissue. MPs were also found between gill filaments, but not within epithelial cells of the gills. Overall, results reinforce the idea that MPs get in contact with mussel gill surfaces and are then transported into the mouth via ciliae movement and later to the digestive system through ingestion (Browne et al., 2008; Von Moos et al., 2012; Brate et al 2018; Kolandhasamy et al.; 2018). Many works have already underlined the importance of MP size for MP ingestion and assimilation in mussels (Browne et al., 2008; Van Cauwenberghe et al., 2015; Kolandhasamay et al., 2018; Qu et al., 2018; Li et al., 2019) although it is not yet clear which particle size has the greatest accumulation potential in mussels and if accumulation can be polymer-type dependent (Li et al., 2019). The 4.5 µm LMPs were similar in size to microalgae provided as food and they were retained and internalized in mussel tissues. On the other hand, 0.5 µm SMPs would possibly not be retained as retention efficiency of particles in gills is close < 15% for particles below 1 µm in size (Ward and Shumway, 2004). However, 0.5 µm particles may enter cells by endocytosis, as shown in mussel hemocytes (Cajaraville & Pal, 1995). Even though 0.5 µm SMPs can be hardly distinguished under the light microscope, these were occasionally observed as large aggregates in the lumen of stomach. Further transmission electron microscopy analyses are necessary to decipher mechanisms of internalization into cells and elimination from cells of mussels.

4.3. Early cellular biomarkers in mussel hemocytes

In the present work, catalase activity (CAT), neutral red (NR) uptake and DNA strand breaks were measured in hemocytes as these cells are pivotal components of the immune and xenobiotic detoxification system of mussels (Gómez-Mendikute et al., 2002) and are known to uptake MPs in a wide range of sizes (Browne et al., 2008; Pittura et al., 2018). The results for CAT in hemocytes of

mussels exposed to LMPB and SMPB followed the classic bell-shaped curve (Viarengo et al., 2007), wherein CAT increased significantly compared to the control at day 7 but was significantly lower than the control at day 26. These results therefore suggest the onset of oxidative stress at day 7, followed by a decrease in catalase activity at day 26 as the antioxidant system was overwhelmed. These results were accompanied by a significant reduction in NR uptake in both treatments of MPs with sorbed BaP at day 26. A decrease in NR uptake is indicative of a decrease in cell viability (Borenfreund & Puerner, 1985; Repetto et al., 2008; Katsumiti et al., 2015). Hence, the results from the NR assay clearly indicate decreased hemocyte viability in mussels exposed to LMPB and SMPB at day 26, which can be related to the increased accumulation of BaP in mussel tissues from day 7 to day 26. The fact that effects on CAT and NR were observed in LMPB and SMPB treatments but not in either of the MP alone groups demonstrates a toxic effect of BaP transferred by the MPs on the oxidative balance and cell viability of mussel hemocytes in these treatments. BaP is known to induce oxidative stress in mussels (Akcha et al., 2000; Banni et al., 2017), and also to cause dose-dependent increases in ROS production and decreases in NR uptake in mussel hemocytes (Gómez-Mendikute et al., 2002; Gómez-Mendikute & Cajaraville, 2003). In agreement with our results, lysosomal membrane stability (LMS) was reduced in hemocytes of mussels exposed for 7 days to LDPE MPs with sorbed BaP compared to LDPE MPs alone, although not after 14 and 28 days (Pittura et al., 2018). Phagocytosis increased in hemocytes of mussels exposed for 7 days to LDPE MPs alone compared to controls but not to LDPE with sorbed BaP whereas at longer exposure times (14 and 28 days) phagocytosis decreased in hemocytes of both mussels exposed to LDPE alone and with sorbed BaP (Pittura et al., 2018). Avio et al. (2015) reported decreased LMS in mussels exposed to PS (<100 µm) alone and with sorbed pyrene. However, antioxidant enzyme activities, including CAT in digestive gland, did not change after MP exposure alone or with adsorbed pyrene (Avio et al., 2015) or BaP (Pittura et al., 2018). Meanwhile, Paul-Pont et al. (2016) found that 7 days of exposure to micro PS alone and with fluoranthene caused reduced CAT and other indications of oxidative stress in mussels. Significant effects on LMS and oxidative stress were also reported in mussels exposed to a virgin high density polyethylene (HDPE) fluff (<80 µm) (van Moos et al., 2012). Détrée and Gallardo-Escárate (2017) also observed oxidative stress and immunological effects in mussels *M. galloprovincialis* after short exposure (24 h) to a high concentration (1.5 x10^7 particle/L) of PE microbeads. Finally, there was no effect of MP size on CAT activity or NR uptake. This contrasts a report of increased antioxidant enzyme activities and intracellular ROS levels with decreasing MP size in rotifers (*Brachionus koreanus*) exposed to PS microspheres (0.05, 0.5, and 6 µm) at 20 µg/mL over 24 hours (Jeong et al., 2016). These effects were accompanied by subsequent reductions in fecundity and survival time.

Background levels of DNA damage observed in the control groups were at similar levels to those found in hemocytes of mussels collected in the same region in previous studies (Katsumiti et al., 2015) and did not change between days indicating no effect of time spent in aquaria on DNA damage. Levels of DNA damage displayed a wide degree of variability at day 7 with only mussels exposed to LMPB showing higher DNA damage than control mussels. However, at day 26 differences were more apparent with all treatments except for LMPB, showing significantly higher levels of DNA strand breaks compared to the day 26 control and to their day 7 counterparts. These results therefore indicate an effect of increased genotoxicity with exposure time in SMP, LMP and SMPB treatments. In contrast to this, levels of DNA damage in mussels exposed to LMPB decreased significantly between day 7 and day 26, although DNA damage in the LMPB treatment at day 26 was still higher than in the day 26 control but not significantly. It is unclear why levels of DNA damage would reduce in the LMPB treatment with time. One possible explanation could be that mussels in this treatment were able to more effectively repair the DNA damage observed than mussels in other treatments. Indeed, BaP not only causes DNA strand breaks but also initiates DNA strand break repair pathways in mice (Tung et al., 2014), as also suggested in mussels (Bihari et al., 1990). Banni et al. (2017) found increased transcription levels of genes involved in DNA repair in mussels exposed to BaP.

At day 26 mussels exposed to LMPB and SMPB both had lower percentages of tail DNA than mussels exposed to LMP and SMP, respectively (significant for the difference between LMP and LMPB), indicating that, despite increased BaP tissue burdens with time in these groups, there was no additional toxic effect of BaP on mussel DNA as compared to MPs and NPs alone. These results could be related to the above mentioned initiation of DNA repair pathways caused by exposure to BaP (Bihari et al. 1990) leading to increased strand break repair in treatments of MPs with sorbed BaP. Avio et al. (2015) also found increased effects of MPs alone as compared to MPs with sorbed pyrene in the comet assay, however none of their results were significantly different from the control. Similarly, Pittura et al. (2018) did not find significant effects on DNA damage in mussels exposed to LDPE and LDPE with sorbed BaP for 28 days, as neither did Santana et al. (2018) after exposing *Perna perna* mussels to polyvinyl chloride (PVC) for 90 days. In contrast, Ribeiro et al. (2017) and Brandts et al. (2018) found DNA damage after exposing clams *Scrobicularia plana* for 7 days to 1 mg/L 20 µm PS MPs and mussels *M. galloprovincialis* for 96 hours to 0.05, 0.5, 5 and 50 mg/L PS nanoparticles, respectively. The effects of MPs alone on DNA strand breaks could be related to their observed pro-oxidant effects in marine organisms (van Moos et al., 2012; Browne et al., 2013; Paul-Pont et al.,

2016; Détrée & Gallardo-Escárate, 2017). The genotoxicity of BaP is due to its metabolism to reactive metabolites such as BaP diol epoxide, which is known to bind covalently to DNA, and BaP quinones which induce oxidative stress (Canova et al., 1998; Tung et al., 2014). Banni et al. (2017) found that DNA strand breaks caused by BaP exposure as measured by the comet assay exhibited a dose response pattern in *Mytilus* spp. Hence, it may be that the BaP tissue burdens in this study were not high enough to cause an increased effect on DNA strand breaks compared to the effects of the plastics alone. The comet assay results also showed that mussels exposed to both SMP and SMPB displayed significantly higher levels of DNA damage compared to mussels exposed to LMP and LMPB, respectively, indicating an effect of MP size on genotoxicity with smaller plastics causing increased levels of DNA damage. To the authors knowledge this effect of size of MPs on DNA damage has not been demonstrated previously and is probably related to the higher particle numbers in the treatments with 0.5 µm NPs and to the increased ability of smaller particles to interact with mussel tissues, translocate and even enter into mussel cells compared to larger particles (Browne et al., 2008), as discussed above.

4.4. Cell and tissue biomarkers in mussel digestive gland and gonad

Background staining in mussel digestive gland cryosections stained for LMS was too high to determine the lysosomal membrane labilization period. The staining seen corresponded largely to partially digested algae but also to the presence of lipofuscins, as evidenced by Schmorl´s reaction. In addition, the possibility of using lipofuscin accumulation as a biomarker for oxidative stress was dismissed as lipofuscin levels in the digestive gland of control mussels were too high to clearly distinguish differences in lipofuscin accumulation between treatments. The presence of the high background staining was due to the fact that the mussels were continually fed in this study whereas usually mussels are starved or fed intermittently in studies investigating LMS in the digestive gland. The same result was found by Izaguirre (2007) who compared the effects of different dietary regimes on ability to measure LMS and Blanco-Rayón et al. (2019) reported increased levels of lipofuscins in continuously fed mussels compared to starved ones. The general appearance of the digestive gland in paraffin histological sections of both control and treated mussels also indicated a high digestive activity. In many digestive tubules epithelial cells were relatively high and the lumen was obliterated. In other tubules, the digestive epithelium was thin and the large lumen appeared full of cell debris (including entire digestive cells). Changes in the cell composition of the digestive epithelium and in the structure of digestive tubules can be measured in terms of volume density of basophilic cells (VvBAS) and mean epithelial thickness to mean diverticular radius (MET/MDR) and mean luminal

radius to MET (MLR/MET), respectively (Bignell et al., 2012; De los Ríos et al., 2013). These parameters are commonly used biomarkers in ecosystem health assessment, as they significantly reflect changes in the general health status of mussels (Marigómez et al., 2006; Zorita et al., 2006; Garmendia et al 2011; De los Ríos et al., 2013). The digestive tubules are lined by a single and dynamic epithelium, comprised of two cell types: digestive and basophilic cells. Under normal physiological conditions, basophilic cells are less abundant than digestive cells in digestive tubules, but this is reversed under stress conditions by basophilic cell hypertrophy and digestive cell loss (Zaldibar et al., 2007). In the present work, at day 7 of exposure values of VvBAS in mussels exposed to SMP and SMPB (0.19 ± 0.01 $\mu m^3/\mu m^3$ and 0.2 ± 0.01 $\mu m^3/\mu m^3$, respectively) were significantly higher than in control mussels and in mussels exposed to LMP. These values indicate a high stress level according to the thresholds reported by Bignell et al. (2012) and have been observed in mussels after the Prestige oil spill (Cajaraville et al., 2006; Marigómez et al., 2006; Garmendia et al., 2011). At day 26 of exposure there were less differences among exposure groups but mussels exposed to SMP still showed higher VvBAS values than those exposed to LMP, clearly demonstrating a significant influence of MP size on the cell composition of digestive tubules, as observed for DNA damage. Additional effects of BaP compared to the plastics alone or effects of exposure time were not observed in VvBAS, also in line with results of DNA damage. These results can be explained taking into account that alterations in the cell composition of digestive tubules is a fast inducible and reversible response (Soto et al., 2002; Zaldibar et al., 2007).

In contrast, the parameters indicative of the structure of digestive tubules evidenced additional effects of BaP compared to the plastics alone and effects of exposure time, but no effect of plastic size. Thus, differences in MET/MDR and MLR/MET among treatments were recorded only at day 26 of exposure, mussels exposed to SMPB showing significantly lower MET/MDR and higher MLR/MET compared to mussels exposed to SMP. These data indicate that mussels treated with NPs with sorbed BaP showed signs of thinning of digestive epithelium and atrophy of digestive tubules, even though values of MLR/MET were below the threshold (0.7 µm/µm) suggested as hallmark of this histopathological condition (Bignell et al., 2012). In general, values of MLR/MET were low for all mussels in the present work, possibly due to the high digestion activity seen in cryostat and paraffin sections, related to the continuous feeding regime during the experiment. Digestive tubule epithelial thinning has been widely associated to exposure of mussels to hydrocarbons (Cajaraville et al., 1992; Garmendia et al., 2011) and may lead to a reduced ability to digest food material (Zorita et al., 2006). Digestive tubules with necrotic areas were observed in few mussels exposed to NPs and MPs alone

(SMP, LMP) but prevalences were too low to reach a consistent conclusion about the influence of NPs and MPs on this histopathological alteration. Similarly, inflammatory responses such as fibrosis, hemocytic infiltration and accumulation of brown cells in the connective tissue and in the epithelium of the digestive tract were observed at low prevalences in mussels exposed to MPs and NPs alone or with sorbed BaP. Due to the pivotal role of hemocytes in internal defense, hemocytic infiltration has been interpreted as a repair process following tissue damage (Des Voigne & Sparks, 1968; Gosling, 2015). In agreement with our results, a general increased presence of hemocytes has been reported in different organs of mussels exposed to MPs (Brate et al., 2018). Formation of granulocytomas has also been observed after exposure of mussels to MPs (Von Moose et al., 2012). Paul-Pont et al. (2016) found increased hemocytic infiltration in stomach and digestive gland of mussels co-exposed to PS MPs and fluoranthene in comparison to mussels exposed to PS alone. In contrast, Pittura et al. (2018) did not observe any histological alterations in mussels exposed to LDPE MPs alone or with sorbed BaP. Clearly further work is necessary to confirm the slight increase in prevalence of inflammatory reactions observed in the present work in mussels exposed to PS MPs alone and with sorbed BaP. On the other hand, in the present work no alterations were observed in gametogenic development nor in gonad histopathology of mussels exposed to MPs of both sizes alone or with sorbed BaP in comparison to control mussels. In oysters after 2 months of exposure to MPs, a reduction in oocyte numbers, oocyte diameter and sperm mobility was observed (Sussarellu et al., 2016). Moreover, parental exposure had detrimental effects on offspring with lower rates of D-larval yield and larval development (Sussarellu et al., 2016), indicating again the need for further work on ecologically relevant endpoints such as reproduction and development of mussels and other marine organisms.

4.5. Whole organism responses

In the present work, effects on condition index (CI) as well as on feeding (CR), food absorption (AE), metabolism (RR) and their combination into an energy budget in the form of scope for growth (SFG) were measured as ecologically relevant whole organism responses. The results for CI suggest that there was no impact of time spent in aquaria on mussel condition. The difference seen between days for mussels exposed to SMP are likely due to differing CIs among mussels at the beginning of the experiment rather than a change caused due to the effects of differing feeding conditions or the effects of the plastics themselves. This explanation is supported by the results from the physiological variables. In agreement with our results, Santana et al. (2018) and Ribeiro et al. (2017) did not observe changes in the CI of mussels *Perna perna* after long (90 days) exposure to 0.1-1 µm PVC

particles and clams *Scrobicularia plana* exposed for 14 days to 1 mg/L 20 µm PS MPs, respectively. In contrast, long term (8 months) dietary exposure to environmentally relevant concentrations of polypropylene rope caused a reduction in condition and feeding activity in the Norwegian lobster *Nephrops norvegicus* (Welden & Cowie, 2016). Differences in polymer and type of material tested and exposure time as well as species differences in feeding strategy may account for the different results.

There was no difference in CR or RR for the control mussels between days and CR and RR did not differ significantly from the control for any treatment across both sampling days indicating that there was no effect of any treatment or of exposure time on CR or RR**.** It is possible that MP and BaP concentrations despite having an effect on cell and tissue level responses were not high enough to cause an effect on mussel feeding and metabolism. Van Cauwenberghe et al. (2015) observed a 25% increase in RR in *M. edulis* following a 14 day exposure to 10, 30 and 90 µm PS microspheres at 110 particles/mL. This increase in RR was interpreted as a stress response as animals have to utilize a greater amount of energy in order to maintain homeostasis (van Cauwenberghe et al., 2015). Alternatively other studies have shown depressed metabolic activity in response to MP exposure, that could occur in order to preserve energy due to reductions in available nutrients caused by alterations in digestive efficiency resulting from gut MP accumulation (Welden & Cowie, 2016). Concerning the lack of response of CR to MP exposure, it should be noted that feeding behavior of mussels is strongly affected by relatively minor changes in the inorganic (not assimilable) fraction of the seston (Navarro et al., 1996). This could account for the contrasting effects that have been attributed to suspended MPs as regards to feeding rates in bivalves, ranging from stimulatory (Sussarellu et al., 2016) to inhibitory effects (Wegner et al., 2012; Rist et al., 2016; Xu et al., 2017) depending on factors such as concentration and size of particles. Responses can also vary depending on the bivalve species studied. Thus, oysters *(O. edulis*) and mussels (*M. edulis*) exposed to 25 µg/L polylactic acid or HDPE MPs presented just the opposite response in relation to filtration rate; while mussels tend to reduce the filtration rate oysters response was to increase it (Green et al., 2017). On the other hand, in mussels *P. perna* exposed for 90 days to PVC MPs no differences in CR were observed between exposed and control mussels. Further, Rist et al. (2016) found no additional effect of exposure to sorbed fluoranthene as compared to PVC MPs alone on CR or RR in *P. viridis* after 44 days exposure.

In contrast to the results for CR and RR significant results were found in AE. Values of this parameter

were not significantly different among treatments in mussels sampled at day 7 but increased significantly with respect to the control for most treatments (namely, SMP, LMPB and SMPB) in those sampled at day 26. The pattern shown is in accordance with the hypothesized order of impact of the treatments i.e. NPs causing more effects than MPs and MPs and NPs with sorbed BaP causing more effects than MPs and NPs alone. Sussarellu et al. (2016) also found an increase in microalgal consumption and in AE in oysters (*Crassotrea gigas*) exposed to virgin 2 and 6 µm PS microspheres over 2 months and Paul-Pont et al. (2016) observed the induction of glycolysis and digestive activity in *Mytilus spp.* following a 7 day exposure to the same PS microspheres. These results were interpreted as a possible compensatory mechanism to cope with the increased energy requirements of stressed conditions. In line with this interpretation, the increased AE observed in this work in mussels exposed for 26 days to NPs alone and to MPs and NPs with sorbed BaP may constitute a mechanism to increase energy intake in response to damage observed at cell level (e.g., oxidative stress, cytotoxicity and DNA damage in hemocytes) and tissue level (structure of digestive tubules).

The integrative parameter SFG largely followed the pattern of results for CR. At day 7, mussels exposed to SMP showed significantly higher SFG than the rest of experimental groups except LMPB whereas at day 26 the only significant difference observed was that mussels exposed to SMPB showed significantly higher SFG than the day 26 control mussels. These results again support the idea of a general compensatory effect of MPs and NPs, regardless of size of plastics or presence of BaP, in line with results of Sussarellu et al. (2016). In contrast, Xu et al. (2017) found that a significant reduction in CR but no change in AE or respiration led to a reduced energy budget in clams *Atactodea striata* exposed to PS (63-250 µm) at the same concentration used in this study for the MPs (1000 particles/mL). The differences compared to the results found in this study could be related to the greater size of MPs used. In crustaceans, reductions in feeding activity leading to reductions in SFG and body mass have been found in *Carcinus maenas* and *N. norvegicus* respectively following chronic dietary exposure to MP fibres (Watts et al., 2015; Welden and Cowie, 2016). Similar reductions in energy budget have also been seen in lugworms following chronic exposure to MPs with reduced feeding and weight loss correlated with increased MP concentration (Besseling et al., 2013; Wright et al., 2013). However, no increased effects of sorbed contaminants have yet been observed on energy budget in comparison to MPs alone (Besseling et al., 2013; Browne et al., 2013; Rist et al., 2016). Further studies are therefore required to better elucidate the effects of MP co-contaminants in relation to MPs alone on integrative indices of physiological condition in an array of marine organisms with different feeding and digestion strategies.

5. CONCLUSIONS

This study demonstrated that BaP transferred from MPs and NPs to mussels and bioaccumulated in mussel tissues with increased exposure time, and that NPs (0.5 µm) posed an increased hazard in terms of the transfer of BaP to tissues than MPs (4.5 µm). Effects of MPs and NPs alone and with sorbed BaP were observed at environmentally relevant concentrations on a range of cellular and tissue level biomarkers and whole organism responses. Effects increased with exposure time or only developed following longer term exposure in the majority of responses studied, highlighting the importance of long term chronic exposure studies in the investigation of the effects of MPs and NPs and their co-contaminants. Increased effects of sorbed BaP compared to MPs and NPs alone were demonstrated on cell viability and catalase activity of hemocytes and on the structure of digestive tubules in the digestive gland but there was no additional effect of sorbed BaP on DNA damage in hemocytes, despite its genotoxic potential. Increased effects of NPs over MPs were observed on DNA damage and on cell composition of digestive tubules, indicating the need of testing a variety of MP sizes in studies investigating MP potential toxicity. At a whole organism level, a hormetic effect was demonstrated on SFG. This appeared to represent a compensatory response, whereby exposed mussels increased their food absorption efficiency in order to increase energy intake to make up for energy expended dealing with stress observed in cell and tissue biomarkers. Thus, the present work evidenced a link between MP effects at different levels of biological organization. Further work is still required under realistic scenarios on the effects of a variety of plastic type, size, shape combinations together with a wide variety of pollutants in order to understand the hazards posed by MPs and NPs and their relevance as carriers of other pollutants in the marine environment.

ACKNOWLEDGEMENTS

This work was funded by Spanish MINECO (NACE project CTM2016-81130-R), Basque Government (consolidated group IT810-13) and predoctoral fellowship to NGS and UPV/EHU (UFI 11/37, VRI grant PLASTOX). Work carried out within EU project PLASTOX (JPI Oceans 005/2015).

REFERENCES

Aebi H. 1984. Catalase *in vitro.* Methods Enzymol 105, 121–126.

Akcha F., Izuel C., Venier P., Budzinski H., Burgeot T., Narbonne J.F. 2000. Enzymatic biomarker measurement and study of DNA adduct formation in benzo[a]pyrene contaminated mussels, *Mytilus galloprovincialis*. Aquatic Toxicology 49, 269-287.

Avio C.J., Gorbi S., Milan M., Benedetti M., Fattorini D., d'Errico G., Pauletto M., Bargelloni L., Regoli F. 2015. Pollutants bioavailability and toxicology risk from microplastics to marine mussels. Environmental Pollution 198, 211-222.

Baini M., Fossia M.C., Gallia M., Clabiania I., Campania T., Finoiac M.G., Pantia C. 2018. Abundance and characterization of microplastics in the coastal waters of Tuscany (Italy): The application of the MSFD monitoring protocol in the Mediterranean Sea. Marine Pollution Bulletin 133, 54-552.

Bakir A., O'Connor I.A., Rowland S.J., Hendriks A.J., Thompson, R. C. 2016. Relative importance of microplastics as a pathway for the transfer of hydrophobic organic chemicals to marine life. Environmental Pollution 219, 56-65.

Banni M., Sforzini S., Arlt V.M., Barranger A., Dallas L.J., Oliveri C., Aminot Y., Pacchioni B., Milino C., Lanfranchi G., Readman J.W., Moore M.N., Viarengo A., Jhan A.N. 2017. Assessing the impact of benzo[a]pyrene on marine mussels: application of a novel targeted low density microarray complementing classical biomarker responses. PloS one 12, e0178460.

Batel A., Borchert F., Reinwald H., Erdinger L., Braunbeck T. 2018. Microplastic accumulation patterns and transfer of benzo[a]pyrene to adult zebrafish (*Danio rerio*) gills and zebrafish embryos. Environmental Pollution 235, 918-930.

Batel A., Linti F., Scherer M., Erdinger L., Braunbeck T. 2016. The transfer of benzo[a]pyrene from microplastics to Artemia nauplii and further to zebrafish via a trophic food web experiment– CYP1A induction and visual tracking of persistent organic pollutants. Environmental Toxicology Chemistry 35, 1656-66.

Bayne B.L., Widdows J., Thompson R.J. 1976. Physiological integrations in Bayne, B.L. (Ed.). Marine mussels: their ecology and physiology. International Biological Programme, 10: pp. 261-291. Cambridge University Press. Cambridge, UK.

Bellas J., Albentosa M., Vidal-Liñán L., Besada V., Franco M.Á., Fumega J., González-Quijano A., Viñas L., Beiras R. 2014. Combined use of chemical, biochemical and physiological variables in mussels for the assessment of marine pollution along the N-NW Spanish coast. Marine Environmental Research 96,105-117.

Bellas J., González-Quijano A., Vaamonde A., Fumega J., Soriano J.A., González J.J. 2011. PCBs in wild mussels (*Mytilus galloprovincialis*) from the N-NW Spanish coast: current levels and long-term trends during the period 1991-2009. Chemosphere 85, 533-41.

Besseling E., Wegner A., Foekema E. M., van den Heuvel-Greve M. J., Koelmans, A. A. 2013. Effects of

microplastic on fitness and PCB bioaccumulation by the lugworm *Arenicola marina* (L.). Environmental Science & Technology 47, 593-600.

Bignell J., Cajaraville M.P., Marigómez I. 2012. Background document: histopathology of mussels (*Mytilus spp.)* for health assessment in biological effects monitoring. Integrated monitoring of chemicals and their effects. IM DAVIES, AD VETHAAK (eds.). ICES Cooperative Research Report N. 315, Copenhagen, Denmark pages, 111-120.

Bihari N., Batel R., Zahn R.K. 1990. DNA damage determination by the alkaline elution technique in the haemolymph of mussel *Mytilus galloprovincialis* treated with benzo[a]pyrene and 4-nitroquinoline-N-oxide. Aquatic Toxicology 18, 13-22.

Blanco-Rayón E., Guilhermino L., Irazola M., Ivanina A.V., Sokolova I.M., Izagirre U., Marigómez I. 2019. The influence of short-term experimental fasting on biomarker responsiveness in oil WAF exposed mussel. Aquatic Toxicology 206, 164-175.

Borenfreund E., Puerner J.A. 1985. Toxicity determined *in vitro* by morphological alterations and neutral red absorption. Toxicology letters 24, 119-124.

Brate I.L., Blazquez M., Brooks S.J., Thomas K.V. 2018. Weathering impacts the uptake of polyethylene microparticles from toothpaste in Mediterranean mussels (*M. galloprovincialis*). Science of the Total Environment 626, 1310-1318.

Brandts I., Teles M., Gonçalves A.P., Barreto A., Franco-Martinez L., Tvarijonaviciute A., Martins M.A., Soares A.M.V.M., Tort L., Oliveira M. 2018. Effects of nanoplastics on *Mytilus galloprovincialis* after individual and combined exposure with carbamazepine. Science of the Total Environment 643, 775-784.

Browne M.A., Crump P., Niven S.J., Teuten E., Tonkin A., Galloway T., Thompson R. 2011. Accumulation of microplastic on shorelines worldwide: sources and sinks. Environmental Science Technology 45, 9175-9.

Browne M.A., Dissanayake A., Galloway T.S., Lowe D.M., Thompson R.C. 2008. Ingested microscopic plastic translocates to the circulatory system of the mussel, *Mytilus edulis* (L.). Environmental Science & Technology 42, 5026-5031.

Browne M.A., Niven S.J., Galloway T.S., Rowland S.J., Thompson R.C. 2013. Microplastic moves pollutants and additives to worms, reducing functions linked to health and biodiversity. Current Biology 23, 2388-2392.

Cajaraville M.P., Bebianno M.J., Blasco J., Porte C., Sarasquete C., Viarengo A. 2000. The use of biomarkers to assess the impact of pollution in coastal environments of the Iberian Peninsula: a practical approach. Science of the Total Environment 247, 295-311.

Cajaraville M.P., Garmendia L., Orbea A., Werding R., Gómez-Mendikute A., Izagirre U., Soto M., Marigómez I. 2006. Signs of recovery of mussels health two years after the Prestige oil spill. Marine Environmental Research 62, 337-341.

Cajaraville M.P., Marigómez J.A., Diez G., Angulo E. 1992. Comparative effects of the water accommodated fraction of three oils on mussels-2. Quantitative alterations in the structure of the digestive tubules. Comparative Biochemistry and Physiology - Part C 102, 113-23.

Cajaraville M.P., Pal S.G. 1995. Morphofunctional study of the haemocytes of the bivalve mollusc *Mytilus galloprovincialis* with emphasis on the endolysosomal compartment. Cell Structure and Function 20, 355-367.

Cajaraville M.P., Robledo Y., Etxeberria M., Marigómez I. 1995. Cellular biomarkers as useful tools in the biological monitoring of environmental pollution: molluscan digestive lysosomes. In: Cell Biology in Environmental Toxicology. M.P. Cajaraville (ed.), University of the Basque Country Press Service, Bilbo, pp 29-55.

Cancio I., Ibabe A., Cajaraville M.P. 1999. Seasonal variation of peroxisomal enzyme activities and peroxisomal structure in mussels *Mytilus galloprovincialis* and its relationship with the lipid content. Comparative Biochemistry and Physiology - Part C: Toxicology & Pharmacology 123, 135-144.

Cancio I., Orbea A., Völkl A., Fahimi H.D., Cajaraville M.P. 1998. Induction of peroxisomal oxidases in mussels: comparison of effects of lubricant oil and benzo(a)pyrene with two typical peroxisome proliferators on peroxisome structure and function in *Mytilus galloprovincialis*. Toxicology and Applied Pharmacology 149, 64-72.

Canova S., Degan P., Peters L.D., Livingstone D.R., Voltan R., Venier P. 1998. Tissue dose, DNA adducts, oxidative DNA damage and CYP1A-immunopositive proteins in mussels exposed to waterborne benzo[a]pyrene. Mutation Research 399, 17-30.

Chen Q., Yin D., Jia Y., Schiwy S., Legradi J., Yang S., Hollert H. 2017. Enhanced uptake of BPA in the presence of nanoplastics can lead to neurotoxic effects in adult zebrafish. Science of the Total Environment 609, 1312-1321.

Cole M., Lindeque P., Halsband C., Galloway T.S. 2011. Microplastics as contaminants in the marine environment: a review. Marine Pollution Bulletin 62, 2588-97.

Conover R.J. 1966. Assimilation of organic matter by zooplankton. Limnology and Oceanography 11, 338-345.

Coughlan J. 1969. The estimation of filtering rate from the clearance of suspensions. Marine Biology 2, 356-358.

Creswell L. 2010. Phytoplankton culture for aquaculture feed. Southern Regional Aquaculture Center (Eds.).

Day R.H., Shaw D.G., Ignell S.E. 1990. The quantitative distribution and characteristics of neuston plastic in the North Pacific Ocean, 1985-88. In R. S. Shomura & M. L. Godfrey (Eds.) Proceedings of the Second International Conference on Marine Debris (pp. 2-7). Honolulu, Hawaii. U.S Dep. Commerce., NOAA Technical. Memorandum. NMFS, NOAATM-SWFSC-154, 2-7 April 1989.

De los Ríos A., Perez L., Ortiz-Zarragoitia M., Serrano T., Barbero M.C., Echavarri-Erasun B., Juanes J.A., Orbea A., Cajaraville M.P. 2013. Assesing the effects of treated and untreated urban discharges to estuarine and coastal waters applying selected biomarkers on caged mussels. Marine Pollution Bulletin 77, 251-265.

Détrée C., Gallardo-Escárate C. 2017. Polyethylene microbeads induce transcriptional responses with tissue-dependent patterns in the mussel *Mytilus galloprovincialis*. Journal of Molluscan Studies 83, 220-225.

Des Voigne D.M., Sparks A.K. 1968. The process of wound healing in the Pacific oyster, *Crassostrea gigas*.

Journal of Invertebrate Pathology 12, 53-65.

Desforges J.P.W., Galbraith M., Dangerfield N., Ross P.S. 2014. Widespread distribution of microplastics in subsurface seawater in the NE Pacific Ocean. Marine Pollution Bulletin 79, 94-99.

Di Y., Aminot Y., Schroeder D.C., Readman J.W., Jha A.N. 2017. Integrated biological responses and tissue-specific expression of p53 and ras genes in marine mussels following exposure to benzo(a)pyrene and C60 fullerenes, either alone or in combination. Mutagenesis 32, 77±90. https://doi.org/10.1093/mutage/gew049 PMID: 28011749.

Eriksen M., Maximenko N., Thiel M., Cummins A., Lattin G., Wilson S., Hafner J., Zellers A., Rifman S. 2013. Plastic pollution in the South Pacific subtropical gyre. Marine Pollution Bulletin 68, 71-76.

Farrell P., Nelson K. 2013. Trophic level transfer of microplastic: *Mytilus edulis* (L.) to *Carcinus maenas* (L.). Environmental Pollution 177, 1-3.

Gamble M., Wilson I. 2002. The hematoxylins and eosin. In: Brancfort J.D., Gamble M. (Eds.), Theory and Practice of Histological Techniques. Churchill Livingstone- Elsevier Science Ltd., London, UK, pp. 125.

Garmendia L., Soto M., Vicario U., Kim Y., Cajaraville M.P., Marigómez I. 2011. Application of a battery of biomarkers in mussel digestive gland to assess long-term effects of the Prestige oil spill in Galicia and Bay of Biscay: tissue-level biomarkers and histopathology. Journal of Environmental Monitoring 13, 915-32.

Gnaiger E. 1983. Heat dissipation and energetic efficiency in animal anoxibiosis: economy contra power. Journal of Experimental Zoology 228, 471-490.

Graham E.R., Thompson J.T. 2009. Deposit- and suspension-feeding sea cucumbers (Echinodermata) ingest plastic fragments. Journal of Experimental Marine Biology and Ecology 368, 22-29.

Green D.S., Boots B., O'Connor N.E., Thompson R., 2017. Microplastics affect the ecological functioning of an important biogenic habitat. Environmental Science and Tecnology 51, 68-77.

Gómez-Mendikute A., Etxeberria A., Olabarrieta I., Cajaraville M.P. 2002. Oxygen radicals production and actin filament disruption in bivalve haemocytes treated with benzo(a)pyrene. Marine Environmental Research 54, 431-436.

Gosling E. 2015. Marine bivalve molluscs, 2nd edn. John Wiley & Sons, Chichester.

Guilhermino L., Vieira L.R., Ribeiro D., Ana Sofia Tavares A.S., Cardoso V., Alves A., Almeida J.M. 2018. Uptake and effects of the antimicrobial florfenicol, microplastics and their mixtures on freshwater exotic invasive bivalve *Corbicula fluminea*. Science of the Total Environment 622-623, 1131-1142.

Hall N.M., Berry K.L.E., Rintoul L., Hoogenboom M.O. 2015. Microplastic ingestion by scleractinian corals. Marine Biology 162, 725-732.

Hartmann N.B., Hüffer T., Thompson R.C., Hassellöv M., Verschoor A., Daugaard A.E., Rist S., Karlsson, T., Brennholt N., Cole M., Herrling M.P., Hess M.C., Ivelva N.P., Lusher A.L., Magner W. 2019. Are we speaking the same language? Recommendations for a definition and categorization framework for plastic debris. Environ. Sci. Technol. 53, 1039-1047.

Hidalgo-Ruz V., Gutow L., Thompson R.C., Thiel M. 2012. Microplastics in the marine environment: A review

of the methods used for identification and quantification. Environmental Science & Technology 46, 3060-3075.

Hoss D.E., Settle L.R. 1990. Ingestion of plastics by teleost fishes. In: Shomura RS, Godfrey ML (eds) Proceedings of the second international conference on marine debris. US Department of Commerce, NOAA Technical Memo, Honolulu, HI, 693-709.

ICES. 2015. OSPAR Request on development of a common monitoring protocol for plastic particles in fish stomachs and selected shell fish on the basis of existing fish disease surveys. Parma, Italy.

Izagirre, U. 2007. Contribution to the interpretation of lysosomal biomarkers in marine organisms based on the mechanistic understanding of the lysosomal responses to pollutants. PhD Thesis, University of the Basque Country, Bilbo, Spain.

Jeong C.B., Won E.J., Kang H.M., Lee M.C., Hwang D.S., Hwang U.K., Zhou B., Souissi S., Lee S.J., Lee J.S., 2016. Microplastic size-dependent toxicity, oxidative stress induction, and p-JNK and p-P38 activation in the monogonont rotifer (*Brachionus koreanus*). Environmental Science & Technology 50, 8849-57.

Jumars P.A. 1993. Gourmands of mud: Diet selection in marine deposit feeders 124-156 in R.N. Hughes, Ed. Mechanisms of Diet Choice, Blackwell Scientific Publishers, Oxford.

Katsumiti A., Gilliland D., Arostegui I., Cajaraville M.P. 2015. Mechanisms of toxicity of Ag nanoparticles in comparison to bulk and ionic Ag on mussel hemocytes and gill cells. PLoS ONE 10, e0129039. doi:10.1371/journal.pone.0129039.

Kim Y., Ashton-Alcox A., Powell E.N. 2006. Histological techniques for marine bivalve molluscs: update NOAA technical memorandum NOS NCCOS 27, 76 pp.

Koelmans A.A. 2015 Modeling the role of microplastics in bioaccumulation of organic chemicals to marine aquatic organisms. A Critical Review. In: Bergmann M., Gutow L., Klages M. (eds) Marine Anthropogenic Litter pp 309-324. Springer, Cham.

Lechner A. Keckeis H., Lumesberger F., Zens B., Krusch R., Tritthart M., Glas M., Schludermann E. 2014. The Danube so colourful: A potpourri of plastic litter outnumbers fish larvae in Europe's second largest river. Environmental Pollution 188, 177-181.

Li J., Green C., Reynolds A., Shi H., Rotchell J.M. 2018. Microplastics in mussels sampled from coastal waters and supermarkets in the United Kingdom. Environmental Pollution 241, 35-44.

Li J., Lusher A.L., Rotchell J.M., Deudero S., Turra A., Brate I.L.N., Sun C., Hossain M.S., Li Q., Kolandhasamy P., Shi H. 2019. Using mussel as a global bioindicator of coastal microplastic pollution. Environmental Pollution 244, 522-533.

Long M., Brivaela M., Morgane G., Christophe L., Arnaud H., Jean R., Philippe S. 2015. Interactions between microplastics and phytoplankton aggregates: impact on their respective fates. Marine Chemistry 175, 39-46.

Long M., Paul-Pont I., Hégareta H., Moriceaua B., Lamberta C., Huveta A., Soudan P. 2017. Interactions between polystyrene microplastics and marine phytoplankton lead to species-specific hetero-aggregation.

Environmental Pollution 228, 454-463.

Lowry O.H., Rosebrough N.J., Farr A.L., Randall R.J. 1951. Determination of proteins. The Journal of Biological Chemistry 193, 265-275.

Lusher A. 2015. Microplastics in the marine environment: Distribution, interactions and effects. In M. Bergmann, L. Gutow & M. Klages (Eds.), Marine anthropogenic litter 245-308. Berlin: Springer.

Lusher A.L., Welden N.A., Sobral P., Cole M. 2017. Sampling, isolating and identifying microplastics ingested by fish and invertebrates. Analytical Methods 9, 1346-1360.

Ma Y., Huang A., Cao S., Sun F., Wang L., Guo H., Ji R. 2016. Effects of nanoplastics and microplastics on toxicity, bioaccumulation, and environmental fate of phenanthrene in fresh water. Environmental Pollution 219, 166-173.

Magni S., Gagné F., André C., Della Torre C., Auclair J., Hanana H., Parenti C.C., Bonasoro F., Binelli A. 2018. Evaluation of uptake and chronic toxicity of virgin polystyrene microbeads in freshwater zebra mussel *Dreissena polymorpha* (Mollusca: Bivalvia). Science of Total Environment 631-632, 778-788.

Marigómez I., Soto M., Cancio I., Orbea A., Garmendia L., Cajaraville M.P. 2006. Cell and tissue biomarkers in mussel, and histopathology in hake and anchovy from Bay of Biscay after the Prestige oil spill (Monitoring Campaign 2003). Marine Pollution Bulletin 53, 287-304.

Martínez-Álvarez I., Le Menach K., Devier M.-H., Cajaraville M.P., Orbea A., Budzinski, H. Characterization of the adsorption/desorption of benzo(a)pyrene to/from polystyrene micro- and nanoplastics for further toxicity assessment. SETAC Europe 28th Annual Meeting, Rome, 13-17 May 2018.

Navarro E., Iglesias J.I.P., Camacho A.P., Labarta U. 1996. The effect of diets of phytoplankton and suspended bottom material on feeding and absorption of raft mussels (*Mytilus galloprovincialis* Lmk). Journal of Experimental Marine Biology and Ecology 198, 175-189.

Navarro E., Iglesias J.I.P., Camacho A.P., Labarta U., Beiras R. 1991. The physiological energetics of mussels (*Mytilus galloprovincialis* Lmk) from different cultivation rafts in the Ria de Arosa (Galicia, NW Spain). Aquaculture 94, 197-212.

Navarro P., Cortazar E., Bartolomé L., Deusto M., Raposo J.C., Zuloaga O., Arana G., Etxebarria N. 2008. Comparison of solid phase extraction, saponification and gel permeation chromatography for the clean-up of microwave-assisted biological extracts in the analysis of polycyclic aromatic hydrocarbons. Journal of Chromatography A 1128, 10-16.

Norén F., Naustvoll F. 2010. Survey of microscopic anthropogenic particle in Skagerrak. Commissioned by KLIMA-OG FORURENSNINGSDIREKTORATET, Norway.

Okay O.S., Tolun L., Tüfekçi V., Telli-Karakoç F. Donkin P. 2006. Effects of pyrene on mussels in different experimental conditions. Environment International 32, 538-544.

Oliveira M., Ribeiro A., Hylland K., Guilhermino L. 2013. Single and combined effects of microplastics and pyrene on juveniles (0+ group) of the common goby *Pomatoschistus microps* (Teleostei, Gobiidae). Ecological Indicators 34, 641-647.

Orbea A. Cajaraville M.P. 2006. Peroxisome proliferation and antioxidant enzymes in transplanted mussels of four Basque estuaries with different levels of polycyclic aromatic hydrocarbon and polychlorinated biphenyl pollution. Environmental Toxicology and Chemistry 25, 1616-26.

Orbea A., Ortiz-Zarragoitia M., Cajaraville M.P. 2002. Interactive effects of benzo(a)pyrene and cadmium and effects of di(2-ethylhexyl) phthalate on antioxidant and peroxisomal enzymes and peroxisomal volume density in the digestive gland of mussel *Mytilus galloprovincialis* Lmk. Biomarkers 7, 33-48.

Ortiz-Zarragoitia M., Cajaraville M.P. 2006. Biomarkers of exposure and reproduction-related effects in mussels exposed to endocrine disruptors. Archives of Environmental Contamination and Toxicology 50, 361-369.

Ortiz-Zarragoitia M., Cajaraville M.P. 2010. Intersex and oocyte atresia in a mussel population from the Biosphere's Reserve of Urdaibai (Bay of Biscay). Ecotoxicology and Environmental Safety 73, 693-701.

Paul-Pont I., Lacroix C., Fernández C.G., Hégaret H., Lambert C., Le Goïc N., Frere L., Cassone A.L., Sussarellu R., Fabioux C., Guyomarch J., Albentosa M, Huvet A., Soudant P. 2016. Exposure of marine mussels *Mytilus* spp. to polystyrene microplastics: Toxicity and influence on fluoranthene bioaccumulation. Environmental Pollution 216, 724-737.

Pearse A.G.E. 1972. Histochemistry, theoretical and applied, Vol. 2. Churchill-Livingstone, London Plastic Europe, 2016. Plastics- the Facts 2016.

Pittura L., Avio C.G., Giuliani M.E., d'Errico G., Keiter S.H., Cormier B., Gorbi S., Regoli F. 2018. Microplastics as vehicles of environmental PAHs to marine organisms: combined chemical and physical hazards to the Mediterranean mussels, *Mytilus galloprovincialis*. Frontiers in Marine Science 5:103. doi: 10.3389/fmars.2018.00103.

Qu X., Su L., Li H., Liang M., Shi H. 2018. Assessing the relationship between the abundance and properties of microplastics in water and in mussels. Science of the Total Environment 621, 679-686.

Raisuddin S., Jha A.N. 2004. Relative sensitivity of fish and mammalian cells to sodium arsenate and arsenite as determined by alkaline single-cell gel electrophoresis and cytokinesis-block micronucleus assay. Environmental and Molecular Mutagenesis 44, 83-89.

Repetto G., Del Peso A., Zurita J.L. 2008. Neutral red uptake assay for the estimation of cell viability/cytotoxicity. Nature protocols 3, 1125.

Ribeiro F., Garcia A.R., Pereira B.P., Fonseca M., Nélia C. Mestre N.C., Fonseca T.G., Laura M. Ilharco L.M., Bebianno M.J. 2017. Microplastics effects in *Scrobicularia plana.* Marine Pollution Bulletin 122, 379-391.

Rist S.E., Assidqi K., Zamani N.P., Appel D., Perschke M., Huhn M., Lenz M. 2016. Suspended micro-sized PVC particles impair the performance and decrease survival in the Asian green mussel *Perna viridis*. Marine Pollution Bulletin 111, 213-220.

Rochman C.M., Hoh E., Kurobe T., Teh S.J. 2013a. Ingested plastic transfers hazardous chemicals to fish and induces hepatic stress. Scientific Reports 3, 3263.

Rochman C.M., Manzano C., Hentschel B.T., Simonich S.L.M., Hoh E. 2013b. Polystyrene plastic: a source and

sink for polycyclic aromatic hydrocarbons in the marine environment. Environmental Science & Technology 47, 13976-13984.

Santana M.F., Moreira F.T., Pereira C.D., Abessa D.M., Turra A. 2018. Continuous exposure to microplastics does not cause physiological effects in the cultivated mussel *Perna perna*. Archives of Environmental Contamination and Toxicology 74, 594-604.

Santana M.F.M., Moreira F.T., Turra A. 2017. Trophic transference of microplastics under a low exposure scenario: Insights on the likelihood of particle cascading along marine food-webs. Marine Pollution Bulletin 121, 154-159.

Ruiz P., Ortiz-Zarragoitia M., Orbea A., Vingen S., Hjelle A., Baussant T., Cajaraville M.P. 2014. Short- and long-term responses and recovery of mussels *Mytilus edulis* exposed to heavy fuel oil no. 6 and styrene. Ecotoxicology 23, 861-879.

Seed R. 1969. The ecology of *Mytilus edulis* L (Lamellibranchiata) on exposed rocky shores. Oecologia 3, 277-315.

Soto M., Zaldibar B., Cancio I., Taylor M.G., Turner M., Morgan A.J., Marigomez I. 2002. Subcellular distribution of cadmium and its cellular ligands in mussel digestive gland as revealed by combined autometallography and X-ray microprobe analysis. The Histochemical Journal 34, 273-280.

Sussarellu R., Suquet M., Thomas Y., Lambert C., Fabioux C., Pernet M.E.J., Corporeau C. 2016. Oyster reproduction is affected by exposure to polystyrene microplastics. Proceedings of the National Academy of Sciences 113, 2430-2435.

Thompson R.C., Olsen Y., Mitchell R.P., Davis A., Rowland S.J., John A.W., Russell A. E. 2004. Lost at sea: where is all the plastic? Science 304, 838-838.

Tsangaris C., Papathanassiou E., Nicolaidou A. 2008. Biochemical biomarkers and overall health status of mussels *Mytilus galloprovincialis* exposed to nickel and chromium. Chemistry and Ecology 24, 315-327.

Tung E.W., Philbrook N.A., Belanger C.L., Ansari S., Winn L.M. 2014. Benzo[a]pyrene increases DNA double strand break repair *in vitro* and *in vivo*: a possible mechanism for benzo[a]pyrene-induced toxicity. Mutation Research/Genetic Toxicology and Environmental Mutagenesis 760, 64-69.

UNEP/RAMOGE. 1999. Manual on the biomarkers recommended for the MED POL biomonitoring programme. UNEP, Athens, Greece.

UNEP .2011. UNEP year book: Emerging issues in our global environment (79 p). Nairobi: United Nations Environmental Programme.

U.E. Water Framework Directive. Environmental Quality Standards Directive (EQSD) 2008/105/EC. http://ec.europa.eu/environment/water/water-framework/priority_substances.htm

U.S. EPA. IRIS Toxicological Review of Benzo[a]pyrene (External Review Draft). U.S. Environmental Protection Agency, Washington, DC, EPA/635/R-14/312, 2014.

Van Cauwenberghe L., Claessens M., Vandegehuchte M.B., Janssen C.R. 2015. Microplastics are taken up by mussels (*Mytilus edulis*) and lugworms (*Arenicola marina*) living in natural habitats. Environmental

Pollution 199, 10-17.

Van Cauwenberghe L., Janssen C.R. 2014. Microplastics in bivalves cultured for human consumption. Environmental Pollution, 193, 65-70.

van Franeker J.A., Blaize C., Danielsen J., Fairclough K., Gollan J., Guse N., Hansen P.L., Heubeck M., Jensen J.K., Le Guillou G., Olsen B., Olsen K.O., Pedersen J., Stienen E.W.M., Turner D.M. 2011. Monitoring plastic ingestion by the northern fulmar *Fulmarus glacialis* in the North Sea. Environmental Pollution 159, 2609-2615.

Vandermeersch, G., Van Cauwenberghe, L., Janssen, C.R., Marques, A., Granby, K., Fait, G., Kotterman, M.J., Diogene, J., Bekaert, K., Robbens, J., Devriese, L., 2015. A critical view on microplastic quantification in aquatic organisms. Environmental Research 143, 46-55.

Velzeboer I., Kwadijk C.J.A.F., Koelmans A.A. 2014. Strong sorption of PCBs to nanoplastics, microplastics, carbon nanotubes, and fullerenes. Envionmental Science and Technology 48, 4869-4876.

Venier P., Maron S., Canova S. 1997. Detection of micronuclei in gill cells and haemocytes of mussels exposed to benzo[a]pyrene. Mutation Research/Genetic Toxicology and Environmental Mutagenesis 390, 33-44.

Viarengo A., Lowe D., Bolognesi C., Fabbri E., Koehler A. 2007. The use of biomarkers in biomonitoring: a 2-tier approach assessing the level of pollutant-induced stress syndrome in sentinel organisms. Comparative Biochemistry and Physiology Part C: Toxicology & Pharmacology 146, 281-300.

Von Moos N., Burkhard-Holm P., Kohler A. 2012. Uptake and effects of microplastics on cells and tissue of the blue mussel *Mytilus edulis* L. after an experimental exposure. Environmental Science & Technology 46, 11327-11335.

Ward J.E., Shumway S.E. 2004. Separating the grain from the chaff: particle selection in suspension- and deposit-feeding bivalves. Journal of Experimental Marine Biology and Ecology 300, 83-130.

Watts A.J., Lewis C., Goodhead R.M., Beckett S.J., Moger J., Tyler C.R., Galloway T.S. 2014. Uptake and retention of microplastics by the shore crab *Carcinus maenas*. Environmental Science & Technology 48, 8823-8830.

Watts A.J., Urbina M.A., Corr S., Lewis C., Galloway T.S. 2015. Ingestion of plastic microfibers by the crab *Carcinus maenas* and its effect on food consumption and energy balance. Environmental Science & Technology 49, 14597-14604.

Wegner A., Besseling E., Foekema E.M., Kamermans P., Koelmans A.A. 2012. Effects of nanopolystyrene on the feeding behavior of the blue mussel (*Mytilus edulis* L.). Environmental Toxicology and Chemistry 31, 2490-2497.

Welden N.A., Cowie P.R. 2016. Long-term microplastic retention causes reduced body condition in the langoustine, *Nephrops norvegicus*. Environmental Pollution 218, 895-900.

Whyte J. 1987. Biochemical composition and energy content of six species of phytoplankton used in mariculture of bivalves. Aquaculture 60, 231-241.

Xu X.Y., Lee W.T., Chan A.K.Y., Lo H.S., Shin P.K.S., Cheung S.G. 2017. Microplastic ingestion reduces energy

intake in the clam *Atactodea striata*. Marine Pollution Bulletin 24, 798-802.

Zaldibar B., Cancio I., Marigómez I. 2007. Reversible alterations in epithelial cell turnover in digestive gland of winkles *(Littorina littorea*) exposed to cadmium and their implications for biomarker measurements. Aquatic Toxicology 81, 183-196.

Ziccardi L.M., Edgington A., Hentz K., Kulacki K.J., Kane Driscoll S. 2016. Microplastics as vectors for bioaccumulation of hydrophobic organic chemicals in the marine environment: A state-of-the science review. Environmental Toxicology and Chemistry 35, 1667-1676.

Zorita I., Ortiz-Zarragoitia M., Soto M., Cajaraville M.P. 2006. Biomarkers in mussels from a copper site gradient (Visnes, Norway): an integrated biochemical, histochemical and histological study. Aquatic Toxicology 78, 109-116.

SUPPLEMENTARY MATERIAL TO CHAPTER 1

Table S1. Tissue distribution of MPs in the digestive gland of mussels dietarily exposed to 4.5 µm MPs (LMP) and to LMP with sorbed BaP (LMPB) along 7 and 26 days. Data are shown as numbers of MPs in one section of the digestive gland per individual mussel and as means and standard errors for 10 mussels per experimental group. Not observed, n.o. and tissue not present in the section, n.t.

			LMP										
			1	**2**	**3**	**4**	**5**	**6**	**7**	**8**	**9**	**10**	**Mean ± SE**
7 d	Stomach	Lumen food	2	229	n.t.	512	n.o.	16	212	n.o.	166	4	126.78 ± 55.08
		Lumen mucus	3	n.o.	n.t.	n.o.	n.o.	2	n.o.	n.o.	n.o.	n.o.	0.56 ± 0.36
		Epithelium	6	3	n.t.	n.o.	n.o.	4	2	n.o.	n.o.	n.o.	1.67 ± 0.69
	Ducts	Lumen	n.o.	n.o.	n.o.	1	n.o.	n.o.	n.o.	n.o.	1	n.o.	0.20 ± 0.13
		Epithelium	1	n.o.	n.o.	n.o.	n.o.	n.o.	n.o.	n.o.	n.o.	n.o.	0.10 ± 0.10
	Digestive tubules	Lumen	n.o.	n.o.	n.o.	n.o.	n.o.	6	n.o.	n.o.	2	n.o.	0.80 ± 0.61
		Epithelium	n.o.	n.o.	n.o.	n.o.	n.o.	2	n.o.	n.o.	1	n.o.	0.30 ± 0.21
	Connective tissue		1	5	n.o.	n.o.	n.o.	5	1	1	2	12	3.10 ± 1.16
	Total MPs		120.60 ± 53.28										
	Total MPs within epithelial cells		1.90 ± 0.84										

			LMPB										
			1	**2**	**3**	**4**	**5**	**6**	**7**	**8**	**9**	**10**	**Mean ± SE**
7 d	Stomach	Lumen food	n.o.	10	3	17	n.o.	2	1	n.o.	n.o.	5	3.80 ± 1.78
		Lumen mucus	n.o.	n.o.	n.o.	n.o.	n.o.	n.o.	2	n.o.	n.o.	n.o.	0.20 ± 0.20
		Epithelium	n.o.	5	n.o.	2	n.o.	n.o.	2	n.o.	2	n.o.	1.10 ± 0.53
	Ducts	Lumen	n.o.	n.o.	n.o.	n.o.	n.o.	2	n.o.	n.o.	2	n.o.	0.40 ± 0.27
		Epithelium	n.o.	n.o.	n.o.	n.o.	n.o.	3	n.o.	n.o.	1	1	0.50 ± 0.31
	Digestive tubules	Lumen	n.o.	n.o.	n.o.	n.o.	n.o.	n.o.	n.o.	8	31	n.o.	3.90 ± 3.11
		Epithelium	n.o.	n.o.	n.o.	n.o.	n.o.	n.o.	n.o.	n.o.	1	n.o.	0.10 ± 0.10
	Connective tissue		1	2	n.o.	2	n.o.	n.o.	6	2	1	3	1.70 ± 0.58
	Total MPs		11.70 ± 3.60										
	Total MPs within epithelial cells		1.70 ± 0.58										

			LMP										
			1	**2**	**3**	**4**	**5**	**6**	**7**	**8**	**9**	**10**	**Mean ± SE**
26 d	Stomach	Lumen food	n.t.	3	4	n.o.	n.o.	1	n.o.	1	106	n.o.	12.78 ± 11.06
		Lumen mucus	n.t.	n.o.	n.o.	n.o.	n.o.	n.o.	n.o.	n.o.	4	3	0.78 ± 0.49
		Epithelium	n.o.	n.o.	2	1	1	n.o.	n.o.	4	n.o.	n.o.	0.89 ± 0.42
	Ducts	Lumen	n.o.	n.o.	n.o.	17	1	1	4	n.o.	n.o.	1	2.40 ± 1.67
		Epithelium	n.o.	n.o.	n.o.	n.o.	n.o.	n.o.	n.o.	n.o.	n.o.	n.o.	n.o.
	Digestive tubules	Lumen	n.o.	n.o.	n.o.	n.o.	n.o.	n.o.	n.o.	n.o.	n.o.	n.o.	n.o.
		Epithelium	n.o.	n.o.	n.o.	n.o.	n.o.	n.o.	n.o.	n.o.	n.o.	n.o.	n.o.
	Connective tissue		n.o.	10	n.o.	n.o.	1	2	1	n.o.	1	1	1.6 ± 0.96
	Total MPs		17 ± 10.57										
	Total MPs within epithelial cells		0.80 ± 0.42										

			LMPB										
			1	**2**	**3**	**4**	**5**	**6**	**7**	**8**	**9**	**10**	**Mean ± SE**
26 d	Stomach	Lumen food	368	n.o.	48	52	14	54	10	12	9	2	56.90 ± 35.20
		Lumen mucus	20	n.o.	n.o.	n.o.	n.o.	3	n.o.	n.o.	n.o.	n.o.	2.30 ± 1.99
		Epithelium	6	3	5	2	n.o.	5	n.o.	n.o.	n.o.	2	2.30 ± 0.75
	Ducts	Lumen	45	n.o.	n.o.	n.o.	n.o.	n.o.	n.o.	n.o.	n.o.	n.o.	4.50 ± 4.50
		Epithelium	n.o.	n.o.	3	n.o.	n.o.	n.o.	n.o.	n.o.	n.o.	n.o.	0.30 ± 0.30
	Digestive tubules	Lumen	n.o.	n.o.	1	1	1	n.o.	n.o.	n.o.	n.o.	1	0.80 ± 0.14
		Epithelium	n.o.	n.o.	n.o.	n.o.	n.o.	n.o.	n.o.	n.o.	n.o.	n.o.	n.o.
	Connective tissue		n.o.	n.o.	n.o.	9	n.o.	8	3	n.o.	n.o.	3	2.30 ± 1.11
	Total MPs		69 ± 41.91										
	Total MPs within epithelial cells		2.60 ± 0.91										

Table S2. Prevalence of histopathological alterations in gonad tissue of control mussels and of mussels dietarily exposed for 7 and 26 days to 4.5 µm MPs (LMP), 0.5 µm NPs (SMP), LMP with sorbed BaP (LMPB) and SMP with sorbed BaP (SMPB). Data are shown in percentages of 8-10 mussels per experimental group (one section per mussel). For oocyte atresia, a semiquantitative scale was used as follows: 0 normal gonad, 1 less than half the follicles are affected, 2 about half the follicles are affected, 3 more than half the follicles are affected and 4 all follicles affected. Not observed, n.o.

				CONTROL	LMP	LMPB	SMP	SMPB
7 D	Fibrosis		Female	n.o.	40	n.o.	n.o.	25
			Male	n.o.	40	40	n.o.	33.33
			Total	n.o.	40	20	n.o.	30
	Hemocytic infiltration	Focal	Female	20	n.o.	20	n.o.	25
			Male	20	20	20	n.o.	n.o.
			Total	20	10	20	n.o.	10
		Diffuse	Female	n.o.	60	20	n.o.	n.o.
			Male	n.o.	n.o.	n.o.	16.66	n.o.
			Total	n.o.	30	10	10	n.o.
	Oocyte atresia		1	40	20	20	50	25
			2	n.o.	n.o.	n.o.	25	n.o.
			3	n.o.	n.o.	20	n.o.	n.o.
			4	n.o.	n.o.	n.o.	25	n.o.
26 D	Fibrosis		Female	n.o.	n.o.	33.33	n.o.	n.o.
			Male	n.o.	n.o.	14.28	n.o.	n.o.
			Total	n.o.	n.o.	20	n.o.	n.o.
	Hemocytic infiltration	Focal	Female	n.o.	n.o.	n.o.	n.o.	n.o.
			Male	25	n.o.	14.28	n.o.	n.o.
			Total	10	n.o.	10	n.o.	n.o.
		Diffuse	Female	n.o.	n.o.	n.o.	n.o.	n.o.
			Male	25	n.o.	n.o.	n.o.	n.o.
			Total	10	n.o.	n.o.	n.o.	n.o.
	Oocyte atresia		1	66.66	50	33.33	20	33.33
			2	n.o.	n.o.	n.o.	20	n.o.
			3	n.o.	n.o.	33.33	20	33.33
			4	n.o.	n.o.	n.o.	n.o.	n.o.

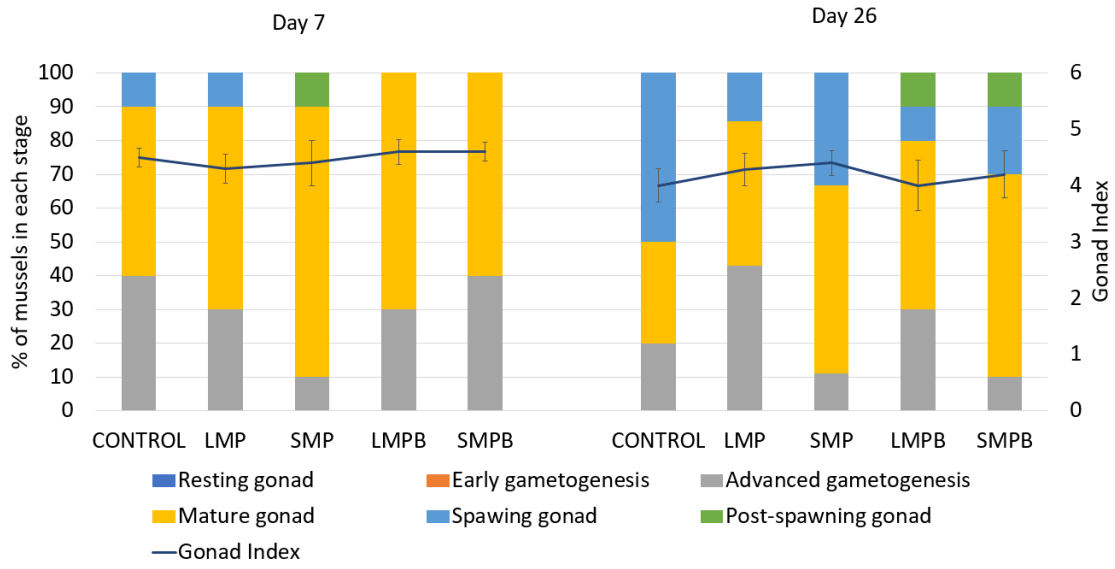

Figure S1. Gonad index (lines) and percentage of animals at each gamete developmental stage (stacked-graphs) in control mussels and in mussels dietarily exposed for 7 and 26 days to 4.5 µm MPs (LMP), 0.5 µm NPs (SMP), LMP with sorbed BaP (LMPB) and SMP with sorbed BaP (SMPB). Gonad index values are given as means and standard errors of 8-10 mussels per experimental group.

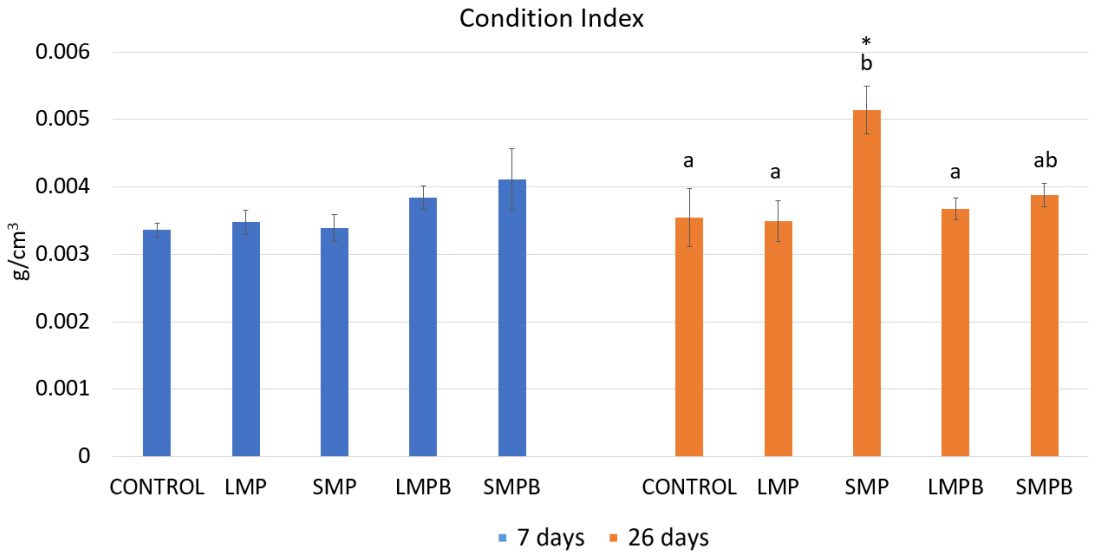

Figure. S2 . Condition index (g/cm^3) in control mussels and in mussels dietarily exposed for 7 and 26 days to 4.5 µm MPs (LMP), 0.5 µm NPs (SMP), LMP with sorbed BaP (LMPB) and SMP with sorbed BaP (SMPB). Data are given as mean values and standard errors of 7 mussels per experimental group. Letters indicate significant differences among treatments within the same day and asterisks indicate a significant difference between days within the same treatment (2-way ANOVA followed by Tukey's post hoc test, $p<0.05$).

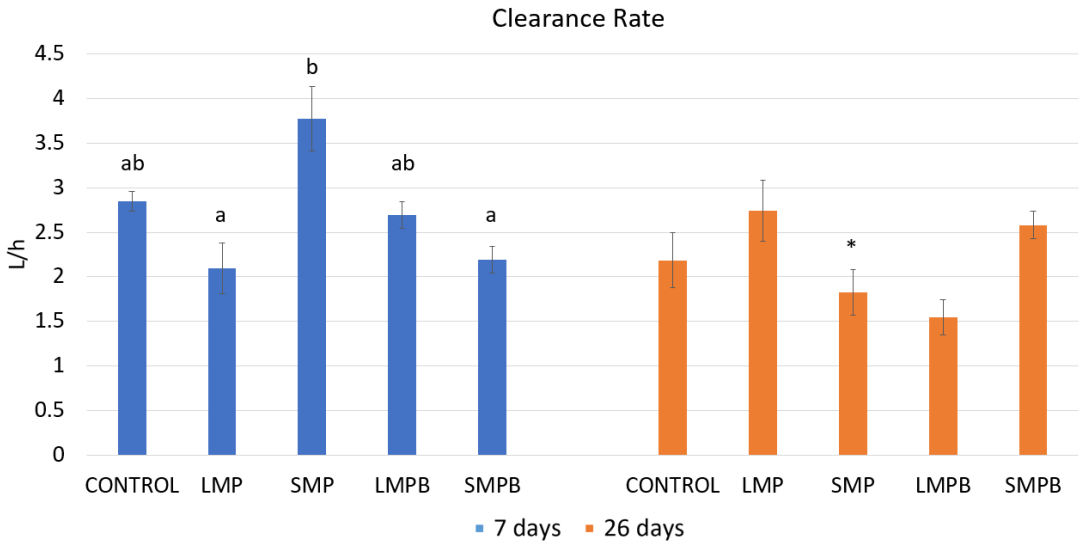

Figure. S3. Clearance rate (L/h) in control mussels and in mussels dietarily exposed for 7 and 26 days to 4.5 µm MPs (LMP), 0.5 µm NPs (SMP), LMP with sorbed BaP (LMPB) and SMP with sorbed BaP (SMPB). Data are given as mean values and standard errors of 7 mussels per experimental group. Letters indicate significant differences among treatments within the same day and asterisks indicate a significant difference between days within the same treatment (2-way ANOVA followed by Tukey's post hoc test, $p<0.05$).

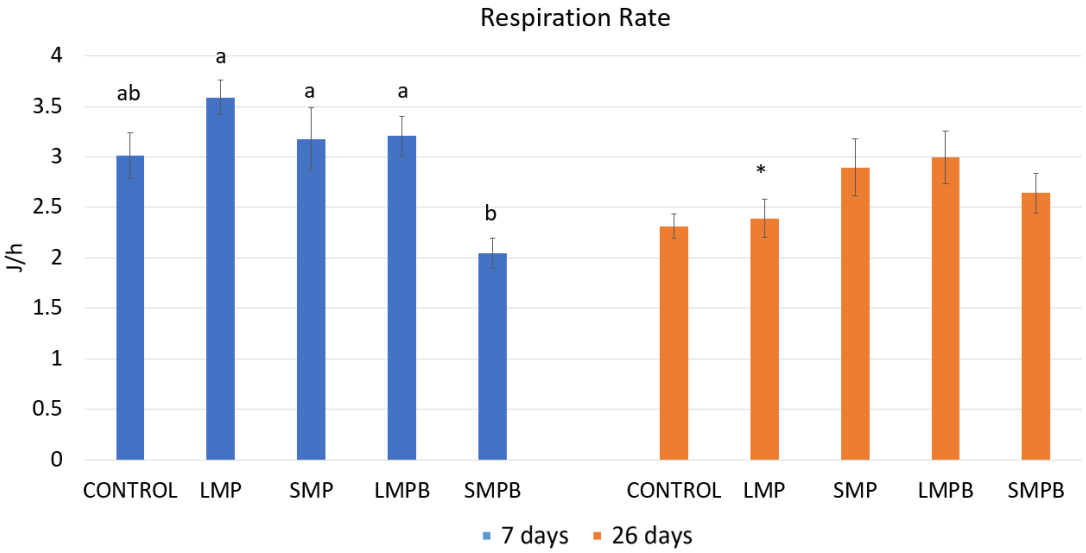

Figure. S4. Respiration rate (J/h) in control mussels and in mussels dietarily exposed for 7 and 26 days to 4.5 µm MPs (LMP), 0.5 µm NPs (SMP), LMP with sorbed BaP (LMPB) and SMP with sorbed BaP (SMPB). Data are given as mean values and standard errors of 7 mussels per experimental group. Letters indicate significant differences among treatments within the same day and asterisks indicate a significant difference between days within the same treatment (2-way ANOVA followed by Tukey's post hoc test, $p<0.05$).

CHAPTER 2:

Effects of microplastics alone or with sorbed oil compounds from the water accommodated fraction of a North Sea crude oil on marine mussels *Mytilus galloprovincialis*

This chapter is being prepared for publication:

GONZÁLEZ-SOTO, N; CAMPOS, L; NAVARRO, E; BILBAO, E., GUILHERMINO, L; CAJARAVILLE, MP. Effects of microplastics alone or with sorbed oil compounds from the water accommodated fraction of a North Sea crude oil on marine mussels (*Mytilus galloprovincialis*). *Environmental Science and Technology*.

This chapter has been/will be presented at:

MICRO 2018- International Conference on Fate and Impact of Microplastics: Knowledge, Actions and Solutions. Lanzarote, 19-23 November 2018. GONZÁLEZ-SOTO, N; KATSUMITI, A; DUROUDIER, N; ORBEA, A; BILBAO, E; NAVARRO, E; CAJARAVILLE, MP. Impact of microplastics alone or with adsorbed oil compounds from the water accommodated fraction of a North Sea crude oil on marine mussels *Mytilus galloprovincialis*. Poster.

21st International Symposium on Pollutant Responses in Marine Organisms (PRIMO), Gothenburg, 22 to 25 May 2022. GONZÁLEZ-SOTO N.; CAMPOS L.; NAVARRO E.; GUILHERMINO L.; BILBAO, E.; CAJARAVILLE, MP. Effects of microplastics alone or with sorbed oil compounds from the WAF of a North Sea crude oil on marine mussels *Mytilus galloprovincialis*. Platform (N González-Soto).

ABSTRACT

Microplastics (MPs) can adsorb persistent organic pollutants such as oil hydrocarbons and may facilitate their transfer to organisms (Trojan horse effect). The aim of this study was to examine the effects of a 21 day dietary exposure to polystyrene MPs of 4.5 μm at 1000 particles/mL, alone and with sorbed oil compounds from the water accommodated fraction (WAF) of a naphthenic North Sea crude oil at two dilutions (25% and 100%), on marine mussels. An additional group of mussels was exposed to 25% WAF for comparison. PAHs were accumulated in mussels exposed to WAF but not in those exposed to MPs with sorbed oil compounds from WAF (MPs-WAF), partly due to the low concentration of PAHs in the studied crude oil. Exposure to MPs or to WAF alone altered the activity of enzymes involved in aerobic and biotransformation metabolism. Prevalence of oocyte atresia and volume density of basophilic cells were higher in mussels exposed to MPs and to WAF than in controls, whereas a decrease in absorption efficiency was observed. After 21 days MPs caused DNA damage in mussel hemocytes. In conclusion, a Trojan horse effect was not observed but both MPs and oil WAF caused an array of deleterious effects on marine mussels at different levels of biological organization.

1. INTRODUCTION

Plastics in oceans tend to accumulate according to their density and to fragment into smaller pieces eventually reaching dimensions lower than 1 mm called microplastics (MPs) (Hartmann et al., 2019). In addition to these MPs, known as secondary ones, particles with original size lower than 1 mm are also introduced into the marine environment and are often indicated as primary MPs. MPs can be found in most parts of world's seas and oceans (Auta et al., 2017; Ying et al., 2020) and may cause disorders in marine organisms (Barnes et al., 2009; Pirsaheb et al., 2020). MPs can be internalized by aquatic organisms with different feeding strategies (Moore, 2008; Andrady, 2011; Lee et al., 2013; Batel et al., 2016; Chae et al., 2017) and they can alter their feeding activity, growth and reproduction or even cause mortality (Browne et al., 2008; Van Moos et al., 2012; Lee et al., 2013; Sussarellu et al., 2016; Oliveira et al., 2018).

Bivalve mollusks, and specially mussels, have been pointed as appropriate organisms to use both in field monitoring programs and laboratory studies to investigate the impact of MPs in the marine environment (Akdogan & Guven, 2019; Li et al., 2019). They are abundant, broadly distributed and sessile filter-feeders that accumulate contaminants in their tissues, reflect levels of environmental pollution and show significant responses to pollutants (Cajaraville et al., 2000; Vethaak et al. 2017). Marine mussels can ingest MPs (Sendra et al., 2021), which have been reported to cause oxidative stress (Paul-Pont et al., 2016), immunological responses (Pittura et al., 2018; Green et al., 2019), alterations in gene expression patterns (Détrée & Gallardo-Escárate, 2017; Capolupo et al., 2018), genotoxicity (Chapter 1), neurotoxicity (Avio et al., 2015) and changes in the physiology of mussels (Wegner et al., 2012; van Cauwenberghe et al., 2015).

An additional risk of MPs to marine biota comes from their ability to adsorb persistent organic pollutants (POPs) from the environment due to their large surface to volume ratio and hydrophobicity (Bakir et al., 2016; Ahmed et al., 2021). Several laboratory studies have demonstrated that POPs such as polycyclic aromatic hydrocarbons (PAHs) sorbed to MPs can bioaccumulate in exposed animals and enhance toxic effects of MPs (Rochman et al., 2013; Avio et al., 2015; O'Donovan et al., 2018; Von Hellfeld et al., 2022; Chapter 1). Moreover, in aquatic

animals exposed to mixtures of MPs and PAHs the presence of the particles influences the biotransformation, bioaccumulation and toxicity of the latter (Oliveira et al., 2013). However, unrealistic high concentrations of POPs are usually used in laboratory studies (Burns & Boxell, 2018). To the best of our knowledge, there are no studies addressing the effects of complex mixtures of PAHs or other oil hydrocarbons sorbed to MPs on bivalves (De Sá et al., 2018).

Crude oil is a complex mixture that contains thousands of different chemicals (Carls & Meador, 2009) and it is one of the most complex and variable products to evaluate toxicologically (Singer et al., 2000). Toxicity of oil in an aquatic system is usually assessed through its water accommodated fraction (WAF). The WAF is a laboratory prepared medium where a test material difficult to dissolve, such as crude oil, is placed in a volume of water and mixed for hours at low energy avoiding the formation of small oil drops (Aurand & Coelho, 1996). Effects of different WAFs on mussels include alterations of enzyme activities, impairment of the lysosomal system, tissue damage, impact on the reproductive capacity, decrease of condition index and mortality (Cajaraville et al., 1991; 1992a ; 1992b; Marigómez & Baybay-Villacorta, 2003; Counihan, 2018; Blanco-Rayón et al., 2019).

This work fills a knowledge gap by studying the impact of a complex mixture of petroleum hydrocarbons derived from WAF sorbed into MPs. For this purpose, the effects of dietary exposure to polystyrene (PS) MPs of 4.5 µm alone or previously incubated in two dilutions (25% and 100%) of WAF of a naphthenic crude oil were investigated in mussels, using a battery of biological responses at molecular, cellular, tissue and organism levels. In parallel, a group of mussels was exposed to a 25% dilution of WAF for comparison.

2. MATERIALS AND METHODS

2.1. Obtention and preparation of MPs, WAF and MPs-WAF

As in previous experiments (Chapter 1), unlabeled 4.5 µm PS microspheres (Polyscience Inc.; density 1.05 g/cm^3) were used.

The WAF of a naphthenic North Sea crude oil was selected as a complex mixture of persistent organic pollutants. The crude oil was kindly provided by Drifts laboratoriet Mongstad, Equinor, Norway (former Statoil) and contained 28.6% w/v of PAHs (Statoil, 2011). WAF was produced at a ratio of 200:1 sea water/crude oil (w/w) at 20 °C based on the protocol of Singer et al. (2000) with modifications. The sand filtered (particle size ≤ 0.2 µm) marine water was added to glass bottles 24 hours prior to the addition of the oil, to achieve the desired temperature. The stirrer was switched on (at low speed, without vortex) once oil was in contact with the water. The bottles were covered with aluminum paper and kept in agitation for 40 hours. The 25% WAF dilution was obtained by diluting the WAF with sand filtered marine water.

For preparation of MPs with sorbed oil compounds from WAF, incubation of MPs with WAF was based on Batel et al. (2016) and Chapter 1. The MPs stock (89.8 µL, 4.9 x 10^8 particles/mL) was incubated with 25% WAF and 100% WAF for 24 hours, to get MP25 and MP100, respectively. The vials were incubated at 300 rpm in an orbital shaker at 18°C in darkness. Then, the suspensions were syringe filtered using sterile 0.45 µm pore sized filters (Merck Millipore, Darmstadt, Germany). The MPs were resuspended in 40 mL of Milli-Q water and added to the algae feed for each respective mussel treatment. MPs were mixed with microalgae (1:100000 MP/microalgae-day-aquarium during the first 7 days and 1:50000 MP/microalgae-day-aquarium after the mussel sampling at day 7) and dosed freshly to mussels as explained in section 2.2 (Figure 1) during the 21 days. Non-contaminated pristine MPs were incubated, filtered and resuspended in the same way but using Milli-Q water.

2.2. Sampling and maintenance of mussels

Roughly 600 mussels *Mytilus galloprovincialis* (3.5-4.5 cm in shell length) were collected in February 2018 in Mundaka, Urdaibai´s Biosphere Reserve (43°24'04.9"N, 2°41' 41.6"W), a

relatively clean area (Puy-Azurmendi et al., 2010; Bellas et al., 2014) and maintained for acclimation in aquarium facilities at the Plentzia Marine Station (PiE) of the University of the Basque Country (UPV/EHU) for 7 days. Mussels were placed in a single large 300 L polypropylene tank with a recirculating filtered seawater system (particle size ≤3 µm) for 2 days without feeding.

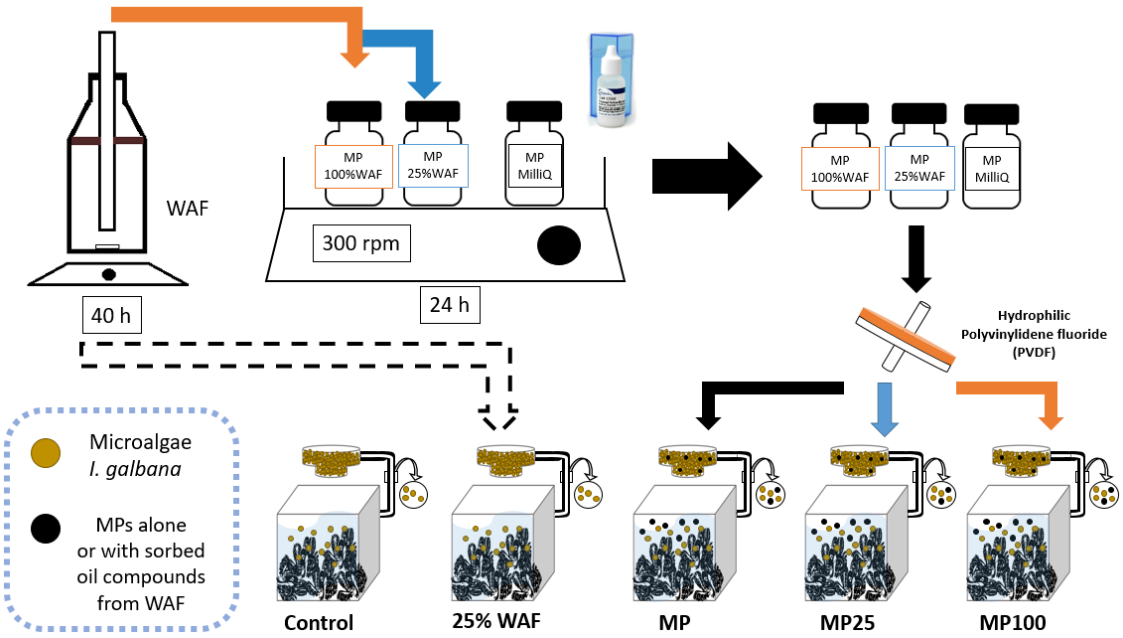

Figure 1. Scheme for the preparation of WAF, MPs alone (MP) and MPs with sorbed oil compounds from WAF (MP25 and MP100).

Then mussels were distributed in 5 glass aquaria (120 mussels per aquarium) with 40 L seawater and fed with a suspension of *Isochrysis galbana* microalgae cells (T-Iso clone) close to maintenance ration (Bayne et al., 1976) for another 5 days. This was achieved by dosing $36x10^9$ cells of *I. galbana*/mussel-day with a multichannel peristaltic pump (Watson-Marlow, United Kingdom) over a period of 22 hours/day as in Chapter 1. During both the acclimation and exposure periods, all tanks were rinsed every day with 10 L of seawater to remove faeces and then water was renewed. During acclimation, water quality was checked daily in all tanks. Light regime was 12L/12D and room temperature was kept at 14 °C. Water parameters were: salinity 28.56 ± 0.28 PSU, dissolved O_2 94.95 ± 2.90%; 8.51 ± 0.25 mg/L, pH 7.3 ± 0.04 and temperature 12.3 °C.

2.3. Mussel exposure experiment

5 experimental groups were set: control, MPs alone (MP), MPs with sorbed oil compounds from WAF at a 25% dilution (MP25) and MPs with sorbed oil compounds from 100% WAF (MP100). Mussels were exposed through the diet, to a mixture of MPs and microalgae, at an environmentally relevant concentration of 1000 MP particles/mL-day as in Chapter 1. In the fifth group (WAF), mussels were exposed to WAF at a dilution of 25%, considering that the hydrocarbon content of this dilution was equivalent to hydrocarbons sorbed to plastics incubated with 100% WAF (Martínez-Álvarez et al., submitted). This approach of using the sorption percentage to select the dose of the "soluble" control has already been described (Chen et al., 2017). On the other hand, the 25% WAF exposure could be compared to the plastics incubated with 25% WAF (MP25) following the approach used by Paul-Pont et al. (2016), where the same concentration was used in the PAH alone exposure and in the exposure to sorbed MPs.

During exposure, mussels were fed with *I. galbana* microalgae or with microalgae mixed with the MPs, in the same way than in the acclimation period. Aeration was used to keep both plastics and algae in suspension. Water from each aquarium was renewed every day, after algae/ algae+MPs dosing finished. During exposure, light regime and room temperature were kept as in acclimation. Water quality was checked every two days in the control tank: salinity 29.13 ± 0.8 PSU, dissolved O_2 90.02 ± 7.9%; 8 ± 0.50 mg/L, pH 7.3 ± 0.05 and temperature 13.29 ± 0.52 °C. Mussels were dissected after 7 and 21 days of exposure. Following sampling on day 7, dosing of algae was recalculated in order to maintain the same microalgae and MP rations.

2.4. Bioaccumulation of PAHs in mussel soft tissues

Whole mussels for chemical analysis (21 per experimental group) were stored at -40 °C and analyzed at the General Services SGiker of UPV/EHU. Measurements were done in 3 pools of 7 animals per each experimental group. Tissues were extracted using MARX microwave (CEM, Mathews, NC, USA) and cleaned through solid phase extraction (SPE Vacuum Manifold System, Millipore). The extracts obtained were concentrated through evaporation with nitrogen flow LV

Evaporator (Zymarck, Hopkinton, MA, USA), filtered and encapsulated in chromatographic vials. Concentrations of 16 EPA PAHs were measured in an Agilent (6890) Gas Chromatograph with Mass Detector (Agilent 5975C) as described by Navarro et al. (2008) and given as ng/g dry weight. Calibration standards were obtained from Dr. Ehrenstorfer GmbH (Augsburg, Germany). In all cases, recovery of analytes was approximately 90%, except for naphthalene that was 60%. The detection limits (LOQ) of the analytical method were: 30 ppb for naphthalene, 1 ppb for acenaphthylene, 10 ppb for acenaphthene, and 0.5 ppb for the rest of PAHs.

2.5. Tissue distribution of MPs in mussels

Digestive gland, gills and mantle tissue of 10 mussels per experimental group were dissected out. Half of the digestive gland, half of the gills and whole mantle were processed for tissue localization of MPs using the N-butyl alcohol protocol as described in Chapter 1. The prevalence of mussels showing MPs in the digestive gland, gills and gonad were calculated as percentages.

2.6. Whole organism responses

After 21 days of exposure, 7 mussels from each treatment were collected to determine physiological parameters (clearance rate, respiration rate, absorption efficiency, scope for growth) and condition index as previously described (Chapter 1).

2.7. Gamete development, gonad index and histopathology of mussel gonad

Gonad tissues of 15 mussels per experimental group were dissected out and processed for histopathological analysis, determination of gamete developmental stages and gonad index as described in Chapter 1. The following alterations were recorded and prevalences given as percentages: occurrence of parasites, fibrosis in the connective tissue, hemocytic infiltration, oocyte necrosis and oocyte atresia (Ortiz-Zarragoitia & Cajaraville, 2006; 2010; Ruiz et al., 2014). Oocyte atresia was semiquantified based on the following scale: 1) ¼ of follicles in the tissue section showed signs of atresia, 2) about half the follicles in the tissue section showed signs of atresia, 3) ¾ of follicles in the tissue section showed signs of atresia and 4) all follicles in the tissue section showed signs of atresia (Kim et al., 2006).

2.8. Cellular biomarkers in mussel hemocytes

The hemolymph of 8 mussels per treatment (same individuals as in sections 2.7.) was withdrawn from the posterior adductor muscle and cell viability, catalase activity and DNA damage were measured in hemocytes of individual mussels.

Cell viability was assessed by the neutral red uptake assay as described in Chapter 1. Cell concentration determined in the hemolymph of each animal using a Bright-Line™ Hemacytometer (Sigma Aldrich, St. Louis, USA) was used to normalize absorbance data. Catalase activity was determined as described in Chapter 1. Protein concentration (Lowry et al. 1951) was used to normalize absorbance data. Catalase activity was expressed as µmol H_2O_2/min*mg protein. The Comet assay was performed on mussel hemocytes following Raisuddin & Jha (2004) with modifications described in Chapter 1.

2.9. Enzyme activities in mussel tissues

Taking into consideration results on the bioaccumulation of PAHs, the presence of MPs in the groups exposed to MP25 and MP100 and the rest of results, enzyme activities were only determined in the control group and in groups exposed to MPs and to WAF.

Gills of 10 mussels and digestive glands of 15 mussels per experimental group (same individuals as in sections 2.7.) were dissected out, frozen in liquid nitrogen and stored at -80°C until analysis. Half of each gills were homogenized in 0.1 M KP buffer (pH = 6.5) to determine the activity of the enzymes glutathione *S*-transferases (GST). The second half of gills was homogenized in 0.1 M KP buffer (pH = 7.4) for catalase and glutathione peroxidase (GPx) activity determination. Digestive glands were divided in three portions. The first one was used for GST activity determination, the second one for palmitoyl-CoA oxidase (AOX1), catalase and GPx activity determination and the last portion was homogenized in 50 mM Tris(hydroxymethyl)-aminomethan buffer (pH = 7.8) for isocitrate dehydrogenase (IDH) activity determination. Tissues were homogenized in each buffer following a 1:10 proportion, tissue weight: volume.

AOX1 activity was determined as described in De los Rios et al. (2013) and expressed as the oxidation of leuco-dichlorofluorescein in mU AOX1/mg prot. IDH activity was determined

according to Ellis & Goldberg (1971) and expressed as the production of nicotinamide adenine dinucleotide phosphate (NADPH) in nmol/min/mg protein. GST activity was determined according to Habig et al. (1974) and expressed as the production of 1-chloro-2,4-dinitrobenzene (CDNB) conjugates with the thiol group of glutathione in nmol/min/mg protein. Catalase activity was determined as explained in section 2.8. GPx activity was determined according to Flohé & Günzler (1984) and expressed as the consumption of NADPH in nmol/min/mg protein. Activity of IDH, GST and GPX were measured in microplates as in Lima et al. (2007). Each enzyme activity was normalized to protein concentration measured using the Bradford method (Bradford, 1976).

2.10. Cell composition, quantitative structure and histopathology of mussel digestive gland

Paraffin sections of the digestive gland stained with hematoxylin/eosin described in section 2.5 were used (from control mussels and mussels exposed to MPs and to WAF). Cell composition of digestive tubules was measured in terms of volume density of basophilic cells (VvBAS, given as $\mu m^3/\mu m^3$) and the structure of digestive tubules was quantified as mean epithelial thickness to mean diverticular radius (MET/MDR, µm/µm) and mean luminal radius to MET (MLR/MET, µm/µm) by using a stereological method (Bignell et al., 2012; De los Ríos et al., 2013). The analysis was performed as previously described in Chapter 1 in 10 mussels per experimental group. Then, parameters were calculated as reported by Bignell et al. (2012).

Prevalences of the following histopathological alterations were recorded for the same 10 mussels per experimental group: occurrence of parasites, fibrosis in the connective tissue, atrophy of digestive tubule epithelium, focal and diffuse hemocytic infiltrations, and accumulation of brown cells in connective tissue and in epithelium of the digestive tract (Bignell et al., 2012; Ruiz et al., 2014; Chapter 1). Results are given as percentages.

2.11. Data analysis

Statistical analyses were carried out using the statistical package SPSS 24 (IBM Analytics, Armonk, NY). When possible outliers were eliminated with the Chauvenet method. All data were tested for normality and homogeneity of variances using Kolmogorov-Smirnov´s and Levene's tests,

respectively. Normally distributed data, which met the assumptions of homogeneity of variances, were assessed via one-way ANOVA and the Tukey's post hoc was used for differences among treatments within the same day, while the Student´s t test was used to assess the differences between days within the same treatment. Data which did not met the above assumptions were analyzed by the one-way Kruskal-Wallis test. The Dunn's post hoc test was used to determine the differences among treatments within the same day and the Mann-Whitney´s U test to determine the differences between days within the same treatment. Since histopathological data were expressed as percentages, the X^2 test was used (Ruiz et al., 2014). In all cases, significance was established at $p < 0,05$.

3. RESULTS

3.1 Bioaccumulation of PAHs in mussels´ soft tissues

PAH concentrations were close to detection limits in control mussels and in mussels exposed to MPs alone and similar to the PAH concentrations measured in mussels exposed to MP25 and MP100 (Table 1, Table S1). The total amount of PAHs recorded ranged from 142 ± 39.27 to 188 ± 40.29 ng/g dry weight (control group and MP100, respectively) at day 7 and from 156 ± 11,42 to 247 ± 59,39 ng/g dry weight (MP and control group, respectively) at day 21 of exposure (Table 1, Table S1). Naphthalene was the main PAH detected in all the cases. Mussels exposed to WAF bioaccumulated PAHs to a great extent, especially at day 7. Main PAHs accumulated were phenanthrene, pyrene, fluorene, acenaphthylene, fluoranthene and crysene. Higher total PAH values were measured at day 7 (ΣPAHs 2306 ± 372.42 ng/g dry weight) than at day 21 (ΣPAHs 1229 ± 165.30 ng/g dry weight) (Table 1, Table S1).

Table 1. Bioaccumulation of **Σ** 16 EPA PAHs in mussel soft tissues (ng/g dry weight). Data is given as mean ± standard deviation for 3 pools of 7 mussels, except for controls at day 21 that were 2 pools.

	Control	MP	MP25	MP100	WAF
7 D	142 ± 39.27	146 ± 21.48	174 ± 36.06	188 ± 40.29	2306 ± 372.42
21 D	247 ± 59.89	156 ± 11.42	157 ± 19.58	169 ± 11.70	1229 ± 165.30

3.2 Tissue distribution of MPs in mussels

MPs were found in different tissues of mussels exposed to MP, MP25 and MP100. 20 to 90% of mussels treated with MPs presented MPs in the digestive gland (Table 2). MPs were mostly found in the lumen of the stomach mixed with the stomach content (Table 3, Figure 2A). MPs were also observed in the lumen of ducts, though to a lesser extent. MPs were observed occasionally in the lumen of the digestive tubules, within the epithelium of the digestive tract and in the connective tissue of the digestive gland (Table 3 Figure 2B;C). MPs were found in the gills of 20 to 70% of treated mussels with the exception of mussels exposed to MP25 for 21 days, whose gills did not show any MP (Table 2). MPs were mostly found interspersed between gills filaments, and occasionally within hemocytes (Figure 2D;E). In gonads, MPs were only found in one of the mussels exposed to MP for 21 days (Table 2). In this individual MPs were localized in the connective tissue and within gonad follicles (Figure 2F).

Overall, the occurrence of MPs showed high variability among individuals of each exposure group. The highest amount of MPs was found in mussels exposed to MP, followed by mussels exposed to MP25 and mussels exposed to MP100 (Table 3). The amount of MPs in tissues of mussels decreased from day 7 to 21 in mussels exposed to MP, whereas it increased in mussels exposed to MP25. No time-dependent differences were detected in mussels exposed to MP100 (Table 3).

Table 2. Prevalence of mussels showing MPs in different tissues of control mussels and mussels exposed to MP, MP25 and MP100 for 7 and 21 days. Data are shown as percentages of 8-10 mussels per experimental group (one section per mussel). Not observed, n.o. No MPs were observed in Control and WAF groups.

	Gonad		**Gill**		**Digestive gland**	
	7D	21D	7D	21D	7D	21D
MP	n.o.	10	33.33	20	90	90
MP25	n.o.	n.o.	22.22	n.o	44.44	50
MP100	n.o.	n.o.	22.22	70	20	30

Table 3. Tissue distribution of MPs in the digestive gland of mussels exposed to MP, MP25 and MP100 for 7 and 21 days (10 mussels per experimental group and one section per mussel). Not observed, n.o.

		MP		**MP25**		**MP100**	
		7D	**21D**	**7D**	**21D**	**7D**	**21D**
Stomach	**Lumen**	35.22 ± 22.24	19.43 ± 9.74	4.33 ± 0.48	45.6 ± 21.02	1 ± 0	2.66 ± 0.66
	Epithelium	1 ± 0	1 ± 0	n.o.	1 ± 0	n.o.	n.o.
Ducts	**Lumen**	2.5 ± 0.22	n.o.	16 ± 0	n.o.	n.o.	n.o.
	Epithelium	n.o.	n.o.	n.o.	n.o.	n.o.	n.o.
Digestive tubules	**Lumen**	1±0	1 ± 0	n.o.	n.o.	n.o.	n.o.
	Epithelium	n.o.	n.o.	n.o.	n.o.	n.o.	n.o.
Connective tissue		1±0	1 ± 0	n.o.	n.o.	1 ± 0	n.o.
Total MPs in DG		**32.8 ± 21.20**	**13.9 ± 8.44**	**2.9 ± 2.18**	**22.9 ± 15.92**	**0.2 ± 0.13**	**0.8 ± 0.51**

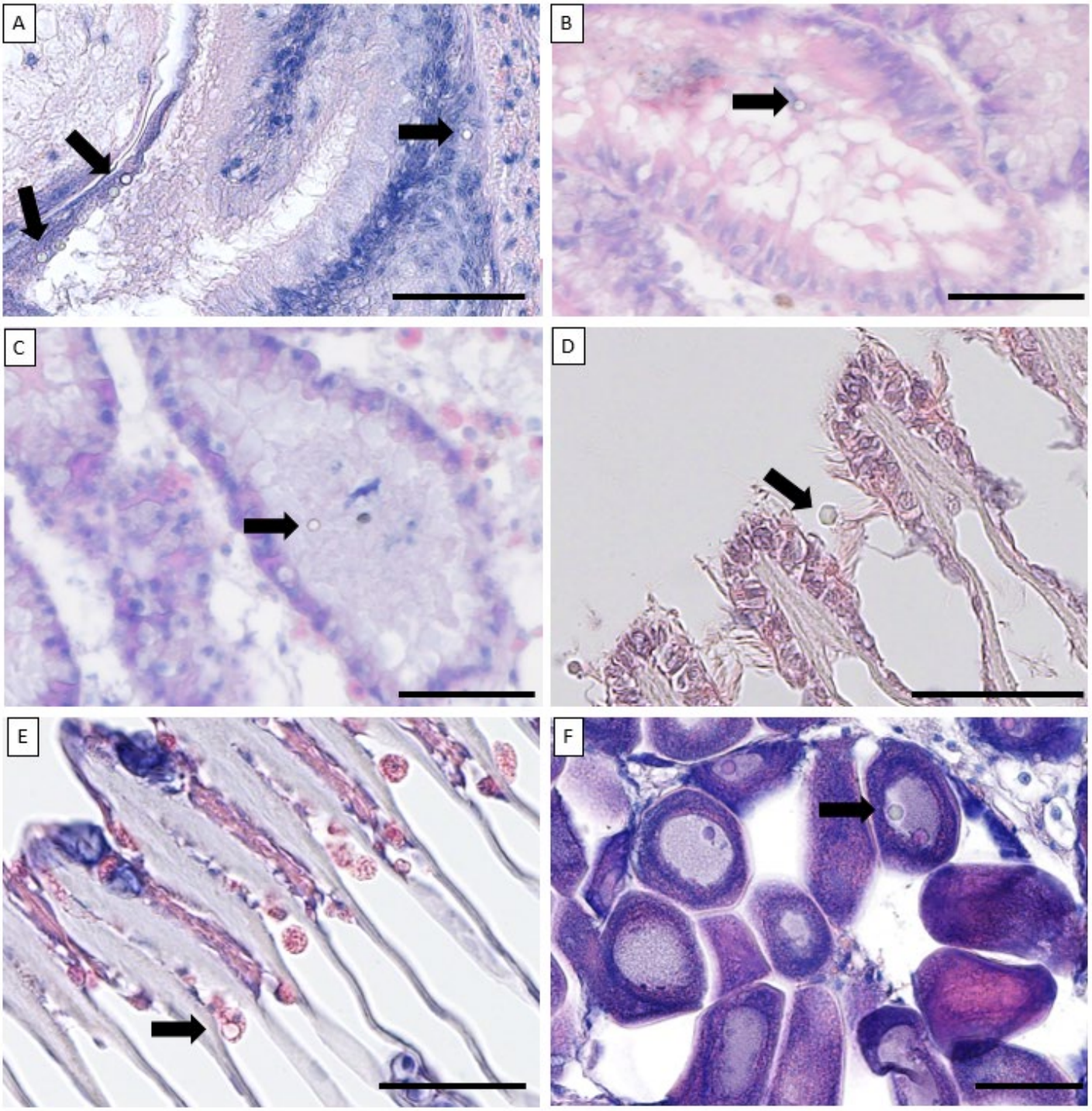

Figure 2 . Light micrographs of mussel paraffin sections showing the presence of 4.5 µm MPs (black arrows) in: A) stomach lumen and epithelium of the digestive tract of a mussel exposed to MPs for 7 days; B) lumen of a digestive duct in a mussel exposed to MPs for 21 days; C) lumen of a digestive tubule in a mussel exposed to MPs for 21 days; D) gill filaments of a mussel exposed to MPs for 7 days; E) gill filaments of a mussel exposed to MP100 for 7 days showing a MP within a hemocyte; E) gonad follicle of a mussel exposed to MPs for 7 days showing a MP within an oocyte. Scale bars: 50 µm.

3.3 Whole organism responses

After 21 days of exposure, there were no significant differences in the condition index, clearance rate and respiration rate among treatments (Figure S1).

Mussels exposed to MP and to WAF showed significantly lower absorption efficiency than controls and mussels exposed to MP25 (Figure 3A) at day 21 of exposure. Mussels exposed to WAF showed lower scope for growth than control mussels and than mussels exposed to MP25 (Figure 3B) at day 21 of exposure.

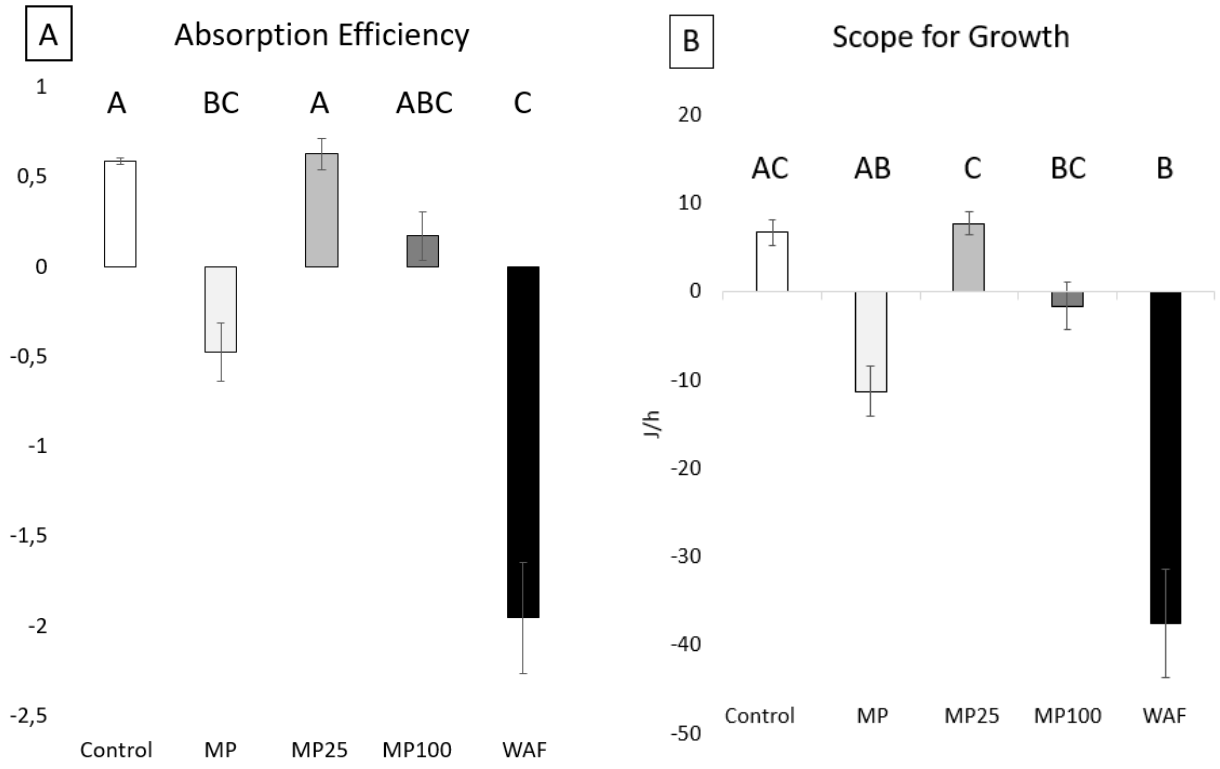

Figure 3. A) Absorption efficiency (ratio) and B) Scope for growth (J/h) of control mussels and mussels exposed to MP, MP25, MP100 and WAF after 21 days of exposure. Data are given as mean values and standard errors of 7 mussels per experimental group. Letters indicate significant differences among treatments (Kruskal-Wallis followed by Dunn's post hoc test, $p < 0.05$).

3.4 Gamete development, gonad index and histopathology of mussel gonad

In all treatments, 3 gametogenic stages were dominant at both exposure times: advanced gametogenesis, mature gonad and spawning gonad (Figure S2). Gonad index (GI) was around 4 in all groups, with a significant increase in mussels exposed to MP25 compared to control mussels and mussels exposed to MP100 and WAF at day 7 of exposure (Figure S2A). No significant differences among groups were recorded at day 21, but GI increased in controls in comparison with day 7 (Figure S2A). In females, no significant differences in the GI were found (Figure S2B) whereas in males a higher GI was observed in mussels exposed to MP25 compared to control mussels and mussels exposed to MP100 and WAF at day 7 of exposure. In addition, mussels exposed to MP100 for 21 days showed lower GI than mussels exposed to MP and the GI of the controls increased from day 7 to day 21 of exposure (Figure S2C).

In general, low prevalences of inflammatory responses such as fibrosis and hemocytic infiltration were recorded in all exposure groups (Figure S3, Table S2) although higher hemocytic infiltration was recorded in mussels exposed to MP25, MP100 and WAF after 21 days of exposure comparing to controls. The prevalence of hemocytic infiltration in controls decreased from day 7 to 21 (Table S2). At day 21 of exposure mussels exposed to MP, MP25, MP100 and WAF showed higher prevalences of oocyte atresia than controls (Table S2). Meanwhile, prevalence of oocyte atresia decreased significantly from day 7 to 21 in controls (Table S2). Oocyte necrosis was observed in a single mussel exposed to MPs at day 21 and a trematode parasite was found in another mussel exposed to MPs for 21 days (Table S2).

3.5 Cellular biomarkers in mussel hemocytes

Neutral red uptake was not significantly affected by any treatment at day 7 whereas it was significantly reduced in mussels exposed to WAF at 21 days in comparison to control mussels, to mussels exposed to MP and MP25 as well as to mussels exposed to WAF at 7 days (Figure 4A).

Catalase activity in hemocytes was not altered after any treatment (Figure S4).

Background levels of DNA damage were observed in control groups (Figure 4B). No significant effects were recorded at day 7 of exposure, while after 21 days of exposure to MP, DNA damage was significantly higher than in the control group (Figure 4B). DNA damage decreased in control mussels along the exposure time (Figure 4B).

3.6 Enzyme activities in mussel tissues

At day 7, IDH activity in mussels exposed to MPs was significantly higher than in control mussels, whereas at day 21 of exposure it was lower than in controls and in mussels exposed to WAF. At the same time, activity in mussels exposed to WAF was significantly lower than in controls. IDH activity increased along the exposure time both in the control and in the WAF group (Figure 5A).

AOX1 activity was not altered at days 7 and 21 of exposure but activity increased significantly along exposure time in the WAF group (Figure S4B).

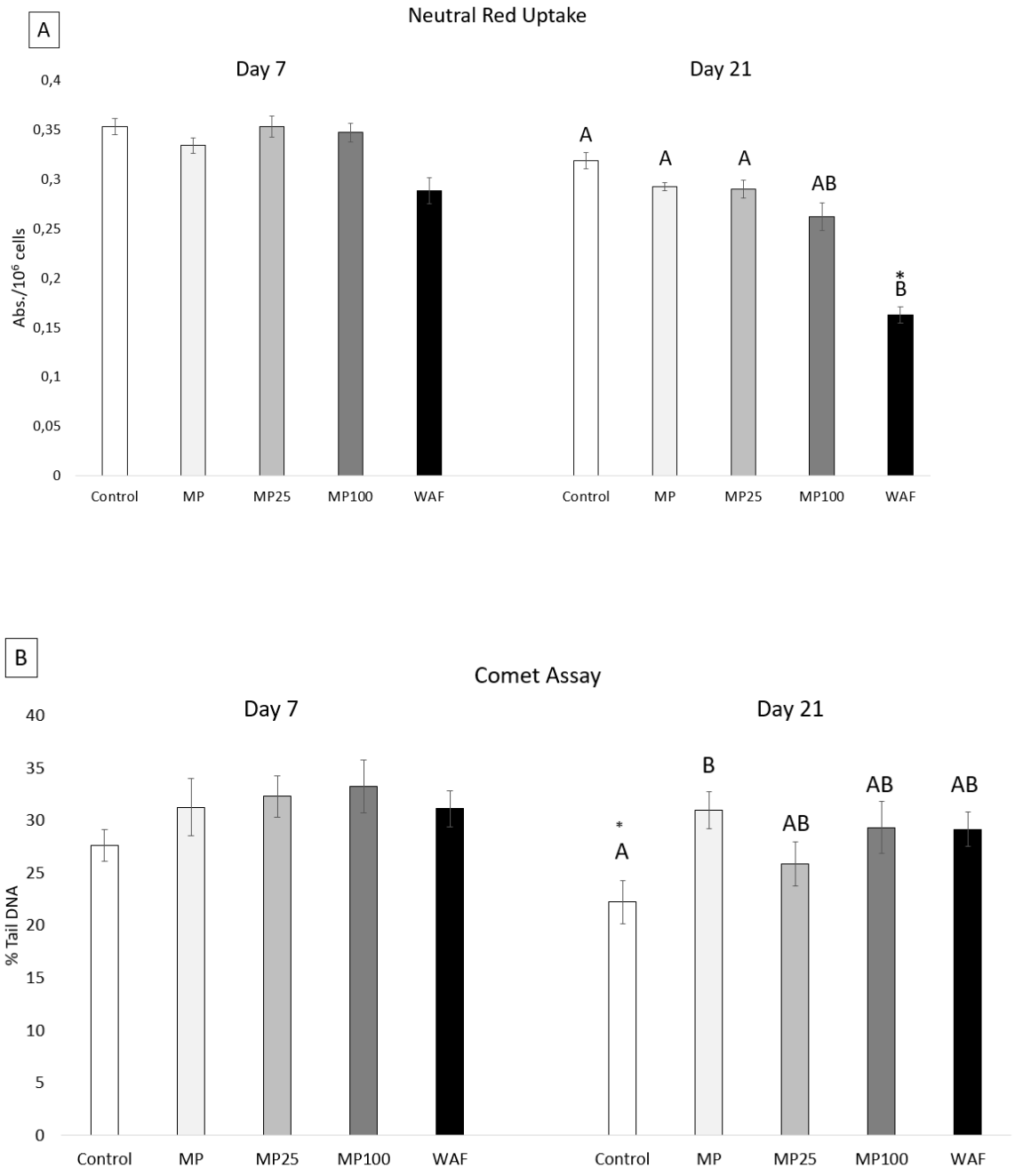

Figure 4. A) Neutral red uptake (given as absorbance/10^6 cells); and B) DNA strand breaks (given as % tail DNA) in hemocytes of control mussels and mussels exposed to MPs, MP25, MP100 and WAF after 7 and 21 days of exposure. Data are given as mean values and standard errors (8 mussels per experimental group, 4 replicates per mussel in A; and 50 cells in 2 slides per mussel in B). Letters indicate significant differences among treatments within the same day (Kruskal-Wallis followed by Dunn's post hoc test, $p < 0.05$). Asterisks indicate significant differences between days within the same treatment (Mann-Whitney´s U test, $p < 0.05$).

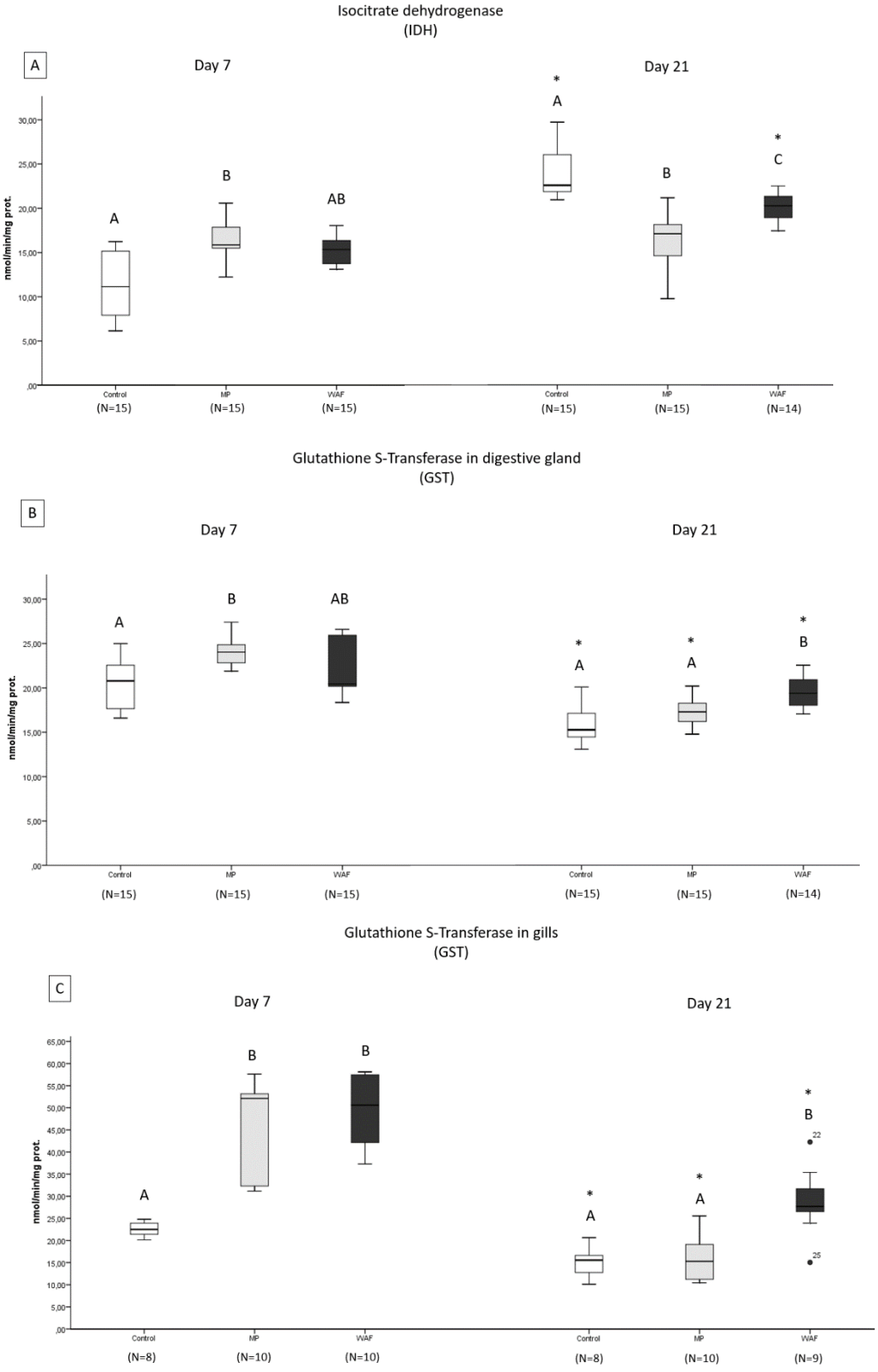
Isocitrate dehydrogenase
(IDH)
A
Day 7
Day 21
nmol/min/mg prot.
Control
MP
WAF
(N=15)
(N=15)
(N=15)
(N=15)
(N=15)
(N=14)
Glutathione S-Transferase in digestive gland
(GST)
B
Day 7
Day 21
Glutathione S-Transferase in gills
(GST)
C
Day 7
Day 21
(N=8)
(N=10)
(N=10)
(N=8)
(N=10)
(N=9)

Figure 5 (previous page) 5. Enzyme activities (given as nmol/min/mg protein) of A) IDH in digestive gland; B) GST in digestive gland and C) GST in gills of control mussels and mussels exposed to MPs and to WAF after 7 and 21 days of exposure. Box-plots show median value (horizontal line), 25%-75% quartiles (box) and standard deviation (whiskers). Dots denote outliers, values that do not fall in the inner fences. Letters indicate significant differences among treatments within the same day (one-way ANOVA followed by Tukey's post hoc or Kruskal-Wallis test followed by Dunn's post hoc, $p<0.05$). Asterisks indicate significant differences between days within the same treatment (Mann-Whitney´s U test, $p < 0.05$).

At day 7 of exposure, GST activity in the digestive gland of mussels exposed to MP was significantly higher than in control mussels. Meanwhile, at day 21 of exposure mussels exposed to WAF showed significantly higher activity than controls and mussels exposed to MP. Along the experiment, GST activity decreased significantly in all the groups (Figure 5B). On the other hand, GST activity in gills of mussels exposed to MP and to WAF for 7 days was significantly higher than in controls. GST activity decreased significantly in all the groups from day 7 to 21; however, after 21 days, mussels exposed to WAF showed significantly higher activity than control mussels and mussels exposed to MPs (Figure 5C).

In the digestive gland, catalase activity was significantly lower in mussels exposed to WAF for 7 days than in controls while, after 21 days of exposure, mussels exposed to WAF showed higher activity than controls. Catalase activity increased significantly in the WAF group from day 7 to day 21 (Figure 6A). On the contrary, no alteration was recorded in the activity of catalase in gills of mussels exposed for 7 days. At day 21 of exposure mussels exposed to WAF showed higher catalase activity than controls, though no differences were recorded along the time (Figure 6B).

GPX activity was not altered significantly in the digestive gland of mussels exposed to MPs or to WAF (Figure 6C). In gills, GPx activity was significantly higher in mussels exposed to MPs and to WAF than in controls, both after 7 and 21 days of exposure (Figure 6D). GPx activity decreased significantly in all groups along the experiment (Figure 6D).

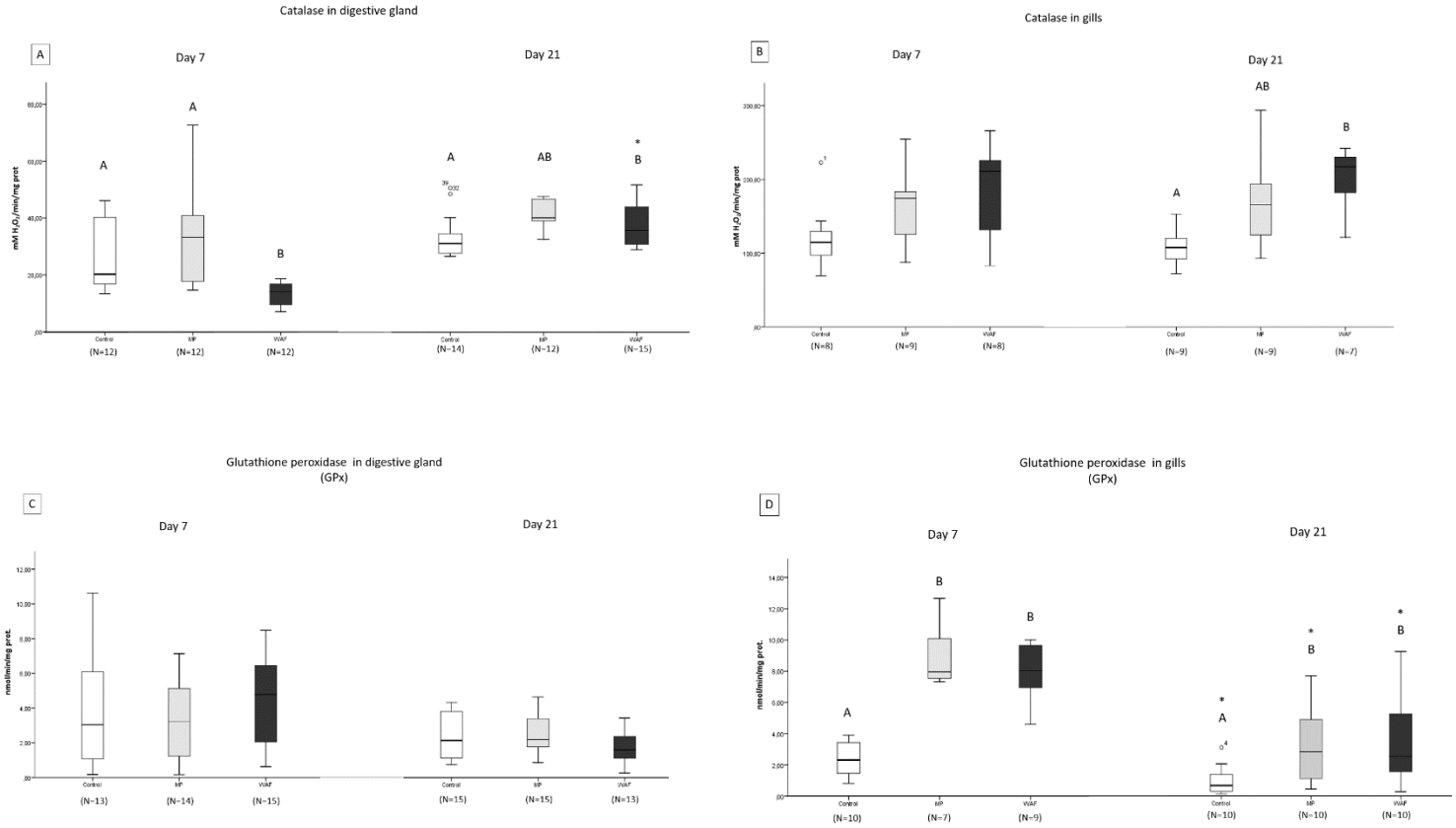

Figure 6. Catalase activity (given as mM H_2O_2/min/mg prot) in A) digestive gland; B) gills; and GPx activity (given as nmol/min/mg protein) in C) digestive gland and D) gills of control mussels and mussels exposed to MPs and to WAF after 7 and 21 days of exposure. Box-plots show median value (horizontal line), 25%-75% quartiles (box) and standard deviation (whiskers). Dots denote outliers, values that do not fall in the inner fences. Letters denote statistical differences among means (one-way ANOVA followed by Tukey's post hoc or Kruskal-Wallis test followed by Dunn's post hoc, $p<0.05$). Asterisk indicates significant differences between days within the same treatment (Mann-Whitney´s U test, $p < 0.05$).

3.7. Cell composition, quantitative structure and histopathology of mussel digestive gland

The volume density of basophilic cells (VvBas) was significantly higher in mussels exposed to MP and to WAF for 7 days than in control mussels (Figure 7A). No significant differences were recorded at day 21 of exposure, as the VvBas in control mussels increased significantly from day 7 to day 21 of exposure (Figure 7A).

No significant differences were found at day 7 of exposure with respect to controls in the two parameters indicative of the structural integrity of the digestive tubules, mean epithelial thickness to mean diverticular radius (MET/MDR) and mean luminal radius to mean epithelial thickness (MLR/MET) (Figure 7B). MET/MDR was significantly lower in mussels exposed to WAF than in mussels exposed to MP and, on the contrary, MLR/MET was significantly higher in mussels exposed to WAF than in mussels exposed to MP (Figure 7C). At day 21 of exposure, mussels exposed to WAF showed significantly higher MET/MDR and lower MLR/MET than controls. During the exposure, MLR/MET significantly increased and MET/MEDR significantly decreased in control mussels while in mussels exposed to WAF MLR/MET decreased along the exposure time (Figure 7B,C).

Digestive tubule atrophy increased in controls along the experiment whereas the prevalence of fibrosis decreased in mussels exposed to MP and to WAF along the experiment. Inflammatory responses such as hemocytic infiltration and accumulation of brown cells were observed in control mussels and in mussels exposed to MP and to WAF for 7 and 21 days (Figure S6, Table S3). The parasites *Mytilicola intestinalis* and *Nematopsis* spp. were observed in the digestive gland of several individuals of all groups at both exposure times (Table S3).

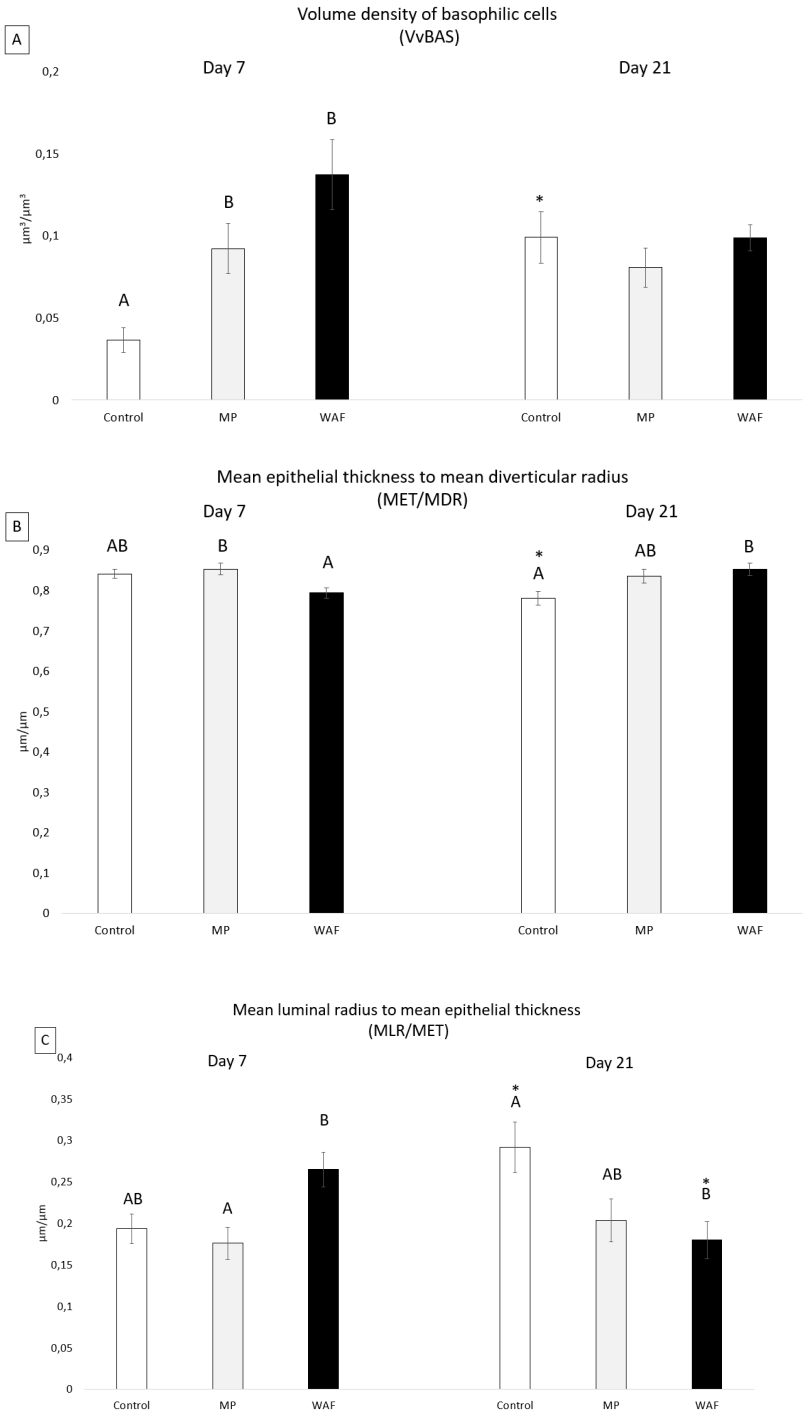

Figure 7. A) Volume density of basophilic cells ($\mu m^3/\mu m^3$); B) Mean epithelial thickness to mean diverticular radius (µm/µm) and C) Mean luminal radius to mean epithelial thickness (µm/µm) of control mussels and mussels exposed to MPs and to WAF after 7 and 21 days of exposure. Data are given as mean values and standard errors of 10 mussels per experimental group. Letters indicate significant differences among treatments within the same day (one-way ANOVA followed by Tukey's post hoc test, $p<0.05$). The asterisk indicates significant differences between days within the same treatment (Mann-Whitney´s U test, $p < 0.05$).

4. DISCUSSION

As far as we know, this is the first work addressing the effects of a complex mixture of hydrocarbons sorbed to MPs in bivalves. The study considers an environmentally realistic scenario in which widely distributed MPs could adsorb a mixture of oil hydrocarbons originating from different sources, including oil spills. Several studies have reported that plastics collected from beaches and oceans presented a complex mixture of POPs, including PAHs (Van et al., 2010; Rios et al., 2012; Zhang et al., 2015). Thus, our study is relevant because most of the experimental works on the impact of MPs with adsorbed or co-exposed organic or metallic pollutants have been performed with single model compounds, usually at doses that are known to be toxic (Burns & Boxell, 2018; Huang et al 2021a; Sendra et al., 2021).

Chemical analysis showed that only mussels exposed to WAF alone bioaccumulated PAHs in their tissues and this accumulation was higher at day 7 of exposure than at day 21. On the contrary, mussels exposed to MPs with sorbed oil compounds from WAF (MP25, MP100) did not accumulate PAHs at any exposure time. This is opposed to what was observed in previous works where transfer of PAHs such as pyrene (Avio et al., 2015) or benzo(a)pyrene (Chapter 1) from MPs to mussels did occur. However, Paul-Pont et al. (2016) already showed that PS MPs exhibited a high sorption capacity for fluoranthene, but fluoranthene did not bioaccumulate in marine mussels. In mussels exposed to WAF alone phenanthrene was the PAH showing the highest concentration at both exposure times. However, in mussels exposed to MPs with sorbed oil compounds from WAF this was not observed, possibly because the sorption of PAHs into MPs was correlated with their initial concentration in the WAF, in which naphthalene was the main component (Martínez-Alvarez et al., submited). In mussels exposed to WAF alone naphthalene represented less than 10% of total bioaccumulated PAHs. Another explanation could be that the MPs were not retained inside mussels long enough to desorb the PAHs, as proposed by Burns & Boxell (2018). In addition, at examining the presence of MPs in mussels exposed to MP25 and MP100, the prevalence and the total number of MPs observed in both exposure groups were lower than in mussels exposed to MPs alone. This reduced presence of MPs in mussels when they have sorbed pollutants has been observed in previous studies (Islam et al., 2021; Chapter 1) and

could be due to a behavioural response of valve closure or to decreased appetite and feeding, that could prevent mussels from the accumulation of associated pollutants sorbed into MPs. If animals can reduce feeding rate or clearance rate, increase the production of pseudofeces or speed up defecation, the toxic impact caused by MPs can be reduced (Huang et al., 2021b). However, these mechanisms will have an impact on the energy budget of the animal (Wegner et al., 2012; van Cauwenberghe et al., 2015; Santana et al., 2018).

In this work, clearance rate was not altered upon exposure to MP, MP25, MP100 or WAF, whereas absorption efficiency (AE) was reduced upon exposure to MPs or to WAF and Scope for Growth (SFG) decreased in mussels exposed to WAF at day 21. Further, in the gonad, prevalence of oocyte atresia increased at day 21 in mussels exposed to MP, MP25, MP100 or WAF and hemocytic infiltration increased in groups MP25, MP100 or WAF. As shown previously in mussels exposed to oil WAF or PAHs (Cajaraville et al*.,* 1992a; Ortiz-Zarragoitia & Cajaraville*.,* 2006), these two alterations suggest the activation of gamete resorption by hemocytes in order to cope with a higher energy demand, especially when energy available from food (i.e., SFG) was, in the present case, reduced to negative values. Similarly, the energy fraction allocated to reproduction seemed to be used to meet the high maintenance costs of stress situations provoked by exposure to MPs in oysters (Sussarellu et al., 2016; Gardon et al., 2018). Thus, gonads appeared to provide the energy to maintain animals' metabolism through the production of metabolites derived from germ cells phagocytosis, which could lead to detrimental effects on reproduction, with potential consequences at the population level (Gardon et al., 2018).

As to the occurrence of MPs in mussels along the exposure period, in mussels exposed to MPs alone the presence of MPs was higher at day 7 of exposure than at day 21, while the opposite was observed in the case of mussels exposed to MP25 and almost no differences between days were recorded in mussels exposed to MP100. This again could indicate a differential modulation of MP uptake, accumulation and elimination in mussels exposed to pristine *versus* contaminated MPs. In agreement with previous works (Browne et al., 2008; Von Moos et al., 2012; Avio et al., 2015; Paul-Pont et al., 2016; Magni et al., 2018; Pittura et al., 2018; Chapter 1) MPs were mainly observed in the digestive tract of the digestive gland, with the only exception of mussels exposed

to MP100 at day 21 of exposure, which showed a higher prevalence of MPs in the gills than in the digestive gland. Two routes have been proposed for the uptake of MPs in bivalves: through gills and mouth (Sendra et al., 2021). Consequently, it is not surprising that the digestive gland and gills are the organs most affected by MPs (Sendra et al., 2021).

Even though PS MPs were seen to translocate into mussel's hemocytes and then they could affect the immune function of these cells (Katsumiti et al., 2021; Sendra et al., 2021), hemocyte viability and catalase activity were not altered in mussels exposed to MP, MP25 or MP100. Only mussels exposed to WAF showed a lower viability of hemocytes after 21 days of exposure, in agreement with results of a previous work of *in vitro* exposure of hemocytes to the same oil WAF (Katsumiti et al., 2019). Meanwhile, damage in DNA was observed in hemocytes of mussels exposed to MPs alone after 21 days of exposure. DNA damage has been observed previously in bivalves after exposure to MPs alone (Ribero et al., 2017; Brandts et al., 2018; Revel et al., 2019; Chapter 1) and in hemocytes exposed to MPs and nanoplastics *in vitro* (Katsumiti et al., 2021). The fact that hemocytes of mussels exposed to MP25 or MP100 did not show increased levels of DNA strand breaks can be explained by the lower occurrence of MPs in tissues of those mussels compared to mussels exposed to MPs alone, as discussed above.

Overall, our results showed a lack of PAH accumulation in mussels exposed to MPs with sorbed oil compounds from WAF (MP25 and MP100), a reduced occurrence of MPs in the same two groups compared to mussels exposed to MPs alone, and no effects on mussel physiology and hemocyte functions in the same two groups. Therefore, further studies on enzyme activities in mussel tissues and on cell composition, quantitative structure and histopathology of mussel digestive gland were carried out only in mussels exposed to MPs or to WAF alone, in comparison to controls.

IDH activity was induced in mussels exposed to MPs for 7 days, suggestingincreased energy needs. However, at 21 days IDH was lower in mussels exposed to MPs and to WAF compared to controls, due to the significant increase in IDH activity in the controls, maybe related to estabulation conditions or to seasonal changes. This enzyme has shown a bell-shaped response in previous studies, with a rise in the activity at the beginning of the exposure to get additional

energy to overcome the toxicity (Oliveira et al., 2013) and a decrease in IDH activity at longer exposures, which implies a reduction of energy obtained through the aerobic pathway. This reduction could be connected with a decrease in feeding (Guilhermino et al., 2018) which agrees well with the reduced AE at day 21 in mussels exposed to MPs and to WAF and with the reduced SFG in the case of mussels exposed to WAF.

The activity of the phase II biotransformation enzyme GST was induced transitorily at day 7 both in digestive gland and gills of mussels exposed to MPs, whereas GST induction under WAF exposure lasted up to day 21 in both organs. The transitory response of GST to MP exposure could be related to the decreased occurrence of MPs in mussels exposed to MPs for 7 days in comparison to 21 days. The antioxidant enzyme GPx was not altered in the digestive gland but exposure to MPs and to WAF caused a significant induction of GPx in the gills at days 7 and 21. The lack of response of GPx activity in the digestive gland of mussels exposed to MPs has also been reported by Paul-Pont et al. (2016). Catalase activity was also induced in the digestive gland and gills of mussels exposed to WAF for 21 days. Different responses of enzyme activities in gills and digestive gland have been recorded in several works (Ribeiro et al., 2017; O'Donovan et al., 2018; Revel et al 2019).

As mentioned before, induction of GST in mussels exposed to WAF lasted until day 21 in both gills and digestive gland but GST activity decreased at day 21 with respect to day 7. This decrease could be due to the decrease in the bioaccumulation of PAHs in mussel tissues, which was reduced almost to the half from day 7 to 21 of exposure. However, mussels exposed to WAF showed higher activity of catalase at day 21 compared to day 7 in the digestive gland. Similarly, the activity of the peroxisomal β-oxidation enzyme AOX1 increased in mussels exposed to WAF from day 7 to day 21 of exposure, but this increase was not enough to cause a significant difference with respect to the control. Both catalase and AOX1 activities are known to vary seasonally in mussels (Cancio et al., 1999) which could explain observed differences along the experiment. In line with our results, no alteration of AOX1 was observed in mussels exposed to MPs alone or in combination with pyrene (Avio et al., 2015), BaP (Pittura et al. 2018; Von Hellfeld et al., 2022) and cadmium (Von Hellfeld et al., 2022).

The cell type composition of the digestive tubules of the digestive gland was altered after 7 days exposure to MPs or to WAF, with a higher volume density of basophilic cells (VvBas) with respect to controls. After exposure to pollutants VvBAS may surpass 0.12 $\mu m^3/ \mu m^3$ (Bignell et al., 2012), as observed in the present work in mussels exposed to WAF for 7 days, possibly related to the high PAH concentrations measured at day 7 in the WAF group. After 21 days of exposure there was no statistically significant difference among treated groups and controls, due to increased values of VvBAS in controls that could be associated again to estabulation conditions or to seasonal changes. For the exposure to MPs, increased values of VvBAS in mussels exposed for 7 days to 0.5 µm nanoplastics have been reported but not in mussels exposed to 4.5 µm MPs (Chapter 1). This difference is probably related to the higher number of MPs found in the digestive ducts and tubules in this work than Chapter 1 which could result in a higher impact on the cellular composition of the digestive tubules.

Higher MET/MDR and lower MLR/MET values were observed at 21 days of exposure to WAF in comparison to the control. These values might possibly be due to increased lysosomal activity related to uptake and elimination of accumulated pollutants (Zorita et al., 2006; Sforzinni et al., 2018), which finally resulted in a reduced SFG in mussels exposed to WAF. Large digestive imbalances, accounting for negative AE (and hence, negative SFG) would be expected to occur associated to these detoxification mechanisms, because of the extensive losses of cell materials voided with the feces that were found to consist mainly of membrane lipids (Ibarrola et al 2000a, b). Finally, it must be taken into consideration that the impact of WAF in mussels´ digestive gland has been observed to be dependent on exposure time, oil type and food ration (Cajaraville et al., 1992b; Marigómez & Baybay-Villacorta, 2003; Blanco-Rayón et al., 2019).

5. CLONCLUSIONS

In conclusion, mussels exposed for 21 days to 4,5 µm PS MPs with sorbed oil compounds from the WAF of a naphthenic North Sea crude oil did not accumulate PAHs in their tissues, which has implications for risk assessment of MPs and associated oil pollution in the marine environment. Importantly, exposure to MPs alone and with sorbed oil compounds from WAF increased oocyte

atresia and MPs alone altered several enzyme activities, caused genotoxicity, increased basophilic cell volume in digestive tubules and decreased absorption efficiency. On the other hand, mussels exposed directly to a 25% dilution of the same WAF did accumulate PAHs in their tissues triggering responses at molecular (alterations of enzyme activities), cellular (decrease of hemocyte viability), tissue (higher prevalences of oocyte atresia and alteration of cell composition and structure of digestive tubules) and organism levels (decrease of absorption efficiency and scope for growth). Future works are needed to elucidate the behavior of other microplastic polymers and sizes towards other types of oil with differing hydrocarbon composition as well as the impact on marine ecosystems under co-exposure scenarios.

ACKNOWLEDGMENTS

This work was funded by Spanish MINECO (NACE project CTM2016-81130-R), Basque Government (consolidated group IT1302-19 and IT1743-22 and predoctoral fellowship to NGS) and UPV/EHU (VRI grant PLASTOX). Work carried out within the EU project PLASTOX (JPI Oceans 005/2015) and the EU H2020-BG-2005-2 project GRACE (grant agreement number 679266). Thanks are due to staff at Drifts laboratoriet Mongstad, Equinor (former Statoil) for supplying the sample of crude oil used in the experiments. Authors gratefully acknowledge Xabier Lekube for handling oil samples, Nerea Duroudier and Alberto Katsumiti for their help in the sample processing for Comet assay and the General Services SGiker of UPV/EHU for the determination of PAHs in mussel tissues.

REFERENCES

Ahmed M.B., Rahman M.S., Alom J., Hasan M.S., Johir M.A.H., Mondal M.I.H., Lee D.Y., Park J., Zhou J.L., Yoon M.H. 2021. Microplastic particles in the aquatic environment: A systematic review. Science of the Total Environment 775, 145793.

Akdogan Z., Guven B. 2019. Microplastics in the environment: A critical review of current understanding and identification of future research needs. Environmental Pollution 254, 113011.

Andrady A.L. 2011. Microplastics in the marine environment. Marine pollution bulletin 62, 1596-605.

Auta H.S., Emenike C.U., Fauziah S.H. 2017. Distribution and importance of microplastics in the marine environment: A review of the sources, fate, effects, and potential solutions. Environment International 102, 165-176.

Avio C.J., Gorbi S., Milan M., Benedetti M., Fattorini D., d'Errico G., Pauletto M., Bargelloni L., Regoli F. 2015. Pollutants bioavailability and toxicology risk from microplastics to marine mussels. Environmental Pollution 198, 211-222.

Aurand D.V., Coelho G.M. 1996. Proceedings of the Fourth Meeting of the Chemical Response to Oil Spills: Ecological Effects Research Forum. Report No. 96-01, Ecosystem Management and Associates, Purcellville, VA. 50p.

Bakir A., O'Connor I.A., Rowland S.J., Hendriks A.J., Thompson R.C. 2016. Relative importance of microplastics as a pathway for the transfer of hydrophobic organic chemicals to marine life. Environmental Pollution 219, 56-65.

Barnes D.K.A., Galgani F., Thompson R.C., Barlaz M. 2009. Accumulation and fragmentation of plastic debris in global environments. Physiological Transactions of the Royal Society, Series B, 364. 1985-1998.

Batel A., Linti F., Scherer M., Erdinger L., Braunbeck T. 2016. The transfer of benzo[a]pyrene from microplastics to *Artemia nauplii* and further to zebrafish via a trophic food web experiment– CYP1A induction and visual tracking of persistent organic pollutants. Environmental Toxicology Chemistry 35, 1656-66.

Bayne B.L., Widdows J., Thompson R.J. 1976. Physiological integrations in Bayne, B.L. (Ed.). Marine mussels: their ecology and physiology. International Biological Programme, 10: pp. 261-291. Cambridge University Press. Cambridge, UK.

Bellas J., Albentosa M., Vidal-Liñán L., Besada V., Franco M.Á., Fumega J., González-Quijano A., Viñas L., Beiras R. 2014. Combined use of chemical, biochemical and physiological variables in mussels for the assessment of marine pollution along the N-NW Spanish coast. Marine Environmental Research 96,105-117.

Bignell J., Cajaraville M.P., Marigómez I. 2012. Background document: histopathology of mussels (*Mytilus spp*.) for health assessment in biological effects monitoring. Integrated monitoring of chemicals and

their effects. IM DAVIES, AD VETHAAK (eds.). ICES Cooperative Research Report N. 315, Copenhagen, Denmark pages, 111-120.

Blanco-Rayón E., Guilhermino L., Irazola M., Ivanina A.V., Sokolova I.M. Izagirre U., Marigómez, I. 2019. The influence of short-term experimental fasting on biomarker responsiveness in oil WAF exposed mussels. Aquatic Toxicology, 206, 164–175.

Bradford MM. 1976. A rapid and sensitive method for the quantitation of microgram quantities of protein utilizing the principle of protein-dye binding. Analytical Biochemistry 72, 248-254.

Brandts I., Teles M., Gonçalves A.P., Barreto A., Franco-Martinez L., Tvarijonaviciute A., Martins M.A., Soares A.M.V.M., Tort L., Oliveira M. 2018. Effects of nanoplastics on *Mytilus galloprovincialis* after individual and combined exposure with carbamazepine. Science of the Total Environment 643, 775-784.

Brate I.L., Blazquez M., Brooks S.J., Thomas K.V. 2018. Weathering impacts the uptake of polyethylene microparticles from toothpaste in Mediterranean mussels (*M. galloprovincialis*). Science of the Total Environmental, 626. 1310-1318.

Browne M.A., Dissanayake A., Galloway T.S., Lowe D.M., Thompson R.C. 2008. Ingested microscopic plastic translocates to the circulatory system of the mussel, *Mytilus edulis* (L.). Environmental Science & Technology 42, 5026-5031.

Burns E.E., Boxall A.B.A. 2018. Microplastics in the Aquatic Environment: Evidence for or Against Adverse Impacts and Major Knowledge Gap. Environmental Toxicology and Chemistry 37, 2776-2796.

Cajaraville M.P., Bebianno M.J., Blasco J., Porte C., Sarasquete C., Viarengo A. 2000. The use of biomarkers to assess the impact of pollution in coastal environments of the Iberian Peninsula: a practical approach. Science of the Total Environment 247, 295-311.

Cajaraville M.P., Marigómez J.A., Angulo E. 1991. Automated Measurement of Lysosomal Structure Alterations in Oocytes of Mussels Exposed to Petroleum Hydrocarbons. Archives of Environmental Contamination and Toxicology 21, 395-400.

Cajaraville M.P., Marigómez J.A., Angulo E. 1992a. Comparative effects of the water accommodated fraction of three oils on mussels-1. Survival, growth and gonad development. Comparative Biochemistry and Physiology. Part C, Comparative, 102, 103–112.

Cajaraville M.P., Marigómez J.A., Diez G., Angulo E. 1992b. Comparative effects of the water accommodated fraction of three oils on mussels-2. Quantitative alterations in the structure of the digestive tubules. Comparative Biochemistry and Physiology - Part C 102, 113-23.

Cancio I., Ibabe A., Cajaraville M.P. 1999. Seasonal variation of peroxisomal enzyme activities and peroxisomal structure in mussels *Mytilus galloprovincialis* and its relationship with the lipid content. Comparative Biochemistry and Physiology Part C: Pharmacology, Toxicology and Endocrinology 123, 135-144.

Carls M.G., Meador J.P. 2009. A perspective on the toxicity of petrogenic PAHs to developing fish embryos related to environmental chemistry Human and Ecological Risk Assessment. 15: 1084–1098.

Capolupo M., Franzellitti S., Valbonesi P., Lanzas C.S., Fabbri E. 2018. Uptake and transcriptional effects of polystyrene microplastics in larval stages of the Mediterranean mussel *Mytilus galloprovincialis*. Environmental Pollution 241, 1038-1047.

Chae Y., An Y. 2017. Effects of micro- and nanoplastics on aquatic ecosystems: Current research trends and perspectives. Marine Pollution Bulletin, 124, 2. 624-632.

Chen Q., Yin D., Jia Y., Schiwy S., Legradi J., Yang S., Hollert H. 2017. Enhanced uptake of BPA in the presence of nanoplastics can lead to neurotoxic effects in adult zebrafish. Science of the Total Environment 609, 1312-1321.

Counihan K.L. 2018. The physiological effects of oil, dispersant and dispersed oil on the bay mussel, *Mytilus trossulus*, in Arctic/Subarctic conditions. Aquatic Toxicology, 199, 220–231.De los Ríos A., Perez L., Ortiz-Zarragoitia M., Serrano T., Barbero M.C., Echavarri-Erasun B., Juanes J.A., Orbea A., Cajaraville M.P. 2013. Assessing the effects of treated and untreated urban discharges to estuarine and coastal waters applying selected biomarkers on caged mussels. Marine Pollution Bulletin 77, 251-265.

De Sá, L.C., Olivera, M., Ribeiro, F., Rocha, T.L, Futter, M.N. 2018. Studies of the effects of microplastics on aquatic organisms: What do we know and where should we focus our efforts in the future? Science of Total Environment, 645. 1029-1039.

Détrée C., Gallardo-Escárate C. 2017. Polyethylene microbeads induce transcriptional responses with tissue-dependent patterns in the mussel *Mytilus galloprovincialis*. Journal of Molluscan Studies 83, 220-225.

Ellis G., Goldberg D.M. 1971. An improved manual and semi-automatic assay for NADP-dependent isocitrate dehydrogenase activity, with a description of some kinetic properties of human liver and serum enzyme. Clinical Biochemistry 2, 175-185.

Flohé L., Günzler W.A. 1984. Assays of glutathione peroxidase. Methods in Enzymology 105, 114–121.

Gardon T., Reisser C., Soyez C., Quillien V., Le Moullac G. 2018. Microplastics Affect Energy Balance and Gametogenesis in the Pearl Oyster *Pinctada margaritifera*. Environmental Science and Technology 52, 5277–5286.

Gonzalez-Soto N., Hatfield J., Katsumiti A., Duroudier N., Lacave J.M., Bilbao E., Orbea A., Navarro E., Cajaraville M.P. 2019. Impacts of dietary exposure to different sized polystyrene microplastics alone and with sorbed benzo[a]pyrene on biomarkers and whole organism responses in mussels *Mytilus galloprovincialis*. Science of the Total Environment 684, 548-566.

Green D.S., Colgan T.J., Thompson R.C., Carolan J.C. 2019. Exposure to microplastics reduces attachment strength and alters the haemolymph proteome of blue mussels (*Mytilus edulis*). Environmental Pollution 246, 423-434

Guilhermino L., Vieira L.R., Ribeiro D., Ana Sofia Tavares A.S., Cardoso V., Alves A., Almeida J.M. 2018. Uptake and effects of the antimicrobial florfenicol, microplastics and their mixtures on freshwater exotic invasive bivalve *Corbicula fluminea*. Science of the Total Environment 622-623, 1131-1142.

Habig W., Pabst M.J., Jakoby W.B. 1974. Glutathione S-Transferases, The first enzymatic step in mercapturic acid formation. The Journal of Biological Chemistry 249, 7130-7139.

Hartmann N.B., Hüffer T., Thompson R.C., Hassellöv M., Verschoor A., Daugaard A.E., Rist S., Karlsson, T., Brennholt N., Cole M., Herrling M.P., Hess M.C., Ivelva N.P., Lusher A.L., Magner W. 2019. Are we speaking the same language? Recommendations for a definition and categorization framework for plastic debris. Environ. Sci. Technol. 53, 1039-1047.

Huang D., Tao J., Cheng M., Deng R., Chen S., Yin L., Li R. 2021a. Microplastics and nanoplastics in the environment: Macroscopic transport and effects on creatures. Journal of Hazardous Materials 407, 124399.

Huang W., Song, B., Liang, J., Niu, Q., Zeng, G., Shen, M., Deng, J., Luo, Y., Wen, X., Zhang, Y. 2021b. Microplastics and associated contaminants in the aquatic environment: A review on their

ecotoxicological effects, trophic transfer, and potential impacts to human health. Journal of Hazardous Materials 405, 124187.

Ibarrola I., Etxeberria M, Iglesias J.I.P., Urrutia M.B., Angulo E. 2000a. Acute and acclimated digestive responses of the cockle *Cerastoderma edule* (L.) to changes in the food quality and quantity. II. Enzymatic, cellular and tissular responses of the digestive gland. Journal of Experimental Marine Biology and Ecology 252, 199-219.

Ibarrola I., Navarro E., Iglesias J.I.P., Urrutia M.B. 2000b. Temporal changes of feeding and absorption of biochemical components in *Cerastoderma edule* fed algal diets. Journal of the Marine Biological Association U.K. 80, 119-125.

Islam, N., Garcia da Fonseca, T., Vilke, J., Gonçalves, J.M., Pedro, P., Keiter, S., Cunha, S.C., Fernandes, J.O. Bebianno, M.J. 2021. Perfluorooctane sulfonic acid (PFOS) adsorbed to polyethylene microplastics: Accumulation and ecotoxicological effects in the clam *Scrobicularia plana*. Marine Environmental Research, 164 https://doi.org/10.1016/j.marenvres.2020.105249

Katsumiti A., Nicolussi G., Bilbao D., Prieto A., Etxebarria N., Cajaraville M. P. 2019. *In vitro* toxicity testing in hemocytes of the marine mussel *Mytilus galloprovincialis* (L.) to uncover mechanisms of action of the water accommodated fraction (WAF) of a naphthenic North Sea crude oil without and with dispersant. Science of the Total Environment 670, 1084–1094.

Katsumiti A., Losada.Carrillo M.P., Barros M., Cajaraville M.P. 2021 Polystyrene nanoplastics and microplastics can act as Trojan horse carriers of benzo(a)pyrene to mussel hemocytes in vitro. Scientific reports 11, 22396.

Kim Y., Ashton-Alcox A., Powell E.N. 2006. Histological techniques for marine bivalve molluscs: update NOAA technical memorandum NOS NCCOS 27, 76 pp.

Lee H., Shim W.J., Kwon O.Y., Kang J.H. 2013. Size-dependent effects of micro polystyrene particles in the marine copepod *Tigriopus japonicas*. Environmental Science and Technology, 47. 19, 11278-11283.

Li J., Lusher A.L., Rotchell J.M., Deudero S., Turra A., Brate I.L.N., Sun C., Hossain M.S., Li Q., Kolandhasamy P., Shi H. 2019. Using mussel as a global bioindicator of coastal microplastic pollution. Environmental Pollution 244, 522-533.

Lima I., Moreira S.M., Rendón-Von Osten J., Soares A.M.V.M., Guilhermino L. 2007. Biochemical responses of the marine mussel *Mytilus galloprovincialis* to petrochemical environmental contamination along the North-Western coast of Portugal. Chemosphere 66, 1230-1242.

Lowry O.H., Rosebrough N.J., Farr A.L., Randall R.J. 1951. Determination of proteins. The Journal of Biological Chemistry 193, 265-275.

Magni S., Gagné F., André C., Della Torre C., Auclair J., Hanana H., Parenti C.C., Bonasoro F., Binelli A. 2018. Evaluation of uptake and chronic toxicity of virgin polystyrene microbeads in freshwater zebra mussel *Dreissena polymorpha* (Mollusca: Bivalvia). Science of Total Environment 631-632, 778-788.

Marigómez I., Baybay-Villacorta L. 2003. Pollutant-specific and general lysosomal responses in digestive cells of mussels exposed to model organic chemicals. Aquatic Toxicology 64, 235–257. Martinez-Alvarez I., Le Menach K., Devier M.H., Cajaraville M.P., Orbea A., Budzinski H. Sorption of PAHs onto polystyrene microplastics depending on particle size. Toxics, submitted.

Moore C.J. 2008. Synthetic polymers in the marine environment: a rapidly increasing long-term threat. Environmental Research, 108. 131-139.

Navarro P., Cortazar E., Bartolomé L., Deusto M., Raposo J.C., Zuloaga O., Arana G., Etxebarria N. 2008. Comparison of solid phase extraction, saponification and gel permeation chromatography for the clean-up of microwave-assisted biological extracts in the analysis of polycyclic aromatic hydrocarbons. Journal of Chromatography A 1128, 10-16.

O'Donovan S., Mestre N.C., Abel S., Fonseca T.G., Carteny C.C., Cormier B., Keiter S.H., Bebianno M.J. 2018. Ecotoxicological Effects of chemical contaminants adsorbed to microplastics in the clam *Scrobicularia plana*. Frontiers in Marine Science 5:143.

Oliveira, P., Barboza, L.G.A.B., Branco, V., Figueiredo, N., Carvalho, C., Guilhermino, L. 2018. Effects of microplastics and mercury in the freshwater bivalve Corbicula fluminea (Müller, 1774): filtration rate, biochemical biomarkers and mercury bioconcentration. Ecotoxicology and Environmental Safety 164, 155-163.

Oliveira M., Ribeiro A., Hylland K., Guilhermino L. 2013. Single and combined effects of microplastics and pyrene on juveniles (0+ group) of the common goby *Pomatoschistus microps* (Teleostei, Gobiidae). Ecological Indicators 34, 641-647.

Ortiz-Zarragoitia M., Cajaraville M.P. 2006. Biomarkers of exposure and reproduction-related effects in mussels exposed to endocrine disruptors. Archives of Environmental Contamination and Toxicology 50, 361-369.

Ortiz-Zarragoitia M., Cajaraville M.P. 2010. Intersex and oocyte atresia in a mussel population from the Biosphere's Reserve of Urdaibai (Bay of Biscay). Ecotoxicology and Environmental Safety 73, 693-701.

Paul-Pont I., Lacroix C., Fernández C.G., Hégaret H., Lambert C., Le Goïc N., Frere L., Cassone A.L., Sussarellu R., Fabioux C., Guyomarch J., Albentosa M, Huvet A., Soudant P. 2016. Exposure of marine mussels *Mytilus spp*. to polystyrene microplastics: Toxicity and influence on fluoranthene bioaccumulation. Environmental Pollution 216, 724-737.

Pirsaheb M., Hossini H., Makhdoumi P. 2020. Review of microplastic occurrence and toxicological effects in marine environment: Experimental evidence of inflammation. Process Safety and Environmental Protection 142, 1–14.

Pittura L., Avio C.G., Giuliani M.E., d'Errico G., Keiter S.H., Cormier B., Gorbi S., Regoli F. 2018. Microplastics as vehicles of environmental PAHs to marine organisms: combined chemical and physical hazards to the Mediterranean mussels, *Mytilus galloprovincialis*. Frontiers in Marine Science 5,103.

Puy-Azurmendi E., Navarro A., Olivares A., Fernandes D., Martínez E., López de Alda M., Porte C., Cajaraville M.P., Barceló D., Piña B. 2010. Origin and distribution of polycyclic aromatic hydrocarbon pollution in sediment and fish the biosphere reserve of Urdaibai (Bay of Biscay, Basque country, Spain). Marine Environmental Research 70, 142-149.

Raisuddin S., Jha A.N. 2004. Relative sensitivity of fish and mammalian cells to sodium arsenate and arsenite as determined by alkaline single-cell gel electrophoresis and cytokinesis-block micronucleus assay. Environmental and Molecular Mutagenesis 44, 83-89.

Revel M., Lagarde F., Perrein-Ettajani H., Bruneau M., Akcha F., Sussarellu R., Rouxel J., Costil K., Decottignies P., Cognie B., Châtel A., Mouneyrac C. 2019. Tissue-specific biomarker responses in the blue mussel *Mytilus spp*. exposed to a mixture of microplastics at environmentally relevant concentrations. Frontiers in Environmental Science 7, 0–14.

Ribeiro F., Garcia A.R., Pereira B.P., Fonseca M., Nélia C. Mestre N.C., Fonseca T.G., Laura M. Ilharco L.M., Bebianno M.J. 2017. Microplastics effects in *Scrobicularia plana*. Marine Pollution Bulletin 122, 379-391.

Rios L.M., Jones P.R., Moore C., Narayan U.V. 2010. Quantitation of persistent organic pollutants adsorbed on plastic debris from the Northern Pacific Gyre's "eastern garbage patch." Journal of Environmental Monitoring 12, 2226–2236.

Rochman C.M., Hoh E., Kurobe T., Teh S.J. 2013. Ingested plastic transfers hazardous chemicals to fish and induces hepatic stress. Scientific Reports 3, 3263.

Ruiz P., Ortiz-Zarragoitia M., Orbea A., Vingen S., Hjelle A., Baussant T., Cajaraville M.P. 2014. Short- and long-term responses and recovery of mussels *Mytilus edulis* exposed to heavy fuel oil no. 6 and styrene. Ecotoxicology 23, 861-879.

Santana M.F., Moreira F.T., Pereira C.D., Abessa D.M., Turra A. 2018. Continuous exposure to microplastics does not cause physiological effects in the cultivated mussel *Perna perna*. Archives of Environmental Contamination and Toxicology 74, 594-604.

Sendra M., Sparaventi E., Novoa B., Figueras A. 2021. An overview of the internalization and effects of microplastics and nanoplastics as pollutants of emerging concern in bivalves. Science of the Total Environment 753, 142024.

Sforzini S., Moore M.N., Oliveri C., Volta A., Jha A., Banni M., Viarengo A. 2018. Role of mTOR in autophagic and lysosomal reactions to environmental stressors in molluscs. Aquatic Toxicology, 195, 114–128.

Singer M.M., Aurand D., Bragin G.E., Clark J.R., Coelho G.M., Sowby M.L., Tjeerdema R.S. 2000. Standardization of the preparation and quantitation of water-accommodated fractions of petroleum for toxicity testing. Marine Pollution Bulletin, 40. 1007–1016.

Sussarellu R., Suquet M., Thomas Y., Lambert C., Fabioux C., Pernet M.E.J., Corporeau C. 2016. Oyster reproduction is affected by exposure to polystyrene microplastics. Proceedings of the National Academy of Sciences 113, 2430-2435.

Statoil. 2011. Crude summary report. Available at: https://www.statoil.com/content/dam/statoil/documents/crude-oil-assays/Statoil-TROLL-BLEND-2011-01.xls. Accessed Nov 2018

Van A., Rochman C.M., Flores E.M., Hill K.L., Vargas E., Vargas S.A., Hoh E. 2012. Persistent organic pollutants in plastic marine debris found on beaches in San Diego, California. Chemosphere 86, 258–263.

Van Cauwenberghe L., Claessens M., Vandegehuchte M.B., Janssen C.R. 2015. Microplastics are taken up by mussels (*Mytilus edulis*) and lugworms (*Arenicola marina*) living in natural habitats. Environmental Pollution 199, 10-17.

Vethaak A.D., Davies I.M., Thain J.E., Gubbins M.J., Martínez-Gómez C., Robinson C.D., Moffat C.F., Burgeot T., Maes T., Wosniok W., Giltrap M., Lang, T. Hylland K. 2017. Integrated indicator framework and methodology for monitoring and assessment of hazardous substances and their effects in the marine environment. Marine Environmental Research 124, 11–20.

Von Hellfeld R., Zarzuelo M., Zaldibar B., Cajaraville M.P., Orbea A. 2022. Accumulation, depuration, and biological effects of polystyrene microplastics spheres and adsorbed cadmium and benzo(a)pyrene on the mussel *Mytilus galloprovincialis*. Toxics 10, 18.

Von Moos N., Burkhard-Holm P., Kohler A. 2012. Uptake and effects of microplastics on cells and tissue of the blue mussel *Mytilus edulis* L. after an experimental exposure. Environmental Science & Technology 46, 11327-11335.

Wegner A., Besseling E., Foekema E.M., Kamermans P., Koelmans A.A. 2012. Effects of nanopolystyrene on the feeding behavior of the blue mussel (*Mytilus edulis* L.). Environmental Toxicology and Chemistry 31, 2490-2497.

Ying Z., Pu S., Xue L., Ya G., Ge L. 2020. Global trends and prospects in microplastics research: A bibliometric analysis. Journal of Hazardous Material 200, 123110.

Zhang W., Ma X., Zhang Z., Wang Y., Wang J., Wang J., Ma D. 2015. Persistent organic pollutants carried on plastic resin pellets from two beaches in China. Marine Pollution Bulletin 99, 28–34.

Zorita I., Ortiz-Zarragoitia M., Soto M., Cajaraville M.P. 2006. Biomarkers in mussels from a copper site gradient (Visnes, Norway): an integrated biochemical, histochemical and histological study. Aquatic Toxicology 78, 109-116.

SUPPLEMENTARY MATERIAL TO CHAPTER 2

Table S1. Bioaccumulation of the 16 EPA PAHs in mussel soft tissues (ng/g dry weight) and the percentage that each compound represents from the total (%). Data is given for 3 pools of 7 mussels ± standard deviation, except for controls at day 21 (2 pools). Naphthalene (NAPH), acenaphthene (ACE), fluorene (FLU), phenanthrene (PHE), anthracene (ANT), fluoranthene (FRT), pyrene (PYR), benzo(a)anthracene (BaA), chrysene (CRY), benzo(b)fluoranthene (BbF), benzo(k)fluoranthene (BkF), indeno pyrene (INP), benzo(a)pyrene (BaP), dibenzo(a,h)anthracene (DahA), benzo(g,h,i)perylene (BghiP), acenaphthylene (ACY).

		NAPH		ACY		FLU		PHE		ANT		FRT		PYR		BaA	
		ng/g	%	ng/g	%	ng/g	%	ng/g	%	ng/g	%	ng/g	%	ng/g	%	ng/g	%
Control	7D	62.39 ± 19.63	43.93	4.35 ± 0	3.06	3.11 ± 3.14	2.19	24.13 ± 4.88	16.99	1.72 ± 0.19	1.21	8.21 ± 4.15	5.78	15.16 ± 7.20	10.68	2.47 ± 0.58	1.74
	21D	185.83 ± 82.88	75.23	<1		0.98 ± 0	0.40	19.37 ± 6.57	7.84	3.23 ± 0.03	1.31	3.65 ± 2.90	1.48	7.40 ± 3.21	3.00	2.10 ± 1.53	0.85
MP	7D	20.71 ± 12.32	14.18	<1		6.73 ± 2.43	4.61	30.36 ± 13.97	20.79	4.13 ± 1.32	2.83	13.61 ± 5.16	9.32	25.90 ± 14.32	17.74	5.64 ± 1.08	3.86
	21D	64.81 ± 14.42	41.54	<1		7.39 ± 1.90	4.74	23.32 ± 5.84	14.95	6.68 ± 1.31	4.28	6.81 ± 0.74	4.37	14.98 ± 2.37	9.60	2.78 ± 0.56	1.78
MP25	7D	62.51 ± 11.96	35.92	22.75 ± 1.26	13.07	4.24 ± 3.05	2.44	17.41 ± 7.30	10.01	3.42 ± 1.26	1.97	12.04 ± 3.10	6.92	20.44 ± 3.22	11.75	4.16 ± 1.23	2.39
	21D	61.16 ± 9.87	38.95	<1		6.20 ± 1.01	3.95	21.81 ± 2.43	13.89	3.23 ± 1.09	2.06	10.16 ± 3.89	6.47	22.18 ± 6.88	14.13	3.30 ± 1.17	2.10
MP100	7D	6.23 ± 44.75	36.29	2.32 ± 0.68	1.23	8.37 ± 3.63	4.45	27.71 ± 3.09	14.74	3.83 ± 1.45	2.04	13.91 ± 3.28	7.40	27.03 ± 6.16	14.38	4.02 ± 0.64	2.14
	21D	57.52 ± 6.46	34.03	1.94 ± 0.60	1.14	9.89 ± 6.59	5.85	25.01 ± 8.90	14.80	2.51 ± 1.29	1.49	10.43 ± 1.25	6.17	18.67 ± 3.88	11,05	1.62 ± 0.28	0.96
WAF	7D	120.25 ± 30.95	5.21	<1		205.32 ± 44.99	8.90	1096.01 ± 81.18	47.53	132.52 ± 11.18	5.75	221.86 ± 19.58	9.62	220.43 ± 17.95	9,56	40.18 ± 14.10	1.74
	21D	116.34 ± 21.54	9.46	1.57 ± 0	0.12	77.02 ± 12.42	6.27	321.52 ± 112.70	26.16	89.66 ± 7.39	7.30	137.74 ± 16.31	11.21	206.11 ± 19.61	16.77	35.99 ± 4.04	2.93

		CRY		BbF		BkF		BaP		INP		DahA		BghiP		ACE	
		ng/g	%	ng/g	%	ng/g	%	ng/g	%	ng/g	%	ng/g	%	ng/g	%	ng/g	%
Control	7D	5.49 ± 0.65	3.87	7.13 ± 2.33	5.02	1.62 ± 1.23	1.14	3.06 ± 0.66	2.15	2.83 ± 1.83	1.99	1.00 ± 0.34	0.70	2.44 ± 0.75	1.72	<10	
	21D	4.00 ± 2.47	1.62	5.37 ± 2.46	2.17	<0.5		8.74 ± 2.24	3.54	2.94 ± 0.78	1.19	1.13 ± 0.38	0.46	2.02 ± 0.04	0.82	<10	
MP	7D	9.93 ± 2.04	6.80	13.11 ± 3.65	8.98	2.58 ± 0.81	1.77	6.64 ± 2.74	4.55	2.87 ± 1.10	1.97	1.20 ± 0.26	0.82	3.04 ± 1.82	2.08	<10	
	21D	5.50 ± 0.83	3.53	6.09 ± 0.24	3.90	1.36 ± 0.20	0.87	8.67 ± 6.89	5.56	3.36 ± 3.06	2.15	1.54 ± 0.85	0.99	2.59 ± 1.21	1.66	<10	
MP25	7D	8.09 ± 1.46	4.65	14.25 ± 1.97	8.19	4.89 ± 0.03	2.81	4.87 ± 3.72	2.80	1.09 ± 0.30	0.63	1.11 ± 0.17	0.64	2.31 ± 0.38	1.33	<10	
	21D	6.89 ± 2.33	4.39	11.93 ± 4.54	7.60	2.48 ± 0	1.58	7.03 ± 5.61	4.48	1.08 ± 0.39	0.69	1.04 ± 0.48	0.66	1.68 ± 0.08	1.07	<10	
MP100	7D	10.68 ± 2.40	5.68	9.63 ± 1.62	5.12	2.29 ± 0.41	1.22	4.98 ±4.09	2.65	1.64 ± 0.76	0.87	1.34 ± 0.58	0.71	2.61 ± 0.80	1.39	<10	
	21D	3.63 ± 0.17	2.15	4.94 ± 0.26	2.92	<0.5		24.43 ± 4.23	14.46	2.70 ± 0.02	1.60	2.39 ± 1.14	1.41	2.91 ± 0.34	1.72	<10	
WAF	7D	118.23 ± 11.07	5.13	51.28 ± 1.70	2.22	8.88 ± 3.88	0.39	45.45 ± 24	1.97	9.84 ± 2.30	0.43	13.09 ± 4.67	0.57	22.17 ± 1.41	0.96	<10	
	21D	152.63 ± 13.68	12.42	47.07 ± 1.06	3.83	9.27 ± 1.22	0.75	14.50 ± 0.87	1.18	4.46 ± 0.72	0.36	6.84 ± 0.92	0.56	9.35 ± 0.97	0.76	<10	

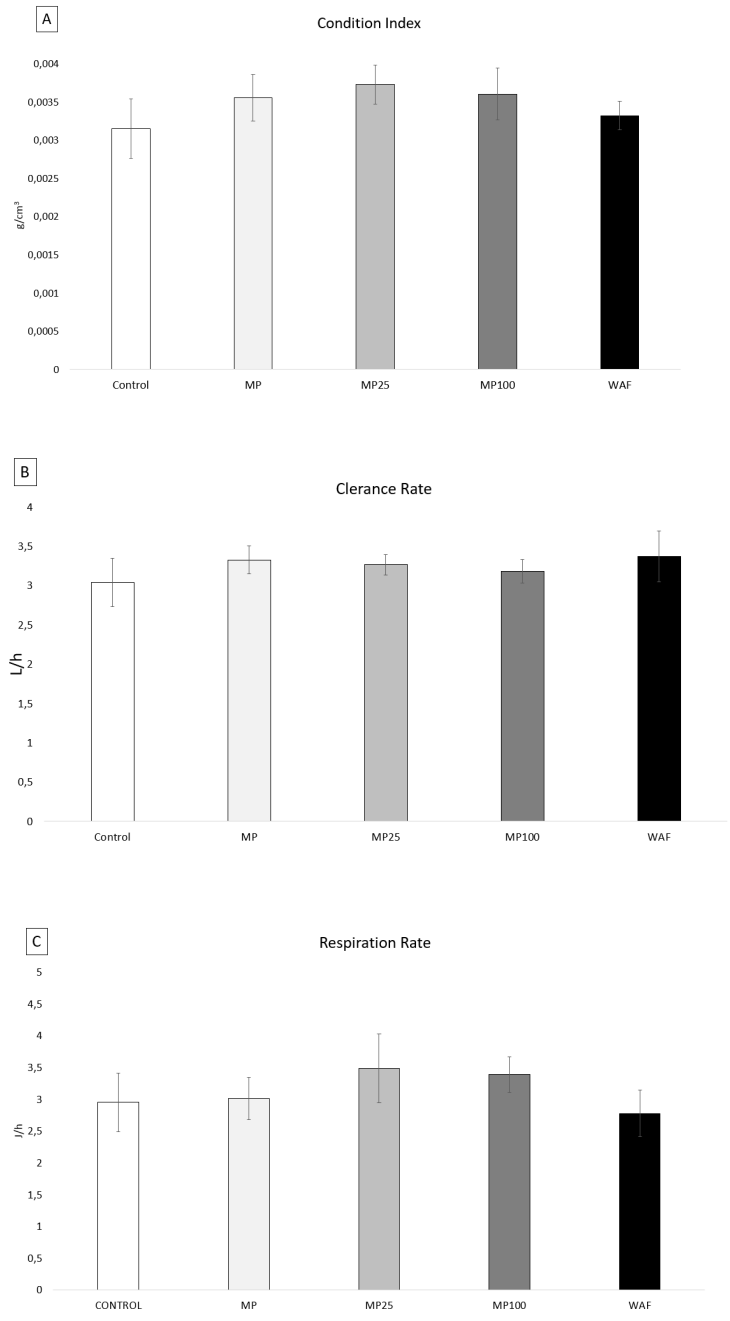

Figure S1. A) Condition index (g dry weight/cm^3); B) Clearance rate (L/h) and C) Respiration rate (J/h) of control mussels and mussels exposed to MP, MP25, MP100 and WAF after 21 days of exposure. Values are given as means and standard errors of 7 mussels per experimental group. No differences were found among treatments (Kruskal-Wallis followed by Dunn's post hoc test, $p > 0.05$).

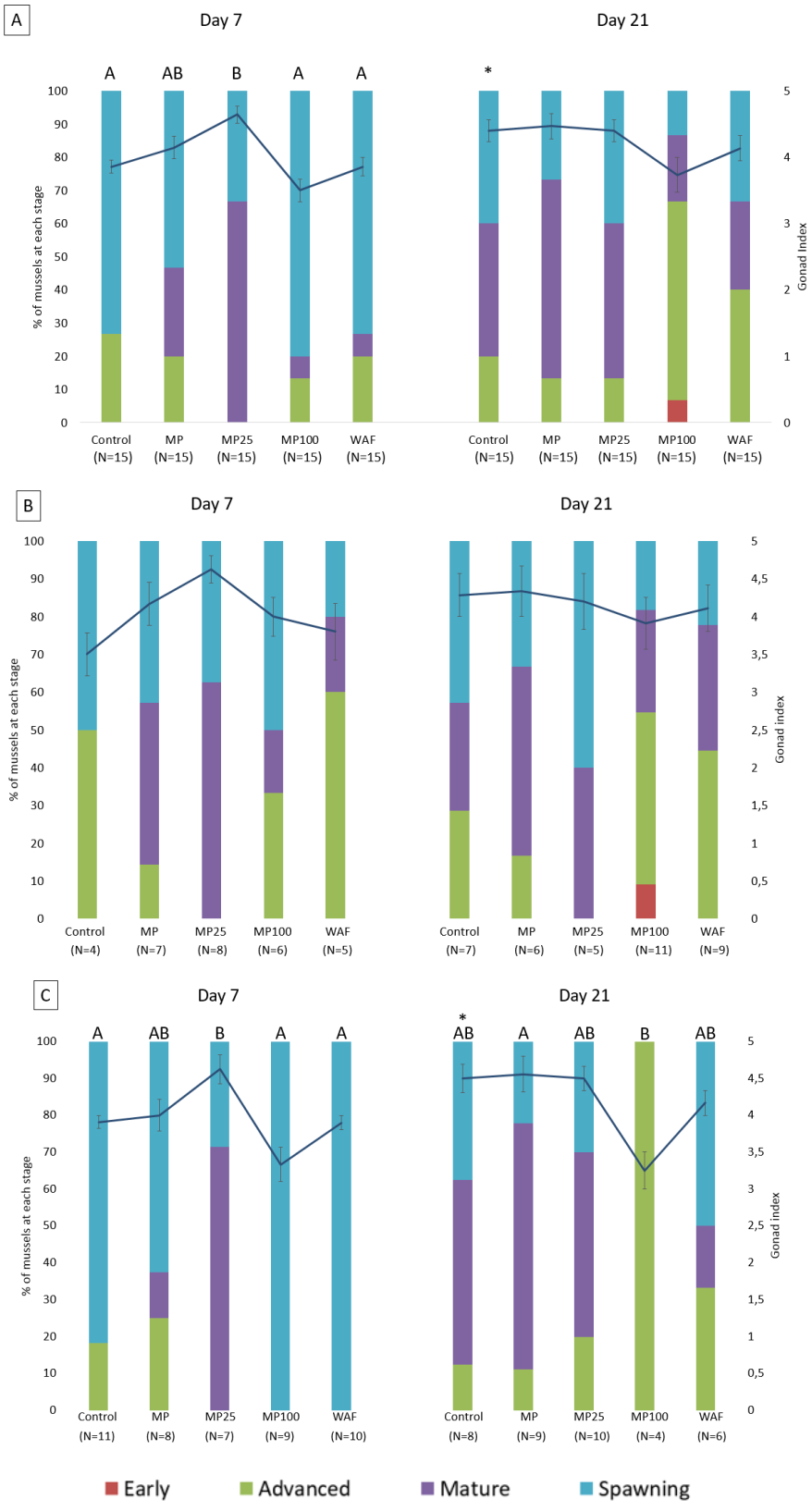

Figure S2. Gonad index (lines) and percentage of animals at each gamete developmental stage (stacked bars) of control mussels and mussels exposed to MP, MP25, MP100 and WAF after 7 and 21 days of exposure. Gonad index values are given as means and standard errors of A) both sexes, B) females, C) males. Letters indicate significant differences for gonad index among treatments within the same day (Kruskal-Wallis followed by Dunn's post hoc test, $p < 0.05$). The asterisk indicates significant differences between days within the same treatment (Mann-Whitney´s U test, $p < 0.05$).

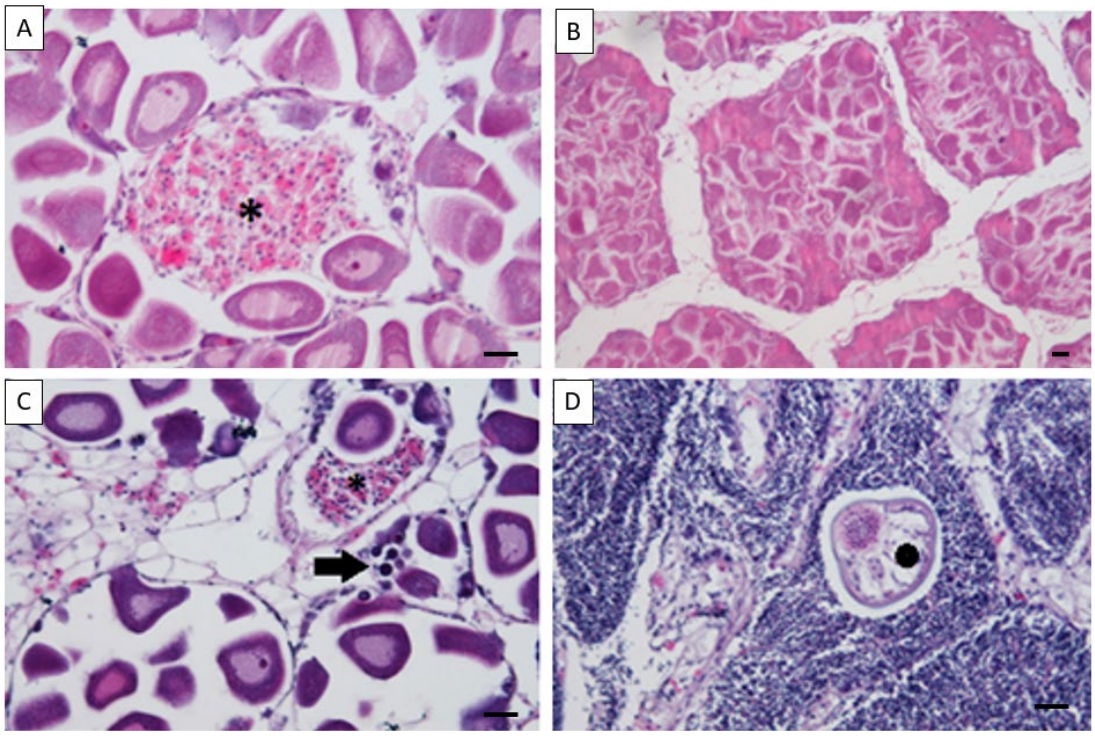

Figure S3. Light micrographs of mussel gonad paraffin sections stained with hematoxylin/eosin showing different histopathological alterations. A) hemocytic infiltration (*) in a female follicle after 7 days of exposure to MP25; B) widespread gamete atresia in a female gonad after 7 days of exposure to MP; C) necrotic oocytes (arrow) in the form of basophilic spheres and hemocytic infiltration (*) in a female mussel after 21 days of exposure to MP100; D) a trematode parasite infestation (dot) in a male gonad after 21 days of exposure to MP. Scale bars: 25 µm.

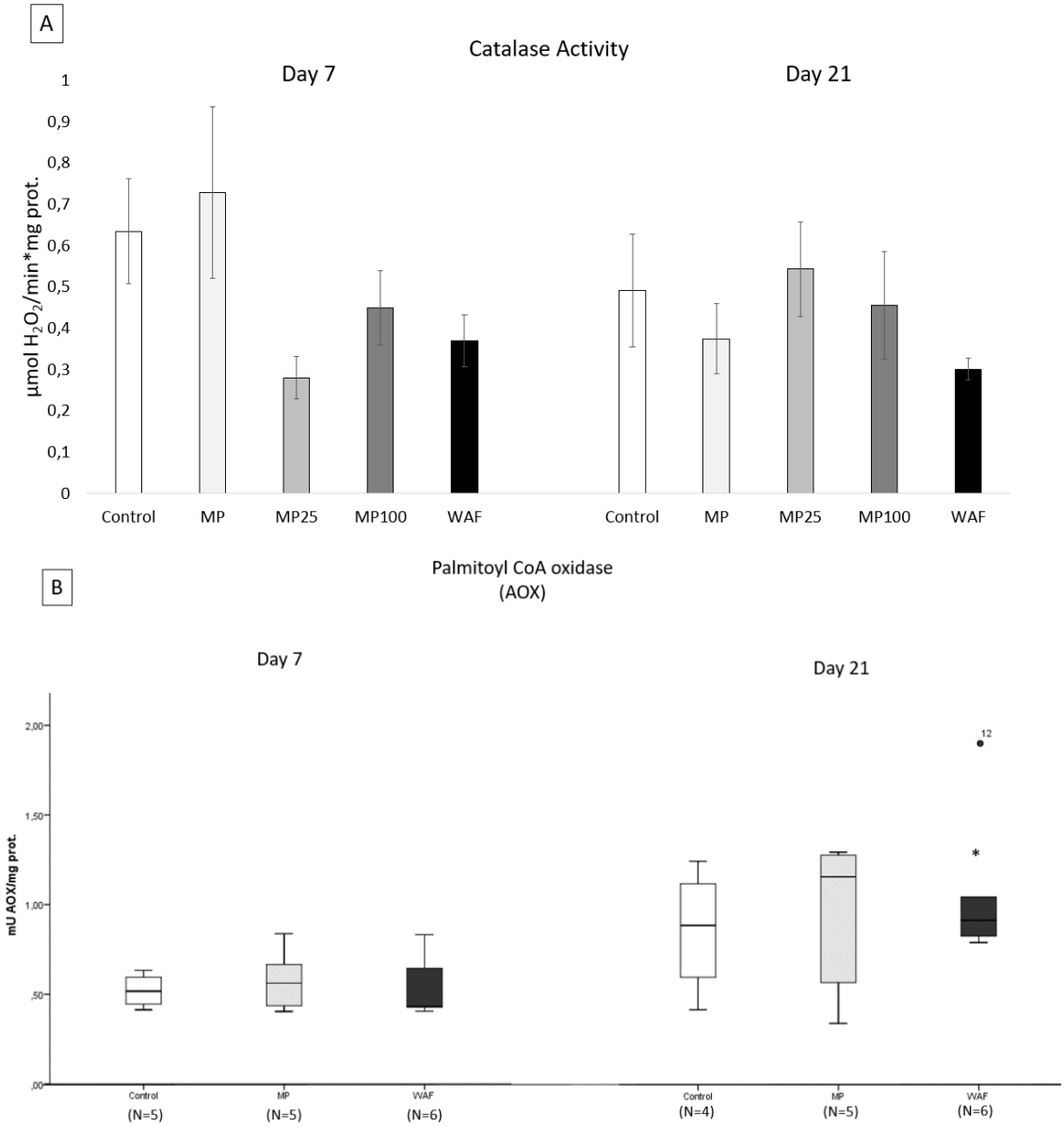

Figure S4. A) Catalase activity (given as µmol H_2O_2/min*mg protein) in hemocytes of control mussels and mussels exposed to MPs, MP25, MP100 and WAF after 7 and 21 days of exposure and B) AOX1 activity (given as mU AOX1/mg protein) in digestive gland of control mussels and mussels exposed to MPs and to WAF after 7 and 21 days of exposure. Data are given as mean values and standard errors 8 mussels per experimental group, 4 replicates per mussel in A and as box-plots which showed median values (horizontal line), 25%-75% quartiles (box) and standard deviation (whiskers) in B. Dot denotes an outlier, a value that does not fall in the inner fences. No differences were observed among treatments ($p>0.05$ after Kruskal-Wallis test followed by Dunn's post hoc). The asterisk indicates significant differences between days within the same treatment (Mann-Whitney´s U test, $p < 0.05$).

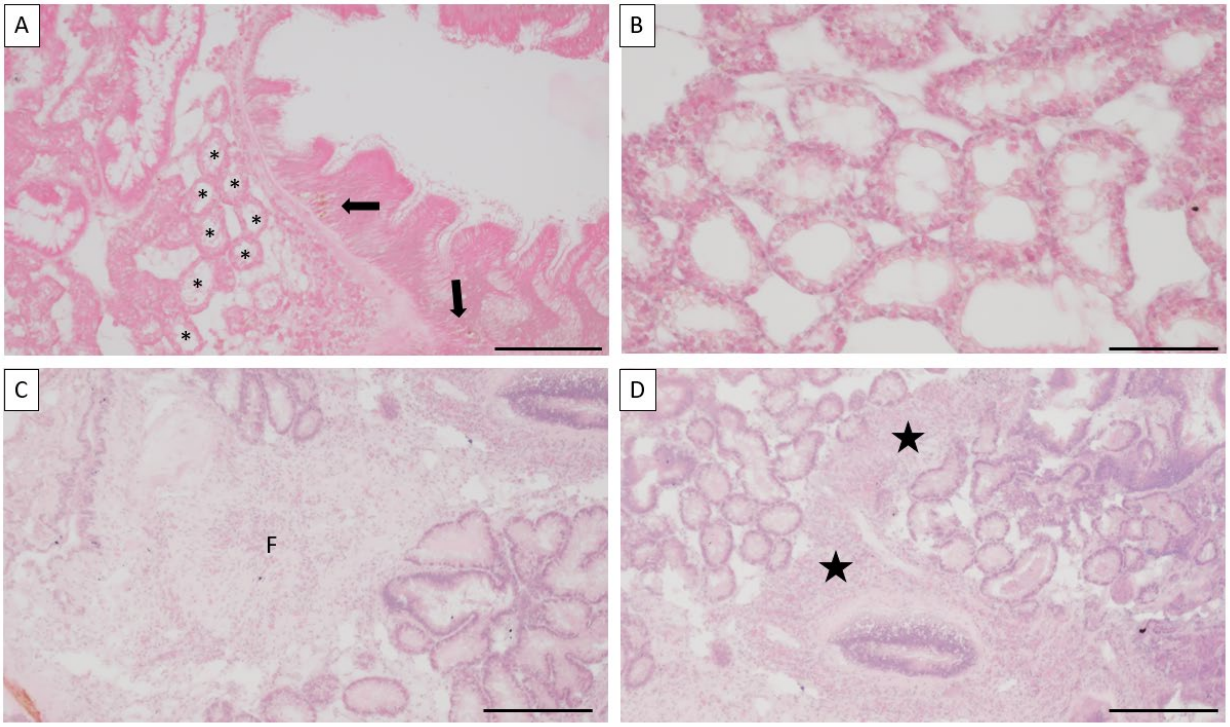

Figure S5. Light micrographs of mussel paraffin sections showing histopathological alterations in digestive glands: A) atrophic digestive tubules (*) and accumulation of brown cells in digestive tract epithelium (arrows) after 21 days of exposure to MPs; B) atrophic digestive tubules after 7 days of exposure to WAF; C) fibrosis (F) after 7 days of exposure to WAF; D) hemocytic infiltration (star) after 7 days of exposure to WAF. Scale bars: A, C and D: 200 µm; B: 100 µm.

Table S2. Prevalence of histopathological alterations in gonad of control mussels and mussels exposed for 7 and 21 days to MP, MP25, MP100 and WAF. Data are shown as percentage for a total of 15 mussels per experimental group (one section per mussel). A semiquantitative index was used for intensity of oocyte atresia, being: 1) ¼ of follicles in the tissue section showed signs of atresia, 2) about half the follicles in the tissue section showed signs of atresia, 3) ¾ of follicles in the tissue section showed signs of atresia and 4) all follicles in the tissue section showed signs of atresia Kim et al. (2006). Not observed, n.o. Letters indicate a significant difference among groups within the same exposure day and asterisks indicate a significant difference between days within treatments (X^2 test; $p<0.05$).

		Control		MP		MP25		MP100		WAF	
		7D	**21D**	**7D**	**21D**	**7D**	**21D**	**7D**	**21D**	**7D**	**21D**
Oocyte atresia	**1**	n.o.	n.o.^{a}	14.29	16.67^{ab}	n.o.	60^{b}	n.o.	45.45^{b}	20	22.22^{ab}
	2	25	n.o.	n.o.	33.33	12.5	n.o.	n.o.	9.09	20	11.11
	3	25	n.o.	14.29	n.o.	n.o.	n.o.	16.67	9.09	n.o.	n.o.
	4	n.o.	n.o.	n.o.	n.o.	n.o.	n.o.	16.67	n.o.	n.o.	22.22
		50	n.o.^{a*}	28.57	50^{b}	12.5	60^{b}	33.33	63.63^{b}	40	55.55^{b}
Hemocytic infiltration		26.67	n.o.^{a*}	20	13.33^{ab}	13.33	33.34^{b}	33.34	26.67^{b}	20	26.67^{b}
Fibrosis		20	20	20	6.67	6.67	20	26.67	20	13.33	20
Oocyte necrosis		n.o.	n.o.	n.o.	n.o.	n.o.	n.o.	n.o.	6.67	n.o.	n.o.
Parasites		n.o.	n.o.	n.o.	6.67	n.o.	n.o.	n.o.	n.o.	n.o.	n.o.

Table S3. Prevalence of histopathological alterations in the digestive gland of control mussels and mussels exposed for 7 and 21 days to MPs and to WAF. Prevalence is given in percentages of 10 mussels per experimental group. Not observed, n.o. Asterisks indicate significant differences between days within treatments (X^2 test; $p<0.05$).

	Control		MP		WAF	
	7D	**21D**	**7D**	**21D**	**7D**	**21D**
Digestive tubule atrophy	10	60*	10	50	20	20
Hemocytic infiltration	100	90	90	90	80	100
Accumulation of brown cells	60	80	60	90	60	80
Fibrosis	50	30	70	10*	80	30*
Parasites ***Nematopsis sp.***	50	60	80	70	70	90
M. intestinalis	80	10	30	20	0	20

CHAPTER 3:

Fate and effects of graphene oxide alone and with sorbed benzo(a)pyrene in mussels *Mytilus galloprovincialis*

This chapter is being prepared for publication:

GONZÁLEZ-SOTO, N; BLASCO, N; IRAZOLA-DUÑABEITIA, M; BILBAO, E., GUILHERMINO, L; CAJARAVILLE, MP. Fate and effects of graphene oxide alone and with sorbed benzo(a)pyrene in mussels *Mytilus galloprovincialis*. *Environmental Science Nano*

This chapter has been presented at:

31st ANNUAL MEETING OF THE SOCIETY OF ENVIRONMENTAL TOXICOLOGY AND CHEMISTRY (SETAC)-EUROPE, virtual, 2-6 May 2021. GONZÁLEZ-SOTO, N; BLASCO, N; IRAZOLA-DUÑABEITIA, M; BILBAO, E; GUILHERMINO, L; CAJARAVILLE, M.P. Toxicity of graphene oxide alone and with sorbed benzo(a)pyrene on mussels *Mytilus galloprovincialis*. Platform (N González-Soto).

ABSTRACT

Among nanomaterials, graphene oxide (GO) has gained a great scientific and economic interest due to its unique properties. As incorporation of GO in consumer products is rising in the last years, it is expected that GO will end up in oceans through direct release, transport through rivers and effluents, among other ways. Due to its high surface to volume ratio, GO can adsorb persistent organic pollutants (POPs), such as benzo(a)pyrene (BaP), and act as carrier of POPs, increasing the bioavailability of these compounds to marine organisms (the so-called Trojan horse effect). Thus, uptake and effects of GO in marine biota represent a major concern. In this context, this work aimed to assess the potential hazards of GO, alone or with sorbed BaP (GO+BaP), and BaP alone in marine mussels (*Mytilus galloprovincialis*) after 7 days of exposure. GO was detected through Raman spectroscopy in the lumen of the digestive tract and in feces of mussels exposed to GO and GO+BaP while BaP was bioaccumulated in mussels exposed to GO+BaP, but especially in those exposed to BaP. Cell viability of hemocytes decreased significantly in mussels exposed to GO+BaP and BaP compared to controls. Frequency of micronuclei was high in hemocytes of mussels exposed to GO and GO+BaP suggesting a genotoxic effect of GO. Interestingly, activity of SOD was higher in the digestive gland of mussels exposed to GO+BaP than in mussels exposed to GO alone, and GST activity was inhibited in mussels exposed to GO+BaP in comparison to controls. At tissue level, inflammation was observed both in the digestive gland and in gonads of all exposed mussels. In addition, oocyte atresia in stages 2 and 3 was found in the gonad of exposed mussels, especially after exposure to GO+BaP. Overall, GO acted as a carrier of BaP to mussels but GO appeared to protect mussels towards BaP accumulation. Enhanced toxicity of GO+BaP with respect to that of GO and/or BaP occurred for some biological responses, whereas carrier effects and synergistic effects were also identified, demonstrating the complexity of the Trojan horse effect. Further work is required in order to understand the hazards of GO, especially at long-term, and its relevance as carrier of other pollutants in the marine environment.

1. INTRODUCTION

Nanomaterials (NMs) are commonly defined as a diverse class of materials with at least one dimension at the nanoscale (<100 nm) (Nel et al., 2006). In 2011, the European Commission defined a nanomaterial as: "*a natural, incidental or manufactured material containing particles, in an unbound state or as an aggregate or as an agglomerate and where, for 50 % or more of the particles in the number size distribution, one or more external dimensions is in the size range 1 nm - 100 nm. In specific cases and where warranted by concerns for the environment, health, safety or competitiveness the number size distribution threshold of 50 % may be replaced by a threshold between 1 and 50 %* (2011/696/EU). Among NMs, carbon-based NMs have attracted great scientific and technological attention due to the physico-chemical properties of their nanometric structures. Carbon-based NMs include among others, fullerenes, carbon nanotubes, carbon black or graphene; but among all of them, graphene stands out for the unique properties that make it the thinnest, strongest and lightest known material (Novoselov et al., 2012).

Graphene family nanomaterials (GFNs) are used in a wide range of applications including electronic devices, a new generation of batteries, sensors (Peng et al., 2020), biomedical applications (Ou et al., 2016), anticorrosion coatings (Ren & Chen, 2014; Yao et al., 2020), agricultural procedures (Kabiri et al., 2017) or environmental applications such as waste water treatments (Peng et al., 2020), water desalination (Le et al., 2021) and pollutants removal (Ahmad et al., 2020; Peng et al., 2020). There are more than 26000 graphene related patents (Scott, 2016) and more than 100 graphene based products (de Marchi et al., 2018). In fact, the production of GFNs is higher in comparison to the rest of NMs (Arvidsson et al., 2018) and it is expected to continue growing as the expensive and low efficient methods used nowadays for graphene production are improved. Therefore, graphene production is expected to reach 3800 tones, with a worth of 300 millions by 2027 (Collins, 2021).

Graphene oxide (GO) is a precursor in graphene synthesis and one of the most studied graphene derivates (Dreyer et al., 2010) whose reactivity and capacity for chemical functionalization (de Marchi et al., 2018) are important characteristics related to the

presence of functional oxygen groups both on the surface (hydroxyl and epoxy groups) and in the edges (carboxyl groups) of the sheet (Chen et al., 2012a). Due to the general interest on GO and its increased production in the last years, GO is being released into the environment during its life cycle (Malina et al., 2020) both through direct release (e.g., sewage effluents, river influx) or indirectly (e.g., aerial deposition, dumping and run off) (Zhao et al., 2014). Therefore, GO will definitely reach coastal and marine ecosystems (de Marchi et al., 2018) and probably will interact with different components of the natural system, which may alter behaviour, transport, fate and toxicity of GO (He et al., 2017). Transport and fate of GFNs are governed mainly by the stability of suspensions, which may be altered by environmental factors such as salinity, organic matter concentration, oxidation status and bioturbation. In aquatic environments, GO can disperse and form relatively stable suspensions that endure in the water column (Zhao et al., 2014; Avant et al., 2019). Such behavior may facilitate the uptake of GO by a large number of organisms through different routes such as ingestion or respiration, as it has been described for other NMs (Moore, 2006). In addition, the high persistence of GO can result in their bioaccumulation and biomagnification in food webs (Dong et al., 2018; Peng et al., 2020), increasing their potential impact in marine ecosystems, even if the GO concentrations released into the environment are relatively low (Arvidsson et al., 2013). Therefore, levels of GO in surface waters should be a primary concern (Han et al., 2019). However, the environmental concentrations of GO are still largely unknown (de Marchi et al., 2018). The presence of GO was already detected in the biomass from wastewater treatment plants (Goodwin et al., 2018). Recent studies consider that the predicted environmental concentration of GO could be similar to that described for other NMs such as multi-walled carbon nanotubes, which is in the range 0.001-1000 µg/L for aquatic environments (Nouara et al., 2013).

Toxicity of NMs is strongly related to their size, shape, surface properties or chemical composition, which are key characteristics for risk assessment (Nel et al., 2006; Katsumiti & Cajaraville, 2019). Overall, at cellular level, GFNs have been reported to decrease integrity of the cell´s plasma membrane, possibly as a consequence of entry of nanosheets into cells by direct penetration or endocytosis (Zhao et al., 2014). Sheets can also disrupt the plasma membrane due to induced invaginations or perforations

(Lammel et al., 2013; Katsumiti et al., 2017), or even by the destructive extraction of lipids (Tu et al., 2013). Disruption of the plasma membrane and internalization of GFNs can provoke the formation of reactive oxygen species (ROS) and lead to oxidative stress (Katsumiti et al., 2017), which is considered one of the main underlying mechanisms of toxicity of NMs (Katsumiti & Cajaraville, 2019). Oxidative damage caused by the increased intracellular production of ROS can lead to mitochondrial and lysosomal dysfunction and finally to a decrease in the viability of hemocyte cells of marine mussels (Katsumiti et al., 2017). In addition, oxidative stress and/or physical cell damage can also cause DNA damage resulting in the fragmentation and destruction of nucleic acids (Wang et al., 2013). These alterations at the cellular level may lead to effects at higher biological levels, such as reduction of metabolic activity (Peng et al., 2020; Britto et al., 2021), histopathological lesions (Souza et al., 2017; Khan et al., 2019a), alterations in behavior and locomotor functions (Audira et al., 2021) and adverse impact on the reproduction capacity, growth and survival (Bortozollo et al., 2021).

In aquatic environments, generally NMs do not appear alone, but are found within complex mixtures of chemical contaminants originated both from natural and anthropogenic sources. Several studies have demonstrated that GFNs show a great adsorption capacity for persistent organic pollutants (POPs) such as polycyclic aromatic hydrocarbons (PAHs), mainly due to their large surface area and hydrophobicity (Apul et al., 2013; He et al., 2013; Ersan et al., 2017; Wang et al., 2021). This adsorption produces accumulation of organic pollutants on the surface of the NM, which may increase their uptake by aquatic organisms (Sanchís et al., 2016) and their potential adverse effects (Ersan et al., 2017), a phenomenon known as Trojan horse effect. Among PAHs, benzo(a)pyrene (BaP) is a priority pollutant (EU, 2008; U.S. EPA, 2014), commonly used in ecotoxicology studies and known to cause effects at different levels of biological organization (Banni et al., 2017). BaP is a genotoxic and carcinogenic agent capable of producing tissue and DNA damage (Di et al., 2011; 2017), oxidative stress (Gómez-Mendikute et al., 2002), peroxisome proliferation (Cancio et al., 1998), lysosomal dysfunction (Marigómez et al., 2005), endocrine disruption (Tian et al., 2013), among other effects in marine organisms, including bivalves. In addition, BaP can interact with emerging pollutants of high concern, such as microplastics and NMs, in marine mussels

resulting in toxicological interactions (Di et al., 2017; Chapter 1). Among target organisms, mussels *(Mytilus sp*.), are considered model organisms for the evaluation of pollutants including micro and nanoscale particulate materials, due to their highly developed mechanisms for cellular internalization of particles through endocytosis and phagocytosis, for physiological functions such as intracellular digestion and cellular immunity (Cajaraville & Pal, 1995; Robledo et al., 2006; Katsumiti & Cajaraville, 2019).

To improve the basis for the risk assessment of GFNs to the marine environment, it is very important to study the toxicity of GFNs, alone and combined with POPs in marine organisms, such as mussels. Therefore, the aim of this work was to investigate the fate and effects of GO, alone or with sorbed BaP, in adult marine mussels (*M. galloprovincialis)* using Raman spectroscopy and a battery of biological responses, respectively. Overall, this work contributes to understand the Trojan horse effect of GFNs towards BaP in mussels.

2. MATERIALS AND METHODS

2.1. Obtention of GO and preparation of GO with sorbed BaP

Commercial nanoplatelets of graphene oxide (GO) were purchased from Graphenea (San Sebastian, Spain) as stable suspensions. According to the supplier, the concentration of GO in the dispersion was 10 mg/mL. The concentration of GO experimentally determined by UV-VIS spectrophotometry was 9.91 mg/mL. According to the manufacturer's information, nanoplatelets showed lateral dimensions ranging from 500 nm to few microns and thickness was < 2 nm. Oxygen content was about 40% wt. Characterization of GO by transmission electron microscopy and atomic force microscopy was reported previously by Martínez-Álvarez et al. (2021).

The protocol to prepare GO with sorbed benzo(a)pyrene (BaP) was based on previous work (Martínez-Álvarez et al*.* 2021). Briefly, after preparing the BaP solution of 100 µg/L containing 0.01% dimethyl sulfoxide (DMSO, purity 99% Sigma, St. Louis, Missouri) in a glass bottle, GO was added in a 0.5 mg:10 mL GO/BaP proportion (weight/volume). Sorption process was allowed by shaking samples in an orbital shaker (300 rpm) for 24

h in the dark at 21±1 °C. After 24 h, samples were centrifuged in an Allegra X30R centrifuge (9509 g, 30 minutes). Supernatant was discarded and the pellet was re-suspended in 50 mL of MilliQ water. Samples were vortexed before dosing into tanks. According to Martínez-Álvarez et al. (2021) the proportion of BaP sorbed onto GO was 96.7% ± 0.5. Samples containing GO alone were processed in the same way, but using only MilliQ water.

2.2. Sampling and acclimation of mussels

Roughly 460 mussels *Mytilus galloprovincialis* (3,5-4,5 cm shell length) were collected in February 2019 in Mundaka, Basque Country (43°24´04.9”N, 2°41´41.6”W). Mussels were maintained in aquaria facilities at the Plentzia Marine Station (PiE) of the University of the Basque Country (UPV/EHU), for acclimation during 21 days. Acclimation was carried out in a 300 L polypropylene tank with a recirculating seawater system. Marine water was collected with a pump at 10 m depth in the mouth of the Butroi estuary (43°24’21”N, 2°56’47”W) and filtered (particles ≤ 3 µm) before reaching the marine station. Mussels were not fed for two days and then they were fed once a day with the *Isochrysis galbana* microalgae ($20x10^6$ cells/mussel-day) for 19 days. *I. galbana* (T-Iso clone) cultures were obtained from the Animal Physiology Laboratory at UPV/EHU. During acclimation, light regime was 12L/12D and room temperature was kept at 18°C. Water parameters were checked daily with a multichannel probe. The variation of water parameters during the acclimation period was (mean ± standard deviation – SD): salinity of 32.40 ± 0.27 PSU, pH of 7.25 ± 0.35 and temperature of 16.02 ± 0.08 °C. The dissolved O_2 was always above 80%.

2.3. Mussel exposure

In order to keep a homogeneous suspension of GO, without aggregation or precipitation, a water recirculation system consisting of two water pumps was installed in the aquaria. Before mussel exposure, tanks were exposed for 24 hours to GO at the same concentration tested in order to saturate the system.

After 21 days of acclimation, mussels were exposed for 7 days to graphene oxide (GO), graphene oxide with sorbed BaP (GO+BaP) or BaP alone in two 20 L replicate tanks per treatment (GO R1 and GO R2, GO+BaP R1 and GO+BaP R2, BaP R1 and BaP R2) with 57 mussels each (Figure.1). Two control tanks, also with 57 mussels each, were run in parallel (Control R1, Control R2). Mussel samples were taken after 7 days of exposure. An exposure concentration of 500 µg/L GO was selected, based on environmentally relevant concentrations for multi-walled carbon nanotubes, which range from 1 µg/L to 1 mg/L (de Marchi et al., 2018). For the GO+BaP exposure groups, the nominal concentration of BaP incubated with GO was 100 µg/L. Finally, for the BaP exposure groups, 96.7 µg/L BaP was used as the equivalent BaP concentration sorbed in GO+BaP preparations (Martínez-Álvarez et al., 2021).

During the experiment, water was changed daily. Throughout exposure, mussels were fed once a day with *I. galbana* (20x10^6 cells/mussel-day) two hours before changing water. While water of tanks was changed, 5 mussels per tank were selected randomly and placed in individual glass containers with clean water to collect feces (Figure 1). The light regime and room temperature were kept at 12L/12D and 18 °C, respectively. Water parameters were checked daily with a multichannel probe: salinity (32.93 ± 0.06 PSU), dissolved O_2 (>77%), pH (7.48 ± 0.23) and temperature (16.62 ± 0.25 °C).

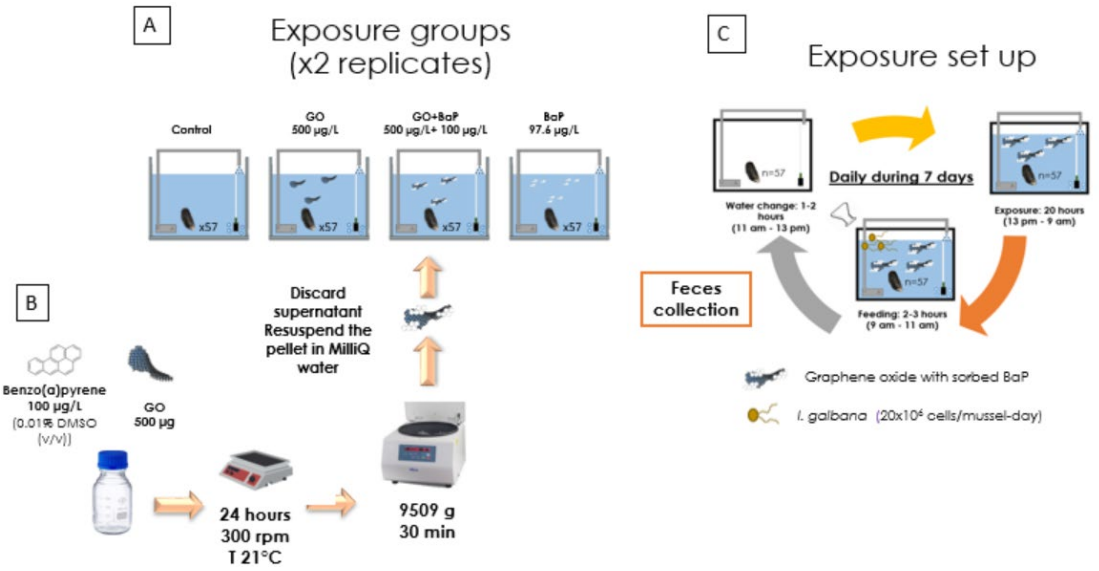

Figure 1: Summary of the experimental design. A: Exposure groups, B: preparation of graphene oxide (GO) with adsorbed benzo(a)pyrene (BaP) and C: exposure set up for the GO+BaP group as an example.

2.4. Bioaccumulation of BaP

The presence of BaP in seawater was checked by gas chromatography in water collected after 20 hours of exposure in all the tanks.

Mussels for chemical analysis (14-18 mussels per tank) were stored at −40°C and analyzed at IPROMA (Castellon, Spain) to determine bioaccumulation of BaP in whole mussel tissues. Mussels were lyophilized and homogenized. Extraction was performed using the QuEChERS method. Concentration of BaP was determined using gas chromatography followed by triple quadrupole mass spectrometry (GC/MS-QqQ). The limit of quantification in the analyses was 5 ng/g dry weight.

2.5. Determination of graphene oxide in mussel tissues and feces

Three mussels per tank were dissected, frozen in liquid nitrogen and maintained at -40°C until further analysis. Then 20 µm sections were obtained in a cryostat (Leica CM 3050S) and observed under an inVia Renishaw microscope in order to get Raman spectra using a 532 nm laser. Conditions were set using the 100x objective as follows: 1-5 µm steps in the tissue, 0.2-0.4 s, 10% laser intensity, 1 accumulation and focused in 1200 nm. For each sample, serial cryotome sections were fixed in Baker's solution (formaldehyde 4% (v/v), NaCl 2% (w/v), calcium acetate 1% (w/v)) for 15 min, rinsed in distilled water and stained 20 s in 0.1% toluidine blue to get the topographic reference of the tissue sample.

Mussels´ feces were also collected and analyzed by Raman spectroscopy. Mussel feces were completely dried and placed in an aluminum foil before getting the Raman spectrum. Conditions were set using a 100x objective as follows: 100% laser intensity, 1 s, 80 accumulation and focused in 1200 nm. As reference, spectra of microalgae *Isochrysis galbana*, BaP stock solution and DMSO were obtained in the same conditions.

2.6. Cellular biomarkers in hemocytes

Hemolymph of 8 mussels per tank was withdrawn from the posterior adductor muscle and cell viability, catalase activity and DNA damage in terms of micronuclei formation

were measured in hemocytes of individual mussels. Neutral red (NR) uptake was assessed according to Borenfreund & Puerner (1985) with modifications explained in Chapter 1. Catalase activity (Cat) was assessed according to Aebi (1984) as modified in Chapter 1. Protein concentration was measured following the Bradford method (Bradford, 1976) to normalize absorbance data. Cat activity was expressed as the consumption of mM H_2O_2/min/mg protein.

The micronucleus assay was performed according to Duroudier et al. (2019). Micronucleated cells were classified following the accepted criteria for mussels: well-preserved cell cytoplasm, micronuclei not touching the main nucleus, similar or weaker staining than the main nucleus and size of micronuclei ≤1/3 in comparison to the main nucleus. Other nuclear abnormalities such as binucleated cells, occurrence of nucleoplasmic bridges and nuclear buds were scored according to Pinto-Silva et al. (2005) and Bolognesi & Fenech (2012). Results are reported in ‰ frequencies.

2.7. Enzyme activities in mussel tissues

Digestive gland, gills and adductor muscle of 10 mussels per tank were dissected out, frozen in liquid nitrogen and maintained at -80°C until further analysis. Adductor muscle was homogenized in 0.1 M potassium phosphate (KP) buffer (pH 7.2) for acetylcholinesterase (AChE) determination. Gills were cut in two halfs; one half was homogenized in 0.1 M KP buffer (pH 6.5) for glutathione *S*-transferase (GST) determination and the second half in 0.1 M KP buffer (pH 7.4) for Cat, glutathione peroxidase (GPx) and superoxide dismutase (SOD) determination. Digestive glands were divided in thee parts. The first part was used for GST determination, the second for Cat, GPx and SOD, and the last piece was homogenized in 50 mM tris buffer (Tris(hydroxymethyl)-aminomethan, pH 7.8) for isocitrate dehydrogenase (IDH) determination. Tissues were homogenized in each buffer following a 1:10 proportion, tissue weight: volume of buffer.

The activity of the enzyme AChE and IDH, GST, GPx and SOD were determined as described in previous studies where some modifications of the original tecnhiques were

made (Guilhermino et al. 1996; Lima et al. 2007). Briefly, AChE activity was determined according to Ellman et al. (1961) at 412 nm and expressed as the production of 5,5'-dithiobis-(2-nitrobenzoic acid) in nmol/min/mg protein. IDH activity was determined according to Ellis & Goldberg (1971) at 340 nm and expressed as the production of nicotinamide adenine dinucleotide phosphate (NADPH) in nmol/min/mg protein. GST activity was determined according to Habig et al. (1974) at 340 nm and expressed as the production of 2,4-Dinitrochlorobenzene (CDNB) conjugates with the thiol group of glutathione in nmol/min/mg protein. Cat activity was determined as previously explained. GPx activity was determined according to Flohé & Günzler (1984) at 340 nm and expressed as the consumption of NADPH in nmol/min/mg protein. SOD activity was determined according to McCord & Fridovich (1969) at 550 nm and given in SOD units (1 SOD unit = 50% inhibition of the reduction of cytochrome C per mg protein). Each enzyme activity was normalized to protein concentration using Bradford method (Bradford, 1976).

2.8. Histopathology of the digestive gland

Digestive glands of 10 mussels per tank were dissected out and processed following a standard protocol for histology (Martoja & Martoja-Pierson, 1970). Briefly, tissues were fixed in 4% formalin in individual cassettes and dehydrated through a graded series of ethanol that finished in xylene using an automatic tissue processor (Leica ASP300; Leica Instruments, Wetzlar, Germany). Then, samples were embedded in paraffin and 5 µm sections were cut in a Leitz 1512 microtome (Leica Instruments, Wetzlar, Germany). Slides were dryed in an oven at 37 °C (24 h) and stained with hematoxylin/eosin (Gamble & Wilson, 2002) using an autostainer XL V2.02 (Leica). Slides were mounted in DPX and analyzed under a BX51 light microscope (Olympus, Tokyo, Japan).

Vacuolization, atrophy and necrosis of the digestive tubule epithelium, fibrosis, hemocytic infiltration, aggregation of brown cells in the connective tissue and in digestive tubules and presence of parasites were assessed in the digestive gland following Villalba et al. (1997), Garmendia et al. (2011) and Bignell et al. (2012). The

prevalence of each alteration (number of individuals showing each pathology divided by the number of individuals of each group) was calculated as percentage.

2.9. Gamete development, gonad index and histopathology of gonad

Mantle of the same animals used for the histopathological analysis of the digestive gland were dissected out and processed following the standard protocol for histology described before.

Sex ratio, gamete developmental stages and gonad index (GI) were determined. Six gamete stages were distinguished (Seed, 1969) and a gonad index (GI) value, ranging from 0 (resting gonad) to 5 (mature gonad), was assigned to each developmental stage as in Chapter 1, adapted from Kim et al. (2006).

Oocyte atresia and necrosis, fibrosis, hemocytic infiltration, aggregation of brown cells, and occurrence of parasites were also assessed in gonads following Ortiz-Zarragoitia & Cajaraville (2006). Prevalences were calculated as for the digestive gland. In addition, intensity of oocyte atresia was assessed using a semiquantitative scale: 0- normal gonad, 1- less than a half of follicles are affected, 2- about half of follicles are affected, 3- more than half of follicles are affected and 4- all follicles are affected (Kim et al., 2006). Intensity was calculated as Sp/NH, where Sp is the score corresponding to the intensity of atresia and NH is the number of specimens with atresia (Garmendia et al., 2011).

2.10. Whole organism responses

Condition index was assessed according to Navarro et al. (1991). Soft tissues of 7 animals per tank were excised from the shells, dried at 80°C for 24 h and weighted. Afterwards, mussel shell lengths were recorded with a Vernier caliper and condition index was calculated as tissue dry weight (g) / [shell length (cm)]^3.

2.11. Data analysis

Statistical analyses were carried out with the aid of the statistical package SPSS 24 (IBM Analytics, Armonk, NY), and the significance level was 0.05. All data sets were tested for normality and homogeneity of variance using Kolmogorov-Smirnov´s and Levene's tests,

respectively. Normally distributed data, which met the assumptions of homogeneity of variances, were assessed via one-way ANOVA. When significant differences were found, the Tukey's post-hoc test was used to identify significant different treatments. Data which did not met the above assumptions were analyzed by the one-way Kruskal-Wallis test, followed by the Dunn's post-hoc test when significant differences were found. For histopathological data expressed as percentages, the X^2 test was used (Ruiz et al., 2014). When no differences were found between the two replicate tanks, data sets were mixed and displayed as: Control, GO, GO+BaP, BaP. However, when differences were found between replicates, data sets were maintained separate and displayed as: Control R1, Control R2, GO R1, GO R2, GO+BaP R1, GO+BaP R2, BaP R1, BaP R2.

3. RESULTS

3.1. Bioaccumulation of BaP

BaP concentration in control mussels and in mussels exposed to GO was below the detection limit (Table 1). BaP was bioaccumulated in mussels exposed to GO+BaP (23-28 ng/g dry weight), but especially in mussels exposed to BaP (18400-18700 ng/g dry weight) (Table 1). In water, BaP was detected only in the tanks exposed to BaP alone.

Table 1: Bioaccumulation of BaP in mussel soft tissues (ng/g dry weight) in control mussels and in mussels exposed to GO, GO+BaP, and BaP for 7 days. N = number of mussels is indicated. LoQ = Limit of Quantification: 5 ng/g dry weight.

Control		**GO**		**GO+BaP**		**BaP**	
R1 N= 14	R2 N= 18	R1 N= 16	R2 N= 14	R1 N= 14	R2 N= 17	R1 N= 15	R2 N= 14
<LoQ	<LoQ	<LoQ	<LoQ	23	28	18700	18400

3.2. Determination of graphene oxide in mussel tissues and feces

GO was detected only in the lumen of the digestive tract of mussels exposed to both GO and GO+BaP (Figure 2), indicating that even if GO was internalized, it was not accumulated in the rest of mussel tissues after 7 days of exposure. Accordingly, GO was detected in feces of mussels exposed to GO and GO+BaP from day one of exposure (Figure S1). Spectra of microalgae *Isochrysis galbana*, BaP stock solution and DMSO were not observed in mussel tissues or feces.

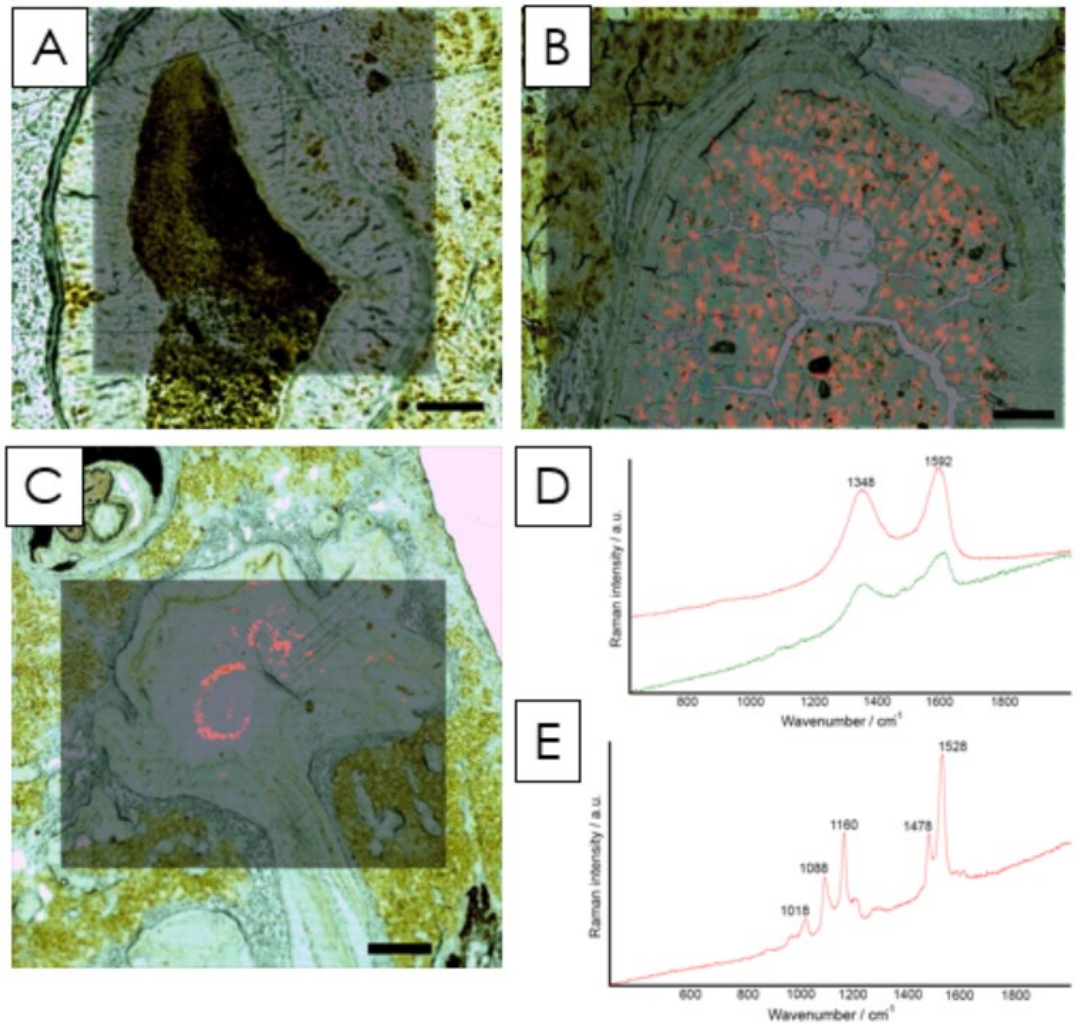

Figure 2: A-C: Heat maps showing the detection of graphene oxide (GO) in cryostat sections of the digestive gland of different mussels; A: Control mussel, B: mussel exposed to GO for 7 days, C: mussel exposed to GO+BaP for 7 days. D: Raman spectra from the zones highlighted in red in map B (green) and the spectrum obtained for the GO stock (red). E: Raman spectrum from the map in A. Scale bars: A and B : 100 µm and C: 500 µm.

3.3. Cellular biomarkers in hemocytes

Viability of hemocytes decreased in mussels exposed to GO+BaP and BaP in comparison to controls (Figure 3A). No differences were observed among groups in the activity of catalase (Cat) (Figure 3B).

Regarding genotoxicity, higher micronuclei frequency was observed in hemocytes of mussels exposed to GO and GO+BaP in comparison to controls (Table 2, Figure 3D, G). In addition, higher frequency of nuclear buds was observed in hemocytes of mussels exposed to GO than in control mussels (Table 2, Figure 3E, H). No differences were observed among groups in binucleated cells (Table 2, Figure 3J) and binucleated cells with a nucleoplasmic bridge (Table 2, Figure 3 F, I).

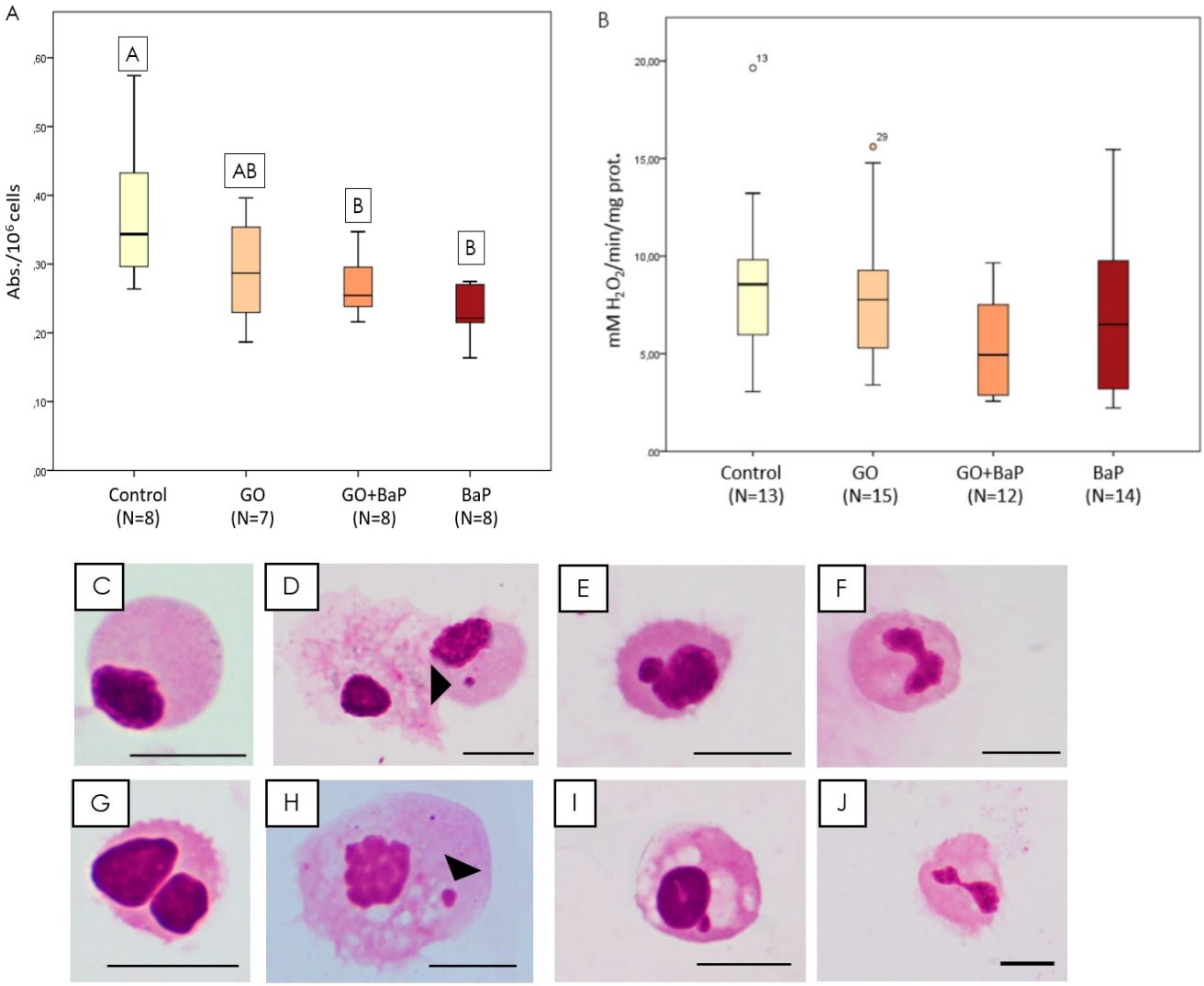

Figure 3: A: Neutral red uptake (given as absorbance/10^6 cells); B: catalase activity (given as mM H_2O_2/min/mg prot) in hemocytes of control mussels and in mussels exposed for 7 days to GO, GO+BaP and BaP . Box-plots show median value (horizontal line), 25%-75% quartiles (box) and standard deviation (whiskers). Dots denote outliers. Letters indicate significant differences among treatments (one-way ANOVA with Tukey's post-hoc, $p<0.05$); C-J: Light micrographs of mussel hemocytes during the micronucleus assay showing C) normal hemocyte of a control mussel; D) hemocyte of a mussel exposed to GO showing a micronucleus (arrow); E) hemocyte of a mussel exposed to GO showing a nuclear bud; F) binucleated cell with nucleoplasmic bridge of a mussel exposed to GO; G) binuclear hemocyte of a mussel exposed to BaP; H) hemocyte of a mussel exposed to GO+BaP showing a micronucleus (arrow); I) hemocyte of a mussel exposed to GO+BaP showing a nuclear bud; J) binucleated cell with nucleoplasmic bridge of a mussel exposed to GO+BaP. Scale bar: 10 µm.

Table 2: Frequency (‰) of micronuclei, binucleated cells, binucleated cells with nucleoplasmic bridges and nuclear buds in control mussels (N=8) and mussels exposed for 7 days to GO (N=7), GO+BaP (N=6) and BaP (N=8). Letters denote statistical differences among groups ($p<0.05$ after Kruskal-Wallis test followed by Dunn's post-hoc).

	Micronuclei	Binucleated cells	Binucleated cells with nucleoplasmic bridges	Nuclear buds
Control	0^{A}	0.125 ± 0.35	2.38 ± 2.67	2.63 ± 2.13 ^{A}
GO	1.86 ± 1.35 ^{B}	0.14 ± 0.38	5.43 ± 2.51	8.71 ± 2.93 ^{B}
GO+BaP	3.67 ± 3.08 ^{B}	0.50 ± 0.55	6.33 ± 2.58	7.17 ± 1.72 ^{AB}
BaP	0.88 ± 0.83 ^{AB}	0.63 ± 0.52	3.88 ± 2.23	5.88 ± 1.73 ^{AB}

3.4. Enzyme activities in mussel tissues

There were statistically significant differences in the activity of acetylcholinesterase (AChE) between replicates and thus, data were treated separately (Figure 4A). Activity of AChE was lower in one of the replicates exposed to GO+BaP (R1) and in both replicates exposed to BaP in comparison to one of the control replicates (R1) (Figure 4A). Inhibition of isocitrate dehydrogenase (IDH) was observed in mussels exposed to BaP in comparison to mussels exposed to GO and GO+BaP (Figure 4B). Similarly, inhibition of Glutathione-S-Transferase (GST) was observed in the digestive gland of mussels exposed to GO+BaP and BaP in comparison to control mussels (Figure 4C), while no response was observed in gills (Figure S2A).

Regarding antioxidant enzymes, induction of Cat activity was observed in the digestive gland of mussels exposed to GO+BaP in comparison to controls (Figure 5A), but no response was observed in gills (Figure S2B). No differences were found in the activity of glutathione peroxidase (GPx) in the digestive gland (Figure S2C), but inhibition was observed in gills of mussels exposed to GO in comparison to mussels exposed to BaP (Figure 5B).

Superoxide dismutase (SOD) was inhibited in the digestive gland of mussels exposed to BaP in comparison to control mussels and mussels exposed to GO+BaP, while induction of SOD was observed in mussels exposed to GO+BaP in comparison to mussels exposed to GO and BaP (Figure 5C). However, no clear trend was observed in gills (Figure S2C).

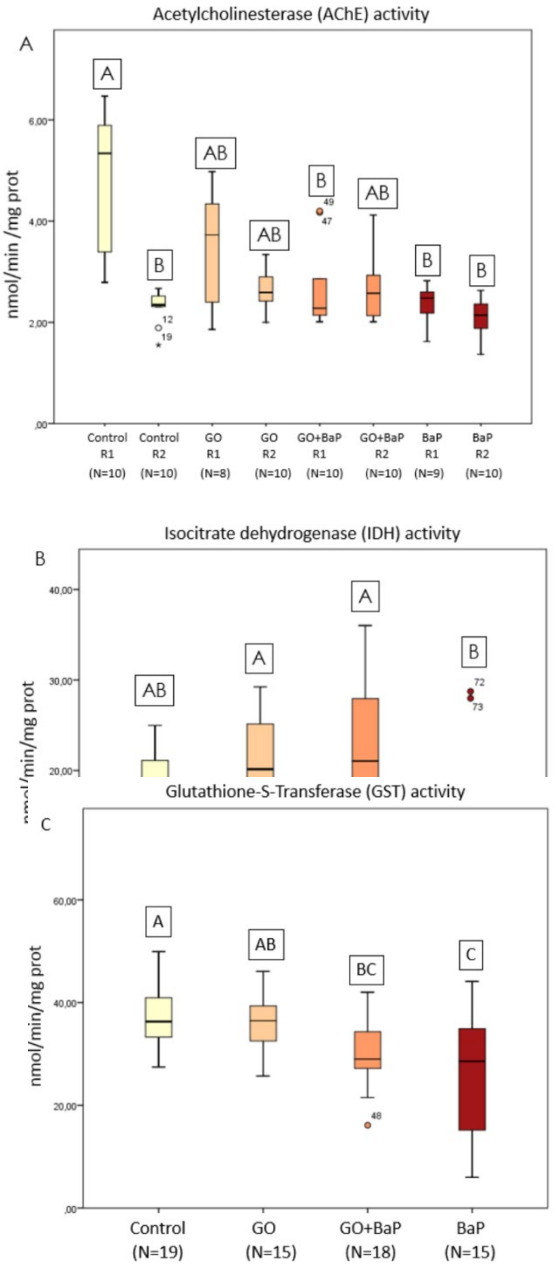

Figure 4: Acetylcholinesterase (AChE) activity in the aductor muscle (given as nmol/min/mg prot);B) Isocitrate dehydrogenase (IDH) activity in the digestive gland (given as nmol/min/mg prot); C)Glutathione-S-Tramsferase (GST) activity in the digestive gland (given as nmol/min/mg prot) control mussels and in mussels exposed for 7 days to GO, GO+BaP and BaP. Box-plots show median value (horizontal line), 25%-75% quartiles (box) and standard deviation (whiskers). Dots denote outliers. Letters denote statistical differences among means (Kruskal-Wallis test followed by Dunn's post-hoc in AChE and GST and one-way ANOVA followed by Tukey's post-hoc in IDH,, $p<0.05$).

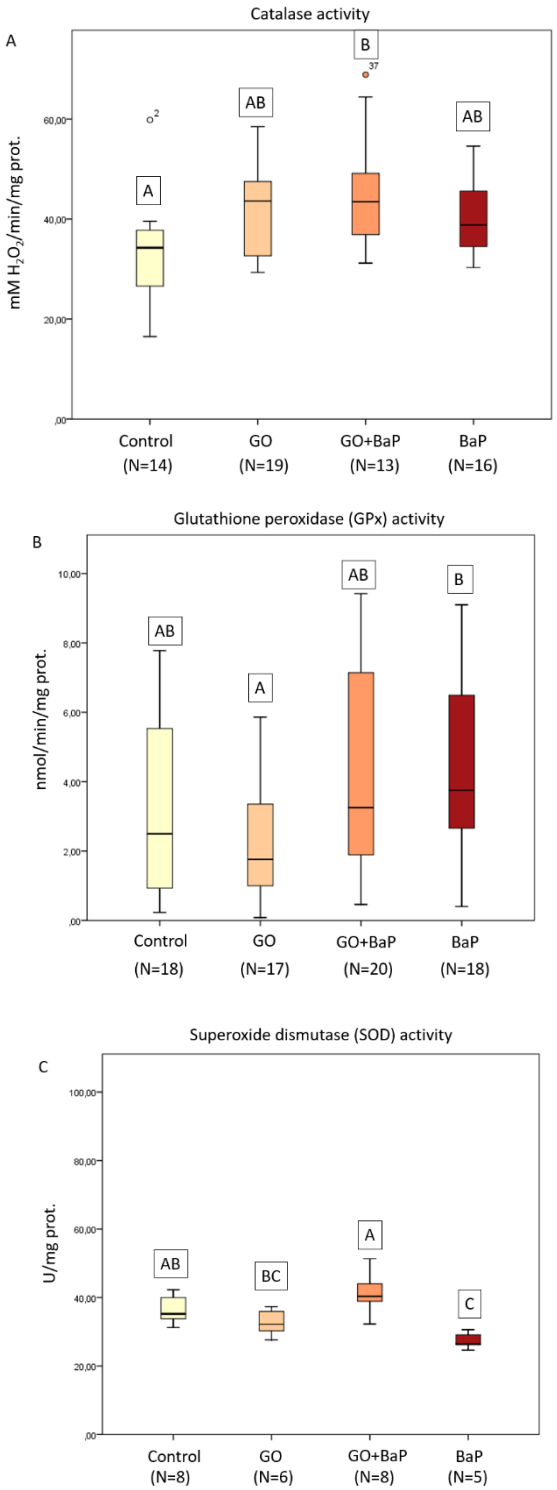

Figure 5: Catalase (Cat) activity in the digestive gland (given as mM H_2O_2/min/mg prot); B: Glutathione Peroxidase (GPx) activity in gills (given as nmol/min/mg prot); C: Superoxide dismutase (SOD) activity in the digestive gland (U/mg prot) of control mussels and in mussels exposed for 7 days to GO, GO+BaP and BaP. Box-plots show median value (horizontal line), 25%-75% quartiles (box) and standard deviation (whiskers). Dots denote outliers. Letters denote statistical differences among means (one-way ANOVA followed by Tukey's post-hoc in Cat and SOD, Kruskal-Wallis test followed by Dunn's post-hoc in GPx, $p<0.05$).

3.5. Histopathology of digestive gland

Statistical differences were found between replicates for some histopathological alterations. In those cases data sets for the two replicates were treated separately (Table 3). Fibrosis (Figure 6A) was widespread in all mussels including controls. All groups showed high prevalences, significantly higher in BaP R1 than in GO R1 (Table 3). Prevalence of hemocytic infiltration (Figure 6B) was similar in control R2 and all exposure groups but it was significantly higher in the GO R2 group than in control R1 (Table 3). Overall, aggregation of brown cells (Figure 6C, D) were more frequent in exposed groups than in controls, at least in one of the replicates (Table 3). Aggregation of brown cells in the connective tissue was significantly higher in mussels exposed to GO, GO+BaP and BaP than in controls (Table 3) while in the digestive tract epithelium, it was significantly higher in GO R2 and GO+BaP R1 than in control R1 (Table 3). In addition, aggregation of brown cells in the digestive tract epithelium was significantly higher in GO+BaP R1 than in GO R1 (Table 3).

Areas of necrosis of digestive tubule epithelium were found in both control and exposed mussels. Prevalence of necrosis was significantly higher in GO+BaP R2 and BaP R2 compared to control R2 (Table 3). Necrosis of digestive tubule epithelium appeared to be associated to the occurrence of an intracellular ciliated protozoan. It was found in the digestive epithelium of mussels of all experimental groups, with its highest prevalence in controls, especially in comparison to mussels exposed to BaP (Table 3). In addition, the protozoan *Nematopsis* sp. was the most common parasite in the digestive gland. It appeared in the connective tissue of almost all mussels, with high prevalences in all the replicates (Table 3). Other parasites such as *Mytilicola intestinalis* were also observed in the digestive gland of some mussels, but with low prevalences (Table 3).

Table 3: Prevalence of histopathological alterations in the digestive gland of both replicates (R1 and R2) of control mussels and mussels exposed to GO, GO+BaP and BaP for 7 days. Data are shown in percentages of 10 mussels per experimental replicate tank. Letters denote statistical differences for each alteration (X^2 test, p<0,05).

		Inflammatory responses				Parasites		
	Fibrosis	**Hemocytic infiltration**	**Brown cells in the connective tissue**	**Brown cells in the digestive tract epithelium**	**Necrosis of digestive tubule epithelium**	**Intracellular ciliated protozoan**	***Nematopsis sp.***	***Mytilicola intestinalis***
Control R1	90 ^{AB}	10 ^{A}	0 ^{A}	10 ^{A}	50 ^{AB}	80 ^{A}	80	10
Control R2	90 ^{AB}	40 ^{AB}	30 ^{A}	30 ^{ABC}	80 ^{A}	70 ^{A}	100	20
GO R1	80 ^{A}	50 ^{AB}	60 ^{B}	20 ^{AB}	50 ^{AB}	60 ^{AB}	90	10
GO R2	60 ^{AB}	60 ^{B}	60 ^{B}	60 ^{CB}	60 ^{AB}	30 ^{AB}	100	0
GO+BaP R1	90 ^{AB}	40 ^{AB}	60 ^{B}	70 ^{C}	60 ^{AB}	60 ^{AB}	80	20
GO+BaP R2	90 ^{AB}	50 ^{AB}	40 ^{B}	20 ^{AB}	30 ^{B}	40 ^{AB}	80	10
BaP R1	100 ^{B}	40 ^{AB}	70 ^{B}	10 ^{A}	80 ^{A}	40 ^{B}	90	10
BaP R2	90 A^{B}	50 ^{AB}	60 ^{B}	30 ^{ABC}	20 ^{B}	40 ^{B}	70	20

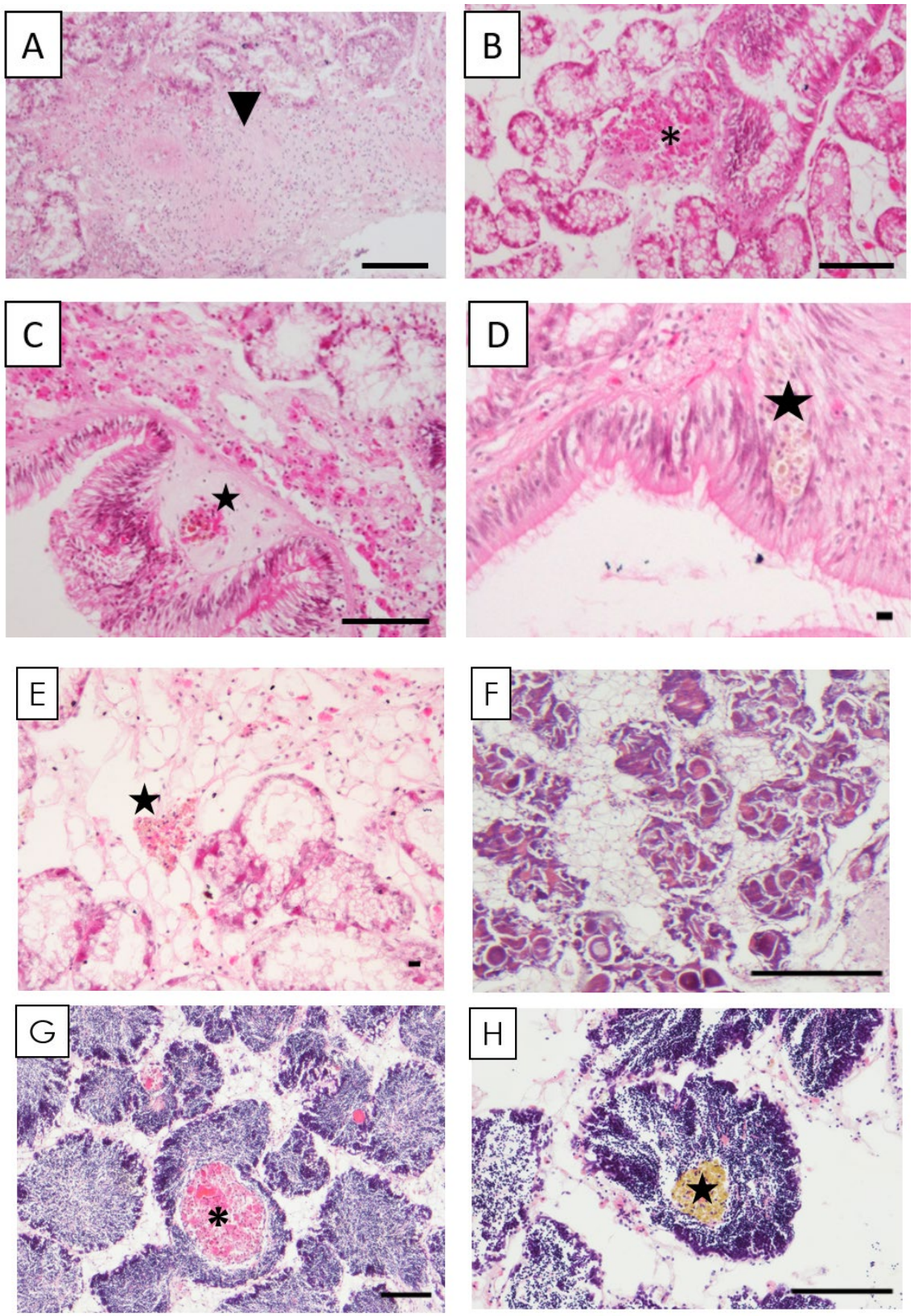

Figure 6: Light micrographs of mussel paraffin sections showing histopathological alterations in mussels digestive gland and gonads: A) mussel after 7 days of exposure to GO+BaP showing fibrosis in the connective tissue (arrow head); B) mussel after 7 days of exposure to GO+BaP showing hemocytic infiltration (*); C) mussel after 7 days of exposure to GO showing aggregation of brown cells in the epithelium of the digestive tract (star); D) mussel after 7 days of exposure to GO+BaP showing aggregation of brown cells in the epithelium of the digestive tract (star); E) mussel after 7 days of exposure to GO showing aggregation of brown cells in the connective tissue (star); F) mussel after 7 days of exposure to GO+BaP showing oocyte atresia; G) mussel after 7 days of exposure to BaP showing hemocytic infiltration within a male follicle (*); H) mussel after 7 days of exposure to BaP showing aggregation of brown cells within a male follicle (star). Scale bar: A, B, C, G, H: 100 µm; D,E: 10 µm; F: 500µm.

3.6. Gamete development, gonad index and histopathology of mussel gonad

Mussels from different groups were in a similar gamete development stage. Spawning was the predominant stage (Figure S3) as expected for the experimental period. There were no differences in the sex ratio and gonad index among groups (Figure S3).

Fibrosis (Figure 6F), hemocytic infiltration (Figure 6G) and aggregation of brown cells (Figure 6H) were widely observed in the gonad of both control and exposed mussels. Prevalence of fibrosis was significantly higher in BaP R2 mussels than in Control R2 mussels (Table 4). Hemocytic infiltration occurred both in the connective tissue and within the gonad follicles and prevalences were higher in GO+BaP R1 and BaP R2 than in both control replicates and in GO R1 (Table 4). Aggregation of brown cells, both in the connective tissues and gonad follicles, was higher in mussels exposed to GO and to BaP than in controls (Table 4). However, the main histopathological alteration observed was oocyte atresia (Figure 6F) with prevalences over 75% in all control and exposed groups (Table 4). Control mussels showed low intensity of atresia which can be linked to the developmental stage of the gonad (Table 4, Figure S3). On the other hand, stages 2 and 3 of oocyte atresia were only recorded in exposed mussels and the highest intensity was found in mussels exposed to GO+BaP (Table 4). *Nematopsis sp*. protozoan was found in the connective tissue of the gonad of almost all mussels (Table 4).

3.7. Whole organism responses

No differences were recorded among groups in mussel condition index (Figure S4).

Table 4: Prevalence of histopathological alterations in gonad of both replicates (R1 and R2) of control mussels and mussels exposed to GO, GO+BaP and BaP for 7 days. Data are shown in percentages of 10 mussels per replicate tank, except for atresia and oocyte necrosis, which were calculated based on the number of females in each group (Figure S3). The intensity of oocyte atresia is given by an index calculated as the average of the intensities based on a scale from 0 to 4. Letters denote statistical differences for each alteration (X^2 test, p<0,05).

	Fibrosis	**Inflammatory responses**		**Oocyte atresia**		**Parasites**
		Hemocytic infiltration	**Aggregation of brown cells**	**Prevalence**	**Intensity**	***Nematopsis sp.***
Control R1	44.44 ^{AB}	44.44 ^{BC}	22.22 ^{A}	100	1 ^{A}	88.89
Control R2	30 ^{A}	40 ^{BC}	30 ^{A}	100	1 ^{A}	80
GO R1	60 ^{AB}	30 ^{C}	50 ^{BC}	100	1 ^{A}	70
GO R2	44.44 ^{AB}	77.78 ^{ABC}	66.67 ^{BC}	100	1.4 ^{AB}	55.56
GO+BaP R1	44.44 ^{AB}	88.89 ^{AE}	33.33 ^{ABC}	100	1.43 ^{B}	66.67
GO+BaP R2	66.67 ^{AB}	55.56 ^{ABC}	33.33 ^{ABC}	100	1.75 ^{B}	66.67
BaP R1	60 ^{AB}	50 ^{ABC}	50 ^{B}	75	0.75 ^{A}	80
BaP R2	77.78 ^{B}	100 ^{DE}	33.33 ^{B}	100	1.33 ^{A}	88.89

4. DISCUSSION

In this work, the toxic effects of short-term (7 days) exposure to GO alone (500 µg/L) and to GO with sorbed BaP (500 µg/L GO incubated with 100 µg/L BaP) has been assessed using a wide selection of biological responses, from molecular to organism levels. For comparison, the effects of exposure to BaP alone at a concentration of 96.7 µg/L, equivalent to that sorbed in GO+BaP preparations (Martínez-Álvarez et al., 2021), were also assessed. In parallel, the fate of GO nanoplatelets in mussels was studied by Raman spectroscopy, as well as BaP bioaccumulation.

After 20 hours of exposure, BaP or GO could not be detected in the water of tanks exposed to GO+BaP, suggesting that mussels had uptaken the GO nanoplatelets with sorbed BaP. Little is known about the desorption dynamics of PAHs from GO and other GFNs in the marine environment. In aqueous solutions, adsorption of phenanthrene into magnetic graphene is mostly irreversible (Huang et al., 2019). The stability of GO with sorbed BaP could explain that BaP was undetectable in water in GO+BaP tanks as mussels would internalize BaP adsorbed into GO nanoplatelets. However, the concentration of BaP bioaccumulated in mussels was much lower in mussels exposed to GO+BaP compared to those exposed to dissolved BaP. Sanchis et al. (2016) reported that the Trojan horse effect is more likely to occur with organic pollutants that present an intermediate affinity to carbon-based NMs, than with non polar compounds showing aromatic rings such as BaP, as the most non polar compounds would be irreversibly bound to the carbon-based NMs decreasing their bioavailability. Alternatively, it could be that BaP bioaccumulation was low in mussels exposed to GO+BaP because of the excretion of GO nanoplatelets with sorbed BaP. This idea is supported by the detection of GO in feces of mussels exposed to GO and to GO+BaP.

At studying the stability of GO in tanks with and without oysters, Khan et al. (2019a; 2019b) concluded that the animals were actively removing the GO from the water, in line with our results. Filtration is the common pathway for the internalization of different NMs during the feeding process of filter-feeding organisms such as mussels. After a first contact with the gills, NM aggregates are ingested and, depending on their size, they can be accumulated in the digestive gland and/or translocated to hemolymph and then distributed to other organs (Faggio et al., 2018). In the present work GO was

not detected in gills, probably due to the short contact between GO and gills. This could explain the lack of effects on enzyme activities studied in gills of mussels exposed to GO and GO+BaP in comparison to controls. Presence of GO was confirmed through Raman spectroscopy in the lumen of the digestive tract and feces of mussels exposed to both GO and GO+BaP, suggesting that GO tends to accumulate in organs related with food intake, as previously reported by Josende and colleagues (Josende et al., 2020). The presence of GO in the digestive tract has been previously reported in exposures to other aquatic invertebrates, such as nematodes (Bortolozzo et al., 2021) and crustaceans (Mesaric et al., 2015; Zhu et al., 2017; Lu et al., 2018; Souza et al., 2018; Zhang. et al., 2019; Josende et al., 2020), but not in bivalves. To the best of our knowledge this is the first time that the presence of GO in the digestive tract of bivalves was confirmed through Raman spectroscopy. As the digestive gland is one of the most important organs in mussels, responsible for intracellular digestion and also for antioxidant defense and pollutant sequestration and detoxification, significant damages in this organ could lead to impact at the organism level (Moore et al., 2013; 2021; Faggio et al., 2018). GO could then be translocated from the digestive system to the rest of organs (Ren et al., 2016; Chatterjee et al., 2017). However, Bortolozzo et al. (2021) observed that carboxyl groups in GO edges can avoid permeability of GO nanoplatelets through the intestine in nematodes. This could explain the presence of GO in feces after each digestive cycle and the absence of GO out of the digestive tract in this work, although there is yet no conclusive data on the distribution and excretion strategies for GFNs inside animal bodies (Ou et al., 2016).

Even though GO was not detected in hemocytes by Raman spectroscopy, cytotoxicity occurred in hemocytes of mussels exposed to GO+BaP and BaP with respect to controls. Further, genotoxic effects were observed in hemocytes of mussels exposed to GO and GO+BaP in comparison to controls. DNA damage has been previously reported in other organisms exposed to GO (Dziewiecka et al., 2017; 2018; Flasz et al., 2020; Zhao et al., 2021), but there is a single work reporting genotoxicity of GFNs to mussels (Meng et al., 2020). Genotoxicity may be provoked by the physical damage caused by nanoplatelets and/or through oxidative stress (Lalwani et al., 2016; Khan et al., 2019b). In most publications the comet assay has been used to measure genotoxicity after exposure to

GFNs, but DNA strand breaks determined by the comet assay can be reversible (Cajaraville et al., 2003). Flaasz et al. (2020) reported that DNA damage measured in crickets *Acheta domesticus* by the comet assay after 5 and 25 days of GO exposure was completely reversed after 10 days of depuration. On the other hand, micronuclei frequency measured in this work assesses DNA damage that remains after cell division (Cajaraville et al., 2003; Ou et al., 2016). Thus, the increased occurrence of micronuclei in hemocytes of mussels exposed to GO+BaP and of nuclear buds in those exposed to GO acquires a great environmental relevance.

Due to its link with genotoxicity, oxidative stress is one of the most studied biomarkers after organism exposure to GO. In this work no differences in hemocyte Cat activity were observed among exposure groups. This could be because exposure was not enough to induce hemocyte Cat activity or because the antioxidant system of hemocytes already reached its maximum after 7 days of exposure. Many antioxidant enzymes follow a bell-shaped curve whereby activation of the synthesis of a specific enzyme causes an initial increase in the activation of the enzyme followed by its decrease, caused by the increased catabolic rate or direct inhibitory effects of toxic chemicals on the enzyme molecules (Viarengo et al., 2007). The fact that viability was reduced in hemocytes of mussels exposed to GO+BaP supports the idea that probably after 7 days of exposure hemocytes were not able to overcome ROS production by inducing Cat activity, thus leading to oxidative stress and non-reversible DNA damage in hemocytes.

In agreement with the occurrence of GO in the lumen of the digestive tract in mussels exposed to GO and GO+BaP, the digestive gland was more sensitive than the gills in terms of effects on biotransformation (GST) and antioxidant enzyme activities Cat and SOD. Inhibition of GST and induction of Cat enzyme activities were observed in the digestive gland of mussels exposed to GO+BaP with respect to the controls. Similarly, the activity of SOD was induced in the digestive gland of mussels exposed to GO+BaP compared to those exposed to GO. Barranger et al. (2019a; 2019b) and Moore et al. (2021) also reported a higher impact in terms of altered enzyme activities in the digestive gland in comparison to the rest of organs in mussels exposed to carbon-based NMs and BaP. Furthermore, it has been reported that Cat and SOD are related to each other and can be activated by BaP exposure alone or in combination with other

pollutants (Chen et al., 2018). In the present study, exposure to dissolved BaP provoked inhibition of GST, SOD and AChE with respect to controls, and also inhibition of IDH with respect to GO and GO+BaP groups and induction of gill GPx with respect to GO groups. These results suggest that effects observed in mussels exposed to GO+BaP could be at least partially due to BaP carried out by GO nanoplatelets to mussels.

In the case of mussels exposed to GO alone, there were no alterations in the enzyme activities related to neurotoxicity, aerobic metabolism, biotransformation or oxidative stress in comparison to control mussels. There are no conclusive results related to the oxidative stress caused by GFNs in bivalves yet. For example, in the study of Copppola et al. (2020) after 28 days of exposure of mussels to GO functionalized with polyethyleneimine (GO-PEI), activities of SOD, CAT and GPx were induced with respect to controls. However, such results were not reproduced in a subsequent report by Coppola et al. (2021). Many works have pointed out that the complex toxicity profiles of GFNs could be related to the reactivity of nanoplatelets used in each study, which depend on the specific molecular structure of the surface of the nanoplatelets and especially on their oxygen content (Katsumiti et al., 2017; Malina et al., 2020; Peng et al., 2020; Bortolozzo et al., 2021). Small variations in the structure of GO, which are inevitable during the production of different batches, would alter its toxicity.

At tissue level, impact of graphene (Meng et al., 2019) and GO-PEI (Coppola et al., 2020) have been previously reported in terms of loss of tissue and digestive tubule atrophy, respectively. Bi et al. (2022) also reported thinning of the digestive tubule epithelium and loss of digestive cells in clams *Corbicula fluminea* after 28 days of exposure to GO. In the present study, a high prevalence of necrosis of the digestive tubule epithelium was found, possibly due to the widespread occurrence of an intraepithelial ciliated protozoan parasite, but prevalence significantly increased in one GO+BaP replicate and one BaP replicate compared to one control replicate. Most importantly, non-specific inflammatory responses such as hemocytic infiltration and accumulation of brown cells in the connective tissue and digestive tract epithelium of the digestive gland were found in mussels exposed to GO and GO+BaP, as well as in mussels exposed to BaP for brown cells in the digestive gland connective tissue. Similarly, non-specific inflammatory responses have been reported in multiple cell lines (Chen et al., 2012b), fishes (Chen et

al., 2020) and oysters (Khan et al., 2019) after exposure to GO. Acute inflammation responses and chronic injury could interfere with normal physiological functions in organs (Ou et al., 2016). Therefore, long-term exposure experiments of bivalves to GO alone and with associated pollutants, including a recovery period, are necessary to decipher whether these damages are reversible or not.

Similar to results in the digestive gland, prevalence of non-specific hemocytic infiltration increased in the gonad of mussels exposed to GO+BaP in comparison to controls and GO, and in one BaP replicate compared to controls, GO+BaP and GO exposure groups. Prevalence of brown cell aggregations was also higher in the gonad of mussels exposed to GO and BaP compared to controls. Further, a higher intensity of oocyte atresia was observed in mussels exposed to GO+BaP in comparison to controls and mussels exposed to BaP. The appearance of atresia in early gametogenic stages has been related with the presence of pollutants such as PAHs in mussels (Aarab et al., 2004; Ortiz-Zarragoitia & Cajaraville, 2006; Baussant et al., 2011). BaP exposure can cause alterations in sex hormones, disintegration of cell membranes, DNA damage, inhibition of ovarian development and increment of atretic follicles in bivalves (Jing-Jing et al., 2009; Yang et al., 2020; 2021). Moreover, developing and mature stages of the gonad are the most susceptible to BaP exposure (Yang et al., 2020). In addition, GO can also provoke degenerative effects in gonads. Bi et al. (2022) reported that clams exposed to GO alone or in combination to perfluorooctane sulfonate (PFOS) showed smaller oocytes. Dziewiecka et al. (2018) suggested that GO might cause degenerative changes in the female gonad due to its sharp edges, although in the present work direct interaction of nanoplatelets with oocytes was unlikely, according to Raman results. In summary, the most severe atresia observed in mussels exposed to GO+BaP was possibly a result of synergistic effects of both GO nanoplatelets and adsorbed BaP.

Neurotoxicity was observed in terms of inhibited AChE activity in mussels exposed to one GO+BaP replicate in comparison to control mussels and in those exposed to BaP in comparison to controls. While it is known that BaP can display neurotoxic effects on bivalves (Banni et al., 2010; Kamel et al., 2012; Chen et al., 2018; Guo et al., 2021), the neurotoxic potential of GFNs is not clear. Alterations of AChE activity and several neurotransmitters have been observed in bivalves and fishes exposed to different GFNs

(Ren et al., 2016; Hu et al., 2017; Coppola et al., 2020), whereas the opposite has also been reported (Audira et al., 2021; Coppola et al., 2021; Urban-Malinga et al., 2021).

Overall, in this work the toxicity of GO+BaP appeared to be explained by effects of GO for certain biological responses (genotoxicity and non-specific inflammatory responses in digestive gland and gonad) and by effects of BaP carried by GO for other responses (decrease in hemocyte viability, changes in enzyme activities and inflammatory and degenerative alterations in digestive gland and gonad) (Figure 7). Most of the alterations observed after BaP exposure have been previously reported: decrease in hemocyte viability (Ding et al., 2020), inhibition of AchE activity (Banni et al., 2010; Kamel et al., 2012), inhibition of GST in digestive gland (Cheung et al., 2004; Wang et al., 2006) and histopathological damage in gonad (Jing-Jing et al., 2009; Yang et al., 2020; 2021). On the other hand, in some biomarkers impact was only observed in mussels exposed to GO+BaP in comparison to the controls, which is taken to imply a synergistic effect between GO and BaP (Figure 7). This was the case of Cat induction in digestive gland and oocyte atresia. Finally, in other cases toxicity of GO+BaP was enhanced in comparison to GO and/or BaP (Figure 7). These results highlight the complexity of the Trojan horse effect of GFNs with sorbed BaP.

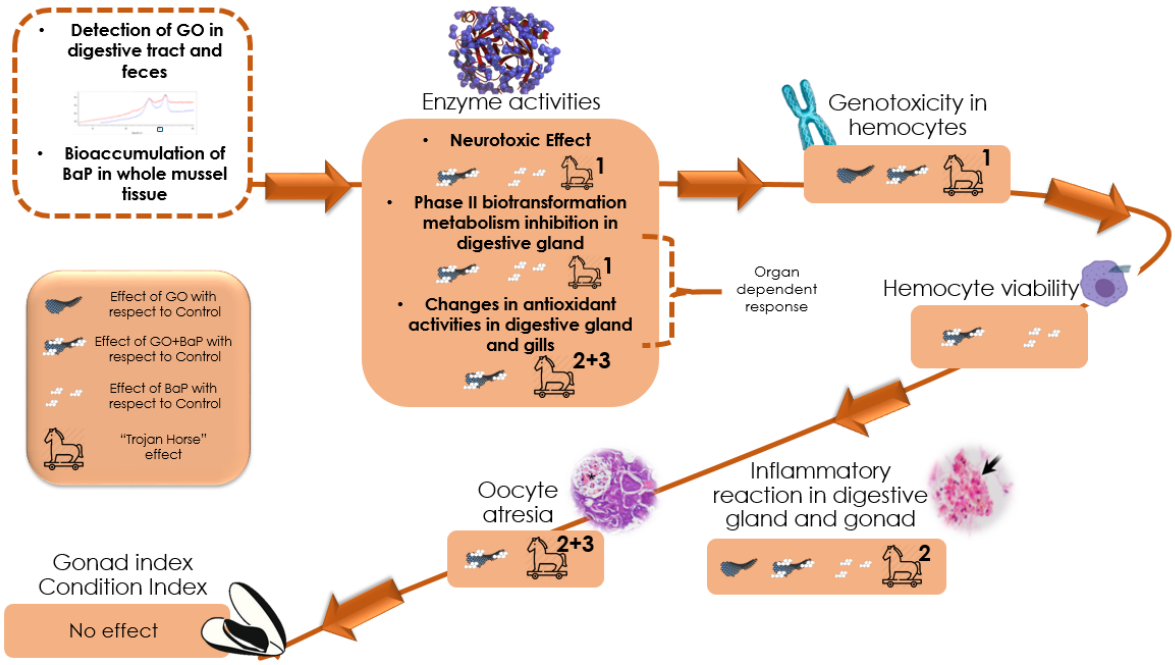

Figure 7. Summary of results obtained at different biological levels. Significant differences in comparison to the control and the Trojan horse effect are represented. The Trojan horse effect includes 1) effects of BaP carried onto GO nanoplatelets, 2) enhanced toxic effects of GO+BaP compared to GO and/or BaP alone, and 3) synergetic effects of GO+BaP that could not be attributted to either GO or BaP alone.

5. CONCLUSIONS

In conclusion, after a short exposure of 7 days to environmentally relevant concentrations of GO and GO with sorbed BaP, GO was observed in the lumen of the digestive tract and feces of mussels suggesting that GO was internalized via ingestion and rapidly excreted. BaP was bioaccumulated in mussels exposed to GO with sorbed BaP, pointing to a carrier role of GO towards BaP. However, the extent of BaP bioaccumulation was much higher in mussels exposed to BaP alone compared to those exposed to GO+BaP at equivalent exposure concentrations of BaP. Thus, it appeared that GO nanoplatelets protected mussels against BaP bioaccumulation, as reported in previous studies with other GFNs and BaP in mussels (Barranger et al., 2019a; 2019b; Moore et al., 2021). Regarding the toxicological impact of exposure to GO+BaP in mussels, complex patterns of interaction between GO and BaP emerged which differed depending on the biological endpoint studied. Some responses could be attributted to the effects caused by GO alone but most responses seemed to be due to a variety of Trojan horse effects, including 1) effects of BaP carried onto GO nanoplatelets, 2) enhanced toxic effects of GO+BaP compared to GO and/or BaP alone, and 3) synergistic effects of GO+BaP that could not be attributted to either GO or BaP alone. This work underlines the necessity of studying GFNs toxicity in combination with other pollutants. Experiments of exposure to single GFNs could lead to an underestimation of their possible impact in the environment, where these NMs would never appear alone. Further work is needed to address the potential hazard that GFNs may pose in the marine environment, particularly at long term.

ACKNOWLEDGEMENTS

This work was funded by Spanish MINECO (NACE project CTM2016-81130-R), Basque Government (consolidated research group IT1302-19 and IT1743-22, and predoctoral fellowship to NGS).

REFERENCES

Aarab N., Minier C., Lemaire S., Unruh E., Hansen P.D., Larsen B.K., Andersen O.K., Narbonne J.F. 2004. Biochemical and histological responses in mussel (*Mytilus edulis*) exposed to North Sea oil and a mixture of North Sea oil and alkylphenols. Marine Environment Research 58, 437–441.

Aebi H. 1984. Catalase *in vitro.* Methods in Enzymology 105, 121–126.

Ahmad S.Z.N., Salleh W.N.W., Ismail A.F., Yusof N., Yusop M.Z.M., Aziz F. 2020. Adsorptive removal of heavy metal ions using graphene- based nanomaterials: Toxicity, roles of functional groups and mechanisms. Chemosphere 248, 126008.

Apul O.G., Wang Q., Zhou Y., Karanfil T. 2013. Adsorption of aromatic organic contaminants by graphene nanosheets: Comparison with carbon nanotubes and activated carbon. Water research 47, 1648-1654.

Arvidsson R., Baun A., Furbe A., Hansen S.F., Molander S., 2018. Proxy measures for simplified environmental assessment of manufactured nanomaterials. Environmental Science & Technology 52, 13670-13680.

Arvidsson R., Molander S., Sandén B. A. 2013. Review of potential environmental and health risks of the nanomaterial graphene. Human and Ecological Risk Assessment: An International Journal 19, 873-887.

Audira G., Lee J.S., Siregar P., Malhotra N., Rolden M.J.M., Huang J.C., Chen K.H.C., Hsu H.S., Hsu Y., Ger T.R., Hsiao C.D. 2021. Comparison of the chronic toxicities of graphene and graphene oxide toward adult zebrafish by using biochemical and phenomic approaches. Environmental Pollution 278, 116907.

Avant B., Bouchard D., Chang X., Hsieh H.S., Acrey B., Han Y., Spear J., Zepp R., Knightes C.D. 2019. Environmental fate of multiwalled carbon nanotubes and graphene oxide across different aquatic ecosystems. NanoImpact 13, 1–12.

Banni M., Sforzini S., Arlt V. M., Barranger A., Dallas L. J., Oliveri C., Aminot Y., Pacchioni B., Milino C., Lanfranchi G., Readman J. W. 2017. Assessing the impact of benzo[a]pyrene on marine mussels: application of a novel targeted low density microarray complementing classical biomarker responses. PloS one 12, e0178460.

Banni M., Negri A., Dagnino A., Jebali J., Ameur S., Boussetta H. 2010. Acute effects of benzo[a]pyrene on digestive gland enzymatic biomarkers and DNA damage on mussel *Mytilus galloprovincialis*. Ecotoxicology and Environmental Safety 73, 842–848.

Barranger A., Langan L.M., Sharma V., Rance G.A., Aminot Y., Weston N.J., Akcha F., Moore M.N., Arlt V.M., Khlobystov A.N., Readman J.W., Jha A.N. 2019a. Antagonistic interactions between benzo[a]pyrene and fullerene (C60) in toxicological response of marine mussels. Nanomaterials 9, 87.

Barranger A., Rance G.A., Aminot Y., Dallas L.J., Sforzini S., Weston N.J., Lodge R.W., Banni M., Arlt V.M., Moore M.N., Readman J.W., Viarengo A., Khlobystov A.N., Jha A.N. 2019b. An integrated approach to determine interactive genotoxic and global gene expression effects of multiwalled carbon nanotubes (MWCNTs) and benzo[a]pyrene (BaP) on marine mussels: evidence of reverse 'Trojan Horse' effects. Nanotoxicology, 1, 1324–1343.

Baussant T., Ortiz-Zarragoitia M., Cajaraville M.P., Bechmann R.K., Taban I.C., Sanni S. 2011. Effects of chronic exposure to dispersed oil on selected reproductive processes in adult blue mussels (*Mytilus edulis*) and the consequences for the early life stages of their larvae. Marine pollution bulletin 62, 1437-1445.

Bi C., Junaid M., Liu Y., Guo W., Jiang X., Pan B., Li Z., Xu N. 2022. Graphene oxide chronic exposure enhanced perfluorooctane sulfonate mediated toxicity through oxidative stress generation in freshwater clam *Corbicula fluminea.* Chemosphere 297, 134242.

Bignell J., Cajaraville M.P., Marigómez I. 2012. Background document: histopathology of mussels (*Mytilus spp*.) for health assessment in biological effects monitoring. Integrated monitoring of chemicals and their effects. In: Davies, I. M., Vethaak, A. D. (Eds.), ICES Cooperative Research Report N. 315, Copenhagen, Denmark, 111-120.

Bolognesi C., Fenech M. 2012 Mussel micronucleus cytome assay. Nature protocols 7, 1125-1137.

Borenfreund E., Puerner J.A. 1985. Toxicity determined in vitro by morphological alterations and neutral red absorption. Toxicology Letters 24, 119–124.

Bortolozzo L.S., Coa F., Khan L.U., Medeiros A.M.Z., Da Silva G.H., Delite F.S., Strauss M., Martinez D.T.S. 2021. Mitigation of graphene oxide toxicity in *C. elegans* after chemical degradation with sodium hypochlorite. Chemosphere 278, 130421.

Bradford MM. 1976. A rapid and sensitive method for the quantitation of microgram quantities of protein utilizing the principle of protein-dye binding. Analytical Biochemistry 72, 248-254.

Britto R.S., Nascimento J.P., Serodre T., Santos A.P., Soares A.M.V.M, Furtado C., Ventura-Lima J., Monserrat J.M., Freitas R. 2021. Oxidative stress in *Ruditapes philippinarum* after exposure to different graphene oxide concentrations in the presence and absence of sediment. Comparative Biochemistry and Physiology, Part C 240, 108922.

Cajaraville M.P., Pal S.G. 1995. Morphofunctional study of the haemocytes of the bivalve mollusc *Mytilus galloprovincialis* with emphasis on the endolysosomal compartment. Cell Struct. Funct. 20, 355–367.

Cajaraville M.P., Hauser L., Carvalho G., Hylland K., Olabarrieta I., Lawrence AJ., Lowe D., Goksoyr A. 2003. Chapter 2: Links between genetic damage by xenobiotics at the individual level and the molecular /cellular response to pollution. In: Effects of Pollution on Fish: molecular effects and population responses. AJ LAWRENCE & KL HEMINGWAY (eds.), Blackwell Science Ltd, Oxford, pp 14-82.

Cancio I., Orbea A., Völkl A., Fahimi H.D., Cajaraville M.P. 1998. Induction of peroxisomal oxidases in mussels: comparison of effects of lubricant oil and benzo(a)pyrene with two typical peroxisome proliferators on peroxisome structure and function in *Mytilus galloprovincialis*. Toxicology and applied pharmacology 149, 64-72.

Chatterjee N., Kim Y., Yang J., Roca C.P., Joo S.W., Choi J. 2017. A system toxicology approach reveals the Wnt-MAPK crosstalk pathway mediated reproductive failure in *Caenorhabditis elegans* exposed to graphene oxide (GO) but not to reduced graphene oxide (rGO). Nanotoxicology 11, 1.

Chen D., Feng H., Li J. 2012a. Graphene oxide: preparation, functionalization, and electrochemical applications. Chemical reviews 112, 6027-6053.

Chen G.Y., Yang H.J., Lu C.H., Chao Y.C., Hwang S.M., Chen C.L., Lo K.W., Sung L.Y., Luo W.Y., Tuan H.Y., Hu Y.C. 2012b. Simultaneous induction of autophagy and toll-like receptor signaling pathways by graphene oxide. Biomaterials 33, 6559–6569.

Chen S., Qu M., Ding J., Zhang Y., Wang Y., Di Y. 2018. BaP-metals co-exposure induced tissue-specific antioxidant defense in marine mussels *Mytilus coruscus*. Chemosphere 205, 286–296.

Chen Z., Yu C., Khan I.A., Tang Y., Liu S., Yang M. 2020. Toxic effects of different-sized graphene oxide particles on zebrafish embryonic development. Ecotoxicology and Environmental Safety 197, 110608.

Cheung C.C.C., Siu W.H.L., Richardson B.J., Luca-Abbott S.B.D., Lam P.K.S. 2004. Antioxidant responses to benzo[a]pyrene and Aroclor 1254 exposure in the greenlipped mussel, *Perna viridis*. Environmental Pollution 128, 393–403.

Collins R. 2021. Graphene Market & 2D Materials Assessment 2021-2031. IDTechEx, 9781913899219.

Coppola F., Bessa A., Henriques B., Russo T., Soares A.M.V.M., Figueira E., Marques P.A.A.P., Polese G., Di Cosmo A., Pereira E., Freitas R. 2020. Oxidative stress, metabolic and histopathological alterations in mussels exposed to remediated seawater by GO-PEI after contamination with mercury. Comparative Biochemistry and Physiology -Part A : Molecular and Integrative Physiology 243, 110674.

Coppola F., Jiang W., Soares A.M.V.M., Marques P.A.A.P., Polese G., Pereira M.E., Jiang Z., Freitas R. 2021. How efficient is graphene-based nanocomposite to adsorb Hg from seawater. A laboratory assay to assess the toxicological impacts induced by remediated water towards marine bivalves. Chemosphere, 277, 130160.

De Marchi L., Pretti C., Gabriel B., Marques P. A., Freitas R., Neto V. 2018. An overview of graphene materials: Properties, applications and toxicity on aquatic environments. Science of the Total Environment 631, 1440-1456.

Di Y., Aminot Y., Schroeder D.C., Readman J.W., Jha A.N. 2017. Integrated biological responses and tissue-specific expression of p53 and ras genes in marine mussels following exposure to benzo(α)pyrene and C60 fullerenes, either alone or in combination. Mutagenesis 32, 77-90.

Di Y., Schroeder D.C., Highfield A., Readman J.W., Jha A.N. 2011. Tissue-specific expression of p53 and ras genes in response to the environmental genotoxicant benzo(α)pyrene in marine mussels. Environmental science & technology 45, 8974-8981.

Ding J., Chen S., Qu M., Wang Y., Di Y. 2020. Trophic transfer affects cytogenetic and antioxidant responses of the mussel *Mytilus galloprovincialis* to copper and benzo(α)pyrene. Marine Environmental Research 154, 104848.

Dong S., Xia T., Yang Y., Lin S., Mao L. 2018. Bioaccumulation of 14C-Labeled Graphene in an Aquatic Food Chain through Direct Uptake or Trophic Transfer. Environmental Science and Technology 52, 541−549.

Dreyer D.R., Park S., Bielawski C.W., Ruoff R.S. 2010. The chemistry of graphene oxide. Chemical Society Reviews 39, 228-240.

Duroudier N., Katsumiti A., Mikolaczyk M., Schäfer J., Bilbao E., Cajaraville M.P. 2019. Cell and tissue level responses in mussels *Mytilus galloprovincialis* dietarily exposed to PVP/PEI coated Ag nanoparticles at two seasons. Science of The Total Environment 750, 141303.

Dziewięcka M., Karpeta-Kaczmarek J., Augustyniak M., Rost-Roszkowska M. 2017. Short-term in vivo exposure to graphene oxide can cause damage to the gut and testis. Journal of Hazardous Materials 328, 80–89.

Dziewięcka M., Witas P., Karpeta-Kaczmarek J., Kwaśniewska J., Flasz B., Balin K., Augustyniak M. 2018. Reduced fecundity and cellular changes in *Acheta domesticus* after multigenerational exposure to graphene oxide nanoparticles in food. Science of the Total Environment 635, 947–955.

Ellis G., Goldberg D.M. 1971. An improved manual and semi-automatic assay for NADP-dependent isocitrate dehydrogenase activity, with a description of some kinetic properties of human liver and serum enzyme. Clinical Biochemistry 2, 175-185.

Ellman G., Courtney K., Andres V., Featherstone, R. 1961. A new and rapid colorimetric determination of acetylcholinesterase activity. Biochemical Pharmacology 7, 88–95.

Ersan G., Apul O. G., Perreault F., Karanfil T. 2017. Adsorption of organic contaminants by graphene nanosheets: A review. Water research 126, 385-398.

EU COM, Commission Recommendation of 18 October 2011 on the definition of nanomaterial Text with EEA relevance OJ L 275, 20.10.2011, p. 38–40 (EN). http://data.europa.eu/eli/reco/2011/696/oj

Faggio C., Tsarpali V., Dailianis S. 2018. Mussel digestive gland as a model tissue for assessing xenobiotics: An overview. Science of the Total Environment, 636, 220–229.

Flohé L., Günzler W.A. 1984. Assays of glutathione peroxidase. Methods in Enzymology 105, 114–121.

Gamble M., Wilson I. 2002. The hematoxylin and eosin. In: Bancroft, J.D., Gamble, M. (Eds.), Theory and Practice of Histological Techniques. Churchill Livingstone-Elsevier Science Ltd., London, IK. 125.

Garmendia L., Soto M., Vicario U., Kim Y., Cajaraville M.P., Marigómez I. 2011. Application of a battery of biomarkers in mussel digestive gland to assess long term effects of the Prestige oil spill in Galicia and Bay of Biscay: tissue-level biomarkers and histopathology. Journal of Environmental Monitoring 13, 915-32.

Gómez-Mendikute A., Etxeberria A., Olabarrieta I., Cajaraville M.P. 2002. Oxygen radicals production and actin filament disruption in bivalve haemocytes treated with benzo(a)pyrene. Marine environmental research 54, 431-436.

González-Soto N., Hatfield J., Katsumiti, A., Duroudier, N., Lacave, J. M., Bilbao, E., Orbea, A., Navarro, E., Cajaraville, M. P. 2019. Impacts of dietary exposure to different sized polystyrene microplastics alone and with sorbed benzo[a]pyrene on biomarkers and whole organism responses in mussels Mytilus galloprovincialis. Science of the Total Environment 684, 548-566.

Goodwin G.D.Jr., Adeleye A.S., Sung L., Ho K.T., Burgess R.M., Petersen E.J. 2018. Detection and Quantification of Graphene-Family Nanomaterials in the Environment. Environmental Science and Technology 52, 4491-4513.

Guilhermino L., Lopes M.C., Carvalho A.P., Soared A.M.V.M. 1996. Inhibition of acetylcholinesterase activity as effect criterion in acute tests with juvenile Daphnia Magna. Chemosphere 32, 727-738.

Habig W., Pabst M.J., Jakoby W.B. 1974. Glutathione S-Transferases, The first enzymatic step in mercapturic acid formation. The Journal of Biological Chemistry 249, 7130-7139

Han Y., Knightes C.D., Bouchard D., Zepp R., Avant B., Hsieh H.S., Chang X., Acrey B., Henderson W.M., Spear J. 2019. Simulating graphene oxide nanomaterial phototransformation and transport in surface water. Environmental Science: Nano 6, 180-194.

He K., Chen G., Zeng G., Peng M., Huang Z., Shi J., Huang T. 2017. Stability, transport and ecosystem effects of graphene in water and soil environments. Nanoscale 9, 5370-5388.

He Y., Liu Y., Wu T., Ma J., Wang X., Gong Q., Kong. W., Xing F., Liu Y., Gao J. 2013. An environmentally friendly method for the fabrication of reduced graphene oxide foam with a super oil absorption capacity. Journal of hazardous materials 260, 796-805.

Huang D., Xu B., Wu J., Brookes P.C., Xu J. 2019. Adsorption and desorption of phenanthrene by magnetic graphene nanomaterials from water: Roles of pH, heavy metal ions and natural organic matter. Chemical Engineering Journal 368, 390–399.

Jing-jing M., Lu-qing P., Jing L., Lin Z. 2009. Effects of benzo[a]pyrene on DNA damage and histological alterations in gonad of scallop *Chlamys farreri*. Marine Environmental Research, 67, 47–52.

Josende M.E., Nunes S.M., de Oliveira Lobato R., González-Durruthy M., Kist L.W., Bogo M.R., Wasielesky W., Sahoo S., Nascimento J.P., Furtado C.A., Fattorini D., Regoli F., Machado K., Werhli A.V., Monserrat J.M., Ventura-Lima J. 2020. Graphene oxide and GST-omega enzyme: An interaction that affects arsenic metabolism in the shrimp *Litopenaeus vannamei*. Science of the Total Environment 716, 136893.

Kabiri S., Degryse F., Tran D.N., da Silva R.C., McLaughlin M.J., Losic D. 2017. Graphene Oxide: A New Carrier for Slow Release of Plant Micronutrients. ACS Applied Materials & Interfaces 9, 43325-43335.

Kamel N., Attig H., Dagnino A., Boussetta H., Banni M. 2012. Increased temperatures affect oxidative stress markers and detoxification response to benzo[a]pyrene exposure in mussel *Mytilus galloprovincialis*. Archives of Environmental Contamination and Toxicology 63, 534–543.

Katsumiti A., Cajaraville M.P. 2019. In Vitro Testing: In Vitro Toxicity Testing with Bivalve Mollusc and Fish Cells for the Risk Assessment of Nanoparticles in the Aquatic Environment. In Ecotoxicology of Nanoparticles in Aquatic Systems (pp. 62-98). CRC Press.

Katsumiti A., Tomovska R., Cajaraville M. 2017. Intracellular localization and toxicity of graphene oxide and reduced graphene oxide nanoplatelets to mussel hemocytes *in vitro*. Aquatic Toxicology 188, 138-147.

Khan B., Adeleye A.S., Burgess R.M., Smolowitz R., Russo S.M., Ho K.T. 2019a. A 72-h exposure study with eastern oysters (*Crassostrea virginica*) and the nanomaterial graphene oxide. Environmental Toxicology and Chemistry 38, 820–830.

Khan B., Adeleye A.S., Burgess R.M., Russo S.M., Ho K.T. 2019b. Effects of graphene oxide nanomaterial exposures on the marine bivalve, *Crassostrea virginica*. Aquatic Toxicology 216, 105297.

Kim Y., Ashton-Alcox A., Powell E.N. 2006. Histological techniques for marine bivalve molluscs: update NOAA technical memorandum NOS NCCOS 27, 76 pp.

Lalwani G., D'Agati M., Khan A.M., Sitharaman B. 2016. Toxicology of graphene-based nanomaterials. Advanced Drug Delivery Reviews, 105, 109–144.

Lammel T., Boisseaux P., Fernández-Cruz M. L., Navas J. M. 2013. Internalization and cytotoxicity of graphene oxide and carboxyl graphene nanoplatelets in the human hepatocellular carcinoma cell line Hep G2. Particle and fibre toxicology 10, 27.

Le V.T., Almomani F., Vasseghian Y., Vilas–Boas J.A., Dragoi E.N. 2021. Graphene-based nanomaterial for desalination of water: A systematic review and meta-analysis. Food and Chemical Toxicology 148, 111964.

Lima I., Moreira S.M., Rendón-Von Osten J., Soares A.M.V.M., Guilhermino L. 2007. Biochemical responses of the marine mussel *Mytilus galloprovincialis* to petrochemical environmental contamination along the North-Western coast of Portugal. Chemosphere 66, 1230-1242.

Lu J., Zhu X., Tian S., Lv X., Chen Z., Jiang Y., Liao X., Cai Z., Chen B. 2018. Graphene oxide in the marine environment: Toxicity to *Artemia salina* with and without the presence of Phe and Cd2+. Chemosphere, 211, 390–396.

Malina T., Maršálkova E., Holá K., Zbořil R., Maršálek B. 2020. The environmental fate of graphene oxide in aquatic environment complete mitigation of its acute toxicity to planktonic and benthic crustaceans by algae. Journal of Hazardous Materials 399, 123027.

Marigómez I., Izagirre U., Lekube X. 2005. Lysosomal enlargement in digestive cells of mussels exposed to cadmium, benzo[a]pyrene and their combination. Comparative Biochemistry and Physiology Part C: Toxicology & Pharmacology 141, 188-193.

Martínez-Álvarez I., Le Menach K., Devier M.H., Barbarin I., Tomovska R., Cajaraville M.P:, Budzinski H., Orbea A. 2021. Uptake and effects of graphene oxide nanomaterials alone and in combination with polycyclic aromatic hydrocarbons in zebrafish. Science of The Total Environment 775, 145669.

Martoja R., Martoja-Pierson M. 1970. Técnicas de Histología Animal. Toray-Masson, Barcelona.

McCord J., Fridovich I. 1969. Superoxide Dismutase, an enzymic function for erythrocuprein (hemocuprein). Journal of Biological Chemistry 244, 6049–6055.

Meng X., Li F., Wang X., Liu J., Ji C., Wu H. 2019. Combinatorial immune and stress response, cytoskeleton and signal transduction effects of graphene and triphenyl phosphate (TPP) in mussel *Mytilus galloprovincialis*. Journal of Hazardous Materials, 378, 120778.

Meng X., Li F., Wang X., Liu J., Ji C., Wu H. 2020. Toxicological effects of graphene on mussel *Mytilus galloprovincialis* hemocytes after individual and combined exposure with triphenyl phosphate. Marine Pollution Bulletin 151, 110838.

Mesarič T., Sepčić K., Drobne D., Makovec D., Faimali M., Morgana S., Falugi C., Gambardella C. 2015. Sperm exposure to carbon-based nanomaterials causes abnormalities in early development of purple sea urchin (*Paracentrotus lividus*). Aquatic Toxicology, 163, 158–166.

Moore M.N. 2006. Do nanoparticles present ecotoxicological risks for the health of the aquatic environment? Environment international 32, 967-976.

Moore M.N., Sforzini S., Viarengo A., Barranger A., Aminot Y., Readman J.W., Khlobystov A.N., Arlt V.M., Banni M., Jha A.N. 2021. Antagonistic cytoprotective effects of C60 fullerene nanoparticles in simultaneous exposure to benzo[a]pyrene in a molluscan animal model. Science of the Total Environment 755, 142355.

Moore M.N., Viarengo A.G., Somerfield P.J., Sforzini S., 2013. Linking lysosomal biomarkers and ecotoxicological effects at higher biological levels. Ecological Biomarkers: Indicators of Ecotoxicological Effects, (Eds. C. Amiard-Triquet, J.C. Amiard, P.S. Rainbow). CRC Press, Boca Raton (Florida), New York & Oxford, pp. 107–130.

Navarro E., Iglesias J.I.P., Camacho A.P., Labarta U., Beiras R. 1991. The physiological energetics of mussels (*Mytilus galloprovincialis* Lmk) from different cultivation rafts in the Ria de Arosa (Galicia, NW Spain). Aquaculture 94, 197–212.

Nel A., Xia T., Mädler L., Li N. 2006. Toxic potential of materials at the nanolevel. Science 311, 622-627.

Nouara A., Wu Q., Li Y., Tang M., Wang H., Zhao Y., Wang D. 2013. Carboxylic acid functionalization prevents the translocation of multi-walled carbon nanotubes at predicted environmentally relevant concentrations into targeted organs of nematode *Caenorhabditis elegans*. Nanoscale 5, 6088-6096.

Novoselov K.S., Fal V.I., Colombo L., Gellert P.R., Schwab M.G., Kim K. 2012. A roadmap for graphene. Nature 490, 192-200.

Ortiz-Zarragoitia M., Cajaraville M.P. 2006. Biomarkers of exposure and reproduction-related effects in mussels exposed to endocrine disruptors. Archives of Environmental Contamination and Toxicology 50, 361-369.

Ou L., Song B., Liang H., Liu J., Feng X., Deng B., Sun T., Shao L. 2016. Toxicity of graphene-family nanoparticles: a general review of the origins and mechanisms. Particle and fibre toxicology 13, 57.

Peng Z., Liu X., Zhang W. Zeng Z., Liu Z. Zhang C., Liu Y., Shao B., Liang Q., Tang W., Yuan X. 2020. Advances in the application, toxicity and degradation of carbon nanomaterials in environment: A review. Environment International 134, 105298

Pinto-Silva C.R.C., Creppy E.E., Matias W.G. 2005. Micronucleus test in mussels *Perna perna* fed with the toxic dinoflagellate *Prorocentrum lima*. Archives of Toxicology 79, 422–426

Ren W., Cheng H.M. 2014. The global growth of graphene. Nature nanotechnology 9, 726-730.

Ren C., Hu X., Li X., Zhou Q. 2016. Ultra-trace graphene oxide in a water environment triggers Parkinson's disease-like symptoms and metabolic disturbance in zebrafish larvae. Biomaterials, 93, 83–94.

Robledo, C., Marigómez, I., Angulo, E., Cajaraville, M.P. 2006. Glycosylation and sorting pathways of lysosomal enzymes in mussel digestive cells. Cell and Tissue Research, 324: 319-333.

Ruiz P., Ortiz-Zarragoitia M., Orbea A., Vingen S., Hjelle A., Baussant T., Cajaraville M.P. 2014. Short- and long-term responses and recovery of mussels *Mytilus edulis* exposed to heavy fuel oil no. 6 and styrene. Ecotoxicology 23, 861-879.

Sanchís J., Olmos M., Vincent P., Farre M., Barceló D. 2016. New insights on the influence of organic co-contaminants on the aquatic toxicology of carbon nanomaterials. Environmental Science & Technology 50, 961-969.

Scott. A. 2016. Graphene's Global Race to Market. Chemical & Engineering news 94, 28−33.

Seed R., 1969. The ecology of *Mytilus edulis* L (Lamellibranchiata) on exposed rocky shores. Oecologia 3, 277–315.

Souza J.P., Baretta J.F., Santos F., Paino I.M.M., Zucolot V. 2017. Toxicological effects of graphene oxide on adult zebrafish (*Danio rerio*). Aquatic Toxicology 186, 11–18.

Souza J.P., Venturini F.P., Santos F., Zucolotto V. 2018. Chronic toxicity in *Ceriodaphnia dubia* induced by graphene oxide. Chemosphere 190, 218–224.

Tian S., Pan L., Sun X. 2013. An investigation of endocrine disrupting effects and toxic mechanisms modulated by benzo[a]pyrene in female scallop *Chlamys farreri*. Aquatic toxicology 144, 162-171.

Tu Y., Lv M., Xiu P., Huynh T., Zhang M., Castelli M., Liu Z., Huang Q., Fan C., Fang H., Zhou R. 2013. Destructive extraction of phospholipids from Escherichia coli membranes by graphene nanosheets. Nature nanotechnology 8, 594-601.

U. S. EPA. 2014. IRIS Toxicological Review of Benzo[a]pyrene (External Review Draft). U.S. Environmental Protection Agency, Washington, DC EPA/635/R-14/312.

U.E. Water Framework Directive. 2008. Environmental Quality Standards Directive (EQSD). 105/EC. https://ec.europa.eu/environment/water/water-framework/priority_substances.htm

Viarengo A., Lowe D., Bolognesi C., Fabbri E., Koehler A. 2007. The use of biomarkers in biomonitoring: a 2-tier approach assessing the level of pollutant-induced stress syndrome in sentinel organisms. Comparative Biochemistry and Physiology Part C: Toxicology & Pharmacology 146, 281-300.

Villalba A., Mourelle S.G., Carballal M.J., Lopez, C. 1997. Symbionts and diseases of farmed mussels *Mytilus galloprovincialis* throughout the culture process in the Rias of Galicia (NW Spain). Diseases of Aquatic Organisms 31, 127-139.

Wang A., Pu K., Dong B., Liu Y., Zhang L., Zhang Z., Duan D., Zhu Y. 2013. Role of surface charge and oxidative stress in cytotoxicity and genotoxicity of graphene oxide towards human lung fibroblast cells. Journal of Applied Toxicology 33, 1156-1164.

Wang J., Zhang J., Han L., Wang J., Zhu L., Zeng H. 2021. Graphene-based materials for adsorptive removal of pollutants from water and underlying interaction mechanism. Advances in Colloid and Interface Science 289, 102360.

Wang C., Zhao Y., Zheng R., Ding X., Wei W., Zuo Z., Chen Y. 2006. Effects of tributyltin, benzo[a]pyrene, and their mixture on antioxidant defense systems in *Sebastiscus marmoratus*. Ecotoxicology and Environmental Safety 65, 381-387.

Yang Y., Pan L., Zhou Y., Xu R., Miao J., Gao Z., Li D. 2021. Damages to biological macromolecules in gonadal subcellular fractions of scallop *Chlamys farreri* following benzo[a]pyrene exposure: Contribution to inhibiting gonadal development and reducing fertility. Environmental Pollution 283, 117084.

Yang Y., Zhou Y., Pan L., Xu R., Li D. 2020. Benzo[a]pyrene exposure induced reproductive endocrine-disrupting effects via the steroidogenic pathway and estrogen signaling pathway in female scallop *Chlamys farreri*. Science of the Total Environment 726, 138585.

Yao W., Zhou S., Wang Z., Lu Z., Houc C. 2020. Antioxidant behaviors of graphene in marine environment: A first-principles simulation. Applied Surface Science 499, 143962.

Zhang Y., Meng T., Shi L., Guo X., Si X., Yang R., Quan X. 2019. The effects of humic acid on the toxicity of graphene oxide to *Scenedesmus obliquus* and *Daphnia magna*. Science of the Total Environment 649, 163–171.

Zhao J., Wang Z., White J. C., Xing B. 2014. Graphene in the aquatic environment: adsorption, dispersion, toxicity and transformation. Environmental science & technology 48, 9995-10009.

Zhao S., Wang, Y., & Duo, L. 2021. Biochemical toxicity, lysosomal membrane stability and DNA damage induced by

Zhu S., Luo F., Chen W., Zhu B., Wang G. 2017. Toxicity evaluation of graphene oxide on cysts and three larval stages of *Artemia salina*. Science of the Total Environment 595, 101–109.

SUPPLEMENTARY MATERIAL TO CHAPTER 3

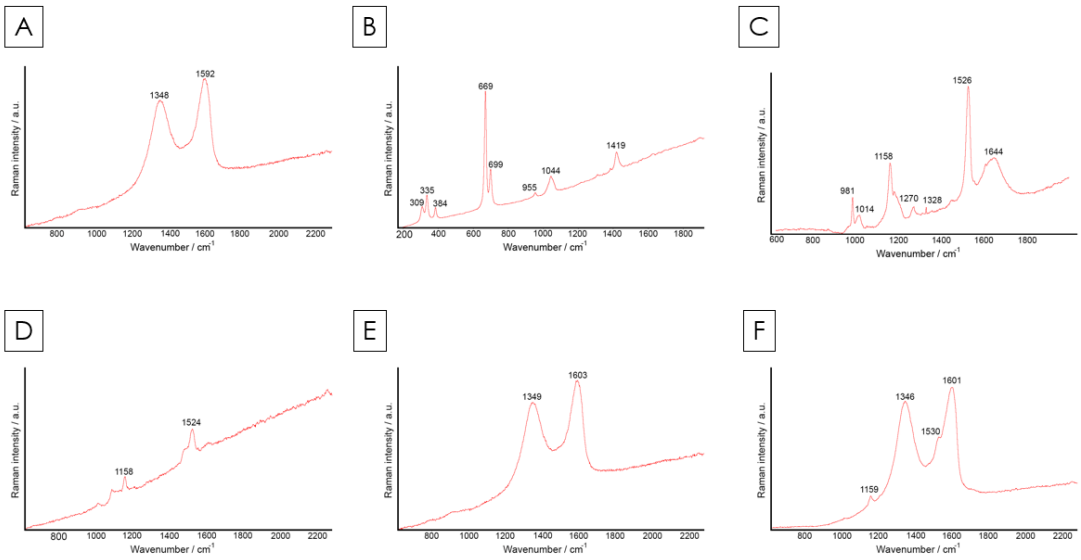

Figure S1: Raman spectra obtained from A: Graphene oxide (GO) stock; B: benzo(a)pyrene (BaP) stock; C: microalgae *Isochrysis galbana* used to feed the mussels during the experiment; D: feces obtained from a control mussel after 1 day of exposure; E: feces obtained from a mussel exposed to GO after 1 day of exposure; F: feces obtained from a mussel exposed to GO+BaP after 1 day of exposure.

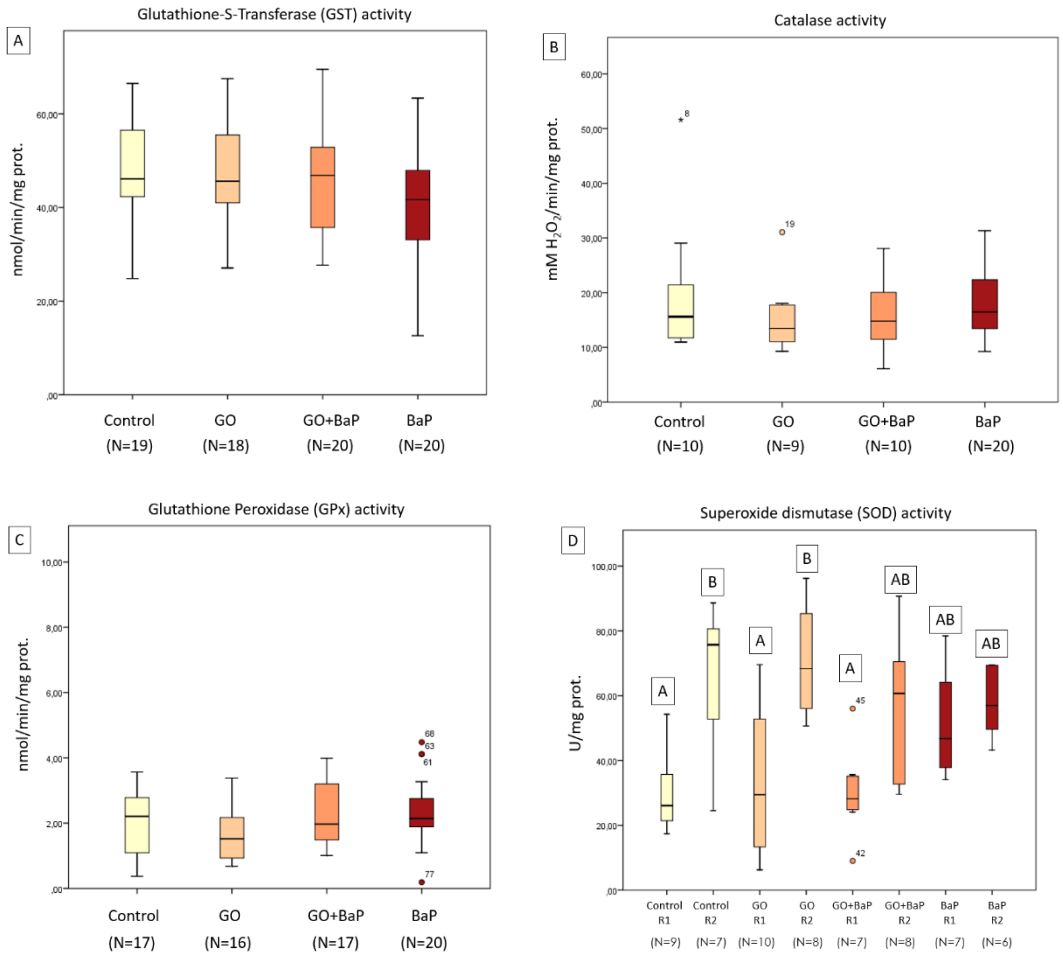

Figure S2: A: Glutathione- S-Transferase (GST) activity in gills (given as nmol/min/mg prot); B: Catalase (Cat) activity in gills (given as mM H_2O_2/min/mg prot); C: Glutathione Peroxidase (GPx) activity in digestive gland (given as nmol/min/mg prot); D: Superoxide dismutase (SOD) activity in gills (U/mg prot) of control mussels and of mussels exposed for 7 days to GO, GO+BaP and BaP. Box-plots show median value (horizontal line), 25%-75% quartiles (box) and standard deviation (whiskers). Dots and star denote outliers. Letters denote statistical differences among means (Kruskal-Wallis test followed by Dunn's post hoc, $p<0.05$).

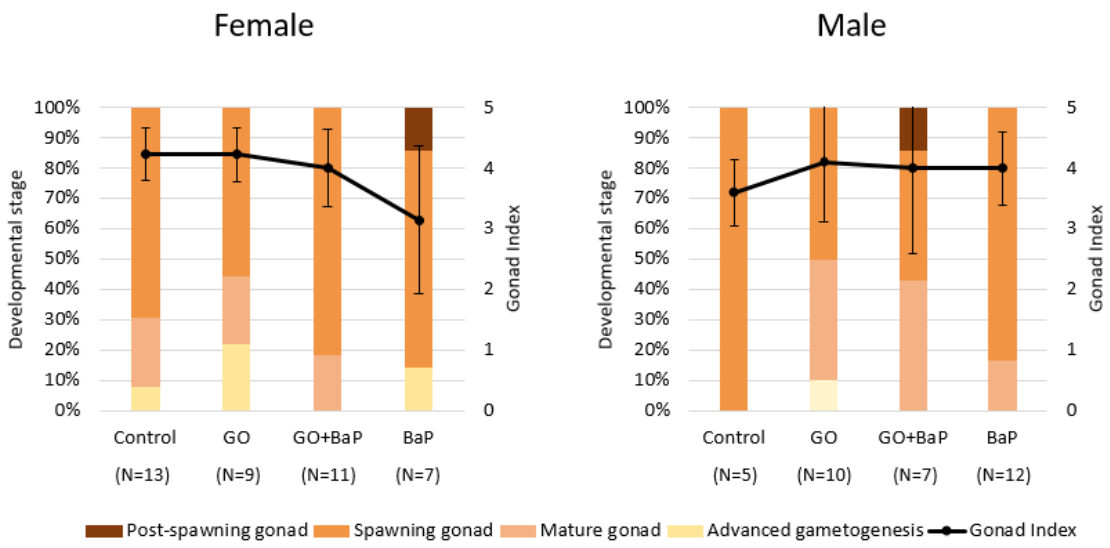

Figure S3: Gonad index (lines) and percentage of animals at each gamete developmental stage (stacked bars) in control mussels and in mussels exposed to GO, GO+BaP and BaP for 7 days. Gonad index values are given as means and standard. No statistically significant differences in Gonad index and developmental stages were found among treatments (Kruskal-Wallis, $p > 0,05$).

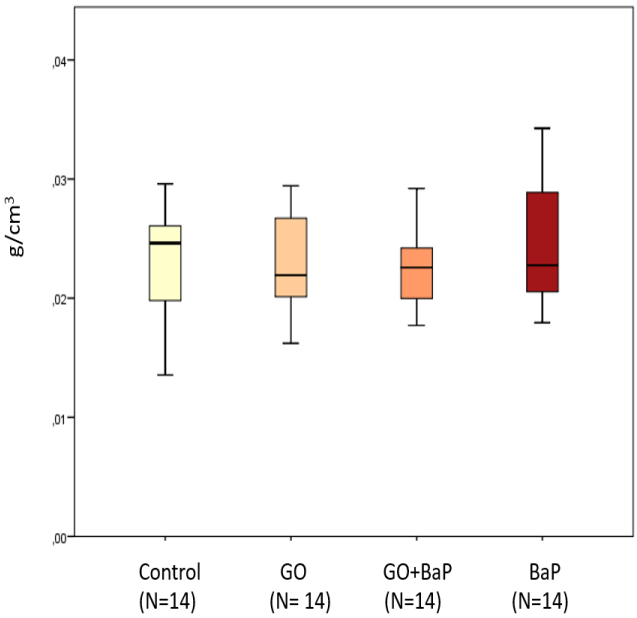

Figure S4: Condition index (g/cm^3) in control mussels and in mussels exposed to GO, GO+ BaP, and BaP for 7 days. Box-plots show median value (horizontal line), 25%-75% quartiles (box) and standard deviation (whiskers) of 14 mussels per group. No significant differences were observed among treatments according to one way-ANOVA ($p > 0,05$).

CHAPTER 4:

Fate and effects of a reduced graphene oxide-silver nanoparticle hybrid material on mussels *Mytilus galloprovincialis*

This chapter is being prepared for publication:

GONZÁLEZ-SOTO, N; IRAZOLA, M; TOMOVSKA, R; SCHÄFER, J; BILBAO, E.; CAJARAVILLE, MP. Fate and effects of a reduced graphene oxide-silver nanoparticle hybrid material on mussels *Mytilus galloprovincialis*.

This chapter will be presented at:

32nd Conference of the European Society of Comparative Physiology and Biochemistry (ESCPB), Naples, 28 to 31 August 2022.

González-Soto, N; Irazola, M; Tomovska, R; Schäfer, J; Bilbao, E.; Cajaraville, MP. Fate and effects of a reduced graphene oxide-silver nanoparticle hybrid material on mussels *Mytilus galloprovincialis*.

ABSTRACT

Research on graphene and related graphene family nanomaterials (GFNs) has bloomed in recent years. Currently, a new generation of hybrid nanomaterials that combine GFNs with silver nanoparticles (Ag NPs) has received increased attention due to their enhanced properties. However, the concern about their possible toxicity is also rising because Ag NPs are known to be toxic for several aquatic organisms and many of the applications of these novel nanocomposites involve their direct application in the environment and especially in the marine environment. In this context, this work aims to assess the potential hazards that a composite of reduced graphene oxide (rGO) with Ag NPs (rGO-Ag) could pose towards marine mussels *Mytilus galloprovincialis.* Mussels were exposed for 21 days to 500 μg/L of rGO-Ag and to the equivalent concentration of rGO (375 μg/L) and Ag NPs (125 μg/L) alone for comparison purposes. rGO nanoplatelets were detected by Raman spectroscopy in the lumen of digestive tract and feces of mussels exposed to rGO and to rGO-Ag. Mussels exposed to rGO-Ag and Ag NPs accumulated Ag in their tissues. Exposure to rGO-Ag altered the activity of AchE, induced catalase activity and oxidative damage in digestive gland at day 3 of exposure and increased the prevalence of brown cell aggregations in mussel gonads. Both rGO and rGO-Ag caused inflammatory responses in mussel gonads and decreased the digestive gland index after 21 days of exposure. Further, rGO caused transitory DNA damage in mussel hemocytes and inhibited catalase activity in digestive gland after 21 days of exposure. Exposure to Ag NPs at the same concentration as in the rGO-Ag hybrid lead to multiple alterations including downregulation of *catalase* and *hsp90* transcription levels in digestive gland, DNA damage in mussel hemocytes, and altered enzyme activities related to aerobic and anaerobic metabolism, neurotransmission and phase 2 biotransformation in different tissues. Further, 21 days of exposure to Ag NPs caused inflammatory responses in mussel gonads and limited mortality. In conclusion, both rGO and rGO-Ag were able to cause deleterious effects to mussels and Ag NPs exerted less toxicity when dosed in the form of rGO-Ag than alone.

1. INTRODUCTION

Since its discovery in 2004, graphene has been one of the great interests of research in recent years (Ding et al., 2022). Graphene is a single-atom-thick sheet with sp^2-bonded carbon atoms with lateral dimensions that can vary from nanometers to the macroscale (Bianco et al 2013). Graphene has shown to have great thermal, optical, mechanical and magnetic properties, among others. These properties make graphene suitable for multiple applications such as the development of a new generation of batteries, electronic engineering, sensors, anticorrosion agents, environmental purification, sea water desalination, drug carriers and tissue engineering (De Marchi et al., 2018; Ding et al., 2022).

Graphene and its derivatives comprise the graphene family nanomaterials (GFNs) which have received increased attention too. According to Bianco et al. (2013) GFNs include graphene oxide (GO), reduced graphene oxide (rGO), few layer graphene, multilayered graphene, graphene quantum dots and materials that use any of these as precursors. Currently, a new generation of hybrid nanomaterials combining GFNs with different polymers or metal nanoparticles are being explored to enhance or acquire new properties and applications. For example, a nanocomposite that combines polyurethane and rGO has been proposed for cardiac tissue engineering (Azizi et al., 2019) and the ecofriendly biodegradable poly(2-ethyl-2-oxazoline) combined with graphene has shown improved antibacterial activity (Shubha et al., 2022).

Among hybrid nanocomposites composed of GFNs and metal nanoparticles, silver nanoparticles stand out. Silver nanoparticles are used for more than a century for multiple applications (Cajaraville et al., 2021), especially due to their antimicrobial activity (Sofi et al., 2022). The combination of GFNs and Ag NPs is being investigated for multiple applications from electronics to biomedicine (De Moraes, 2015; Zhou et al., 2016; Sharma et al., 2017; Xu et al., 2017). Since many of these applications involve direct application of the nanocomposite in the environment and especially in the marine environment (Chen et al., 2016; Koushik et al., 2016; Yee et al., 2016; Jin et al., 2021), concentrations of GFNs and Ag NPs are expected to increase in the environment. Although GFNs have already been detected in biomass from wastewater treatment

plants (Goodwin et al., 2018) there is no data regarding their environmental concentration yet (De Marchi et al., 2018). It is expected that GFNs concentration will reach 0.001–1000 μg/L in the aquatic environment based on estimations for carbon nanotubes (De Marchi et al., 2018). A similar environmental concentration range has been predicted for Ag NPs (Blaser et al., 2008; Gottschalk et al., 2009; Tiede et al., 2009; Dumont et al., 2015; Giese et al., 2018) though the recent use of metal containing nanocomposites could increase it.

Deleterious effects caused by both nanomaterials, GFNs and Ag NPs, have been reported in aquatic animals. Ag NPs are a well described pollutant able to cause inhibition of microalgal growth, oxidative stress, genotoxicity, lysosomal damage and tissue alterations in bivalves, embryotoxicity in echinoderms and fishes, alterations in the development of polychaetes and mortality of crustaceans, among others (Cajaraville et al., 2021). On the other hand, GFNs can cause oxidative stress (Katsumiti et al., 2017), DNA damage (Wang et al., 2013), damage to cell membranes (Katsumiti et al., 2017), tissue damage (Souza et al., 2017; Khan et al., 2019), alterations in energy reserves (Peng et al., 2020; Britto et al., 2021), reproduction and growth or mortality (Bortolozo et al., 2021) in different organisms. Consequently, it is relevant to investigate the possible impact of a nanocomposite formed by GFNs and Ag NPs, especially taking into account that inconclusive data on its toxicity have been reported (De Luna et al., 2016; Kim et al., 2018; Alian et al., 2019; Medeiros et al., 2021; Krishnaraj et al., 2022). Importantly, as far as we know, there are no studies on the impact of these hybrid materials on marine animals.

Marine mussels *Mytilus sp.* comprise a well recognized target group to study the toxicity of different nanomaterials, including nanoparticles. As filter-feeders, mussels are prone to trap nanomaterials in their gills, that once in the organism can be internalized into cells depending on several factors such as size, shape, surface properties, aggregation and dissolution behavior in experimental media (Moore, 2006; Canesi et al., 2012; Corsi et al., 2014). In addition, mussels are well known as sentinels of environmental pollution since they accumulate pollutants in their tissues and can survive in harsh environments but, at the same time, they are relatively sensitive and show consistent responses to pollutants (Goldberg, 1986; Cajaraville et al., 2000). The aim of this work is to assess the

toxicity of a reduced graphene oxide (rGO)-silver nanoparticle (Ag NP) hybrid material (rGO-Ag) at different levels of biological organization in mussels *Mytilus galloprovincialis* and to compare its toxicity with that produced by rGO and Ag NPs separately, at concentrations equivalent to those in the hybrid material.

2. MATERIALS AND METHODS

2.1. Production and characterization of rGO and rGO-Ag nanoplatelets and Ag NPs

The synthesis of the hybrid nanomaterial reduced graphene oxide (rGO) with silver nanoparticles (Ag NPs), rGO-Ag, was carried out at the POLYMAT Institute (UPV/EHU). Briefly, graphene oxide (GO) in aqueous dispersions of 4 mg/mL, with a monolayer content >95 %, in a pH range between 2.2- 2.5 was purchased from Graphenea (San Sebastian, Spain). The Ag NPs were prepared *in situ* from silver nitrate ($AgNO_3$) ACS reagent, ≥99.0% by simultaneous reduction of the GO and $AgNO_3$ performed in aqueous dispersion with ascorbic acid 99% (AsA) from ACROS. To stabilize colloidally the hybrid rGO-Ag in aqueous dispersion, 2% in weight of polyvinylpyrrolidone (PVP) with average Mw of 10,000 was used. For the synthesis of the batch of rGO-Ag used in this work, 125 mL of GO dispersion (500 mg GO), 120 mg of $AgNO_3$ (diluted in 4 mL of H_2O), 5 mg of PVP (diluted in 5 mL of H_2O) and 620 mg of AsA (diluted in 6 mL of H_2O) were used.

The GO aqueous dispersion was sonicated for 20 min with amplitude of 70% and energy pulsed at 0.5 Hz at room temperature. In a second step, PVP was added drop by drop and left stirring for 10 min. Subsequently, $AgNO_3$ was added drop by drop and left stirring for 30 min. In the last step, AsA was also added drop by drop. The mixture was left to stir for 72 h at room temperature. After the 72 h the rGO-Ag mixture was transferred into a membrane for dialysis (12– 14,000 Da spectral/Por® membranes, Spectru mLabs), in order to remove unreacted species. The excess PVP was also removed from the dispersion. The water of the dialysis was changed two times per day for a period of 10 days until neutral pH was obtained.

rGO samples were prepared following the same procedure without addition of precursor $AgNO_3$, as described in Katsumiti et al. (2017) and Martínez-Álvarez et al. (2021).

For the characterization of the materials, the elemental composition of GO was determined by Scanning Electron Microscopy (SEM, Hitachi TM3030 tabletop model, Krefeld, Germany) equipped with an EDX. The structure of the rGO and distribution of Ag NPs decorated onto rGO surfaces were investigated with a Philips TECNAI G2 20 TWIN Transmission Electron Microscope (TEM). The size of Ag NPs was determined using Dynamic Light Scattering (DLS).

The thermogravimetric analysis (TGA) of the materials was performed to determine the chemical composition and relative fraction of each of the components in the final products (rGO-Ag and Ag NPs). For this purpose, 6 mg of each material were heated in a TGA5500 apparatus (TA Instruments), under N_2 atmosphere (10 °C/min) until 500 °C to eliminate all oxygen species including PVP, and then the gas was switched to O_2 (10 °C/min) and the analysis was performed until 800 °C to eliminate all carbon material.

2.2. Sampling and acclimation of mussels

Mussels *Mytilus galloprovincialis* (3,5-4,5 cm shell length) were collected in February 2021 in Plentzia (43°24'00.0"N, 2°56'00.0"W). 51 mussels were dissected on the sampling day (t=0) and the rest (500) were maintained in aquaria facilities at the Plentzia Marine Station (PiE) of the University of the Basque Country (UPV/EHU), for acclimation during 20 days. Acclimation was carried out in a 300 L polypropylene tank with a recirculating seawater system. Marine water was collected with a pump at 10 m depth in the mouth of the Butroi estuary (43°24’21”N, 2°56’47”W) and filtered (particles ≤ 3 µm) before reaching the marine station. Mussels were not fed for two days and then they were fed once a day with *Isochrysis galbana* microalgae ($20x10^6$ cells/mussel-day) for 18 days. *I. galbana* (T-Iso clone) cultures were obtained from the Animal Physiology Research Group of the Department of Genetics, Physical Anthropology and Animal Physiology at UPV/EHU. During acclimation, light regime was 12L/12D and room temperature was kept at 15°C. Water parameters were checked daily with a multichannel probe: salinity (32.40 ± 0.27 PSU), dissolved O_2 (>90%), pH (7.425 ± 0.049) and temperature (13.5 ± 0.02 °C). No mussels died during the acclimation period.

2.3. Mussel exposure

After 20 days of acclimation, 125 mussels were transferred to each 125 L glass tanks and four experimental groups were established: control mussels and mussels exposed to rGO, rGO-Ag and Ag NPs. A nominal concentration of 500 μg/L of rGO-Ag was selected as environmentally relevant concentration, based on data for multi-walled carbon nanotubes that range from 1 μg/L to 1 mg/L (de Marchi et al., 2018). The nominal concentrations of rGO and Ag NPs were selected taking into consideration their initial proportions in the production of the rGO-Ag, that were 75% and 25%, respectively. In consequence, mussels were exposed to 375 μg/L of rGO and 125 μg/L of Ag NPs. In order to keep a homogeneous suspension of the different NMs in water and to avoid their aggregation or precipitation, a water recirculation system consisting of 2 pumps was installed in the aquaria.

During the experiment, whole aquarium volume was changed every day and mussels were fed once a day with *I. galbana* ($20x10^6$ cells/mussel-day) two hours before changing the water. At each water change, 5 random mussels per tank were placed in individual glass containers with clean water to collect feces. The light regime and room temperature were kept at 12L/12D and 15°C, respectively. Water parameters were checked daily with a multichannel probe: salinity (32.19 ± 0.02 PSU), dissolved O_2 (>92%), pH (7.86 ± 0.27) and temperature (14.43 ± 1.09°C). 6 mussels died in the Ag NPs exposure tank along the experiment. Mussels were sampled after 3 and 21 days of exposure. Following sampling on day 3, dosing of microalgae was recalculated in order to maintain rations after removing mussels.

2.4. Analysis of rGO, rGO-Ag and Ag in water

Water samples were collected from each exposure tank 30 minutes and 24 hours post-exposure in 3 replicates. Presence of rGO, rGO-Ag was checked by UV/Vis spectrophotometry at 230 nm in a Shimadzu 1800 UV spectrophotometer.

To determine Ag content, water samples were sent to the Environnments et Paléoenvironnments Océaniques et Continentaux (EPOC) research unit of the University of Bordeaux. Analysis of Ag content in water was performed using an Inductively

Coupled Plasma-Tandem Mass Spectrometry (ICP-MS/MS; Thermo Scientific®; iCAP TQ). The analytical performance of the digestion procedure was assessed using the external calibration made from commercially available standard solutions (PlasmaCAL, SCP Science®). Ag concentrations measured were consistent (RSD <2%) among replicates. The detection limit for dissolved total Ag measurements was 10 ng/ L

2.5. Bioaccumulation of Ag in mussel tissues

For analysis of Ag in mussel samples, between 5 and 8 individuals per experimental group were dissected and weighted to make homogeneous pools of 4-5 animals per experimental group and time. Pooled samples were then freeze-dryed and sent to the EPOC research unit of the University of Bordeaux.

Mussel samples (pools of 4-5 mussels ~ 1 g) were weighed and turned to ashes in acid-cleaned porcelain crucibles at 650 °C during 5 h (removal of organic matter). Samples were then transferred to polypropylene tubes and mineralized using 2 ml of HNO_3 (67%, Ultrex® II J.T.Baker) and 1 ml of HCl (33%, Ultrex® J.T.Baker), for 3 h in a hot plate at 110°C (Analab®) (adapted from Abdou et al. 2018). Then, digestates were diluted and analyzed for Ag concentration by ICP-MS (Thermo Scientific®; iCAP TQ) using external calibration (from commercially available standard solutions of Ag, PlasmaCAL, SCP Science®). Accuracy and precision were controlled during each analytical session by SRM 1643f, Trace Elements in Water, NIST® (recovery 94%, RSD 5%, n=18). Results are expressed as µg Ag/g.

2.6. Determination of rGO and rGO-Ag in mussel tissues and feces

To determine the occurrence of rGO and rGO-Ag in mussels´ tissues, the hemolymph of 3 mussels per experimental group was withdrawn and then the same mussels were dissected after 3 and 21 days of exposure. All samples were frozen in liquid nitrogen and maintained at -40°C until further analysis. For tissue samples, 20 µm sections of each mussel were obtained in a cryostat (Leica CM 3050S) and observed under an inVia Renishaw microscope in order to get Raman spectra using a 532 nm laser. Conditions

were set using the 50x objective as follows: 1 µm steps in the tissue, 0.5 s, 10% laser intensity, 1 accumulation and focused in 1350 nm.

Mussel's feces were also collected (as described in section 2 of materials and methods) and analyzed by Raman spectroscopy. Mussel feces were completely dried and placed in an aluminum foil before getting the Raman spectrum. Conditions were set using a 100x objective as follows: 100% laser intensity, 1s, 80 accumulation and focused in 1350 nm. Hemolymph samples were defrosted and transferred to 1 mL glass vials to be analyzed in the same conditions as mussel feces.

2.7. Cellular biomarkers in hemocytes

Hemolymph of 8 mussels per tank used for enzyme activity determination (see section 9 of materials and methods) was withdrawn from the posterior adductor muscle and cell viability, catalase activity and DNA damage were measured in hemocytes of individual mussels. Neutral red uptake was assessed as explained in Chapter 1. Catalase activity was assessed as detailed in Chapter 1) and protein concentration was measured following the Bradford method (Bradford, 1976) to normalize absorbance data. Catalase activity was expressed as the consumption of hydrogen peroxide in mM H_2O_2/min/mg protein. The comet assay was a performed as explained in Chapter 1with the following modifications. Two slides per animal were stained with GreenSafe Premium (NZYTech) (1:100 dilution) and 50 randomly selected cells per slide were analyzed under an Olympus BX61 fluorescence microscope (Hamburg, Germany) and scored using the Opencomet, ImageJ software (Gyori et al., 2014).

2.8. Gene transcription levels in the digestive gland

A third of the digestive gland (50-100 mg) of 15 animals per experimental group were individually immersed in RNA later® (Sigma-Aldrich, St. Louis, Missouri, USA) and frozen in liquid nitrogen. Samples were stored at -80°C until further processing. A piece of the mantle of the same animals was also dissected for histological observation. As sex dependent gene transcription patterns have been reported in mussels (Banni et al., 2011), 6 males per experimental group were selected for the analysis.

Each sample were homogenized individually in Trizol® Reagent (Invitrogen, Carlsbad, USA) at 4°C in a 24 Precellys 21 (Bertin Instruments). RNA was isolated following the manufacturer´s recommendations and then purified by using the RNeasy Mini Kit (Qiagen). After checking RNA purity and integrity, 2 µg of total RNA were retrotranscribed using the Affinity Script Multiple Temperature cDNA synthesis Kit (Agilent Technologies) following manufacturer's conditions in a A24811 simpliAMP Thermal Cycler (ThermoFisher Scientific).

Transcription levels of selected genes were quantified by qRT-PCR using the SYBR®Green Dye (Roche Diagnostics, Basel, Switzerland). Selected genes were: the antioxidant enzymes catalase (*cat,* ID: AY743716*)* and superoxide dismutase *(sod,* ID: FM177867*)*; glutathione S-transferase pi 1 (*gstpi1*, ID: AF527010.1) involved in the biotransformation metabolism; palmitoyl-CoA oxidase (aox*1*, ID:EF525542.1) as marker of peroxisome proliferation and heat shock protein 90-1 (*hsp90,* ID:AM236589) as gene related to stress response.

Specific primers (Table 1) for SYBR®Green qRT-PCR were designed using the PRIMER-3 free software and confirmed by the Primer Express 3.0 software (Applied Biosystems) (Table 1). Each gene was amplified separately in an 384 well-plate in a Applied Biosystems ViiA7 realtime thermocycler (ThermoFisher Scientific) using melting temperatures reported in Table 1. cDNA was diluted 1:10 for *cat, sod* and *aox1* and 1:100 for *gstpi1* and *hsp90*.

Relative transcription levels were calculated based on the RQ= $(1+E)^{-\Delta\Delta ct}$ method (Livak and Schmittgen, 2001) using the mean value of each exposure time control group as calibrator. The relative transcription of each gene was normalized to the cDNA concentration measured using the Quan-it OliGreen ssDNA AssayKit (Invitrogen). Results are represented as $\log_2$ RQ.

Table 1: Forward (Fw) and reverse (Rv) primers and specific melting temperatures (Tm) used to quantify transcription levels of target genes. GenBank accession number of each gene is also shown.

GENE	Accession nº	Primer	Tm
cat	AY743716.2	Fw: TCA TTA CAC TTC GAC CAG AGA CAA C Rv: GGG TTC CAC GGT CAG AGA AC	61
sod	FM177867.1	Fw: GGT GCA CCA GGA GAT GAA GAA Rv: CCC TCT GCA TTG GCT AAT ACA TT	59
gstpi1	AF527010.1	Fw: GAA AAC TGG AAC CAA AGA TGC A Rv: TGGAAACCGTCATCATCTGTGT	57
aox1	AF527010	Fw: ACTACCAGACCCAGCAGTATAGATT Rv: TAAGCTGAGGCTAACAAGGG	57
Hsp90	AM236589.2	Fw: CCT CCC CTT GTT GCA TTG TT Rv: CTT GGG CTT TCA TGA TCC TTT C	57

2.9. Enzyme activities in mussel tissues

Digestive gland, gills, foot and adductor muscle of 15 mussels per exposure group were dissected out, frozen in liquid nitrogen and maintained at -80°C until further analysis. The adductor muscle was homogenized in 0.1 M potassium phosphate (KP) buffer (pH 7,2) to determine the activity of acetylcholinesterase (AchE). Gills were cut in two halves, one half was homogenized in 0.1 M KP buffer (pH 6,5) to determine the activity of Glutathione S-Transferase (GST) and the second half was homogenized in 0.1 M KP buffer (pH 7,4) for Catalase activity. Digestive glands were also divided in halves. The first part was homogenized in 0.1 M KP buffer (pH 6,5) for GST activity determination and the second half was homogenized in 0.1 M KP buffer (pH 7,4) for Catalase, Palmitoyl-CoA oxidase (AOX1) and Lipid Peroxide (LPO) determination. Foots were divided in two, one half was homogenized in 50 mM Tris buffer (Tris(hydroxymethyl)-aminomethan, pH 7.8) to determine the activity of Isocitrate dehydrogenase (IDH) and the second part was homogenized in 20 nM Tris buffer (with 1mM Na_2EDTA, 1mM DTT, pH 7.5) for Octopine dehydrogenase (ODH) activity. Tissues were homogenized in each buffer following a 1:10 proportion, tissue weight: volume of buffer**.** Enzyme activities were determined according to the following literature: AchE: Ellman et al. (1961); IDH: Ellis & Goldberg (1971); ODH: Livingstone et al. (1990); GST: Habig et al. (1974); AOX1: De los Rios et al. (2013) and LPO: Ohkawa et al. (1979). Catalase activity was determined as in section 7

of materials and methods. Measurements of AchE and IDH, ODH and GST were adapted to microplates by Guilhermino et al. (1996) and Lima et al. (2007), respectively. Each enzyme activity was normalized using protein concentration measured by the method of Bradford (Bradford, 1976).

2.10. Gamete development, gonad index and histopathology of gonad

A piece of mantle of the same mussels used to determine gene transcription levels were dissected out and processed following a standard protocol for histology (Martoja & Martoja-Pierson, 1970) in a Leica Tissue processor ASP 3000 (Leica Instruments, Wetzlar, Germany) for paraffin embedding. After sectioning at 5 µm and staining with hematoxylin-eosin, sex, gamete developmental stage and gonad index (GI) of each animal were determined. Six gamete stages were distinguished according to Seed (1969) and GI values ranging from 0 (resting gonad) to 5 (mature gonad) were assigned depending on the developmental stage according to Chapter 1.

Prevalence of oocyte atresia and necrosis, hemocytic infiltration, aggregation of brown cells, and occurrence of parasites (Ortiz-Zarragoitia & Cajaraville, 2006) were determined as percentages. In addition, intensity of oocyte atresia was assessed using a semiquantitative scale: 0- normal gonad, 1- less than a half of follicles are affected, 2- about half of follicles are affected, 3- more than half of follicles are affected and 4- all follicles are affected (Kim et al., 2006). An intensity index of oocyte atresia was calculated as Sp/NH, where Sp was the score corresponding to the intensity of atresia and NH was the number of specimens with atresia (Garmendia et al., 2011).

2.11. Whole organism responses

The digestive gland index was calculated according to Cartier et al. (2004) in the same mussels used to determine enzyme activities. Results were expressed as wet digestive gland weight/wet soft tissue weight. In addition, soft tissues of 7 mussels per exposure group were excised from the shells, dried at 80°C for 24 h and weighted. Then, mussel shell lengths were recorded with a Vernier caliper and condition index was calculated as tissue dry weight (g) / [shell length (cm)]^3 (Navarro et al., 1991).

2.12. Data analysis

Statistical analyses were carried out with the aid of the statistical package SPSS 24 (IBM Analytics, Armonk, NY). Outliers were eliminated following the Chauvenet method. All data were tested for normality and homogeneity of variances using the Kolmogorov-Smirnov´s and Levene's tests, respectively. Significant differences were studied via one-way ANOVA followed by the Tukey's post-hoc test when homogeneity of variances was confirmed. In case normality or homogeneity of variances were not confirmed, data were analyzed by the Kruskal-Wallis test followed by the Dunn's post-hoc test. Since results on histopathology were expressed as percentages, the X^2 test was used (Ruiz et al., 2014). In all cases, significance was established at $p < 0,05$.

3. RESULTS

3.1. Characterization of rGO and rGO-Ag nanoplatelets and Ag NPs

The elemental analysis (EDX) of GO showed the following composition C: 49-56%, H: 0-1%, N: 0-1%, S: 2-4% and O: 41-50%, which agreed with the information obtained from the provider. According to the TGA analysis of rGO-Ag, its composition was: 78,47% rGO + 19,4% Ag NPs + 2,13% PVP (Figure 1A) and in the case of Ag NPs it was 15.15% PVP and 84.85% Ag NPs (Figure 1A). At TEM, platelets of rGO-Ag with different sizes and shapes were observed. The maximum length of rGO-Ag platelets was 6 µm and the size of Ag NPs present in the nanoplatelets was between 100 -200 nm (Figure 1B-D). DLS showed two populations of Ag NPs, one with an average diameter of about 95 nm, and a second with an average diameter of 15 nm (Figure 1E-G; H).

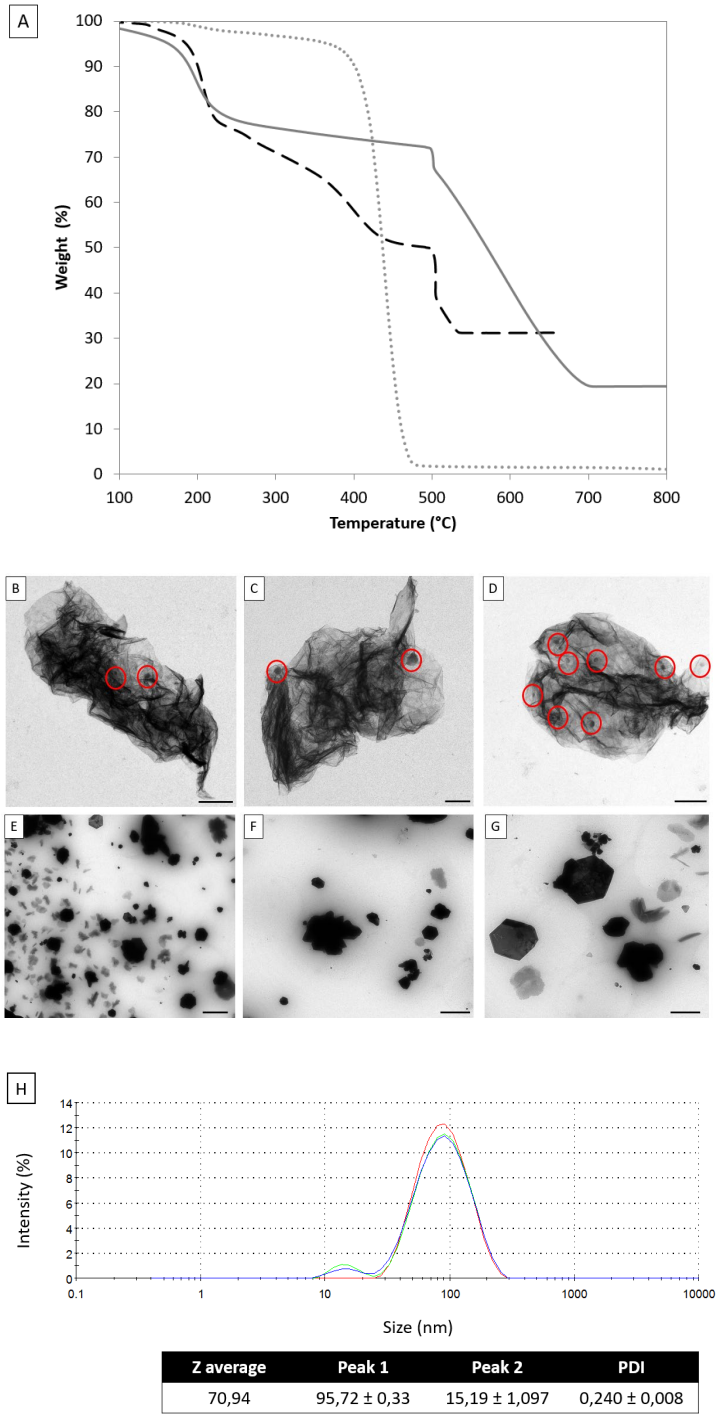

Z average	Peak 1	Peak 2	PDI
70,94	95,72 ± 0,33	15,19 ± 1,097	0,240 ± 0,008

Figure 1. Characterization of rGO-Ag and Ag NPs. A) Thermogravimetric analysis of rGO-Ag (solid grey), Ag NPs (black dots) and PVP (grey dots); Transmission Electron Microscopy images of B-D) rGO-Ag nanoplatelets Ag NPs in circles and E-G) Ag NPs alone; Scale bars: B, D, E: 1 µm and C, F, G: 500 nm. H) DLS analysis of Ag NPs (3 replicates).

3.2. Determination of rGO, rGO-Ag and Ag in water

After 30 minutes, rGO and rGO-Ag were not detected in water in rGO and rGO-Ag exposure groups, respectively. On the contrary, at the same sampling time, concentration of Ag in water in the rGO-Ag exposure group was higher than in the Ag NPs exposure group (Table 2A). However, after 20 h, both concentrations were similar since Ag concentration in water decreased, especially in the rGO-Ag NPs exposure group.

3.3. Bioaccumulation of Ag in mussel soft tissues

At day 3 of exposure, silver accumulation was higher (52,95% more) in mussels exposed to Ag NPs in comparison to mussels exposed to rGO-Ag. At day 21 of exposure silver accumulation in both exposure groups was similar (Table 2B, Figure 2) since accumulation of silver in mussels exposed to rGO-Ag increased and accumulation of silver in mussels exposed to Ag NPs decreased during exposure (Table 2B).

Table 2. Ag concentration in A) water samples (µg/L) at 30 minutes and at 20 hours post exposure and B) soft tissues (µg/g) of mussels from the t0 group, from the control group and after exposure to rGO, rGO-Ag and Ag NPs for 3 and 21 days. Data are given for three replicates at each exposure time ± standard deviation in A and for 5-8 mussels per exposure group and time in B.

A µg/L

Control		rGO-PVP		rGO-Ag		Ag NPs	
30 min	20 h	30 min	20 h	30 min	20 h	30 min	20 h
0,016 ± 0,007	0,033 ± 0,015	0,007 ± 0	0,023 ± 0,032	15,993 ± 13,307	0,508 ± 0,284	5,823 ± 0,748	0,708 ± 0,858

B µg/g

t0	t3				t21			
	Control	rGO-PVP	rGO-Ag	Ag NPs T3	Control	rGO-PVP	rGO-Ag	Ag NPs
0,213 ± 0,038	0,305 ± 0,015	0,204 ± 0	1,094 ± 0,13	2,325 ± 0	0,164 ±0,012	0,305 ± 0	1,627 ± 0,125	1,896 ± 0

3.4. Determination of rGO and rGO-Ag in mussel tissues and feces

Both rGO and rGO-Ag were determined in feces of mussels exposed to rGO and rGO-Ag, respectively, from day 1 of exposure (Figure S1). In addition, rGO and rGO-Ag were present in the lumen of the digestive tract after 3 and 21 days of exposure and between lamellae in gills of mussels exposed for 21 days (Figure 2). No presence of rGO or rGO-Ag was detected in the hemolymph of the same mussels or in the rest of tissues (Figure S1).

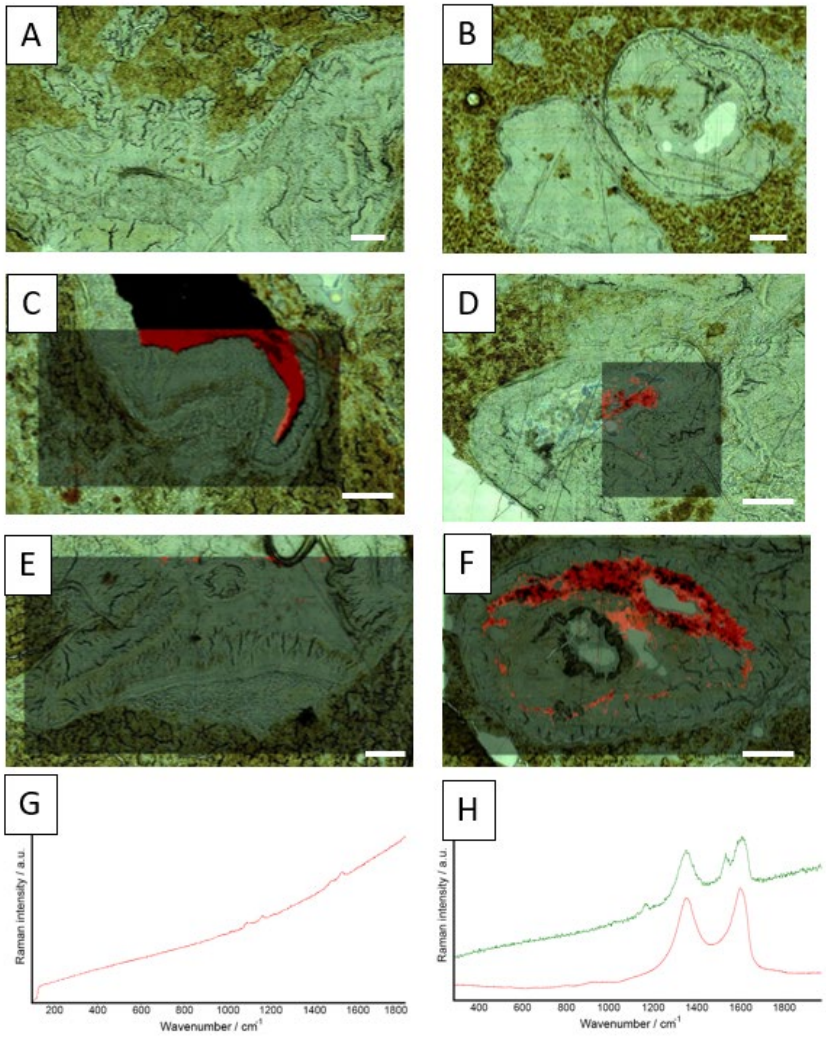

Figure 2: Heat maps showing the detection of rGO and rGO-Ag in cryostat sections of the digestive gland of different mussels; A: Control mussel, B: mussel exposed to Ag NPs for 21 days, C: mussel exposed to rGO for 3 days; D: mussel exposed to rGO for 21 days; E: mussel exposed to rGO-Ag for 3 days; F: mussel exposed to rGO-Ag for 21 days.; G: Raman spectra from the map in A; H: Raman spectra from the zones highlighted in red in map C (green spectrum) and the spectra obtained for the rGO stock (red spectrum). Scale bars: 200 µm.

3.5. Cellular biomarkers in hemocytes

Neutral red uptake did not reveal any impact in the viability of hemocytes in mussels exposed for 3 or 21 days or during the exposure (Figure S2). Catalase activity did not show any significant difference among exposure groups but, activity in control mussels and mussels exposed to rGO increased from day 3 to day 21 (Figure S2).

After 3 days of exposure DNA damage was observed in mussels exposed to rGO and to Ag NPs in comparison to control mussels. At day 21 of exposure hemocytes of mussels exposed to Ag NPs showed more DNA damage than controls. In addition, DNA damage in hemocytes of mussels exposed to rGO-Ag and to Ag NPs increased from day 3 to day 21 (Figure 3).

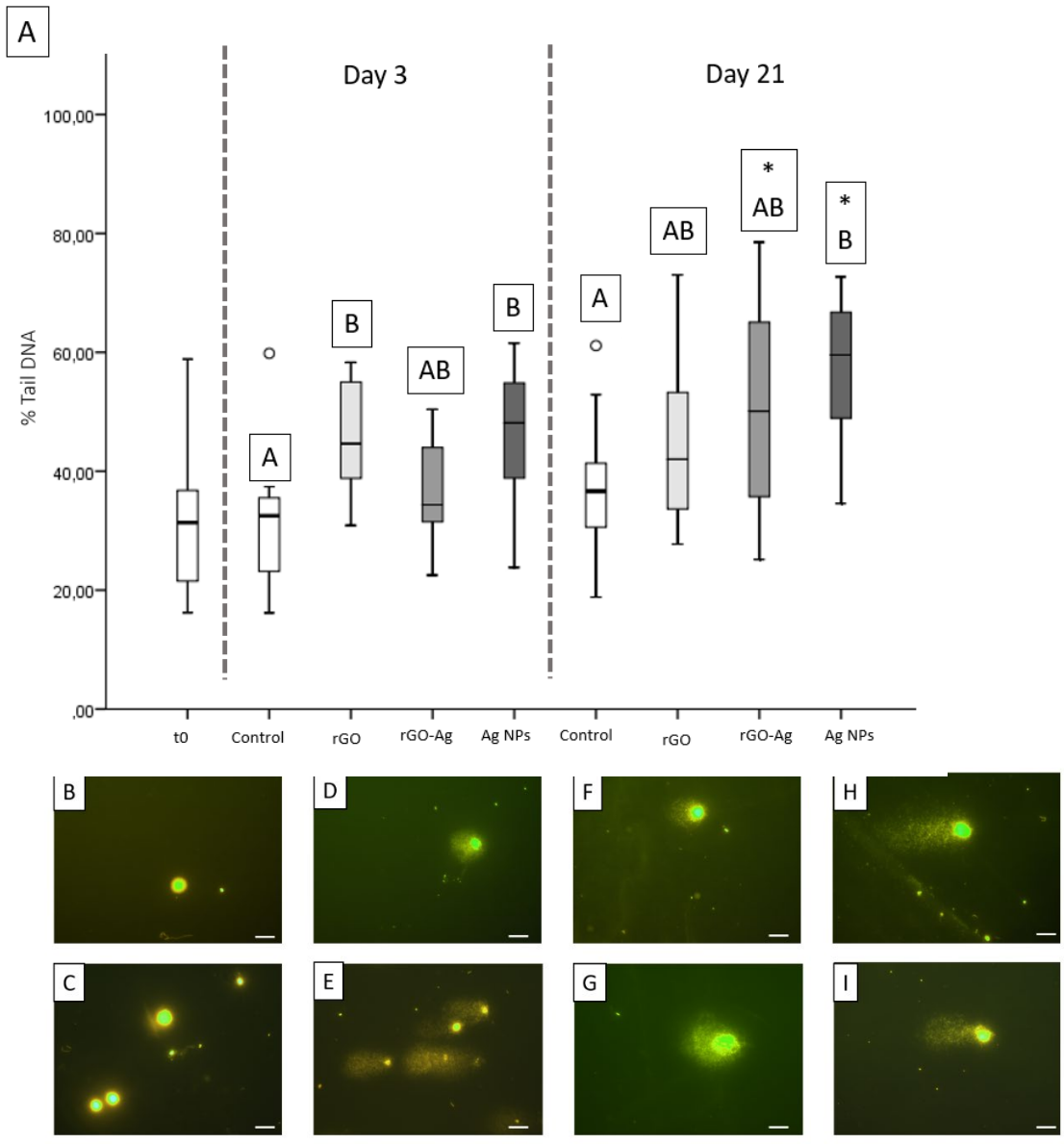

Figure 3 (previous page). A) DNA strand breaks (given as % tail DNA) in hemocytes of mussels from t0, control mussels and mussels exposed to rGO, rGO-Ag and Ag NPs after 3 and 21 days of exposure. Box-plots show median value (horizontal line), 25%-75% quartiles (box) and standard deviation (whiskers). Dots denote outliers, values that do not fall in the inner fences. Data are given for 50 cells in 2 slides per mussel. Letters indicate significant differences among treatments within the same day (Kruskal-Wallis followed by Dunn's post hoc test, $p < 0.05$). Asterisks indicate significant differences between days within the same treatment (Mann-Whitney´s U test, $p < 0.05$). Comet assay fluorescence micrographs displaying typical levels of DNA strand breaks for hemocytes from Control (B-C), rGO- (D-E), rGO-Ag (F-G) and Ag NPs (H-I), treatments at day 3 (B,D,F,H) and 21 (C,E,G,I) of exposure. Scale bars: 20 µm

3.6. Gene transcription levels in the digestive gland

cat was downregulated in mussels exposed to Ag NPs for 21 days in comparison to control mussels and mussels exposed to rGO and rGO-Ag. In addition, *cat* transcription levels decreased in mussels exposed to Ag NPs from day 3 to day 21 (Figure 4A). *aox1* transcription levels were similar among exposure groups but mRNA levels decreased during the exposure in mussels exposed to Ag NPs (Figure 4B). Similarly, *hsp90* transcription levels decreased along the experiment in mussels exposed to rGO and Ag NPs (Figure 4C). In addition, downregulation of *hsp90* was observed in mussels exposed to Ag NPs for 21 days in comparison to control mussels. No differences were observed in the transcription levels of *sod* (Figure 4D) and *gstpi1* (Figure 4E).

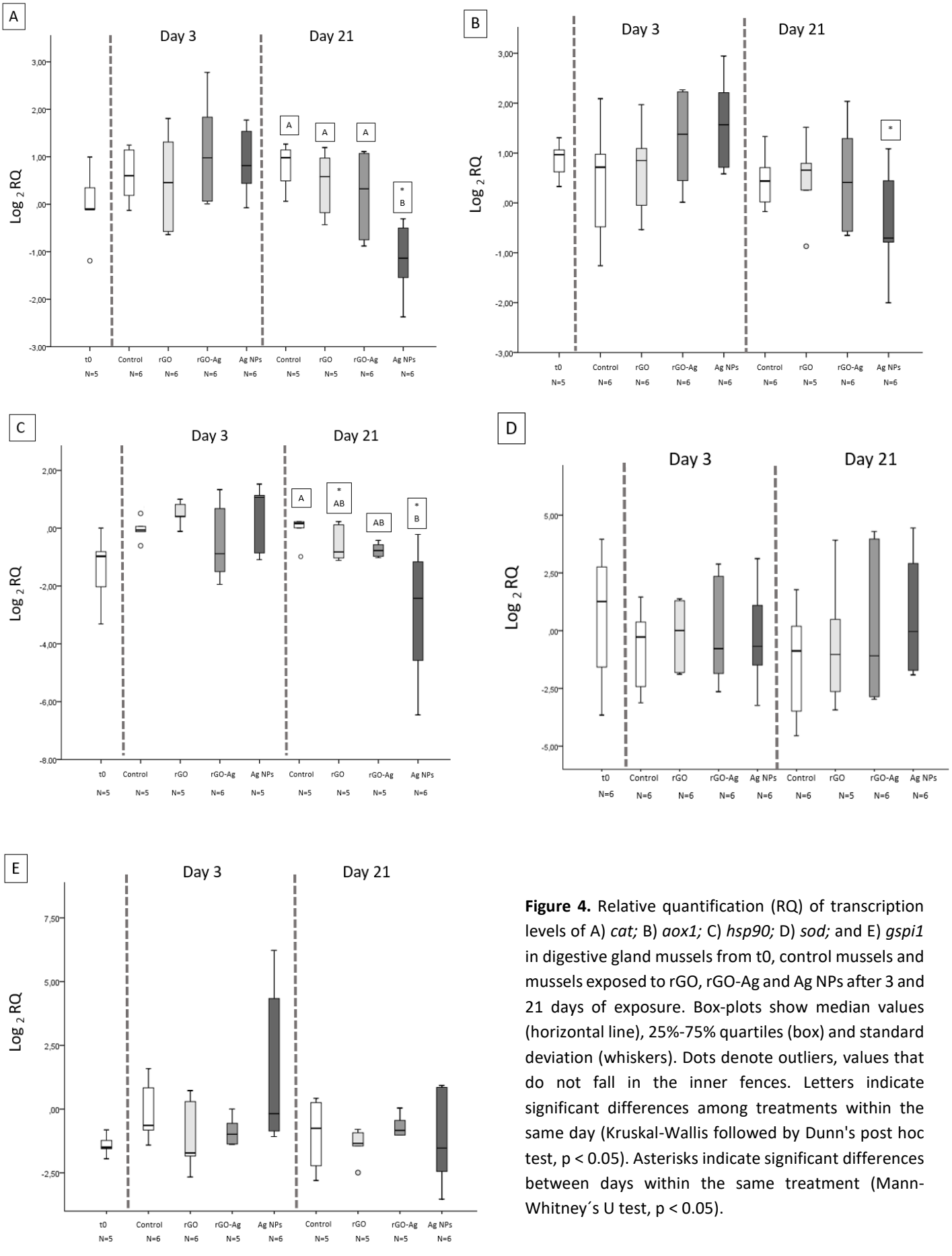

Figure 4. Relative quantification (RQ) of transcription levels of A) *cat;* B) *aox1;* C) *hsp90;* D) *sod;* and E) *gspi1* in digestive gland mussels from t0, control mussels and mussels exposed to rGO, rGO-Ag and Ag NPs after 3 and 21 days of exposure. Box-plots show median values (horizontal line), 25%-75% quartiles (box) and standard deviation (whiskers). Dots denote outliers, values that do not fall in the inner fences. Letters indicate significant differences among treatments within the same day (Kruskal-Wallis followed by Dunn's post hoc test, $p < 0.05$). Asterisks indicate significant differences between days within the same treatment (Mann-Whitney´s U test, $p < 0.05$).

3.7. Enzyme activities in mussel tissues

Regarding aerobic metabolism, mussels exposed to Ag NPs showed lower IDH activity than control mussels and mussels exposed to rGO at day 3 of exposure, whereas after 21 days of exposure, no differences were observed among groups. In control mussels and in mussels exposed to rGO and rGO-Ag IDH activity decreased during the experiment (Figure 5A). On the contrary, the anaerobic metabolism measured in terms of ODH, did not show any difference at day 3 of exposure while after 21 days of exposure, mussels exposed to Ag NPs showed higher ODH activity than control mussels. ODH activity decreased duringthe exposure period in control mussels and in mussels exposed to rGO-Ag (Figure 5B). The first and rate limiting enzyme of the peroxisomal β oxidation, AOX1, did not show any significant difference among exposure groups or exposure days (Figure S3A).

The activity of the enzyme involved in neurotransmission AchE, was lower in mussels exposed to Ag NPs in comparison to mussels exposed to rGO-Ag after 3 days of exposure, though no differences were detected with respect to the control. Overall, after 21 days of exposure, AchE activity was higher than after 3 days in all the groups and mussels exposed to Ag NPs and rGO-Ag showed higher activity than controls (Figure 6A).

The phase 2 biotransformation metabolism was assessed based on the activity of GST, which was lower in gills of mussels exposed to Ag NPs than in control mussels and in mussels exposed to rGO-Ag after 3 days of exposure. On the contrary, at day 21 of exposure, mussels exposed to Ag NPs showed higher GST activity than controls and mussels exposed to rGO-Ag due to the time-dependent increase of the activity in mussels exposed to Ag NPs (Figure 6B). In the digestive gland, GST activity was similar among groups, but it decreased during the experiment in exposed mussels (Figure S3B).

Regarding oxidative stress, catalase activity in gills did not show significant differences among exposure groups at day 3 and day 21 of exposure, but the activity increased during the exposure period in control mussels and in mussels exposed to rGO and rGO-Ag (Figure S3C). In the digestive gland, mussels exposed to rGO-Ag for 3 days showed higher catalase activity than control mussels. After 21 days of exposure, lower catalase activity was found in mussels exposed to rGO than in controls. Catalase activity

increased through the experiment in control mussels and in mussels exposed to Ag NPs (Figure 7A).

On the other hand, higher LPO was measured in mussels exposed to rGO-Ag in comparison to control mussels at day 3 of exposure whereas no differences were found among groups at day 21 of exposure. In addition, LPO decreased through the experiment in mussels exposed to rGO-Ag (Figure 7B).

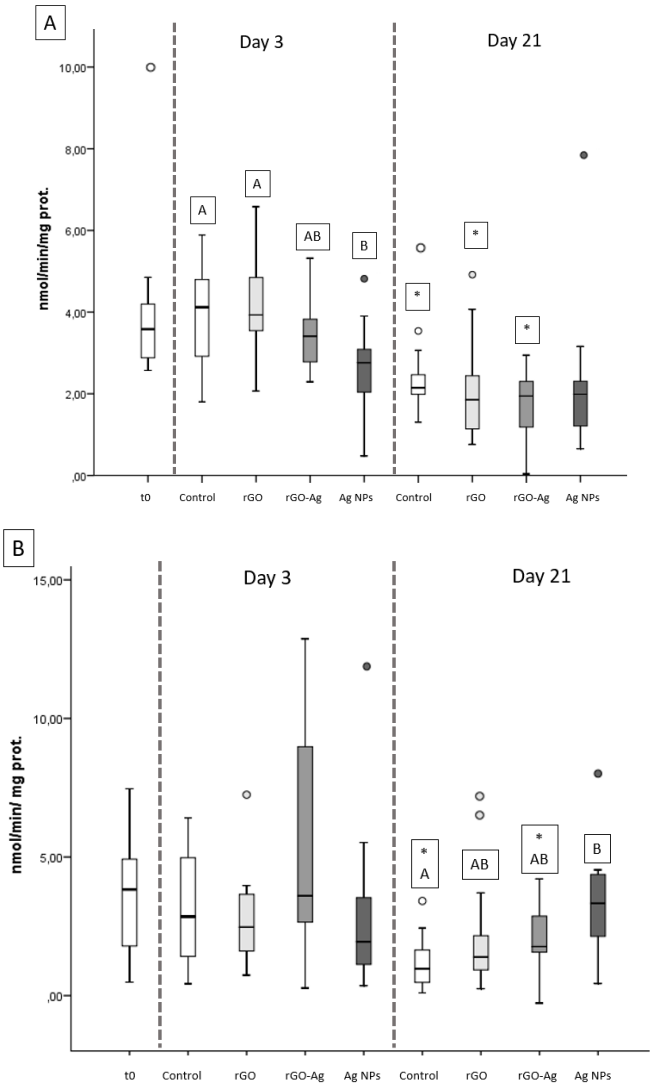

Figure 5. Activities (given as nmol/min/mg protein) of A) IDH and B) ODH in foot of mussels from t0, control mussels and mussels exposed to rGO, rGO-Ag and Ag NPs after 3 and 21 days of exposure. Box-plots show median value (horizontal line), 25%-75% quartiles (box) and standard deviation (whiskers). Dots denote outliers, values that do not fall in the inner fences. Letters indicate significant differences among treatments within the same day (one-Way Anova followed by Tukey's post hoc in A and Kruskal-Wallis test followed by Dunn's post hoc in B, $p<0.05$). Asterisks indicate significant differences between days within the same treatment (Mann-Whitney´s U test, $p < 0.05$).

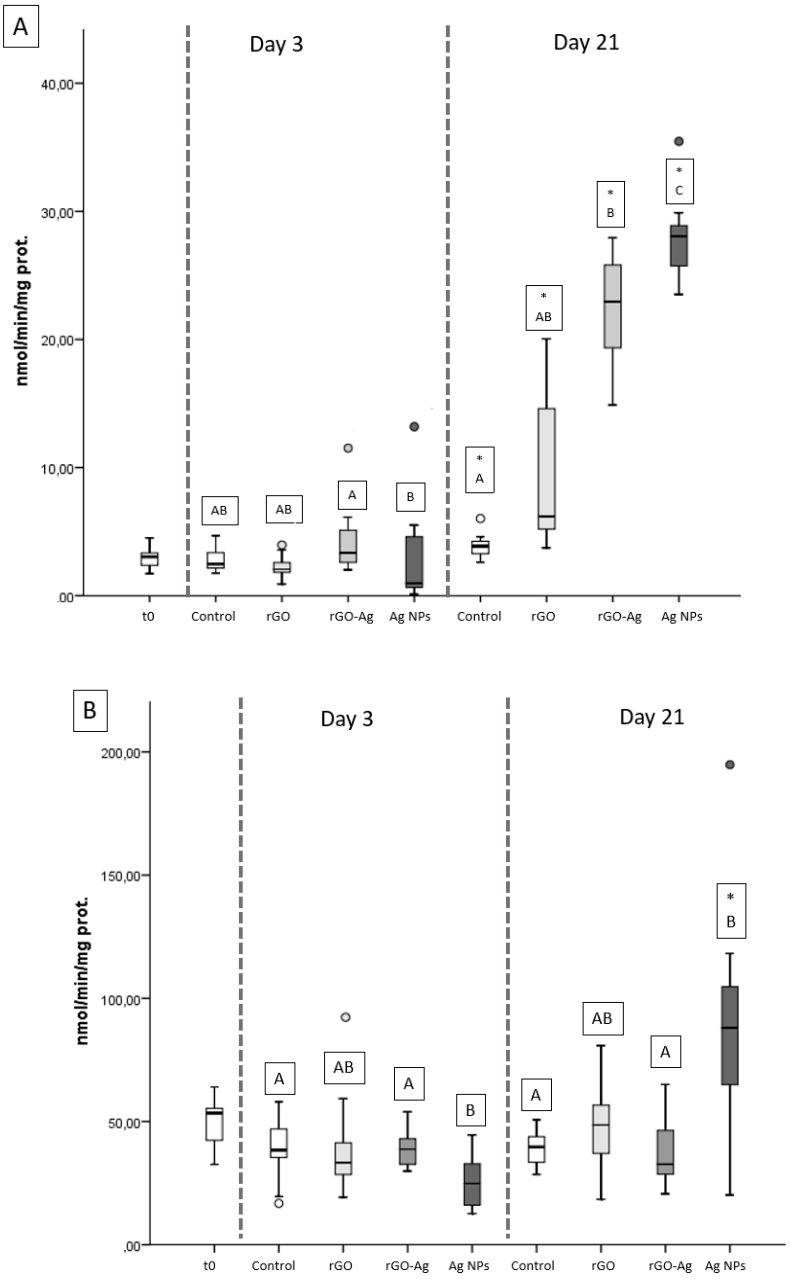

Figure 6. Activities (given as nmol/min/mg protein) of A) AchE in adductor muscle; B) GST in gills of mussels from t0, control mussels and mussels exposed to rGO, rGO-Ag and Ag NPs after 3 and 21 days of exposure. Box-plots show median value (horizontal line), 25%-75% quartiles (box) and standard deviation (whiskers). Dots denote outliers, values that do not fall in the inner fences. Letters indicate significant differences among treatments within the same day (Kruskal-Wallis test followed by Dunn's post hoc, $p<0.05$). Asterisks indicate significant differences between days within the same treatment (Mann-Whitney´s U test, $p < 0.05$).

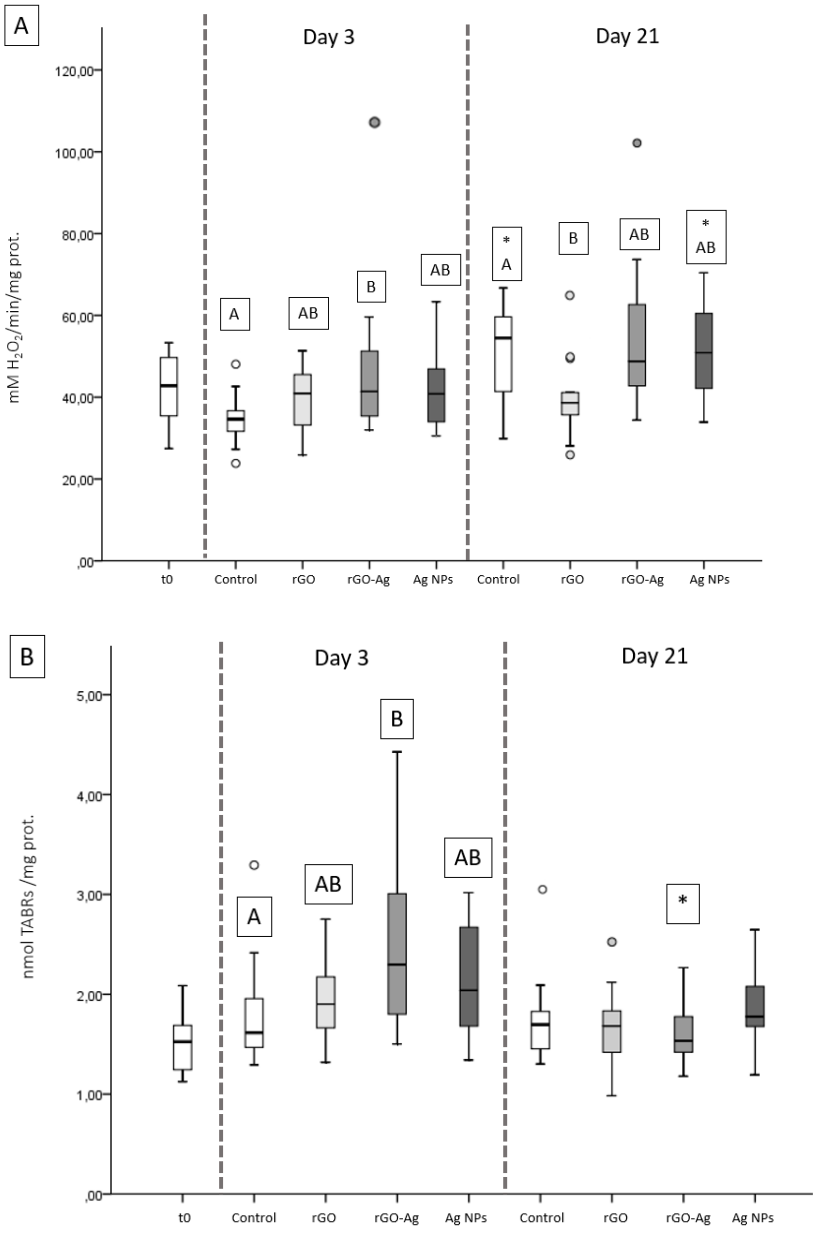

Figure 7. A) Catalase activity (given as mM H_2O_2/min/mg prot) and B) Lipid peroxidation (given as nmol TBARS /mg prot) in digestive gland of mussels from t0, control mussels and mussels exposed to rGO, rGO-Ag and Ag NPs after 3 and 21 days of exposure. Box-plots show median value (horizontal line), 25%-75% quartiles (box) and standard deviation (whiskers). Dots denote outliers, values that do not fall in the inner fences. Letters indicate significant differences among treatments within the same day (Kruskal-Wallis test followed by Dunn's post hoc, $p<0.05$). Asterisks indicate significant differences between days within the same treatment (Mann-Whitney´s U test, $p < 0.05$).

3.8. Gamete development, gonad index and histopathology of mussel gonad

Most of the animals studied were in a mature or spawning gamete developmental stage (Figure S4). Gonad index (GI) was between 3 and 4, with no differences among exposure groups (Figure S4). GI increased in controls at day 21 of exposure in comparison with day 3 (Figure S4A). In females, GI was around 3 and no differences were observed among exposure groups or exposure days (Figure S4B). In males, GI was around 4 with no differences among exposure groups but with a higher GI in controls of day 21 of exposure in comparison with day 3 (Figure S4C).

In general, low prevalences of non-specific inflammatory responses were observed in all exposure groups (Table 3). At day 21 of exposure, mussels exposed to rGO, rGO-Ag and Ag NPs showed higher hemocytic infiltration than control mussels and prevalence of brown cell aggregation was higher in mussels exposed to rGO-Ag than in control mussels (Table 3). In addition, oocyte atresia tended to increase at day 21 of exposure in all the groups, but a higher prevalence of atresia was especially evident in mussels exposed to rGO and rGO-Ag and intensity of atresia in mussels exposed to Ag NPs (Table 3). A similar trend was observed in oocyte necrosis, with slightly higher prevalences in mussels exposed to rGO and rGO-Ag (Table 3). Parasites such as *Nematopsis spp.* were observed in several individuals and a trematode was observed in a single individual exposed to rGO for 3 days (Table 3).

3.9. Whole organism responses

During the experiment, 6 mussels exposed to Ag NPs were found death.

At day 3 of exposure, the digestive gland index did not reveal any difference among exposure groups, but at day 21, the index was lower in mussels exposed to rGO and rGO-Ag than in control mussels and mussels exposed to Ag NPs (Figure 8A). In addition, the digestive gland index of control mussels increased during the experiment, whereas it decreased in mussels exposed to rGO (Figure 8A).

Condition index did not vary among groups at 3 and 21 days of exposure, but it increased from day 3 to day 21 in all the exposure groups (Figure 8B).

Table 3. Prevalence of histopathological alterations in gonad of mussels from t0, control mussels and mussels exposed to rGO, rGO-Ag and Ag NPs after 3 and 21 days of exposure. Data are shown as percentage for a total of 15 mussels per experimental group (one section per mussel). A semiquantitative index was used to determine the intensity of oocyte atresia. Not observed, n.o. Letters indicate a significant difference among groups within the same exposure day and asterisks indicate a significant difference between days within treatments (X^2 test; $p<0.05$).

		Atresia		Oocyte necrosis	Hemocytic infiltration	Brow cell aggregation	*Nematopsis sp.*
		Pevalence	**Intensity**				
	t0	88.89	1.33	0	20	6.67	0
t3	**Control**	25	1	12.5	33,33	13.33	33-33[a]
	rGO	37.5	1	37.5	20	20	6.67[ab]
	rGO-Ag	37.5	1	37.5	20	20	6.67[ab]
	Ag NPs	33.33	1	16.67	40	6.67	n.o.[b]
t21	**Control**	50	1	n.o.	13.33[a]	n.o.[a]	6.67
	rGO	66.67	1	55.56	60[b*]	20[ab]	6.67
	rGO-Ag	80	1	40	53.33[b]	26.67[b]	13.33
	Ag NPs	42.85	2,33	14.29	46.67[b]	20[ab]	6.67

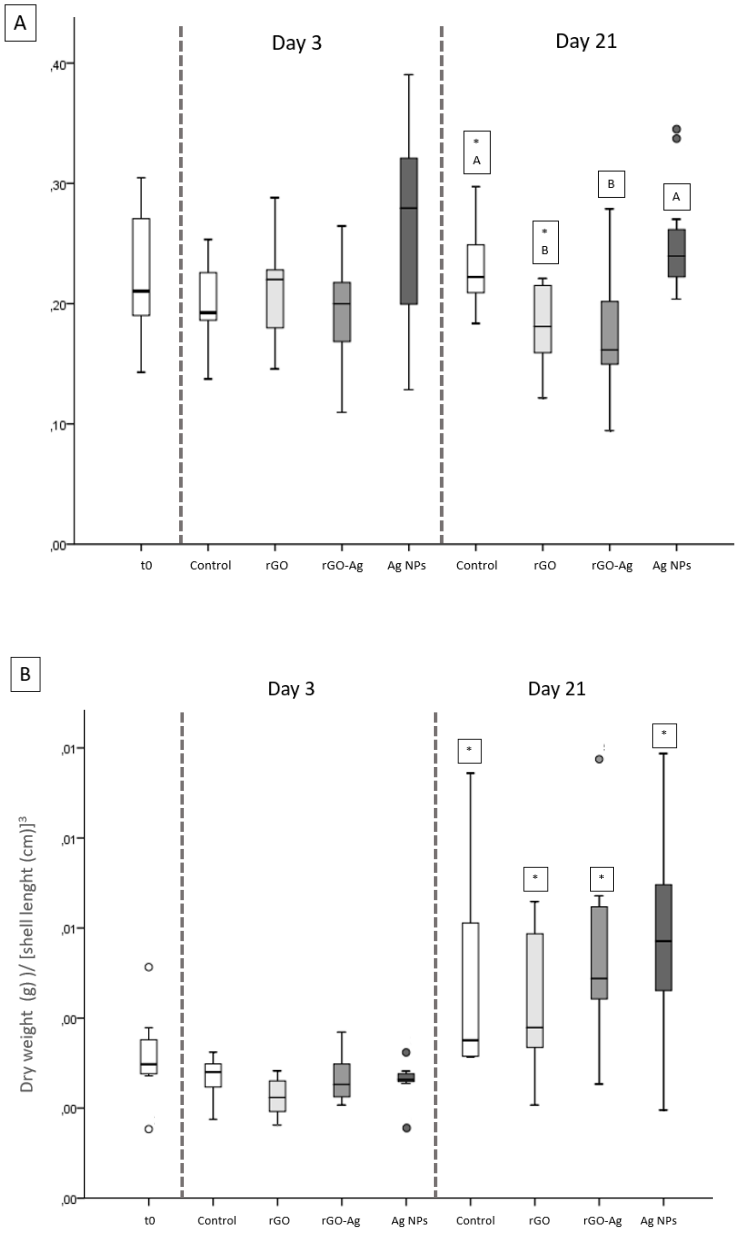

Figure 8. A) Digestive gland index; B) Condition index (g dry weight/cm^3) of mussels from t0 control mussels and mussels exposed to rGO, RGO-Ag and Ag NPs after 3 and 21 days of exposure. Box-plots show median value (horizontal line), 25%-75% quartiles (box) and standard deviation (whiskers). Dots denote outliers, values that do not fall in the inner fences. Letters indicate significant differences among treatments within the same day (Kruskal-Wallis test followed by Dunn's post-hoc, $p<0.05$). Asterisks indicate significant differences between days within the same treatment (Mann-Whitney´s U test, $p < 0.05$).

4. DISCUSSION

Assessment of GFNs toxicity requires consideration on the great impact that small variations in the structure and properties of GFNs have in their environmental fate and behavior and as a consequence, in their toxicity (Goodwin et al., 2018; Malina et al., 2020; Peng et al., 2020; Zhao et al., 2021). Addition of Ag NPs on rGO platelets, changes the structure of platelets from 2D to a 3D appearance, which probably difficults their penetration through cell membranes (Peng et al., 2020) and helps to explain the lack of response in hemocytes of mussels exposed to rGO-Ag unlike exposure to rGO platelets that caused DNA damage in hemocytes. Ag NPs that form rGO-Ag NPs nanocomposites were difficult to observe in TEM images, but the diameter of visible Ag NPs was between 100 and 200 nm. Thus, particles in the rGO-Ag hybrid were bigger than those present in the Ag NPs suspension. This difference should be considered to compare toxicity of both treatments since the toxicity of Ag NPs is known to be size dependent (Kim et al., 2012). In addition, shape of particles in the Ag NPs suspension was heterogeneous, including dot-like and needle like particles, may be due to a slow reduction reaction during the synthesis process that allowed aggregation of particles and formation of different geometries.

Production of rGO-Ag started with a 75% of rGO and 25% of silver, however the TGA analysis showed that in the final rGO-Ag product, Ag NPs were 19,4% of the compound. This low presence of Ag NPs could explain why after 3 days of exposure, mussels exposed to rGO-Ag accumulated less silver than mussels exposed to Ag NPs alone. Moreover, the Raman spectroscopy showed that mussels exposed to rGO and rGO-Ag excreted GFNs in feces from the first day of exposure, which could have reduced the amount of Ag able to accumulate in tissues in mussels exposed to rGO-Ag NPs in comparison to mussels exposed to Ag NPs. However, rGO-Ag was not internalized in the epithelium of the digestive gland or rest of tissues and it was only observed in the lumen of the digestive tract. This was in agreement with results in Chapter 3 which show that adult mussels exposed to GO and GO with sorbed benzo(a)pyrene presented GO in the lumen of the digestive tract and feces, but not in the rest of tissues. Similarly, GFNs have been previously localized in the digestive tract of other aquatic invertebrates (Mesaric et al., 2015; Zhu et al., 2017; Lu et al., 2018; Souza et al., 2018; Zhang. et al., 2019; Josende et

al., 2020; Bortozollo et al., 2021), but rarely in the rest of tissues. Therefore, this heterogeneous distribution as well as intake and excretion mechanisms of NMs will determine toxicity to organisms after *in vivo* exposures Ou et al. (2016).

Silver accumulation in mussels exposed to rGO-Ag was higher after 21 days than after 3 days. On the contrary, in mussels exposed to Ag NPs, higher concentration of silver was found at day 3 of exposure in comparison to day 21. In both sampling days, concentration in mussels exposed to Ag NPs was higher than in mussels exposed to rGO-Ag. This reduction in the accumulation of silver in mussels exposed to Ag NPs, could be due to a defense mechanism of mussels which could have closed their valves to avoid toxicity and thus, less water, including nutrients and Ag NPs entered in the organism. In fact, 5 mussels died in the Ag NPs exposure group and exposure to Ag NPs affected almost all the biological organization levels examined in this work. Ag NPs altered gene transcription levels as well as enzyme activities related to neurotransmission, aerobic and anaerobic metabolism and phase 2 biotransformation metabolism and caused DNA damage in mussel hemocytes and inflammatory reactions in the gonad. Most of these effects have been previously described after exposure to Ag NPs (Cajaraville et al., 2021).

In general, rGO-Ag as well as rGO showed lower toxicity than Ag NPs alone. Exposure to rGO-Ag and rGO did not alter viability and catalase activity of hemocytes and though exposure to rGO damaged DNA of hemocytes in mussels exposed for 3 days, DNA damage caused by the exposure to Ag NPs remained even after 21 days of mussel exposure. Genotoxicity caused by GFNs has been already described in several organisms including insects, fish, crustaceans and lugworms (Chen et al., 2015; 2016; Fernandes et al., 2017; Souza et al., 2017; Zhang et al., 2017; Dziewiecka et al 2018; Flasz et al., 2020; Zhao et al., 2021). Before Chapter 3 was develop, a single publication had reported genotoxicity caused by GFNs in mussels (Meng et al., 2020). In addition, the transitory effect observed after exposure to rGO-Ag NPs was already described in crickets exposed to GFNs (Flasz et al., 2020).

At molecular level, exposure to rGO-Ag and rGO did not alter transcription levels of any of the target genes (*cat, sod, gstpi1, aox1* and *hsp90*). Similarly, *cat, sod* and *gst* were not altered in zebrafish exposed for 3 and 21 days to GO (Martinez-Alvarez et al., 2021). On the other hand, Meng et al. (2019) reported up-regulation of *hsp90* in mussels

exposed to graphene alone and co-exposed with triphenyl phosphate. On the contrary, *hsp90* and *cat* were downregulated in the present study after 21 days of exposure to Ag NPs. Heat shock proteins are a big family of proteins that have been related to the physiological plasticity of bivalves towards multiple stressors (Cruz-Rodriguez & Chu, 2002; Fabbri et al., 2008). Bebianno et al. (2015) described a slight downregulation of *hsp70* in gills of mussels exposed to Ag NPs while Gomes et al. (2014) reported downregulation of the *hsp70* in the same experimental conditions as Bebianno et al. (2015). In addition, Bebianno et al. (2015) also reported a non-significant downregulation of *cat* after Ag NPs exposure, which was not followed by the enzyme activity as reported by Gomes et al. (2014).

IDH activity involved in the aerobic metabolism decreased in mussels exposed to Ag NPs at short term exposure. Consequently, activity of ODH involved in the anaerobic metabolism increased in the same mussels after 21 days of exposure. Downregulation of the gene coding for IDH was observed in the microalgae *Chlorella pyrenoidesa* after exposure to Ag NPs (Cao et al., 2021). In bivalves, IDH activity has showed to be a sensitive biomarker for multiple contaminants including metals (Rodriguez-Ortega et al., 2001; Lima et al., 2007; Oliveira et al., 2018). On the other hand, the increase in the activity of ODH could respond to the defense mechanism of mussels to the exposure to Ag NPs also mentioned above. It is known that under untoward conditions mussels tend to reduce filtration, by closing their valves. This could cause reduction of cellular respiration and activation of the anaerobic metabolism in order to obtain energy (Storey & Storey, 1983; Long et al., 2003). Osswald et al. (2013) recorded that in trouts exposed to anatoxin-a showed enzyme activities related to the anaerobic metabolism and AchE activity increased in an attempt to obtain extra energy to defend themselves against pollutants. Accordingly, in the present study, AchE activity was increased in mussels exposed to rGO-Ag and Ag NPs after 21 days of exposure.

The phase 2 biotransformation metabolism was only alter after exposure to Ag NPs. GST activity decreased at day 3 of exposure in mussels exposed to Ag NPs and increased after 21 days of exposure in gills. However, no significant responses were observed in the digestive gland. Tissue dependent GST activity responses have been already reported in crabs exposed to Ag NPs (Walters et al., 2015). In mussels, gills are the first barrier

towards environmental contaminants and thus, higher detoxification rates such as higher GST activities could be expected in comparison to other tissues such as digestive gland (Cheung et al., 2001). In addition, gills have been also reported as the most sensitive organ for other NMs such as Cd quantum dots (Rocha et al., 2015).

Mussels exposed to rGO-Ag for 3 days showed higher catalase activity and higher lipid peroxidation in the digestive gland. This response seemed to be transitory as no effect was observed at day 21 of exposure. The fact that rGO-Ag showed higher toxicity in the digestive gland than in gills could be due to its internalization form. As it was mentioned before, rGO-Ag was localized in the lumen of the digestive tract where due to digestive process release of Ag from rGO-Ag is expected. On the other hand, rGO alone caused inhibition of catalase activity after 21 days of exposure in the digestive gland. Interestingly, this inhibition could be linked to the transitory DNA damage observed in hemocytes of mussels exposed to rGO. Therefore, the late response in the antioxidant defense could compensate DNA damage, although catalase activity was not altered in hemocytes. In addition, catalase activity was not altered in hemocytes, gills or digestive gland of mussels exposed for 7 days to GO alone in Chapter 3. This lack of agreement on the antioxidant response in organisms exposed to GFNs has already been addressed in the literature. One of the main explanations for this phenomenon is the inevitable difference among the nanoplatelets used, as their surface elements are linked to the reactivity of nanoplatelets and therefore to their toxicity (Katsumiti et al., 2017; Malina et al., 2020; Peng et al., 2020; Bortolozzo et al., 2021).

Oxidative stress was not evidenced in mussels exposed to Ag NPs, which could be explained by the lower bioaccumulation of Ag observed from day 3 to day 21 of exposure. This decrease could have been promoted by the activation of detoxification processes through exocytosis of lysosomes. Exocytosis of lysosomes containing xenobiotics has been previously proposed as a possible detoxification mechanism in mussels (Cajaraville et al., 1995a, 1995b; Cancio et al., 1995; Zorita et al., 2006). Decrease in Ag accumulation in exposures longer than 2 weeks due to the elimination of nanoparticles through the activation of detoxification processes has already being reported for mussels (Gomes et al., 2013).

Zorita et al. (2006) observed metal deposits in the lumen of digestive tubules that corresponded to mussel metal levels. In addition, Zorita et al. (2006) also reported a high amount of brown cell accumulations related to metal exposure. Similarly, in the present work a higher prevalence of brown cell aggregations was observed in the gonad of mussels exposed to rGO-Ag in comparison to controls at day 21 of exposure. This could point to a synergetic effect after exposure to rGO-Ag. The enhanced toxicity caused by hybrid nanocomposites formed by GFNs and Ag NPs, has been already discussed in the literature (De Luna et al., 2016).

Moreover, at day 21 of exposure, hemocytic infiltration was observed in gonad of mussels exposed to rGO-Ag, rGO, and Ag NPs. A similar result was described in Chapter 3, where a general inflammatory response was found in mussels exposed to GO and GO with sorbed benzo(a)pyrene in gonads and digestive glands, in agreement also with the literature that pointed to the capacity of GFNs to cause inflammatory reactions (Chen et al., 2012; 2020; Khan et al., 2019). It was reported that these reactions might be caused by the physical hazard that sharp edges of GFNs may do in tissues (Dziewiecka et al. 2018). In addition, combination of GFNs with metal compounds could induce necrosis and apoptosis in oocytes (Coppola et al. 2020). In the present study, a slightly higher prevalence of oocyte necrosis was observed in mussels exposed to rGO-Ag and rGO after 21 days in comparison with the controls.

GFNs have been reported to cause tissue loss and digestive tubule atrophy in digestive gland of bivalves (Meng et al., 2019; Coppola et al., 2020; Bi et al., 2022). Similarly, digestive gland index decreased in the present study in mussels exposed to rGO-Ag and rGO at day 21 of exposure. Exposure to pollutants has been related to the loss of the digestive gland epithelium through epithelial thinning and atrophy (Lowe et al., 1981; Couch, 1984; Lowe and Clarke, 1989; Vega et al., 1989; Cajaraville et al., 1992; Garmendia et al., 2010; Lopes et al., 2016), which indicates that health condition in mussels was reduced (Marigómez et al., 2006; Garmendia et al., 2011).

5. CONCLUSIONS

The hybrid nanocomposite rGO-Ag as well as rGO were internalized via ingestion and rapidly excreted in mussels as detected by Raman spectroscopy. Ag bioaccumulation occurred upon exposure to rGO-Ag but at much lower extent than in mussels exposed to equivalent concentrations of Ag nanoparticles. Exposure to rGO-Ag altered enzyme activities and caused oxidative damage in digestive gland at 3 days of exposure, increased inflammatory responses and decreased the digestive gland index after 21 days of exposure. These cell, tissue and organism level alterations were partially comparable to impacts caused by rGO and by Ag nanoparticles alone though Ag nanoparticles exerted less toxicity when dosed as rGO-Ag than alone.

ACKNOWLEDGEMENTS

This work was funded by Spanish MINECO (NACE project CTM2016-81130-R), Basque Government (consolidated research group IT1302-19 and IT1743-22, and predoctoral fellowship to NGS).

REFERENCES

Alian, R., Dziewięcka, M., Kędziorski, A., Majchrzycki, Ł., & Augustyniak, M. (2021). Do nanoparticles cause hormesis? Early physiological compensatory response in house crickets to a dietary admixture of GO, Ag, and GOAg composite. Science of the Total Environment, 788

Azizi M., Navidbakhsh M., Hosseinzadeh S., Sajjadi M. 2019. Cardiac cell differentiation of muscle satellite cells on aligned composite electrospun polyurethane with reduced graphene oxide, Journal of Polymer Research 26, 258.

Banni M., Negri A., Mignone F., Bousetta H., Viarengo A. and Dondero F. 2011. Gene expression rythms in the mussel *Mytilus galloprovincialis* (Lam.) across an annual cycle. PLoS ONE 6 (5): e18904.

Bebianno M.J., Gonzalez-Rey M., Gomes T. Mattos J.J., Flores-Nunes F., Bainy A.C.D. 2015. Is gene transcription in mussel gills altered after exposure to Ag nanoparticles? Environmental Science and Pollution Research 22, 17425-17433.

Bi C., Junaid M., Liu Y., Guo W., Jiang X., Pan B., Li Z., Xu N. 2022. Graphene oxide chronic exposure enhanced perfluorooctane sulfonate mediated toxicity through oxidative stress generation in freshwater clam *Corbicula fluminea*. Chemosphere 297, 134242.

Bianco A., Cheng H.-M., Enoki T., Gogotsi Y., Hurt R.H., Koratkar N., Kyotani T., Monthioux M., Park C.R.,. Tascon J.M.D, Zhang J. 2013. All in the graphene family - a recommended nomenclature for two-dimensional carbon materials. Carbon 65, 1–6.

Blaser S.A., Scheringer M., Macleod M., Hungerbühler K. 2008. Estimation of cumulative aquatic exposure and risk due to silver: contribution of nano-functionalized plastics and textiles. Science of the Total Environment 390: 396-409.

Bortolozzo L.S., Coa F., Khan L.U., Medeiros A.M.Z., Da Silva G.H., Delite F.S., Strauss M., Martinez D.T.S. 2021. Mitigation of graphene oxide toxicity in *C. elegans* after chemical degradation with sodium hypochlorite. Chemosphere 278, 130421.

Bradford MM. 1976. A rapid and sensitive method for the quantitation of microgram quantities of protein utilizing the principle of protein-dye binding. Analytical Biochemistry 72, 248-254.

Britto R.S., Nascimento J.P., Serodre T., Santos A.P., Soares A.M.V.M, Furtado C., Ventura-Lima J., Monserrat J.M., Freitas R. 2021. Oxidative stress in *Ruditapes philippinarum* after exposure to different graphene oxide concentrations in the presence and absence of sediment. Comparative Biochemistry and Physiology, Part C 240, 108922.

Cajaraville M.P., Duroudier N., Bilbao E. 2021. Mechanisms of toxicity of engineered nanoparticles: adverse outcome pathway for dietary silver nanoparticles in mussels. Health and Environmental Safety of Nanomaterials (Second Edition) Polymer Nancomposites and Other Materials Containing Nanoparticles Woodhead Publishing Series in Composites Science and Engineering, 39-82.

Cajaraville MP, Abascal I, Etxeberria M, Marigómez I. 1995a. Lysosomes as cellular markers of environmental pollution time-dependent and dose-dependent responses of the digestive lysosomal system of mussels after petroleum hydrocarbon exposure. Environmental Toxicology and Water Quality 10, 1–8.

Cajaraville MP, Marigómez JA, Díez G, Angulo E. 1992. Comparative effects of the water accommodated fraction of three oils on mussels—2. Quantitative alterations in the structure of the digestive tubules. Comparative Biochemistry and Physiology 102C, 113-123.

Cajaraville MP, Robledo Y, Etxeberria M, Marigómez I. 1995b. Cellular biomarkers as useful tools in the biological monitoring of environmental pollution: molluscan digestive lysosomes. In: Cajaraville, M.P. (Ed.), Cell Biology in Environmental Toxicology. University of the Basque Country, Press Service

Cajaraville, M.P., Bebianno, M.J., Blasco, J., Porte, C., Sarasquete, C., Viarengo, A., 2000. The use of biomarkers to assess the impact of pollution in coastal environments of the Iberian Peninsula: a practical approach. Sci. Total Environ. 247, 295-311.

Cancio, I., Gwynn, I.A., Ireland, M.P., Cajaraville, M.P., 1995. The effects of sublethal lead exposure on ultrastructure and on the distribution of acid phosphatase activity in chloragocytes of earthworms (Annelida, Oligochaeta). Histochem. J. 27, 965–973.

Canesi L., Ciacci C., Fabbri R., Marcomini A., Pojana G. and Gallo G. 2012. Bivalve molluscs as a unique target group for nanoparticle toxicity. Marine Environmental Research 76, 16-21.

Cao M., Huang X., Wang F., Zhang Y., Zhou B., Chen H., Yuan R., Ma S., Geng H., Xu D., Yan C., Xing B. 2022. Transcriptomics and metabolimics revealed the biological response of *Chlorella pyrenoidesa* to single and repeated exposures of Ag NPs at different concentrations. Environmental Science and Technology 55, 15776-15787.

Cartier S., Pellerin J., Fournier M., Tamigneaux E., Girault L., Lemaire N. 2004. Use of an index based on the blue mussel (*Mytilus edulis* and *Mytilus trossulus*) digestive gland weight to asses the nutritional quality of mussel farm sites. Aquaculture 241, 633-654.

Chen L., Hu P., Zhang L., Huang S., Luo L., Huang C., 2012. Toxicity of graphene oxide and multi-walled carbon nanotubes against human cells and zebrafish. Science China Chemistry 55 2209-2216.

Chen Y., Hu X., Sun J., Zhou Q. 2015. Specific nanotoxicity of graphene oxide during zebrafish embryogenesis. Nanotoxicology 10, 42–52.

Chen Z., Yu C., Khan I.A., Tang Y., Liu S., Yang M. 2020. Toxic effects of different-sized graphene oxide particles on zebrafish embryonic development. Ecotoxicology and Environmental Safety 197, 110608.

Chen, J., Sun, L., Cheng, Y., Lu, Z., Shao, K., Li, T., Hu, C., Han, H., 2016. Graphene oxide-silver nanocomposite: novel agricultural antifungal agent against *fusarium graminearum* for crop disease prevention. ACS Applied Materials & Interfaces 8, 24057–24070

Cheung, C.C.C., Zheng, G.J., Li, A.M.Y., Richardson, B.J., Lam, P.K.S., 2001. Relationships between tissue concentrations of polycyclic aromatic hydrocarbons and antioxidative responses of marine mussels*, Perna viridi*s. Aquatic. Toxicology. 52, 189–203.

Cruz-Rodríguez L.A., Chu F.L.E. 2002. Heat-shock protein (HSP70) response in the eastern oyster, Crassostrea virginica, exposed to PAHs sorbed to suspended artificial clay particles and to suspended field contaminated sediments. Aquatic Toxicology 60, 157–168.

Coppola F., Bessa A., Henriques B., Russo T., Soares A.M.V.M., Figueira E., Marques P.A.A.P., Polese G., Di Cosmo A., Pereira E., Freitas R. 2020. Oxidative stress, metabolic and histopathological alterations in mussels exposed to remediated seawater by GO-PEI after contamination with mercury. Comparative Biochemistry and Physiology -Part A : Molecular and Integrative Physiology 243, 110674.

Corsi I., Cherr G.N., Lenihan H.S., Labille J., Hassellov M., Canesi L., Dondero F., Frenzilli G., Hristozov D., Puntes V., Della Torre C., Pinsino A., Libralato G., Marcomini A., Sabbioni E., Matranga V. 2014. Common strategies and technologies for the ecosafety assessment and design of nanomaterials entering the marine environment. ACS Nano 8: 9694-9709

Couch JA. 1984. Atrophy of diverticular epithelium as an indicator of environmental irritants in the oyster, *Crassostrea virginica*. Marine Environmental Research 14, 525-526.

De los Ríos A., Perez L., Ortiz-Zarragoitia M., Serrano T., Barbero M.C., Echavarri-Erasun B., Juanes J.A., Orbea A., Cajaraville M.P. 2013. Assessing the effects of treated and untreated urban discharges to estuarine and coastal waters applying selected biomarkers on caged mussels. Marine Pollution Bulletin 77, 251-265.

De Luna, L. A. V., Moraes, A. C. M., Consonni, S. R., Pereira, C. D., Cadore, S., Giorgio, S., & Alves, O. L. (2016). Comparative in vitro toxicity of a graphene oxide-silver nanocomposite and the pristine counterparts toward macrophages. Journal of Nanobiotechnology, 14(1), 1–17.

De Marchi L., Pretti C., Gabriel B., Marques P. A., Freitas R., Neto V. 2018. An overview of graphene materials: Properties, applications and toxicity on aquatic environments. Science of the Total Environment 631, 1440-1456.

de Medeiros, A. M. Z., Khan, L. U., da Silva, G. H., Ospina, C. A., Alves, O. L., de Castro, V. L., & Martinez, D. S. T. (2021). Graphene oxide-silver nanoparticle hybrid material: an integrated nanosafety study in zebrafish embryos. Ecotoxicology and Environmental Safety, 209.

De Moraes A.C.M. 2015. Graphene oxide-silver nanocomposite as a promising biocidal agent against methicillin- resistant *Staphylococcus aureus*. International Journal of Nanomedicine 10, 6847–6861.

Ding X., Pu Y., Tang M., Zhang T. 2022. Environmental and health effects of graphene-family nanomaterials: potential release pathways, transformation, environmental fate and health risks. NanoToday 42, 101379.

Dumont E., Johnson A.C., Keller V.D.J., Williams R.J. 2015. Nano silver and nano zinc-oxide in surface waters-Exposure estimation for Europe at high spatial and temporal resolution. Environmental Pollution 196: 341-349.

Duroudier, N., Katsumiti, A., Mikolaczyk, M., Schäfer, J., Bilbao, E., Cajaraville, M.P., 2019. Dietary exposure of mussels to PVP/PEI coated Ag nanoparticles causes Ag accumulation in adults and abnormal embryo development in their offspring. Science of Total Environment 655, 4860.

Dziewięcka M., Witas P., Karpeta-Kaczmarek J., Kwaśniewska J., Flasz B., Balin K., Augustyniak M. 2018. Reduced fecundity and cellular changes in *Acheta domesticus* after multigenerational exposure to graphene oxide nanoparticles in food. Science of the Total Environment 635, 947–955.

Ellis G., Goldberg D.M. 1971. An improved manual and semi-automatic assay for NADP-dependent isocitrate dehydrogenase activity, with a description of some kinetic properties of human liver and serum enzyme. Clinical Biochemistry 2, 175-185.

Ellman G., Courtney K., Andres V., Featherstone, R. 1961. A new and rapid colorimetric determination of acetylcholinesterase activity. Biochemical Pharmacology 7, 88–95.

Fabbri E., Valbonesi P., Franzellitti S. 2008. HSP expression in bivalves. ISJ-Invertebrate Survival Journal 5,135–161.

Fernandes A.L., Josende M.E., Nascimento J.P., Santos A.P., Sahoo S.K., Rodrigues da Silva Júnior F.M., Romano L.A., Furtado C.A., Wasielesky W., Monserrat J.M., Ventura-Lima J. 2017. Exposure to few-layer graphene through diet induces oxidative stress and histological changes in the marine shrimp *Litopenaeus vannamei*. Toxicology Research 6, 205-214.

Flasz B., Dziewięcka M., Kędziorski A., Tarnawska M., Augustyniak M. 2020. Vitellogenin expression, DNA damage, health status of cells and catalase activity in *Acheta domesticus* selected according to their longevity after graphene oxide treatment. Science of the Total Environment 737, 140274

Garmendia L., Soto M., Vicario U., Kim Y., Cajaraville M.P., Marigómez I. 2011. Application of a battery of biomarkers in mussel digestive gland to assess long term effects of the Prestige oil spill in Galicia and Bay of Biscay: tissue-level biomarkers and histopathology. Journal of Environmental Monitoring 13, 915-32.

Giese B., Klaessig F., Park B., Kaegi R., Steinfeldt M., Wigger H., von Gleich A., Gottschalk F. 2018. Risks, release and concentrations of engineered nanomaterials in the environment. Scientific Reports 8: 1565-1582

Goldberg E.D. 1986. The Mussel Watch Concept. Environmental Monitoring and Assessment 7.

Gomes T., Araújo O., Pereira R., Almeida A.C., Cravo A., Bebianno M.J. 2013. Genotoxicity of copper oxide and silver nanoparticles in the mussel *Mytilus galloprovincialis*. Marine Environmental Research 84, 51-59.

Gomes T., Chora S., Pereira C.G., Cardoso C., Bebianno M.J. 2014. Proteomic response of mussels *Mytilus galloprovincialis* exposed to CuO NPs and Cu2+: an exploratory biomarker discovery. Aquatic Toxicology 155, 327–336.

Goodwin G.D.Jr., Adeleye A.S., Sung L., Ho K.T., Burgess R.M., Petersen E.J. 2018. Detection and Quantification of Graphene-Family Nanomaterials in the Environment. Environmental Science and Technology 52, 4491-4513.

Gottschalk F., Sonderer T., Scholz R.W., Nowack B. 2009. Modeled environmental concentrations of engineered nanomaterials (TiO2, ZnO, Ag, CNT, fullerenes) for different regions. Environmental Science and Technology 43: 9216-9222

Guilhermino L., Lopes M.C., Carvalho A.P., Soared A.M.V.M. 1996. Inhibition of acetylcholinesterase activity as effect criterion in acute tests with juvenile *Daphnia Magna*. Chemosphere 32, 727-738.

Gyori B.M., Venkatachalam G., Thiagarajan P.S., Hsu D., Clement M.V. 2014. Open comet: an automated tool for comet assay image analysis. Redox Biology 2, 457-465.

Jin H., Tian L., Bing W., Zhao J., Ren L. 2021. Toward the application of graphene for combating marine biofouling. Advanced sustainable systems 5, 2000076.

Josende M.E., Nunes S.M., de Oliveira Lobato R., González-Durruthy M., Kist L.W., Bogo M.R., Wasielesky W., Sahoo S., Nascimento J.P., Furtado C.A., Fattorini D., Regoli F., Machado K., Werhli A.V., Monserrat J.M., Ventura-Lima J. 2020. Graphene oxide and GST-omega enzyme: An interaction that affects arsenic metabolism in the shrimp *Litopenaeus vannamei*. Science of the Total Environment 716, 136893.

Katsumiti A., Tomovska R., Cajaraville M. 2017. Intracellular localization and toxicity of graphene oxide and reduced graphene oxide nanoplatelets to mussel hemocytes *in vitro*. Aquatic Toxicology 188, 138-147.

Khan B., Adeleye A.S., Burgess R.M., Smolowitz R., Russo S.M., Ho K.T. 2019. A 72-h exposure study with eastern oysters (*Crassostrea virginica*) and the nanomaterial graphene oxide. Environmental Toxicology and Chemistry 38, 820–830.

Kim T.H., Kim M., Park H.S., Shin U.S., Gong M.S., Kim H.W. 2012. Size dependent cellular toxicity of silver nanoparticles. Journal of Biomedical Materials Research 100A, 1033-1043.

Kim Y., Ashton-Alcox A., Powell E.N. 2006. Histological techniques for marine bivalve molluscs: update NOAA technical memorandum NOS NCCOS 27, 76 pp.

Kim M.J., Ko D., Ko K., Kim D., Lee J. Y., Woo S.M., Kim W., Chung H. 2018. Effects of silver-graphene oxide nanocomposites on soil microbial communities. Journal of Hazardous Materials, 346, 93–102.

Koushik D., Sen S., Maliyekkal S.M., Pradeep T. 2016. Rapid dehalogenation of pesticides and organics at the interface of reduced graphene oxide – silver nanocomposite. Journal of Hazardous Materials 308, 192–198.

Krishnaraj C., Kaliannagounder V.K., Rajan R., Ramesh T., Kim C.S., Park C.H., Liu B., Yun S.Il. (2022). Silver nanoparticles decorated reduced graphene oxide: Eco-friendly synthesis, characterization, biological activities and embryo toxicity studies. Environmental Research 210, 112864.

Lima I., Moreira S.M., Rendón-Von Osten J., Soares A.M.V.M., Guilhermino L. 2007. Biochemical responses of the marine mussel *Mytilus galloprovincialis* to petrochemical environmental contamination along the North-Western coast of Portugal. Chemosphere 66, 1230-1242.

Livingstone D.R., Stickle W.B., Kapper M.A., Wang S. Zurburg W. 1990. Further studies on the phylogenetic distribution of pyruvate oxidoreductase activities. Comp. Biochem. Physiol., 97B, 4, 661-666.

Long S.M., Ryder K.J., Holdway D.A. 2003. The use of respiratory enzymes as biomarkers of petroleum hydrocarbon exposure in *Mytilus edulis planulatus*. Ecotoxicology and Environmental Safety 55, 261–270.

Lopes T, Texeira S, Bebianno MJ. 2016. Histopathological assessment and inflammatory response in thedigestive gland of marine mussel *Mytilus galloprovincialis* exposed to cadmium-based quantum dots. Aquatic Toxicology 177, 306-315.

Lowe DM, Moore MN, Clarke KR. 1981. Effects of oil in the digestive cells in mussels: Quantitative alterations in cellular and lysosomal structure. Aquatic toxicology 1, 213-226

Lu J., Zhu X., Tian S., Lv X., Chen Z., Jiang Y., Liao X., Cai Z., Chen B. 2018. Graphene oxide in the marine environment: Toxicity to *Artemia salina* with and without the presence of Phe and Cd2+. Chemosphere, 211, 390–396.

Malina T., Maršálkova E., Holá K., Zbořil R., Maršálek B. 2020. The environmental fate of graphene oxide in aquatic environment complete mitigation of its acute toxicity to planktonic and benthic crustaceans by algae. Journal of Hazardous Materials 399, 123027.

Marigómez I, Soto M, Cancio I, Orbea A, Garmendia L, Cajaraville MP. 2006. Cell and tissue biomarkers in mussel, and histopathology in hake and anchovy from Bay of Biscay after the Prestige oil spill (Monitoring Campaign 2003). Marine Pollution Bulletin 53, 287-304

Martínez-Álvarez I., Le Menach K., Devier M.H., Barbarin I., Tomovska R., Cajaraville M.P:, Budzinski H., Orbea A. 2021. Uptake and effects of graphene oxide nanomaterials alone and in combination with polycyclic aromatic hydrocarbons in zebrafish. Science of The Total Environment 775, 145669.

Martoja R., Martoja-Pierson M. 1970. Técnicas de Histología Animal. Toray-Masson, Barcelona.

Meng X., Li F., Wang X., LiU J., Ji C., Wu H. 2019. Combinatorial immune and stress response, cytoskeleton and signal transduction effects of graphene and triphenyl phosphate (TPP) in mussel *Mytilus galloprovincialis.* Journal of Hazardous Materials 378, 120778.

Meng X., Li F., Wang X., LiU J., Ji C., Wu H. 2020. Toxicological effects of graphene on mussel *Mytilus galloprovincialis* hemocytes after individual and combined exposure with triphenyl phosphate. Marine Pollution Bulletin 151, 110838.

Mesarič T., Sepčić K., Drobne D., Makovec D., Faimali M., Morgana S., Falugi C., Gambardella C. 2015. Sperm exposure to carbon-based nanomaterials causes abnormalities in early development of purple sea urchin (*Paracentrotus lividus*). Aquatic Toxicology, 163, 158–166.

Moore M.N. 2006. Do nanoparticles present ecotoxicological risks for the health of the aquatic environment? Environment international 32, 967-976.

Navarro E., Iglesias J.I.P., Camacho A.P., Labarta U., Beiras R., 1991. The physiological energetics of mussels (*Mytilus galloprovincialis* Lmk) from different cultivation rafts in the Ria de Arosa (Galicia, NW Spain). Aquaculture 94, 197–212.

Ohkawa H., Ohishi N., Yagi K. 1979. Assay for lipid peroxides in animal tissues by thiobarbituric acid reaction. *Analytical Biochemistry, 95:* 351-358.

Oliveira P., Barboza L.G.A., Branco V., Fuigueiredo N., Carvalho C., Guilhermino L. 2018. Effects of microplastics and mercury in the freshwater bivalve *Corbicula fluminea* (Müller, 1774): Filtration rate, biochemical biomarkers and mercury bioconcentration. Ecotoxicology and Environmental Safety 164, 155-163.

Ortiz-Zarragoitia M., Cajaraville M.P. 2006. Biomarkers of exposure and reproduction-related effects in mussels exposed to endocrine disruptors. Archives of Environmental Contamination and Toxicology 50, 361-369.

Osswald J., Carvalho A.P., Guimaraes L., Guilhermino L. 2013. Toxic effects of pure anatoxin-a on biomarkers of rainbow trout, *Oncorhynchus mykiss.* Toxicon 70, 162-169.

Ou L., Song B., Liang H., Liu J., Feng X., Deng B., Sun T., Shao L. 2016. Toxicity of graphene-family nanoparticles: a general review of the origins and mechanisms. Particle and fibre toxicology 13, 57.

Peng Z., Liu X., Zhang W. Zeng Z., Liu Z. Zhang C., Liu Y., Shao B., Liang Q., Tang W., Yuan X. 2020. Advances in the application, toxicity and degradation of carbon nanomaterials in environment: A review. Environment International 134, 105298

Rocha T.L., Gomes T., Mestre N.C., Cardoso C., Bebiano M.J. 2015. Tissue specific responses to cadmium-based quantum dots in the marine mussel *Mytilus galloprovincialis.* Aquatic Toxicology 169, 10-18.

Rogriguez-Ortega M.J., Alhama J., Fune V., Romero-Ruiz A., Rodriguez-Ariza A., Lopez-Barea J. 2002. Biochemical biomarkers of pollution in the clam *Chamaelea gallina* from south-Spanish littoral. Environmental Toxicology and Chemistry 21, 542-549.

Ruiz P., Ortiz-Zarragoitia M., Orbea A., Vingen S., Hjelle A., Baussant T., Cajaraville M.P. 2014. Short- and long-term responses and recovery of mussels *Mytilus edulis* exposed to heavy fuel oil no. 6 and styrene. Ecotoxicology 23, 861-879.

Seed R., 1969. The ecology of *Mytilus edulis* L (Lamellibranchiata) on exposed rocky shores. Oecologia 3, 277–315.

Sharma S., Prakash V., Mehta S.K. 2017. Graphene/silver nanocomposites-potential electron mediators for proliferation in electrochemical sensing and SERS activity. TrAC Trends in Analytical Chemistry Journal 86, 155–171.

Shubha A., Manohara S.R., Siddlingeshwar B., Daima H.K., Singh M., Revaprasadu N. 2022. Ternary poly(2-ethyl-2-oxazoline). Polyvinylpyrrolidone-graphene nanocomposites: thermal, electrical, dielectric, mechanical and antibacterial profiling. Diamond and Related Materials *in press.*

Sofi A.A., Sunitha S., Sofi M.A., Pasha K., Choi D. 2022. An overview of antimicrobial and anticancer potential of silver nanoparticles. Journal of King Saud Aniversity-Science 34, 101791.

Souza J.P., Baretta J.F., Santos F., Paino I.M.M., Zucolot V. 2017. Toxicological effects of graphene oxide on adult zebrafish (*Danio rerio*). Aquatic Toxicology 186, 11–18.

Souza J.P., Venturini F.P., Santos F., Zucolotto V. 2018. Chronic toxicity in *Ceriodaphnia dubia* induced by graphene oxide. Chemosphere 190, 218–224.

Storey K.B., Storey J.M. 1983. Carbohydrate metabolism in cephalopod molluscs. In: Hochachka, P.W. (Ed.), The Mollusca – Metabolic Biochemistry and Molecular Biomechanics. Academic Press, New York, USA, pp. 91–136.

Tiede K., Hassellöv M., Breitbarth E., Chaudhry Q., Boxall A.B.A. 2009. Considerations for environmental fate and ecotoxicity testing to support environmental risk assessments for engineered nanoparticles. Journal of Chromatography A 1216: 503-509.

Vega M.M., Marigómez I., Angulo E.. 1989. Quantitative alterations in the structure of digestive cells of *Littorina littorea* on exposure to cadmium. Marine Biology 103, 547-553

Walters C.R., Cheng P., Pool E., Somerset V. 2015. Effect of temperature on oxidative stress parameters and enzyme activity in tissues of Cape River crab (*Potamanautes perlatus*) following exposure to silver nanoparticles (AgNP). Journal of Toxicology and Environmental Health, Part A 79, 61-70.

Xu J., Wang Y., Hu S., 2017. Nanocomposites of graphene and graphene oxides: Synthesis, molecular functionalization and application in electrochemical sensors and biosensors. a review. Microchimica Acta 184, 1–44.

Yee M.S.L., Khiew P.S., Chiu W.S., Tan Y.F., Kok Y.Y., Leong C.O. 2016. Green synthesis of graphene-silver nanocomposites and its applications as a potent marine antifouling agent. Colloids ans Surfaces B: BIointerfaces 148, 392.401.

Zhang X., Zhou Q., Zou W., Hu X., 2017. Molecular mechanisms of developmental toxicity induced by graphene oxide at predicted environmental concentrations. Environmental Science & Technology 51, 7861–7871.

Zhang Y., Meng T., Shi L., Guo X., Si X., Yang R., Quan X. 2019. The effects of humic acid on the toxicity of graphene oxide to *Scenedesmus obliquus* and *Daphnia magna*. Science of the Total Environment 649, 163–171.

Zhao Y., Liu Y., Zhang X., Liao W. 2021. Environmental transformation of graphene oxide in the aquatic environment. Chemosphere 262, 127885.

Zhou Y., Chen R., He T., Xu K., Du D., Zhao N., Cheng X., Yang J., Shi H., Lin Y. 2016. Biomedical potential of ultrafine Ag/ AgCl nanoparticles coated on graphene with special reference to antimicrobial performances and burn wound healing. ACS Applied Materials & Interfaces 8, 15067–15075.

Zhu S., Luo F., Chen W., Zhu B., Wang G. 2017. Toxicity evaluation of graphene oxide on cysts and three larval stages of *Artemia salina*. Science of the Total Environment 595, 101–109.

Zorita I., Ortiz-Zarragoitia M., Soto M., Cajaraville M.P. 2006. Biomarkers in mussels from a copper site gradient (Visnes, Norway): an integrated biochemical, histochemical and histological study. Aquatic Toxicology 78, 109-116.

SUPPLEMENTARY MATERIAL TO CHAPTER 4

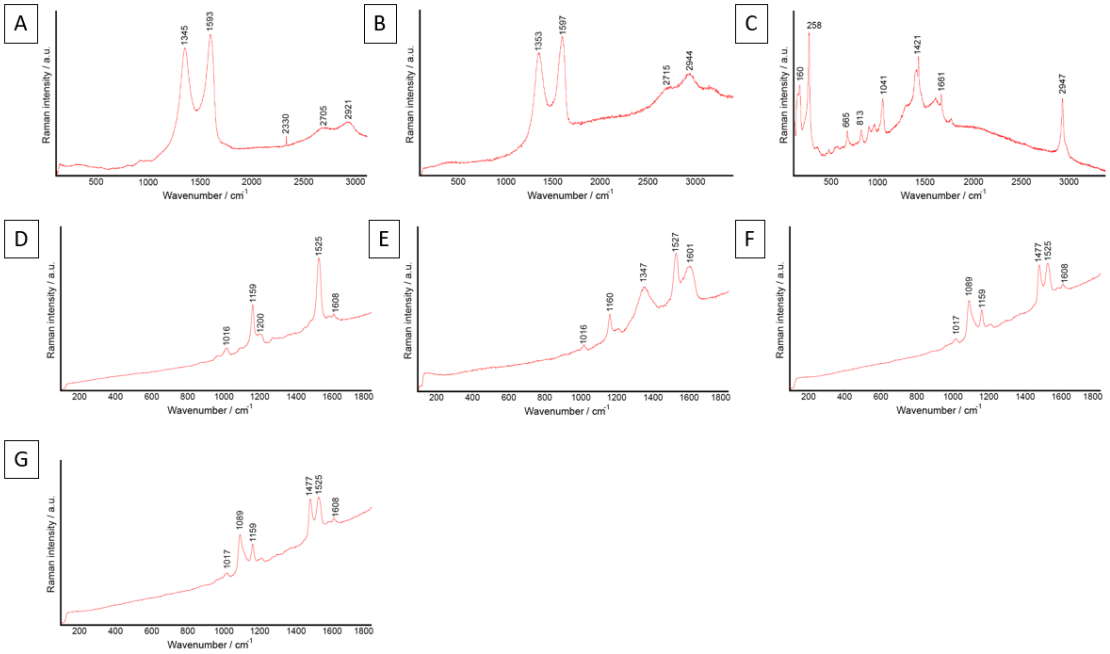

Figure S1. Raman spectra obtained from A: rGO stock; B: rGO-Ag stock; C: Ag NPs stock; D: feces obtained from a control mussel after 1 day of exposure; E: feces obtained from a mussel exposed to rGO after 1 day of exposure; F: feces obtained from a mussel exposed to rGO-Ag after 1 day of exposure ; G: feces obtained from a mussel exposed to Ag NPs after 1 day of exposure.

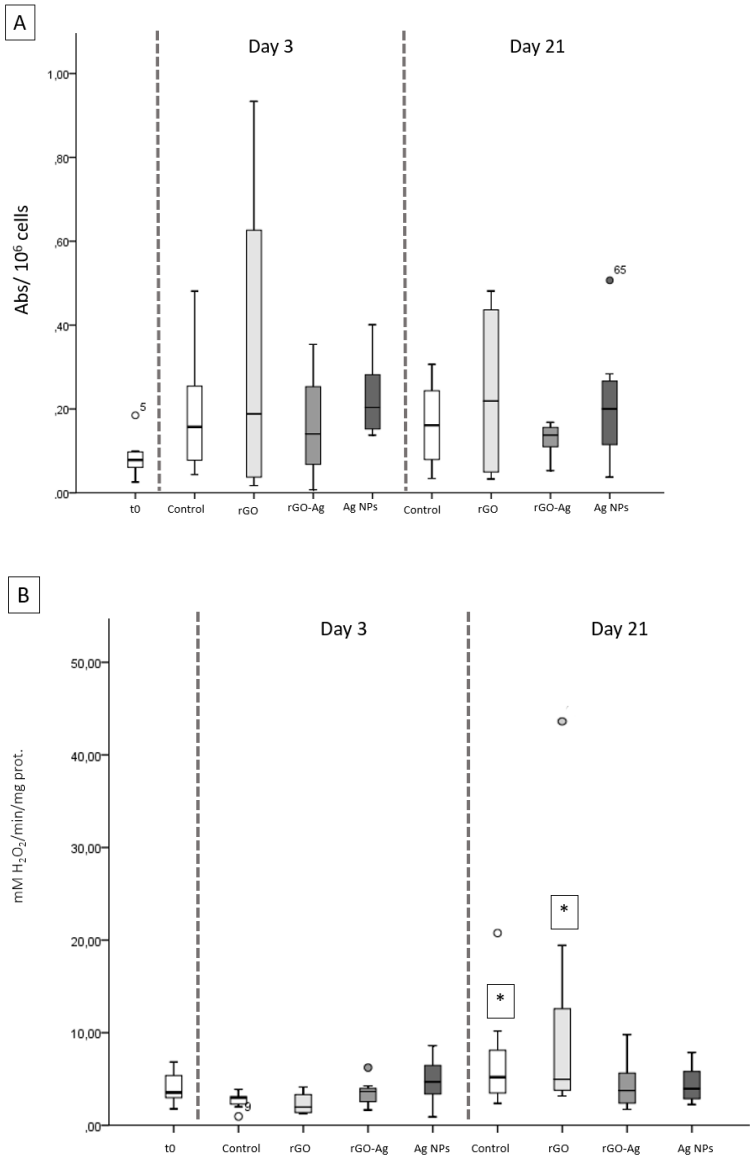

Figure S2. A) Neutral red uptake (given as absorbance/10^6 cells) and B) Catalase activity (given as mM H_2O_2/min/mg prot.) in hemocytes of mussels from t0 , control mussels and mussels exposed to rGO, rGO-Ag and Ag NPs after 3 and 21 days of exposure. Box-plots show median values (horizontal line), 25%-75% quartiles (box) and standard deviation (whiskers). Dots denote outliers, values that do not fall in the inner fences. Letters indicate significant differences among treatments within the same day (Kruskal-Wallis followed by Dunn's post hoc test, $p < 0.05$). Asterisks indicate significant differences between days within the same treatment (Mann-Whitney´s U test, $p < 0.05$).

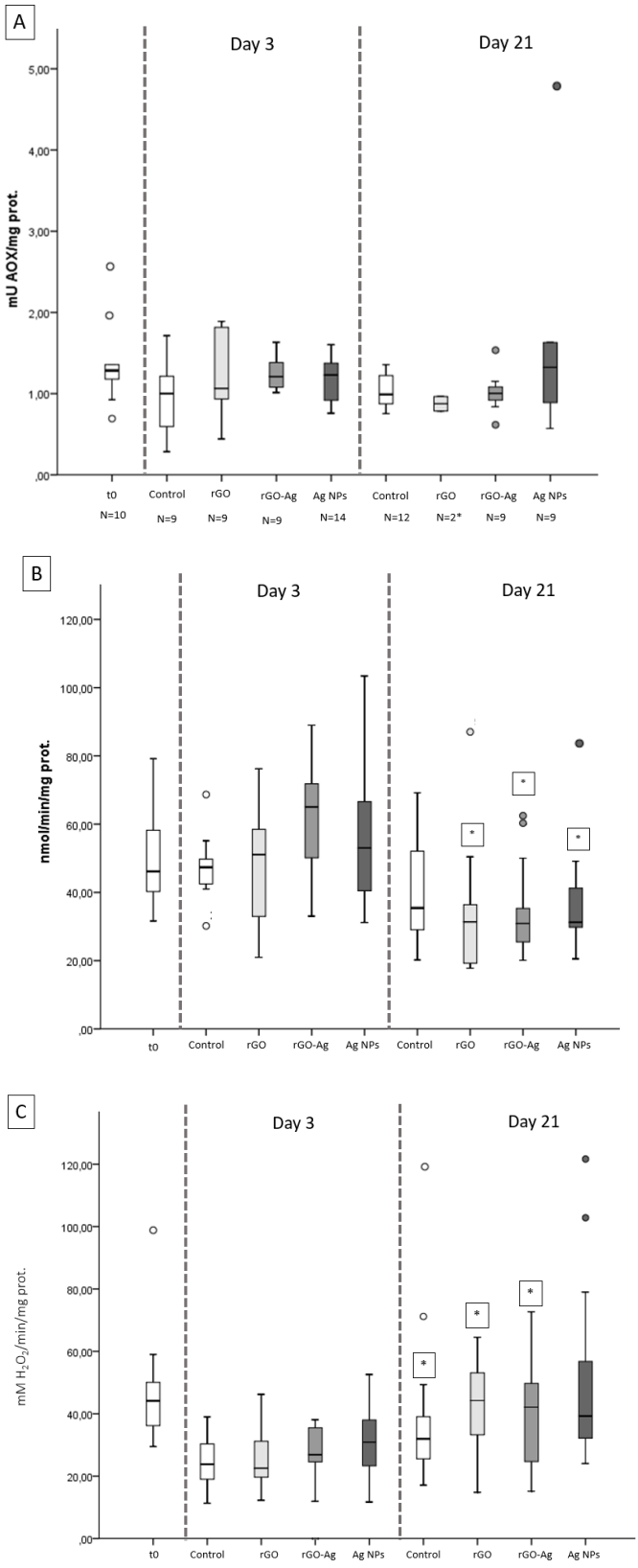

Figure S3. A) AOx1 activity given as mU AOX1/mg prot. in digestive gland; B) GST activity given as nmol/min/mg prot. in digestive gland and C) catalase activity given as mM H_2O_2/min/mg prot in gills of mussels from t0, control mussels and mussels exposed to rGO, rGO-Ag and Ag NPs after 3 and 21 days of exposure. Box-plots show median value (horizontal line), 25%-75% quartiles (box) and standard deviation (whiskers). Dots denote outliers, values that do not fall in the inner fences. No differences were found among treatments within the same day (Kruskal-Wallis test followed by Dunn's post hoc in A and one-Way Anova followed by Tukey's post hoc in B and C, $p>0.05$). Asterisks indicate significant differences between days within the same treatment (Mann-Whitney´s U test, $p < 0.05$).

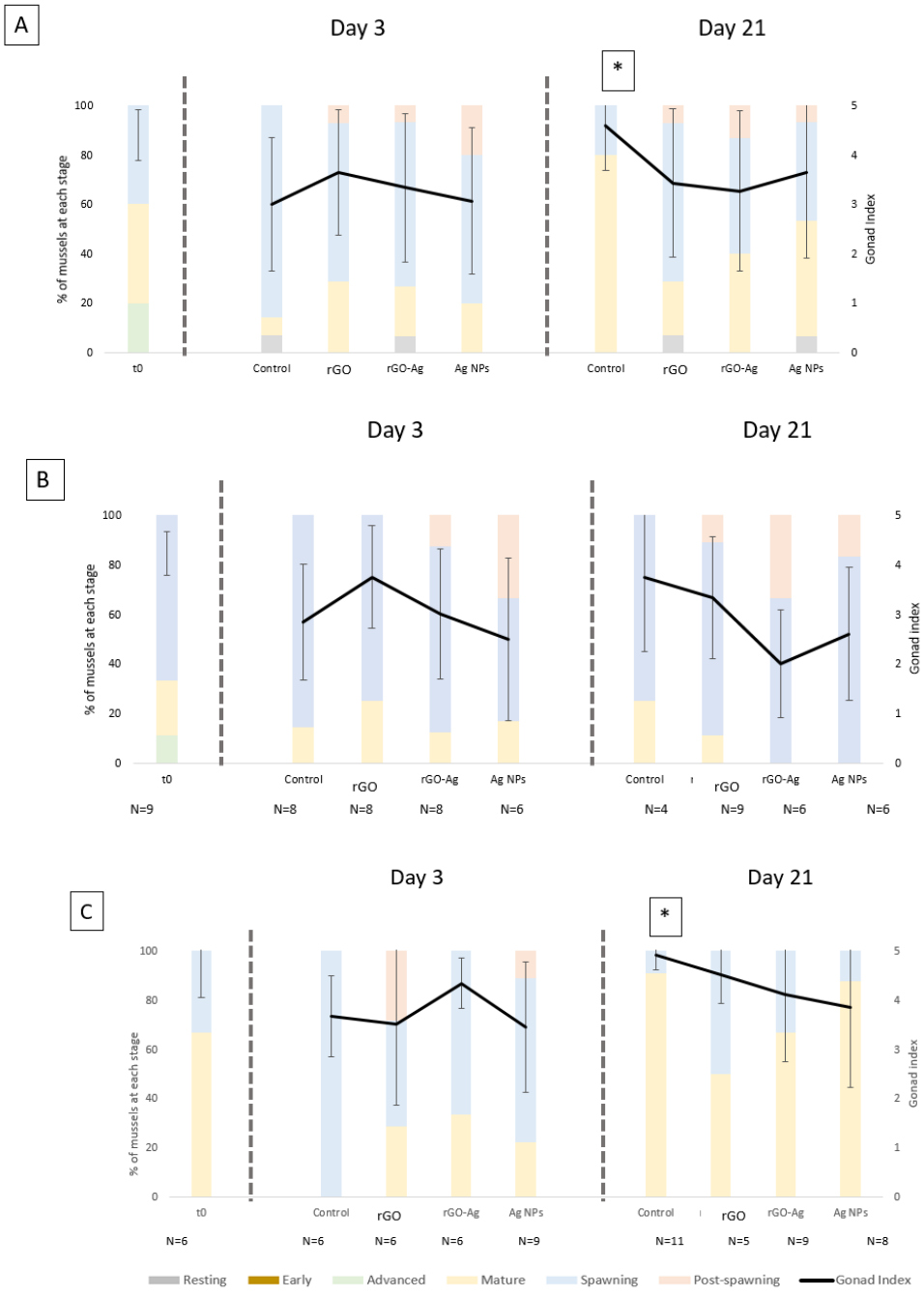

Figure S4. Gonad index (lines) and percentage of animals at each gamete developmental stage (stacked bars) of mussels from the t0, control mussels and mussels exposed to rGO, rGO-Ag and Ag NPs after 3 and 21 days of exposure. Gonad index values are given as means and standard deviation of A) both sexes, B) females, C) males. No significant differences were observed for gonad index among treatments within the same day (Kruskal-Wallis followed by Dunn's post hoc test, $p > 0.05$). The asterisk indicates significant differences between days within the same treatment (Mann-Whitney´s U test, $p < 0.05$).

CHAPTER 5:

Toxicity of graphene family nanomaterials alone and with associated benzo(a)pyrene on early embryo developmental stages of mussels *Mytilus galloprovincialis*

This chapter is being prepared for publication:

GONZÁLEZ-SOTO, N; BLASCO, N; SCHÄFER, J; BILBAO, E.; CAJARAVILLE, MP. Toxicity of graphene family nanomaterials alone and with associated benzo(a)pyrene on early developmental stages of mussels *Mytilus galloprovincialis*.

This chapter will be presented at:

21st International Symposium on Pollutant Responses in Marine Organisms (PRIMO), Gothenburg, 22 to 25 May 2022. GONZÁLEZ-SOTO, N; BLASCO, N; TOMOVSKA, R; BILBAO, E.; CAJARAVILLE, MP. Impact of graphene family nanomaterials alone and with associated pollutants on early developmental stages of mussels *Mytilus galloprovincialis*. Platform (N González-Soto)

ABSTRACT

In the last years graphene family nanomaterials (GFNs) have been incorporated in an increasing number of consumer products and this may cause their entry into the marine environment. Thus, understanding the fate and effects of GFNs on marine biota represents a major concern, especially on embryos as they are considered the most vulnerable life stage and represent a direct link to population level consequences. An additional hazard of GFNs is due to their ability to adsorb persistent organic pollutants (POPs), thus enabling GFNs to act as carriers of POPs to marine organisms (Trojan horse effect). The present study aimed to assess the potential embryotoxicity of different GFNs alone or with sorbed benzo(a)pyrene (BaP) on early developmental stages of marine mussels. First, mussel embryos were statically exposed for 48 hours to 0.001-100 mg/L of graphene oxide (GO), GO with sorbed BaP (500 µg/L GO + 100 µg/L BaP; GO+BaP) and to the equivalent BaP concentration sorbed in the GO+BaP mixture (96.7 µg/L). In a second experiment, mussel embryos were exposed to 0.001-10 mg/L of a hybrid material consisting of reduced GO with silver nanoparticles (rGO-Ag). For comparison purposes embryos were also exposed to equivalent concentrations of reduced GO (rGO, 0.0007847-7.847 mg/L) and silver nanoparticles (Ag NPs, 0.000194-1.94 mg/L) present in rGO-Ag and to the filtrated medium obtained from rGO-Ag. After 48 h, EC_{50} of GO was 0.470 mg/L and the most common malformation observed was the protuberant mantle. Sorption of BaP into GO nanoplatelets did not alter the toxicity of either GO or BaP at equivalent concentrations, suggesting that BaP sorbed onto GO platelets did not pose an additional risk to mussel embryos. rGO-Ag was more toxic than GO (EC_{50} for rGO-Ag 0.017 mg/L), followed by the filtrated medium derived from rGO-Ag (EC_{50} 0.039 mg/L) and Ag NPs resulted the most toxic compound tested (EC_{50} 0.001 mg/L). Meanwhile, rGO did not show a dose-dependent response and the EC_{50} could not be calculated in this case. Among embryos surviving in the second experiment, arrested development was the most common abnormality found. The relative low embryotoxicity of GO and rGO could be associated with their aggregation and sedimentation behavior in seawater while Ag NPs seemed to contribute largely to the embryotoxicity of rGO-Ag, highlighting the toxic potential of GFN-Ag NP composites in the marine environment.

1. INTRODUCTION

The production of nanomaterials (NMs) has raised in the last decades leading to an unprecedented growth of nanotechnology and nanoindustry (Sajid, 2021). Among NMs, graphene and its derivatives (the graphene family NMs, GFNs) are outstanding due to their unique characteristics and multiple applications (Ren & Chen, 2014). In the last years the production of GFNs-polymer composites (Stankovich et al., 2006; Bai & Shi, 2011; Mu et al., 2021) and of nanocomposites of GFNs and metal nanoparticles (NPs) (Hassandoost et al., 2019) is rising. This new generation of graphene hybrid nanocomposites show enhanced functionalities and provide novel properties to GFNs that may result in new applications (Hassandoost et al., 2019). GFN nanocomposites with silver NPs (Ag NPs) are most promising because they present improved electrical and thermal conductivity than pure graphene, among other properties (Huang et al., 2014). In addition, the large surface of GFNs can act as a stabilizing support for Ag NPs and avoid their aggregation in the media, which improves the reactivity of Ag NPs, increasing for example their antibacterial activity (Krishnaraj et al., 2022). Consequently, applications for GFN-Ag NPs nanocomposites are studied in different fields, from electronics to biomedicine, including the environment (Fatima et al., 2021). For instance, GFN-Ag NPs nanocomposites are promising materials as antifouling agents in the shipping industry and in the treatment and purification of water (Fatima et al., 2021; Pourhashem et al., 2022). These applications could result in a direct release of GFN-Ag NPs nanocomposites into aquatic environments. Thus, preventive studies are needed that evaluate the impact of such nanocomposites on human and ecosystems health (Hutchison, 2016; Kim et al., 2018; Ziat et al., 2020). Moreover, it is expected that GFNs will finally tend to sink in seas an oceans (Zhao et al., 2014) but currently there is no data on levels of GFNs in the marine environment (de Marchi et al., 2018; Goodwin et al., 2018).

Dynamics and fate of NMs in the marine environment depend on the physico-chemical properties of each NM, including size, shape and surface charge (de Marchi et al., 2019; Katsumiti & Cajaraville, 2019), which may change due to UV exposure and reaction with other molecules, among others (Zhao et al., 2021). These phenomena cause a gap between what is known based on laboratory works and real behavior of GFNs in the

environment (Goodwin et al., 2018; Zhao et al., 2021) and complicates estimation of the potential impacts of GFNs onto aquatic organisms (de Marchi et al., 2018; Goodwin et al., 2018). Once in the environment, due to their hydrophobicity and largesurface to volume ratio, GFNs may adsorb other pollutants (Wang et al., 2021) increasing their uptake and toxicity to marine organisms, through the so-called Trojan horse effect (Sanchís et al., 2016; Ersan et al., 2017). Among the vast variety of pollutants present in the marine environment, persistent organic pollutants (POPs) and particularly polycyclic aromatic hydrocarbons (PAHs) such as benzo(a)pyrene (BaP) are extremely worrying. BaP is a carcinogen and teratogen compound, listed as priority contaminant by several agencies as highly toxic to aquatic organisms (EU, 2008; U.S. EPA, 2014;). BaP has been widely investigated in ecotoxicology and it is known to cause detrimental effects at molecular, cellular, tissue and whole organism level in marine organisms such as mussels (Cancio et al., 1998; Gómez-Mendikute et al., 2002; Marigómez et al., 2005; Di et al., 2011; 2017; Tian et al., 2013; Banni et al., 2017). Consequently, the potential impact of GFNs alone or in combination with other pollutants such as BaP on marine organisms is of high concern though scarce data on the subject is available yet (de Marchi et al., 2018).

Early life stages of aquatic organisms are known to be especially sensitive to pollution. In addition, impacts on early life stages can have severe consequences at the population level (Pörtner et al., 1998; Carls et al., 2008; Wale & Gardiner, 2016). Therefore, it would be essential to consider different life stages of a species to establish its sentivity towards any pollutant and especially towards NMs (Ringwood et al., 2009; Fabbri et al., 2014). In particular, it would be necessary to establish the sensitivity of marine sessile invertebrates living in coastal ecosystems, which are especially affected by anthropogenic pressures and whose resilience or spatial dispersion is linked to their planktonic embryo and larval stages (Gamain et al. 2017; Capolupo et al., 2018). Among species with planktonic embryo and larval stages, bivalves and specially mussels are widely used as sentinels in toxicological studies (Cajaraville et al., 2000; Vethaak et al. 2017). However, little information is available regarding the impact of pollutants on their early life stages, even though the life cycle of bivalves is well known (Capela et al., 2020). The objective of this work is to assess the impact of different GFNs alone or in

combination with sorbed pollutants (BaP) on embryos of mussels *Mytilus galloprovincialis.*

2. MATERIALS AND METHODS

2.1. Obtention and behaviour of GO, rGO, rGO-Ag and Ag NPs in marine water

The same batch of GO used in Chapter 3 and the same rGO, rGO-Ag and Ag NPs used in Chapter 4 were used for embryotoxicity assays.

In addition to the characterization of the different nanomaterials reported in Chapters 3 and 4, the behaviour of GO, rGO, rGO-Ag and Ag NPs was checked visually both in marine water and in MilliQ water. Suspensions of GO, rGO, rGO-Ag and Ag NPs were prepared at the same concentrations as for embryo toxicity tests and maintained for 48 h in an orbital shaker at minimum speed under the same conditions as for the assays.

2.2. Preparation of GO with sorbed BaP

Preparation of GO with sorbed BaP (GO+BaP) was based on Martínez-Álvarez et al. (2021) using the same concentrations of GO and BaP as in Chapter 3. Briefly, once the BaP solution (100 µg/L) was prepared in a glass bottle, GO was added in a 0.5 mg to 10 mL GO/BaP proportion. Sorption process was allowed by shaking glass bottles in an orbital shaker (300 rpm) for 24 h in the dark at 21 ± 1 °C. After 24 h, mixtures were centrifuged in an Allegra X30R centrifuge (9509 g, 30 minutes). Supernatant was discarded and the pellet was resuspended in 50 mL of MilliQ water. According to Martínez-Álvarez et al. (2021) the proportion of BaP sorbed onto GO was 96.7% ± 0.5.

2.3. Preparation of rGO-Ag filtrated medium and analysis of Ag

In order to elucidate the contribution of soluble Ag ions to the overall toxicity of the rGO-Ag hybrid, toxicity of rGO-Ag filtrates was tested following the protocol of de

Medeiros et al. (2021) with modifications. Briefly, a 100 mg/L rGO-Ag dispersion prepared in autoclavated seawater was mantained under the same conditions (photoperiod, temperature, agitation, time) as embryos. Then, the solution was filtered (Filtropour S 0,2 µm, Sardstedt, Germany) to eliminate all solid particles. The absence of rGO-Ag was checked through UV spectroscopy and the remaining filtrated medium was diluted as the rGO-Ag stock (100 mg/L) for toxicity assays.

To determine Ag content in the rGO-Ag filtrated medium, samples were sent to the Oceanic and Continental Environments and Paleoenvironments (EPOC) research unit of the University of Bordeaux. Analysis of Ag content was performed using an Inductively Coupled Plasma-Tandem Mass Spectrometry (ICP-MS/MS; Thermo Scientific®; iCAP TQ). The analytical performance of the digestion procedure was assessed using the external calibration made from commercially available standard solutions (PlasmaCAL, SCP Science®). Ag concentrations measured were consistent (RSD <2%) among replicates. The detection limit for dissolved total Ag measurements was 10 ng/ L.

2.4. Sampling of mussels

30 mussels *Mytilus galloprovincialis* per assay were collected in May-July 2020 and 2021 in Plentzia (43°24´43.02”N, 2°56´58.84”W) and maintained in aquaria facilities at the Plentzia Marine Station (PiE) of the University of the Basque Country (UPV/EHU) for depuration during 24 h under continued seawater flow. The marine water was collected with a pump at 10 m depth in the mouth of the Butroi estuary (43°24’21”N, 2°56’47”W) and filtered (particles ≤ 3 µm) before reaching the marine station.

2.5. Embryo toxicity assays

GO, rGO, rGO-Ag, Ag NPs and the filtrated medium of rGO-Ag were diluted in sea water to reach target nominal concentrations. First, GO was diluted to reach 0.001; 0.01; 0.1; 0.5; 1; 5, 10; 25; 50; and 100 mg/L. Then, 500 µg/L of GO were mixed with 100 µg/L BaP to prepare the GO+BaP mix as described in section 2. Embryos were exposed to different concentrations of GO, to GO+BaP, to the equivalent BaP concentration sorbed in the

GO+BaP (96.7 µg/L) Martínez-Álvarez et al. (2021) and to the equivalent concentration of GO alone (500 µg/L).

For the second batch of assays, GO-Ag was diluted to 0.001; 0.01; 0.1; 0.5; 1; 5; and 10 mg/L. Embryos were exposed to those concentrations of GO-Ag, to the equivalent concentrations of rGO (0.0007847; 0.007847; 0.007847; 0.039235; 0.07847; 0.39235; and 7.847 mg/L) and Ag NPs (0.000194; 0.00194; 0.0194; 0.097; 0.194; 0.97; 1.94 mg/L) present in the rGO-Ag nanocomposite and to the filtrated medium obtained from rGO-Ag suspensions at 0.001; 0.01; 0.1; 0.5; 1; 5; and 10 mg/L.

Embryo toxicity tests were performed based on His et al. (1997) and Duroudier et al. (2019) with modifications. Briefly, 30 glass beakers of 100 mL were filled with 80 mL of seawater and placed in a plastic container filled 2/3 with warm water (26-27 °C). Mussels were placed individually in each glass beaker to induce their spawning by thermal stimulation. Obtained sperm and eggs were sieved through a nylon filter of 30 µm and 100-150 µm, respectively, and their quality was checked using a light microscope. A sperm pool (from 3 individuals) was prepared with those individuals that showed greater sperm density and mobility. The eggs from 4 females were individually fertilized in a 2:20 mL sperm/eggs proportion. After 30 minutes, the total number of eggs and the number of fertilized eggs were counted in 40 µL of suspension to calculate the fertilization rate. Round eggs with expelled polar bodies were considered as fertilized (His et al., 1999). The volume corresponding to 300-400 fertilized eggs per female was transferred to 4 glass vials with 15 mL of medium corresponding to each treatment. Vials were mixed manually after addition of eggs and covered with aluminum foil in the case of photosensitive compounds, GO+BaP and BaP. Four replicates per female and per treatment were performed (16 vials in total per treatment). Vials were incubated for 48 h in an orbital shaker (200 rpm) at room temperature. The tap of vials was not completely closed to allow oxygen exchange. After incubation, 100 µL of formalin was added to each vial for their storage at 4 °C until observation. The percentage of abnormal embryos among randomly selected 100 embryos per each vial was determined under the inverted microscope (Nikon Eclipse Ti, Nikon instruments, Tokio, Japan). In total 1600 embryos were examined for each treatment to establish the malformation ratio.

Normal larvae were defined as those showing a perfect D-veliger shell while abnormal larvae were classified as: (a) segmented eggs, (b) normal or malformed embryos that did not reach the D-larval stage, (c) D-larvae with protuberant mantle and (d) D-larvae with convex hinge (His et al., 1997).

2.6. Data analysis

Statistical analyses were carried out with the aid of the statistical package SPSS 24 (IBM Analytics, Armonk, NY). Raw data and data resulting after arcsin transformation did not follow a normal distribution. Thus, statistical differences were analyzed by the one-way Kruskal-Wallis test followed by the Dunn´s post-hoc test (Fabbri et al., 2014; Beiras et al., 2018). In all cases, significance was established at $p<0.05$. EC_{50} values were calculated through Probit analysis.

3. RESULTS

3.1. Behaviour of GO, rGO, rGO -Ag and Ag NPs in marine water

GO, rGO and rGO-Ag formed a homogeneous suspension in MilliQ water but not in marine water. GO formed large aggregates in less than 24 hours in marine water at concentrations higher than 1 mg/L, whereas rGO and rGO-Ag needed 48 hours to form aggregates and sink, at concentratrions equal or above 0.7847 mg/L and 0.5 mg/L, respectively (Figure 1). No differences were observed between the behavior of GO+BaP and the equivalent concentration of GO alone (Figure 1).

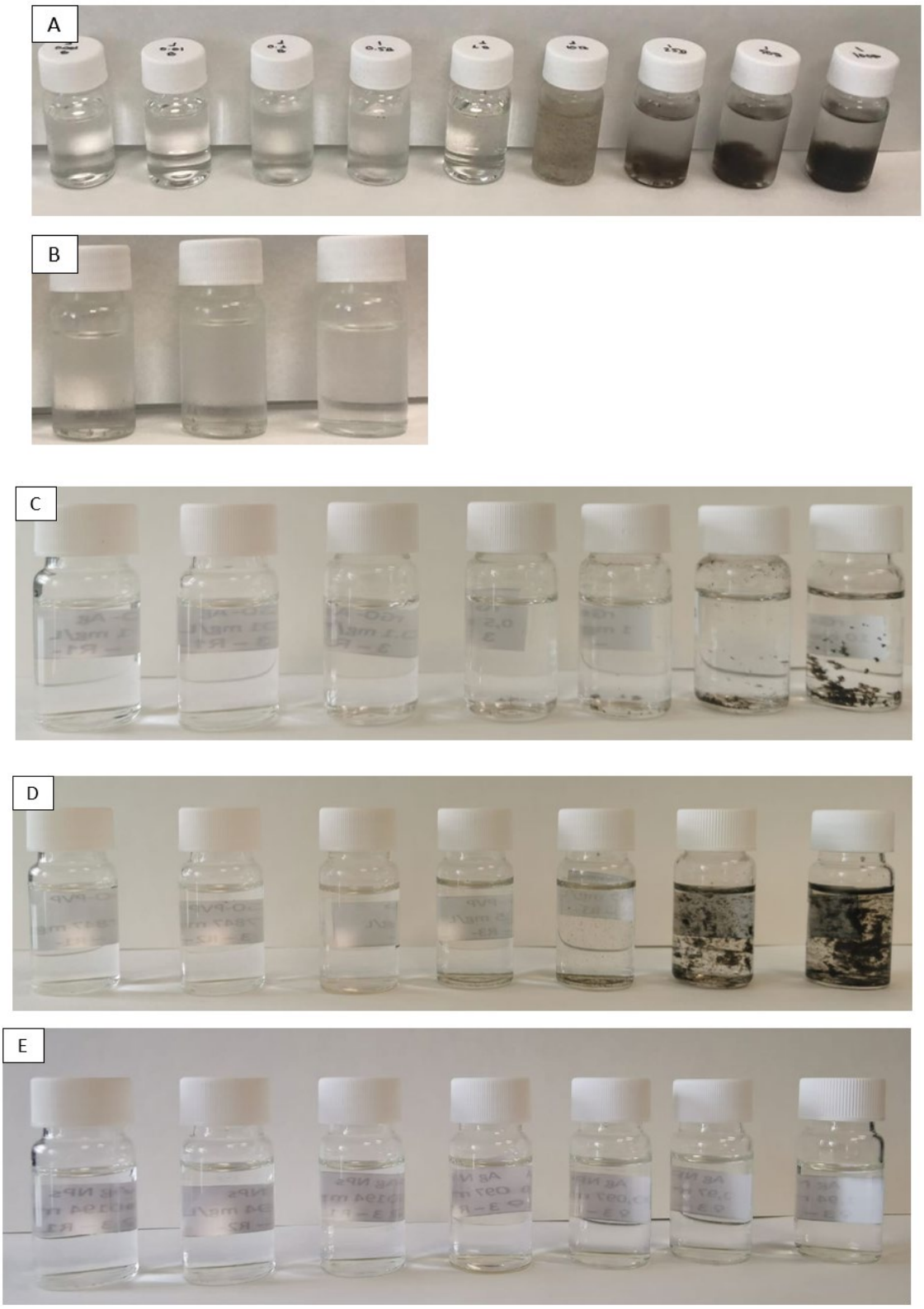

Figure 1. Stability after 48 hours in marine water (left to right) of A) 0.001 to 100 mg/L of GO; B) 500 µg/L GO, GO+BaP (500 µg/L GO + 100 µg/L BaP) and BaP (96.7 µg/L); C) 0.001 to 10 mg/L of rGO-Ag; D) 0.0007847-7.847 mg/L of rGO; E) 0.000194-1.94 mg/L of Ag NPs.

3.2. Effects of GO alone and with sorbed BaP on embryo development

After 48 hours post-fertilization, controls presented >80% of normal D larvae which ensured the quality of the tests. Embryos exposed from 0.001 mg/L to 0.5 mg/L of GO showed a dose dependent response , whereas toxicity was reduced from 0.5 mg/L to 10 mg/L of GO and full mortality was recorded at higher concentrations (>25 mg/L) (Figure 2A, Table S1). Considering the whole range of concentrations tested, the EC_{50} of GO was 0.47 mg/L (Table 1). Exposure of embryos to GO with sorbed BaP gave rise to an increased percentage of malformed embryos with respect to controls but values did not differ with respect to those exposed to GO or BaP at equivalent concentrations (Figure 2B, Table S1).

Table 1. EC_{50} values obtained in mussel embryos exposed to GO alone (0.001-100 mg/L), rGO (0.0007847-7.847 mg/L), rGO-Ag (0.001-10 mg/L), Ag NPs (0.000194-1.94 mg/L), and filtrated medium of rGO-Ag (0.001-10 mg/L) in mg/L after 48 hours of exposure. n.d: not determined.

	mg/L
GO	0.47
rGO	n.d
rGO-Ag	0.017
Ag NPs	0.001
Filtrated medium	0.039

Among embryos exposed to GO the most common malformation was the protuberant mantle (>60%) (Figures 3,4A, Table S2), followed by arrested development (12.45-31.75%) (Figure 4A, Table S2), then embryos completely malformed that could not be classified (<8%) (Figure 4A, Table S2) and embryos showing shell deformities (<1%) (Figures 3,4A, Table S2). The proportion of embryos showing arrested development was higher at 0.001 mg/L than at 10 mg/L (Figure 4A, Table S2). Embryos exposed to GO+BaP and to the equivalent concentrations of GO or BaP alone showed similar results, with the exception that a higher proportion of shell deformities was observed in embryos exposed to BaP alone in comparison to controls (3.47 %) (Figure 4B, Table S2).

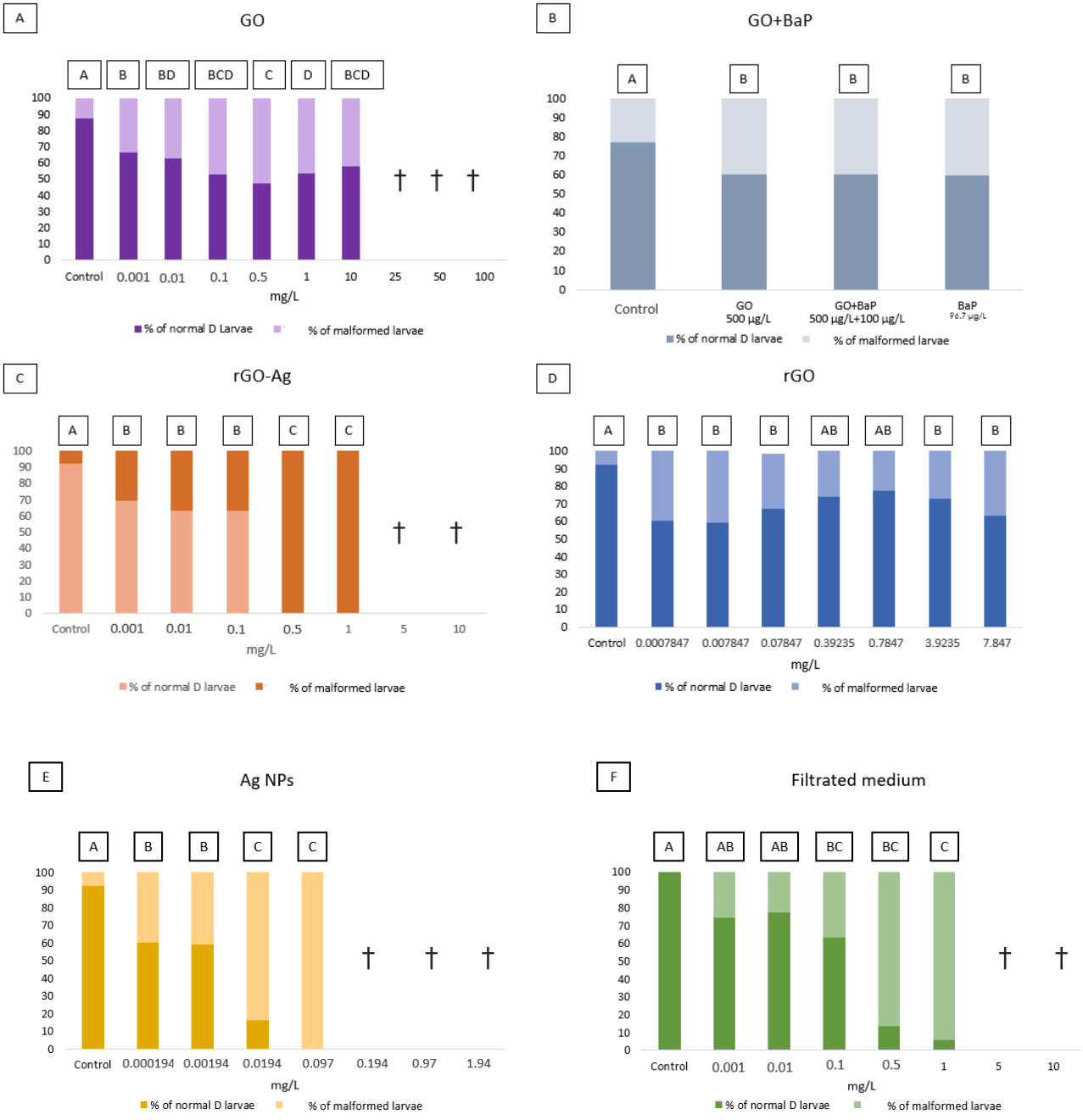

Figure 2. Percentage of normal D larvae and malformed larvae after 48 hours of exposure to A) GO, B) GO with sorbed BaP compared to GO or BaP alone, C) rGO-Ag, D) rGO at equivalent concentrations found in rGO-Ag, E) Ag NPs at equivalent concentrations found in rGO-Ag, F) Filtrated medium of rGO-Ag. The mean value of 4 experiments (4 replicates for each experiment) is given in each case. Bars which do not share the same letter are significantly different according to the Kruskal-Wallis test followed by the Dunn's post-hoc test ($p < 0.05$). † denotes 100% of mortality.

3.3. Effects of rGO-Ag, rGO, Ag NPs and filtrated medium derived from rGO-Ag on embryo development

As in the previous set of experiments, after 48 hours post-fertilization the controls presented >80% of normal D larvae which ensured the quality of the tests. Among GFNs tested, rGO-Ag was the most toxic (EC_{50} 0.017 mg/L) followed by the filtrated rGO-Ag medium (EC_{50} 0.039 mg/L) but, among all treatments, Ag NPs were the most toxic (EC_{50} 0.001 mg/L). rGO did not cause a dose-dependent response and thus, the EC_{50} could not be calculated (Table 1).

rGO-Ag concentrations above 0.1 mg/L did not show any normal D larvae while concentrations above 1 mg/L resulted in death of all embryos (Figure 2C, Table S1).

The toxicity pattern observed in embryos exposed to rGO was similar to that observed in embryos exposed to GO alone at similar concentrations (Figure 2D, Table S1).

Embryos exposed to Ag NPs and to the filtrated medium obtained from the rGO-Ag showed the same toxicity pattern as rGO-Ag (Figure 2E,F, Table S1). Ag NPs were confirmed as the most toxic compound to mussel embryos. No normal D larvae were present in concentrations above 0.0194 mg/L and no surviving embryos were found at concentrations higher than 0.097 mg/L (Figure 2E, Table S1). Exposure to the filtrated medium showed a toxicity halfway between Ag NPs and rGO-Ag exposure, with no surviving embryos at concentrations above the equivalent of 1 mg/L of rGO-Ag, but with normal D embryos still present in concentrations equivalent to 0.001 to 1 mg/L of rGO-Ag (Figure 2F, Table S1). Chemical analysis showed that 967 ± 119.38 µg/L of Ag were present in the filtrated medium derived from rGO-Ag at a concentration of 100 mg/L.

In mussels exposed to rGO alone, rGO-Ag, Ag NPs or filtrated medium derived from rGO-Ag the most common abnormality was the arrested development (>60%) (Figure 4C-F, Table S2). In addition, in embryos exposed to rGO-Ag a higher proportion of larvae with protuberant mantle was observed at 0.5 mg/L in comparison with the control and embryos exposed to 0.001 mg/L, while a higher proportion of shell deformities and lower arrested development were observed at 0.1 mg/L in comparison to the control (Figure 4C, Table S2). A similar pattern was observed after exposure to rGO, with arrested development being the most prevalent abnormality and the proportion of shell

deformities and protuberant mantle increasing with the exposure concentration. However, percentages of abnormalities were not significantly different among controls and different concentrations of rGO (Figure 4D, Table S2).

In the case of embryos exposed to Ag NPs alone a significantly higher proportion of protuberant mantle was observed in mussel embryos exposed to 0000194; 0.00194 and 0.0194 mg/L in comparison to the control. Lower arrested development was observed in embryos exposed to 0.000194 mg/L in comparison to those exposed to 0.0194 mg/L and in embryos exposed to 0.0194 mg/L in comparison to embryos exposed to 0.097 mg/L (Figure 4E, Table S2).

Regarding the filtrated medium derived from rGO-Ag, a decreasing percentage of shell deformities with increasing concentration was observed in all the concentrations with surviving embryos, being significantly higher the percentage of shell deformities in mussels exposed to the filtrated medium equivalent to the 0.01 mg/L of rGO-Ag in comparison to the control. All the exposure concentrations showed a higher percentage of arrested development than the control and the embryos exposed to the filtrated medium equivalent to the 0.5 mg/L of rGO-Ag also showed a higher percentage of protuberant mantle than the control (Figure 4F, Table S2).

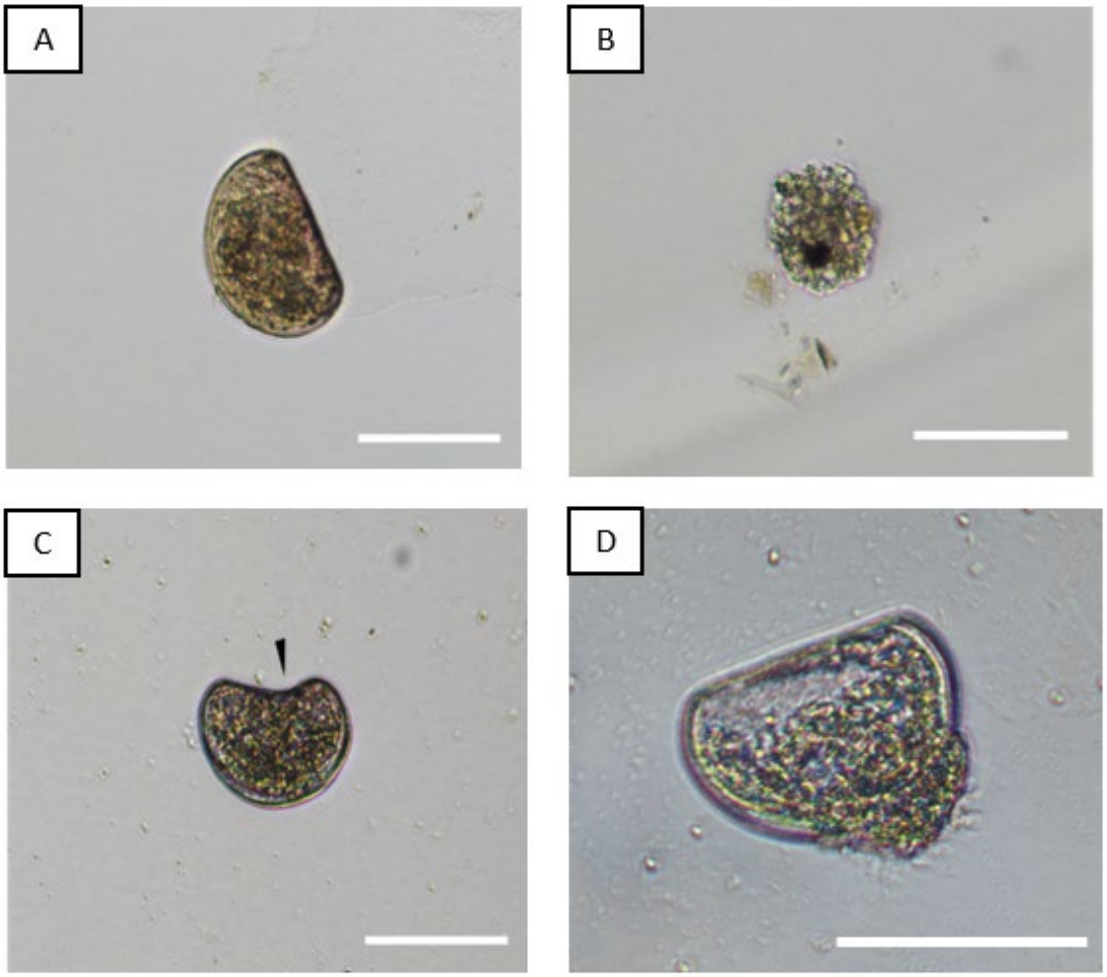

Figure 3. Micrographs of mussel embryos after 48 hours post-fertilization. A) Control D-larvae; B) Embryo whose development was arrested at the trochophore stage after exposure to GO with sorbed BaP; C) embryo whose development was arrested at the trochophore stage after exposure rGO abnormal larvae showing a shell deformity (arrowhead) after BaP exposure; D) Abnormal larvae showing a protuberant mantle after Ag NPs exposure. Scale bars: 100 µm.

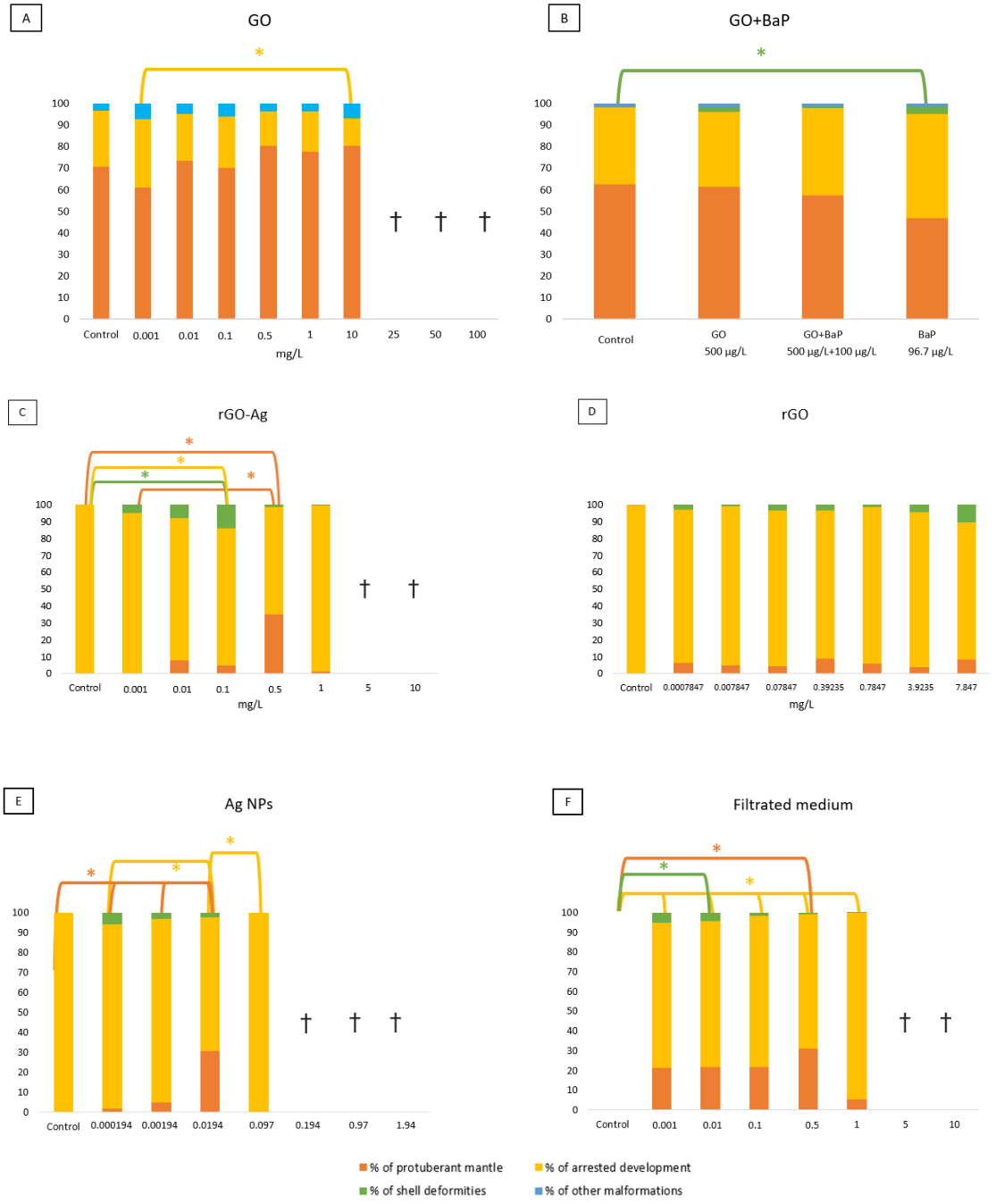

Figure 4. Percentage of each type of abnormality observed in control embryos and in embryos exposed to A) GO alone, B) GO with sorbed BaP compared to GO or BaP alone C) rGO-Ag, D) rGO at equivalent concentrations found in rGO-Ag, E) Ag NPs at equivalent concentrations found in rGO-Ag, F) Filtrated medium of rGO-Ag. The mean value of 4 experiments (4 replicates for each experiment) is given in each case. Asterisks denote a significant difference according to the Kruskal-Wallis test followed by the Dunn's post-hoc test ($p < 0.05$). † denotes 100% of mortality and no bar in the control in graph F means no malformed larvae.

4. DISCUSSION

GFNs are frequently claimed to be biocompatible materials but, however, they present a relative toxicity that can pose a risk for environmental and human health (Peng et al., 2020). In adult forms of bivalves GFNs have shown to alter gene transcription patterns and energy reserves, cause oxidative stress, immune toxicity, lysosomal membrane destabilization, DNA damage and inflammatory reactions, among others (Barrick et al., 2019; Britto et al., 2020;2021; Khan et al., 2019a;b; Meng et al., 2019; 2020; Coppola et al., 2020). In addition, Katsumiti et al. (2017) observed that the *in vitro* exposure of mussel hemocytes to GFNs decreased cell membrane integrity and increased production of reactive oxygen species. In some cases, GFNs have been categorized as not highly toxic or showing transitory toxicity (Katsumiti et al. 2017; Flasz et al., 2020). However, as far as we know, there are no studies addressing the effects of GFNs on early life stages of bivalves and especially of mussels, although embryo and larval stages are usually considered more sensitive to NMs than adult forms and different life stages should be considered to establish the toxicity of pollutants (Pörtner et al., 1998; Ringwood et al., 2009; Fabbri et al., 2014).

In the present study, GO and rGO alone showed low toxicity towards mussel embryos. This low toxicity could be related to the dispersability of these materials in marine water. At low GO concentrations a dose-response pattern of toxicity was observed, but once the materials started to aggregate and sink, toxicity decreased until it sharply went to full mortality at the highest concentrations tested. Similarly, Anand et al. (2019) reported that at medium concentrations (25–50 mg/mL) GO created "*floating scaffolds*" in saline solutions reducing its toxicity, but at higher concentrations toxicity increased again due to the formation of large aggregates. Though rGO showed the same trend to aggregate and sink at concentrations higher than 0.7847 mg/L, full mortality was not observed in embryos exposed to this compound. Toxicity of GFNs has been reported to be more dependent on the oxygen content (C/O proportion) than on the concentration (Guo & Mei, 2014; Barrios et al., 2019; Malina et al., 2020) as their reduction degree is correlated with their reactivity in aquatic environments (Guo & Mei, 2014; Ahmad et al., 2020), which could explain the difference in embryotoxicity between GO and rGO.

In addition, the proportion of each malformation phenotype observed in embryos exposed to GO and rGO was different. No shell deformities were observed in the embryos exposed to GO alone, but they were observed in embryos exposed to rGO. Further, the predominant malformation in embryos exposed to GO was the protuberant mantle, whereas in embryos exposed to rGO arrested development was the main malformation. Similarly, Martínez-Álvarez et al. (2021) also reported different percentages of malformation phenotypes in zebrafish larvae exposed to the same concentrations of GO and rGO and Liu et al. (2014) reported a reduction in the length of zebrafish larvae exposed to rGO, but not in those exposed to the same concentration of GO.

In the aquatic environment GFNs will interact with other pollutants (Ahmad et al., 2020) and organisms will inevitably be co-exposed to them (Zhao et al., 2020). Due to the physicochemical properties of GFNs, the functional groups present on the surface of GFNs tend to sorb a wide variety of compounds already present in the marine environment including metals, oils, antibiotics and PAHs (Ersan et al., 2017; Naasz et al., 2018; Peng et al., 2020). These interactions may enhance their bioavailability and toxicity (Britto et al., 2020). However, few works have studied this potential Trojan horse effect of GFNs and most of them are based on co-exposures of GFNs and metal compounds (Dziewicka et al., 2017; Liu et al., 2018; Lu et al., 2018; Britto et al., 2020; Coppola et al., 2020). In addition, in general, toxicity of organic compounds has been much less studied in mussel embryos than that of metals (Beiras & Bellas, 2008). Few works have addressed the impact of the model PAH benzo(a)pyrene (BaP) on the embryo development of bivalves but none of these have been performed in mussels *Mytilus sp.*, althought embryotoxicity of BaP towards bivalve larvae has been reported to be species-dependent (Lyons et al., 2002; Jeong & Chong, 2005; Wessel et al., 2007; Wang et al., 2012). In this work, sorption of BaP to GO did not alter the embryotoxicity profile of either GO or BaP at equivalent concentrations, discarding the occurrence of a Trojan horse effect. However in Chapter 3 we have shown the occurrence of different types of Trojan horse effects of GO with sorbed BaP in adult mussels. It must be taken into consideration that in the present work exposure to GO+BaP and BaP alone were

conducted in the dark, while a photo-dependent increase in the toxicity of BaP has been reported in oyster and clam embryos (Lyons et al., 2002; Fathalth et al., 2012).

Similar to our results, toxicity of GO to zebrafish embryos was not altered with sorbed BaP or with sorbed oil compounds from the water accommodated fraction of a naphthenic North Sea crude oil (Martínez-Álvarez et al., 2021). On the contrary, Meng et al. (2020) reported that the adsorption of triphenyl phosphate on the surface of graphene could inhibit its surface activity and thus, reduced its toxicity.

After exposure to BaP alone, a higher proportion of shell deformities were recorded in comparison to controls. Shell biogenesis is a key process in the development of mussels (Balbi et al., 2016; Wathsala et al., 2018). Different authors have suggested that disruption of larval shell formation may trigger on structural alterations in adult shells, which would make adult mussels more vulnerable towards numerous stressors, thus endangering the population resilience (Gizzi et al., 2016; Ramesh et al., 2017). Wang et al. (2012) reported that embryo/larvae of *Meretrix meretrix* were sensitive towards BaP in terms of metamorphosis. In addition, DNA damage and embryotoxicity have been correlated in bivalve larvae exposed to BaP (Wessel et al., 2007; Xie et al., 2017) and genes related to stress response, infectious diseases and innate immunity have been reported to be altered too (Jiang et al., 2016).

Ag NPs are one of the most widely used metal NPs, especially due to their antimicrobial properties (Nowack et al., 2012). These properties of Ag NPs are exploited for several applications and recently, novel nanocomposites consisting of Ag NPs combined with GFNs have been developed that could provide enhanced functionalities (Kumar et al., 2019). However, Ag NPs are toxic to a variety of organisms living in aquatic and marine environments (Cajaraville et al., 2021) where many of the applications of GFN-Ag NP hybrid materials are planned to be applied (Fatima et al., 2021; Pourhashem et al., 2022). In the case of bivalve embryos, a detrimental effect of Ag NPs has been observed at concentrations as low as µg/L (Ringwood et al., 2009; Auguste et al., 2018). In this work Ag NPs were the most toxic compound tested, with a EC_{50} of 0.001 mg/L, similar to previous results on Ag NP toxicity to bivalve embryos (Ringwood et al., 2009; Auguste et al., 2018). Auguste et al. (2018) observed that mussel larvae were especially withheld at trocophora stage after exposure to Ag NPs, but other malformations such as

protuberant mantle and shell deformities were also observed, in agreement with our results.

Chemical analysis showed that a 100 mg/L suspension of rGO-Ag released 967 ± 119,38 µg/L of silver ions in 48 hours in marine water. Consequently, a relatively high toxicity was observed in embryos exposed to rGO-Ag, with a EC_{50} of 0.017 mg/L. In contrast to exposures to plain GO and rGO, a dose-dependent response was observed in embryos exposed to rGO-Ag and all embryos were dead or malformed at concentrations lower than those needed for this compound to aggregate and sink. Comparison of the toxicity profile of rGO-Ag with those of Ag NPs and rGO at equivalent concentrations found in rGO-Ag pointed out that the toxicity of the latter came largely from the Ag NPs. However, results obtained from the filtrated medium suggested that the composite has a synergistic effect in terms of embryotoxicity, as exposure to the equivalent concentration of the filtered medium, where the rGO-Ag particles were removed and embryos were only exposed to silver ions, caused a lower toxicity than when exposed to rGO-Ag. For instance, the malformations observed in embryos exposed to equivalent concentrations of rGO-Ag and Ag NPs were almost comparable, whereas a higher proportion of larvae showing protuberant mantle was observed in embryos exposed to the filtrated medium. Some authors pointed that the large surface of GFNs will increase the contact area of Ag NPs with the target, thus increasing their toxic potential (De Luna et al., 2016). However, the toxicity of this type of nanocomposite has not been clarified yet: some researchers claimed that it is a suitable material for biomedical and antimicrobial applications, while others showed that it could cause hazard to humans and other organisms (Gurunathan et al., 2015; De Luna et al., 2016; Kim et al., 2018; de Medeiros et al., 2021). On the other hand, our data showed that Ag NPs were less toxic when combined with rGO in the rGO-Ag composite than when dosed alone at equivalent concentrations, pointing to a protective role of rGO against Ag NP toxicity. Overall, results obtained in mussel embryos were in agreement with those reported previously in Chapter 4 for adult mussels.

5. CONCLUSIONS

GO and rGO showed relatively low toxicity to mussel embryos, partly due to their aggregation and sedimentation behaviour in seawater. Nevertheless, they provoked significant embryotoxicity even at the lowest concentrations tested, which were environmentally realistic. Exposure to GO with sorbed BaP did not pose an additional risk to mussel embryos, discarding the occurrence of a Trojan horse effect. Ag NPs contributed largely to the embryotoxicity of the rGO-Ag nanocomposite, pointing to the toxic potential of GFN-Ag NP nanocomposites in the marine environment. At the same time, rGO appeared to extert a protective role against Ag NP toxicity.This work highlights the need to include embryotoxicity data in target species for the environmental risk assessment of GFNs and associated pollutants.

ACKNOWLEDGEMENTS

This work was funded by Spanish MINECO (NACE project CTM2016-81130-R), Basque Government (consolidated research group IT1302-19 and IT1743-22, and predoctoral fellowship to NGS).

REFERENCES

Ahmad S.Z.N., Wan Salleh W.N., Ismail A.F., Yusof N., Mohd Yusop M.Z., Aziz F. 2020. Adsorptive removal of heavy metal ions using graphene-based nanomaterials: Toxicity, roles of functional groups and mechanisms. Chemosphere 248, 126008.

Anand A., Unnikrishnan B., Wei S.C., Chou C.P., Zhang L.Z., Huang C.C. 2019. Graphene oxide and carbon dots as broad spectrum antimicrobial agents- a minireview. Nanoscale Horizons 4,117.

Auguste M., Ciacci C., Balbi T., Brunelli A., Caratto V., Marcomini A., Cuppini R., Canesi L. 2018. Effects of nanosilver on *Mytilus galloprovincialis* hemocytes and early embryo development. Aquatic Toxicology 203, 107–116.

Bai H., Li C., Shi G. 2011. Functional Composite Materials based on Chemically converted graphene. Advanced Materials 23, 1089-1115.

Balbi T., Franzellitti S., Fabbri, R., Montagna, M., Fabbri, E., Canesi, L. 2016. Impact of bisphenol A (BPA) on early embryo development in the marine mussel *Mytilus galloprovincialis*: Effects on gene transcription. Environmental Pollution 218, 996–1004.

Banni M., Sforzini S., Arlt V.M., Barranger A., Dallas L.J., Oliveri C., Aminot Y., Pacchioni B., Millino C., Lanfranchi G., Readman J.W., Moore M.N., Viarengo A., Jha A.N. 2017. Assessing the impact of Benzo[a]pyrene on Marine Mussels: Application of a novel targeted low density microarray complementing classical biomarker responses. PLoS ONE 12, 1–26.

Barrick A., Manier N., Lonchambon P., Flahaut E., Jrad N., Mouneyrac C., Châtel A. 2019. Investigating a transcriptomic approach on marine mussel hemocytes exposed to carbon nanofibers: An *in vitro/in vivo* comparison. Aquatic Toxicology 207, 19–28.

Barrios A., Wang Y., Gilbertson L.M., Perreault F. 2019. Structure-property-toxicity relationships of graphene oxide: role of surface chemistry on the mechanisms of interactions with bacteria. Environ. Sci. Technol. 53, 14679-14687.

Beiras R., Bellas J. 2008. Inhibition of embryo development of the *Mytilus galloprovincialis* marine mussel by organic pollutants; assessment of risk for its extensive culture in the Galician Rias. Aquaculture 277, 208–212.

Beiras R., Bellas J., Cachot J., Cormier B., Cousin X., Engwall M., Gambardella C., Garaventa F., Keiter S., Le Bihanic F., López-Ibáñez S., Piazza V., Rial D., Tato T., Vidal-Liñán L. 2018. Ingestion and contact with polyethylene microplastics does not cause acute toxicity on marine zooplankton. Journal of Hazardous Materials 360, 452–460.

Britto R.S., Nascimento J.P., Serode T., Santos A.P., Soares A.M.V.M., Figueira E., Furtado C., Lima-Ventura J., Monserrat J.M., Freitas R. 2020. The effects of co-exposure of graphene oxide and copper under different pH conditions in Manila clam *Ruditapes philippinarum*. Environmental Science and Pollution Research 27, 30945–30956.

Britto R.S., Nascimento J.P., Serodre T., Santos A.P., Soares A.M.V.M., Furtado C., Ventura-Lima J., Monserrat J.M., Freitas R. 2021. Oxidative stress in *Ruditapes philippinarum* after exposure to different graphene oxide concentrations in the presence and absence of sediment. Comparative Biochemistry and Physiology Part - C: Toxicology and Pharmacology, 240.

Cajaraville M.P., Bebianno M.J., Blasco J., Porte C., Sarasquete C., Viarengo A. 2000. The use of biomarkers to assess the impact of pollution in coastal environments of the Iberian Peninsula: a practical approach. Science of the Total Environment 247, 295-311.

Cajaraville M.P., Duroudier N., Bilbao E. 2021. Chapter 2 - Mechanisms of toxicity of engineered nanoparticles: adverse outcome pathway for dietary silver nanoparticles in mussels, Editor(s): James Njuguna, Krzysztof Pielichowski, Huijun Zhu, In Woodhead Publishing Series in Composites Science and Engineering, Health and Environmental Safety of Nanomaterials (Second Edition), Woodhead Publishing, Pages 39-82, ISBN 9780128205051.

Cancio I., Orbea A., Völkl A., Fahimi H.D., Cajaraville M.P. 1998. Induction of peroxisomal oxidases in mussels: comparison of effects of lubricant oil and benzo(a)pyrene with two typical peroxisome proliferators on peroxisome structure and function in *Mytilus galloprovincialis*. Toxicology and applied pharmacology 149, 64-72.

Capela R., Garric J., Castro L.F.C., Santos M.M. 2020. Embryo bioassays with aquatic animals for toxicity testing and hazard assessment of emerging pollutants: A review. Science of the Total Environment 705, 135740.

Capolupo M., Franzellitti S., Valbonesi P., Lanzas C.S., Fabbri E. 2018. Uptake and transcriptional effects of polystyrene microplastics in larval stages of the Mediterranean mussel *Mytilus galloprovincialis*. Environmental Pollution 241, 1038–1047.

Carls M.G., Holland L., Larsen M., Collier T.K., Scholz N.L., Incardona J. P. 2008. Fish embryos are damaged by dissolved PAHs, not oil particles. Aquatic Toxicology. 88: 121-127.

Coppola F., Bessa A., Henriques B., Russo T., Soares A.M.V.M., Figueira E., Pereira E., Marques P., Polese G., Freitas R. 2020. The role of temperature on the impact of remediated water towards marine organisms. Water 12, 1–17.

De Luna L.A.V., Moraes A.C.M., Consonni S.R., Pereira C.D., Cadore S., Giorgio S., Alves O.L. 2016. Comparative *in vitro* toxicity of a graphene oxide-silver nanocomposite and the pristine counterparts toward macrophages. Journal of Nanobiotechnology 14, 1–17.

De Marchi L., Coppola F., Soares A.M.V.M., Pretti C., Monserrat J.M., Torre C., Freitas R. 2019. Engineered nanomaterials: From their properties and applications, to their toxicity towards marine bivalves in a changing environment. Environmental Research 178, 108683.

De Marchi L., Pretti C., Gabriel B., Marques P.A.A.P., Freitas R., Neto V. 2018. An overview of graphene materials: Properties, applications and toxicity on aquatic environments. Science of the Total Environment 631–632, 1440–1456.

de Medeiros A.M.Z., Khan L.U., da Silva G.H., Ospina C.A., Alves O.L., de Castro V.L., Martinez D. S.T. 2021. Graphene oxide-silver nanoparticle hybrid material: an integrated nanosafety study in zebrafish embryos. Ecotoxicology and Environmental Safety, 209.

Di Y., Aminot Y., Schroeder D.C., Readman J.W., Jha A.N. 2017. Integrated biological responses and tissue-specific expression of p53 and ras genes in marine mussels following exposure to benzo(α)pyrene and C60 fullerenes, either alone or in combination. Mutagenesis 32, 77-90.

Di Y., Schroeder D.C., Highfield A., Readman J.W., Jha A.N. 2011. Tissue-specific expression of p53 and ras genes in response to the environmental genotoxicant benzo(α)pyrene in marine mussels. Environmental science & technology 45, 8974-8981.

Dziewięcka M., Karpeta-Kaczmarek J., Augustyniak M., Rost-Roszkowska M. 2017. Short-term in vivo exposure to graphene oxide can cause damage to the gut and testis. Journal of Hazardous Materials, 328, 80–89.

Ersan G., Apul O.G., Perreault F., Karanfil T. 2017. Adsorption of organic contaminants by graphene nanosheets: A review. Water Research 126, 385–398.

Fabbri R., Montagna M., Balbi T., Raffo E., Palumbo F., Canesi L. 2014. Adaptation of the bivalve embryotoxicity assay for the high throughput screening of emerging contaminants in *Mytilus galloprovincialis*. Marine Environmental Research 99, 1–8.

Fathallah S., Medhioub M.N. Kraiem M.M. 2012. Photo-induced toxicity of four polycyclic aromatic hydrocarbons (PAHs) to embryos and larvae of the carpet shell clam *Ruditapes decussatus*. Bulletin of Environmental Contamination and Toxicology, 88(6), 1001–1008.

Fatima N., Qazi U.Y., Mansha A., Bhatti I.A., Javaid R., Abbas Q., Nadeem N., Rehan Z.A., Noreen S., Zahid M. 2021. Recent developments for antimicrobial applications of graphene-based polymeric composites: A review. Journal of Industrial and Engineering Chemistry 100, 40–58.

Flasz B., Dziewięcka M., Kędziorski A., Tarnawska M., Augustyniak M. 2020. Vitellogenin expression, DNA damage, health status of cells and catalase activity in *Acheta domesticus* selected according to their longevity after graphene oxide treatment. Science of the Total Environment 737.

Gamain P., Gonzalez P., Cachot J., Clérandeau C., Mazzella N., Gourves P.Y., Morin B. 2017. Combined effects of temperature and copper and S-metolachlor on embryo-larval development of the Pacific oyster, *Crassostrea gigas*. Marine Pollution Bulletin, 115, 201–210.

Gizzi F., Caccia M.G., Simoncini G.A., Mancuso A., Reggi M., Fermani S., Brizi L., Fantazzini P., Stagioni M., Falini G., Piccinetti C., Goffredo S. 2016. Shell properties of commercial clam Chamelea gallina are influenced by temperature and solar radiation along a wide latitudinal gradient. Sci. Rep. 6, 36420.

Gómez-Mendikute A., Etxeberria A., Olabarrieta I., Cajaraville M.P. 2002. Oxygen radicals production and actin filament disruption in bivalve haemocytes treated with benzo(a)pyrene. Marine environmental research 54, 431-436.

Goodwin D.G., Adeleye A.S., Sung L., Ho K.T., Burgess R.M., Petersen E.J. 2018. Detection and Quantification of Graphene-Family Nanomaterials in the Environment. Environmental Science and Technology, 52, 4491–4513.

Guo X., Mei N. 2014. Assessment of the toxic potential of graphene family nanomaterials. Journal of Food and Drug Analysis 22, 105–115.

Gurunathan S., Han J.W., Park J.H., Kim E., Choi Y.J., Kwon D.N., Kim J.H. 2015. Reduced graphene oxide-silver nanoparticle nanocomposite: A potential anticancer nanotherapy. International Journal of Nanomedicine, 10, 6257–6276.

Hassandoost R., Pouran S.R., Khataee A., Orooji Y., Joo S.W.2019. Hierarchically structured ternary heterojunctions based on Ce3+/ Ce4+ modified Fe3O4 nanoparticles anchored onto graphene oxide sheets as magnetic visible-light-active photocatalysts for decontamination of oxytetracycline. Journal of Hazardous Materials 376, 200-211.

His E., Beiras R., Seaman M.N.L. 1999. The assessment of marine pollution bioassays with bivalve embryos and larvae. In Advances in Marine Biology (Vol. 37, Issue 37). Elsevier Masson SAS.

His E., Seaman M.N.L., Beiras R. 1997. A simplification the bivalve embryogenesis and larval development bioassay method for water quality assessment. Water Research, 31(2), 351–355.

Huang S.Y., Zhang K., Yuen M.M.F., Fu X.Z., Sun R., Wong C.P. 2014. Facile synthesis of flexible graphene-silver composite papers with promising electrical and thermal conductivity performances. RSC Advances 4, 34156-34160.

Hutchison J.E. 2016. The road to sustainable nanotechnology: challenges, progress and opportunities. ACS Sustain. Chem. Eng. 4, 5907–5914.

Jeong W.G., Cho S.M. 2005. The effects of polycyclic aromatic hydrocarbon exposure on the fertilization and larva development of the Pacific oyster, *Crassostrea gigas*. Journal of Shellfish Research 24,209–213.

Jiang X., Qiu L., Zhao H., Song Q., Zhou H., Han Q., Diao X. 2016. Transcriptomic responses of *Perna viridis* embryo to Benzo(a)pyrene exposure elucidated by RNA sequencing. Chemosphere, 163, 125–132.

Katsumiti A., Cajaraville M.P. 2019. Chapter 3: *In vitro* testing: *In Vitro* Toxicity Testing with Bivalve Mollusc and Fish Cells for the Risk Assessment of Nanoparticles in the Aquatic Environment. In: Ecotoxicology of Nanoparticles in Aquatic Systems. J BLASCO, I CORSI (eds), Science Publishers CRC Press/ Taylor & Francis Group, Boca Raton, London, New York, pp 62-98, ISBN 9781138067264.

Katsumiti A., Tomovska R., Cajaraville M.P. 2017. Intracellular localization and toxicity of graphene oxide and reduced graphene oxide nanoplatelets to mussel hemocytes *in vitro*. Aquatic Toxicology 188, 138–147.

Khan B., Adeleye A.S., Burgess R.M., Russo S.M., Ho K.T. 2019a. Effects of graphene oxide nanomaterial exposures on the marine bivalve, *Crassostrea virginica*. Aquatic Toxicology 216, 105297.

Khan B., Adeleye A.S., Burgess R.M., Smolowitz R., Russo S.M., Ho K.T. 2019b. A 72-h exposure study with eastern oysters (*Crassostrea virginica*) and the nanomaterial graphene oxide. Environmental Toxicology and Chemistry 38, 820–830.

Kim M.J., Ko D., Ko K., Kim D., Lee J.Y., Woo S.M., Kim W., Chung H. 2018. Effects of silver-graphene oxide nanocomposites on soil microbial communities. Journal of Hazardous Materials 346, 93–102.

Krishnaraj C., Kaliannagounder V.K., Rajan R., Ramesh T., Kim C.S., Park C.H., Liu B., Yun S. 2022. Silver nanoparticles decorated reduced graphene oxide: Eco-friendly synthesis, characterization, biological activities and embryo toxicity studies. Environmental Research, 210, 112864.

Kumar P., Huo P., Zhang R., Liu B. 2019. Antibacterial Properties of Graphene Based Nanomaterials. Nanomaterials 9, 737.

Liu S., Ge H., Wang C., Zou Y., Liu J. 2018. Agricultural waste/graphene oxide 3D bio-adsorbent for highly efficient removal of methylene blue from water pollution. Science of the Total Environment 628–629, 959–968.

Liu X.T., Mu X.Y., Wu X.L., Meng L.X., Guan W.B., Ma Y.Q., Sun H., Wang C.J., Li X.F. 2014. Toxicity of multi-walled carbon nanotubes, graphene oxide, and reduced graphene oxide to zebrafish embryos. Biomedical and Environmental Sciences 27, 676–683.

Lu J., Zhu X., Tian S., Lv X., Chen Z., Jiang Y., Liao X., Cai Z., Chen B. 2018. Graphene oxide in the marine environment: Toxicity to *Artemia salina* with and without the presence of Phe and Cd2+. Chemosphere, 211, 390–396.

Lyons B.P., Pascoe C.K., McFadzen I.R.B. 2002 Phototoxicity of pyrene and benzo(a)pyrene to embryo-larval stages of the pacific oyster *Crassostrea gigas*. Marine Environmental Research 54, 627-631.

Malina T., Maršálková E., Holá K., Zbořil R., Maršálek B. 2020. The environmental fate of graphene oxide in aquatic environment—Complete mitigation of its acute toxicity to planktonic and benthic crustaceans by algae. Journal of Hazardous Materials 399, 123027.

Marigómez I., Izagirre U., Lekube X. 2005. Lysosomal enlargement in digestive cells of mussels exposed to cadmium, benzo[a]pyrene and their combination. Comparative Biochemistry and Physiology Part C: Toxicology & Pharmacology 141, 188-193.

Martínez-Álvarez I., Le Menach K., Devier M.H., Barbarin I., Tomovska R., Cajaraville M.P., Budzinski H., Orbea A. 2021. Uptake and effects of graphene oxide nanomaterials alone and in combination with polycyclic aromatic hydrocarbons in zebrafish. Science of the Total Environmente 775, 145669.

Meng X., Li F., Wang X., Liu J., Ji C., Wu H. 2019. Combinatorial immune and stress response, cytoskeleton and signal transduction effects of graphene and triphenyl phosphate (TPP) in mussel *Mytilus galloprovincialis*. Journal of Hazardous Materials 378, 120778.

Meng X., Li F., Wang X., Liu J., Ji C., Wu H. 2020. Toxicological effects of graphene on mussel *Mytilus galloprovincialis* hemocytes after individual and combined exposure with triphenyl phosphate. Marine Pollution Bulletin 151, 110838.

Mu J., Gao F., Cui G., Wang S., Tang S., Li Z. 2021. A comprehensive review of anticorrosive graphene-composite coatings. Progress in organic coating 157, 106321.

Naasz S., Altenburger R., Kühnel D. 2018. Environmental mixtures of nanomaterials and chemicals: The Trojan-horse phenomenon and its relevance for ecotoxicity. Science of the Total Environment 635, 1170–1181.

Nowack B., Krug H.F., Height. 2011. 120 Years of nanosiver history: implications for policy makers. Environmental Science Technology 45, 1177-1183.

Peng Z., Liu X., Zhang W., Zeng Z., Liu Z., Zhang C., Liu Y., Shao B., Liang Q., Tang W., Yuan X. 2020. Advances in the application, toxicity and degradation of carbon nanomaterials in environment: A review. Environment International 134, 105298.

Pörtner H.O., Reipschlager A., Heisler N. 1998. Acid-base regulation, metabolismand energetics in *Sipunculus nudus* as a function of ambient carbon dioxide level. The Journal of Experimental Biology 201, 43–55.

Pourhashem S., Seif A., Saba F., Nezhad E.G., Ji X., Zho Z., Zhai X., Mirzaee M., Duan J., Rashidi A., Hou B. 2022. Antifouling nanocomposite polymer coatings for marine applications: a review on experiments, mechanisms and theoretical studies. Journal of Materials & Technology 118, 73-113.

Ramesh K., Hu M.Y., Thomsen J., Bleich M., Melzner F. 2017. Mussel larvae modify calcifying fluid carbonate chemistry to promote calcification. Nat. Commun. 8, 1–8.

Ren W., Cheng H.M. 2014. The global growth of graphene. Nature Nanotechnology 9, 726–730.

Ringwood A.H., Levi-Polyachenko N., Carroll D.L. 2009. Fullerene exposures with oysters: Embryonic, adult, and cellular responses. Environmental Science and Technology 43, 7136–7141.

Sajid M. 2021. Nanomaterials: types, properties, recent advances, and toxicity concerns. Current Opinion in Environmental Science and Health 25, 100319.

Sanchís J., Olmos M., Vincent P., Farré M., Barceló D. 2016. New Insights on the Influence of Organic Co-Contaminants on the Aquatic Toxicology of Carbon Nanomaterials. Environmental Science and Technology 50, 961–969.

Stankovich S., Dikin D.A., Dommett G.H.B., Kohlass K.M., Zimney E.J., Stach E.A., Piner R.D., Nguyen S.T., Ruoff R.S. 2006. Graphene based composite material. Nature 442, 282–286

Tian S., Pan L., Sun X. 2013. An investigation of endocrine disrupting effects and toxic mechanisms modulated by benzo[a]pyrene in female scallop *Chlamys farreri*. Aquatic toxicology 144, 162-171.

U. S. EPA. 2014. IRIS Toxicological Review of Benzo[a]pyrene (External Review Draft). U.S. Environmental Protection Agency, Washington, DC EPA/635/R-14/312.

U.E. Water Framework Directive. 2008. Environmental Quality Standards Directive (EQSD). 105/EC. https://ec.europa.eu/environment/water/water-framework/priority_substances.htm.

Vethaak A.D., Davies I.M., Thain J.E., Gubbins M.J., Martínez-Gómez C., Robinson C.D., Moffat C.F., Burgeot T., Maes T., Wosniok W., Giltrap M., Lang T., Hylland K. 2017. Integrated indicator framework and methodology for monitoring and assessment of hazardous substances and their effects in the marine environment. Marine Environmental Research, 124, 11–20.

Wale P.L., Gardner D.K. 2016. The effects of chemical and physical factors on mammalian embryo culture and their impostance for the practice of assisted human reproduction. Human Reproduction Update 22,2 –22.

Wang J., Zhang J., Han L., Wang J., Zhu L., Zeng H. 2021. Graohene based materials for adsorptive removal of pollutants from water and underlying interaction mechanism. Advances in Colloid and Interface Science 289, 102360.

Wang Q., Yang H., Liu B., Wang X. 2012. Toxic effects of benzo[a]pyrene (Bap) and Aroclor1254 on embryogenesis, larval growth, survival and metamorphosis of the bivalve *Meretrix meretrix*. Ecotoxicology 21, 1617–1624.

Wathsala R.H.G.R., Franzellitti S., Scaglione M., Fabbri E. 2018. Styrene impairs normal embryo development in the Mediterranean mussel (*Mytilus galloprovincialis*). Aquatic Toxicology 201, 58–65.

Wessel N., Rousseau S., Caisey X., Quiniou F., Akcha F. 2007. Investigating the relationship between embryotoxic and genotoxic effects of benzo[a]pyrene, 17α-ethinylestradiol and endosulfan on *Crassostrea gigas* embryos. Aquatic Toxicology 85, 133–142.

Xie J., Yang D., Sun X., Cao R., Chen L., Wang Q., Li F., Wu H., Ji C., Cong M., Zhao J. 2017. Individual and Combined Toxicities of Benzo[a]pyrene and 2,2”,4,4”-Tetrabromodiphenyl

Ether on Early Life Stages of the Pacific Oyster, *Crassostrea gigas*. Bulletin of Environmental Contamination and Toxicology 99, 582–588.

Zhao J., Ning F., Cao X., Yao H., Wang Z., Xing B. 2020. Photo-transformation of graphene oxide in the presence of co-existing metal ions regulated its toxicity to freshwater algae. Water Research 176, 115735.

Zhao J., Wang Z., White J.C., Xing, B. 2014. Graphene in the aquatic environment: Adsorption, dispersion, toxicity and transformation. Environmental Science and Technology 48, 9995–10009.

Zhao Y., Liu Y., Zhang X., Liao W. 2021. Environmental transformation of graphene oxide in the aquatic environment. Chemosphere 262, 127885.

Ziat Y., Hammi M., Zarhri Z., Laghlimi C. 2020. Epoxy coating modified with graphene: A promising composite against corrosion behavior of copper surface in marine media. Journal of Alloys and Compounds, 820, 153380.

SUPPLEMENTARY MATERIAL TO CHAPTER 5

Table S1. Mean and standard deviation of percentage of normal D larvae and malformed larvae given in figure 2. † denotes 100% of mortality.

		% of normal D larvae	% of malformed larvae
Control		92.07 ± 10.54	7.93 ± 10.54
GO	0.001 mg/L	66.16 ± 2.90	11.6 ± 2.90
	0.01 mg/L	62.82 ± 20.31	37.18 ± 20.31
	0.1 mg/ L	53.1 ± 28.24	46.9± 28.24
	0.5 mg/ L	47.3 ± 21.70	52.7 ± 21.70
	1 mg/ L	53.75 ± 16.21	46.25 ± 16.21
	10 mg/ L	57.84 ± 12.71	42.16 ± 12.71
	25 mg/ L	†	†
	50 mg/ L	†	†
	100 mg/ L	†	†
GO	500 µg/L	60.37 ± 13.77	39.63 ± 13.77
GO+BaP	500 µg/L+100 µg/L	59.96 ± 15.13	40.04 ± 15.13
BaP	96.7 µg/L	59.43 ±18.54	40.57 ±18.54
rGO-Ag	0.001 mg/ L	69.56 ± 18.32	30.44 ± 18.52
	0.01 mg/ L	62.99 ± 19.40	37.01 ± 19.40
	0.1 mg/ L	63.38 ± 19.91	36.61 ± 19.91
	0.5 mg/ L	0.44 ± 1.33	99.55 ± 1.33
	1 mg/ L	0	100
	5 mg/ L	†	†
	10 mg/ L	†	†
rGO	0.0007847 mg/ L	60.27 ± 29.29	39.73 ±29.29
	0.007847 mg/ L	59.28 ± 29.40	40.72 ±29.49
	0.07847 mg/ L	66.98 ± 19.73	31.38 ± 19.93
	0.39235 mg/ L	74.05 ±17.09	25.95 ± 17.09
	0.7847 mg/ L	77.52 ± 17.48	22.48 ± 17.48
	3.9235 mg/ L	72.6 ±18.13	27.4 ± 18.13
	7.847 mg/ L	63.11 ±20.63	36.89 ±20.63
Ag NPs	0.000194 mg/ L	59.98 ± 29.36	40.02 ± 29.36
	0.00194 mg/ L	59.33 ± 28.05	40.67 ± 28.05
	0.0194 mg/ L	16.19 ± 23	83.81 ± 23
	0.097 mg/ L	0	100
	0.194 mg/ L	†	†
	0.97 mg/ L	†	†
	1.94 mg/ L	†	†
Filtrated medium	0.001 mg/ L	74.36 ± 20.61	25.64 ± 20.61
	0.01 mg/ L	77.21 ± 15.96	22.79 ± 15.96
	0.1 mg/ L	63.36 ± 23.03	36.64 ± 23.03
	0.5 mg/ L	13.72 ± 12.24	86.28 ± 12.24
	1 mg/ L	5.64 ± 18.04	94.36 ± 18.04
	5 mg/ L	†	†
	10 mg/ L	†	†

Table S2. Mean and standard deviation of percentage of each type of abnormality given in figure 4. † denotes 100% of mortality.

		% of protuberant mantle	% of arrested development	% of shell deformities	% of other malformations
GO	0.001 mg/L	61.09 ± 28.36	31.75 ± 20.69	0	7.16 ± 13.26
	0.01 mg/L	73.4 ± 17.99	21.65 ± 13.51	0	4.95 ± 9.18
	0.1 mg/ L	70.2 ± 20.41	23.82 ± 12.53	0	5.98 ± 10.61
	0.5 mg/ L	80.5 ± 16.76	15.82 ± 12.46	0	3.68 ± 7.92
	1 mg/ L	77.52 ± 16.73	18.7 ± 11.40	0	3.77 ± 6.94
	10 mg/ L	80.47 ± 15.26	12.46 ± 9.44	0.4 ± 1.10	6.67 ± 11.23
	25 mg/ L	†	†	†	†
	50 mg/ L	†	†	†	†
	100 mg/ L	†	†	†	†
GO	500 µg/L	62.14 ± 18.05	34.30 ± 19.95	1.83 ± 3.36	1.73 ±2.42
GO+BaP	500 µg/L+100 µg/L	62.66 ± 19.86	39.42 ± 32.45	0.58 ± 0.81	1.61 ± 1.28
BaP	96.7 µg/L	49.25 ± 13.09	46.11 ± 41.92	3.36 ± 5.03	1.61 ± 1.11
rGO-Ag	0.001 mg/ L	0.36 ± 0.99	94.8 ± 9.17	4.84 ± 9.28	0
	0.01 mg/ L	7.89 ± 23.22	84.43 ± 27.67	7.68 ± 18.04	0
	0.1 mg/ L	4.86 ±7.23	81.34 ± 21.64	13.8 ± 16.70	0
	0.5 mg/ L	35.08 ±41.76	63.59 ± 43.50	1.33 ± 2.92	0
	1 mg/ L	1.17 ± 1.60	98.64 ± 1.50	0.19 ± 0.47	0
	5 mg/ L	†	†	†	†
	10 mg/ L	†	†	†	†
rGO	0.0007847 mg/ L	6.19 ± 10.10	91.04 ± 12.61	2.77 ± 6.12	0
	0.007847 mg/ L	4.69 ± 12.79	94.53 ± 12.87	0.78 ± 3.13	0
	0.07847 mg/ L	4.57 ± 11.02	92.21 ± 12.55	3.21 ± 8.23	0
	0.39235 mg/ L	9.06 ± 22.42	87.41 ±23.62	3.54 ± 9.74	0
	0.7847 mg/ L	5.96 ± 8.16	92.48 ± 8.09	1.56 ± 3.43	0
	3.9235 mg/ L	3.85 ± 5.79	91.53 ± 7.90	4.63 ± 7.91	0
	7.847 mg/ L	8.21 ± 11.98	81.37 ± 20.37	10.42 ± 19.15	0
Ag NPs	0.000194 mg/ L	1.57 ± 3.58	92.59 ± 12.82	5.83 ± 13.08	0
	0.00194 mg/ L	4.89 ± 7.06	91.98 ± 10.71	3.13 ± 7.43	0
	0.0194 mg/ L	30.78 ± 28.22	66.87 ± 26.05	2.35 ± 4.54	0
	0.097 mg/ L	0	100	0	0
	0.194 mg/ L	†	†	†	†
	0.97 mg/ L	†	†	†	†
	1.94 mg/ L	†	†	†	†
Filtrated medium	0.001 mg/ L	21.06 ± 27.77	73.83 ± 20.92	5.11 ± 8.31	0
	0.01 mg/ L	21.68 ± 22.61	73.85 ±21.15	4.48 ± 11.69	0
	0.1 mg/ L	21.53 ± 24.34	76.62 ± 22.93	1.85 ± 3.93	0
	0.5 mg/ L	31.13 ±31.23	67.94 ± 32.01	0.93 ± 1.44	0
	1 mg/ L	5.31 ± 12.76	94.47 ± 13.44	0.23 ± 0.75	0
	5 mg/ L	†	†	†	†
	10 mg/ L	†	†	†	†

4. GENERAL DISCUSSION

4. GENERAL DISCUSSION

Nanomaterials (NMs) are a diverse class of materials with at least one dimension at the nanoscale (<100 nm), that possess unique properties due their nanosize (Nel et al., 2006; Heinz et al., 2017). The rapid development of nanotechnology and nanoindustry would result, as for any other material, in their introduction into the environment, which has led to a growing concern about their possible impacts (Gottschalk & Nowack, 2011). The marine environment merits special consideration because NMs tend to end up in waterways and finally in the oceans (Rocha et al., 2015a; de Marchi et al., 2019). In consequence, studies on the uptake and potential bioaccumulation and toxicity of NMs to marine organisms are urgently needed. In contrast with the growing knowledge on the toxicity of metal-bearing nanoparticles (NPs) in marine organisms, works on the impact of carbon-based nanomaterials such as graphene family nanomaterials (GFNs) is scarce, even though graphene and its derivatives have become one of the main research interest of the latest years due to their astonishing properties and their applicability in several fields (Ren & Chen, 2014; Peng et al., 2020). On the other hand, plastic marine litter is one of the biggest global concerns nowadays (Kühn et al., 2015). Especially, the smallest fraction of plastic litter, the nanoplastics (NPs, <1 μm) and microplastics (MPs, <1 mm), which comprise the least studied most dangerous part of marine litter due to their size-specific properties (Koelmans., 2015; Hartmann et al., 2019). Moreover, pollutants do not appear alone in the marine environment. Thousands of organic compounds, including persistent organic pollutants (POPs) such as polycyclic aromatic hydrocarbons, are released into water bodies derived from natural, but mostly from anthropogenic activities and oil spills anthropogenic activity and oil spills (Meador et al., 1995; Abdel-Shafy & Mansour, 2016). As other carbon based NMs, GFNs are prone to adsorb different compounds including organic pollutants and thus, their potential use in water pollution remediation is being extensively studied (Ersan et al., 2017; Younis et al., 2020), but the ability of both GFNs and NPs and MPs to adsorb POPs could cause an additional threat to marine organisms because GFNs, NPs and MPs could act as vehicles or carriers of pollutants to marine organisms, increasing their bioavailability and toxicity through the so-called Trojan horse effect (Deng et al., 2017; Freixa et al., 2018; Naasz et al., 2018; Sendra et al., 2021). In addition, in order to perform a realistic assessment of

the hazards of nano and micro scale particulate pollutants, their possible interactions with other pollutants in the marine environment must be considered (Deng et al., 2017). Bivalve molluscs such as mussels (*Mytilus sp.*) are used all over the globe as sentinel organisms in environmental pollution (Viarengo et al., 2007). In addition, due to their filter-feeding activity and well-developed endo-lysosomal system, mussels have been considered an important target for NMs in the marine environment and thus, have been proposed as model organisms to study the toxicity of NMs, NPs and MPs and their associated contaminants (Canesi et al., 2012; Li et al., 2019). In view of the complex responses that could be triggered in mussels by a diverse range of NMs and associated pollutants, in this PhD we adopted a holistic approach involving the use of a wide battery of biomarkers and biological responses at different levels of biological organization in both embryo and adult stages of mussels in order to determine the potential impact of GFNs and NPs and MPs alone and in combination with adsorbed POPs in the marine environment.

4.1. The Trojan horse effect

In this PhD we have studied the hypothesis that sorption of POPs such as PAHs to GFNs and to NPs and MPs could increase the bioavailability and thus toxicity of POPs by the so-called Trojan horse effect. This hypothesis has been investigated with NPs and MPs in Chapters 1, MPs in Chapter 2 and with GFNs in Chapters 3 and 5.

Regarding plastics, the fate and impact of polystyrene (PS) NPs and MPs alone and with sorbed benzo(a)pyrene (BaP) (Chapter 1) and of PS MPs alone or with sorbed oil compounds from the water accommodated fraction (WAF) of a naphthenic North Sea crude oil (Chapter 2) were studied after a long-term dietary exposure that lasted for 26 days in Chapter 1 and 21 days in Chapter 2. In both Chapters an environmentally relevant concentration of 0.058 mg/L (1000 particles/mL in the case of 4.5 µm MPs and 7.44×10^5 particles/mL for 0.5 µm NPs) was used (Eriksen et al., 2013; Lechner et al., 2014).

In the case of GFNs, in Chapter 3 adult mussels were exposed for 7 days to graphene oxide (GO) alone, GO with sorbed BaP (GO+BaP) and to the equivalent concentration of

BaP sorbed into GO+BaP whereas in Chapter 5 newly fertilized mussel embryos were exposed to the same conditions for 48 hours.

As to the Trojan horse effect, in Chapter 1 we did not include in the experimental design a group of exposure to BaP. Thus, we could not compare the effects of 0.5 µm NPs and 4.5 µm MPs with sorbed BaP with those caused by dissolved BaP at equivalent concentrations. In terms of BaP bioaccumulation, NPs and MPs were demonstrated to act as carriers of BaP to mussels but we could not determine the extent of BaP bioaccumulation compared to exposure to BaP alone. In terms of toxicological impact, increased effects of NPs and MPs with sorbed BaP compared to NPs and MPs alone were observed for some endpoints (cell viability and catalase activity of mussel hemocytes and structure of digestive tubules), but not for others (such as DNA damage or cell composition of digestive tubules) in which the size of the particles was more important at defining the toxicity profile of NPs and MPs (Figure 1). The particle size also had a clear influence on the bioaccumulation of BaP, mussels exposed to 0.5 µm NPs accumulating at least 2 times more BaP in their tissues than mussels exposed to 4.5 µm (Figure 1). In addition, bioaccumulation of BaP in mussel tissues increased along the exposure time. Exposure time was also a crucial factor to explain differences observed in many of the parameters studied in Chapter 1, with a different response being observed at 7 and 26 days of exposure (Figure 1).

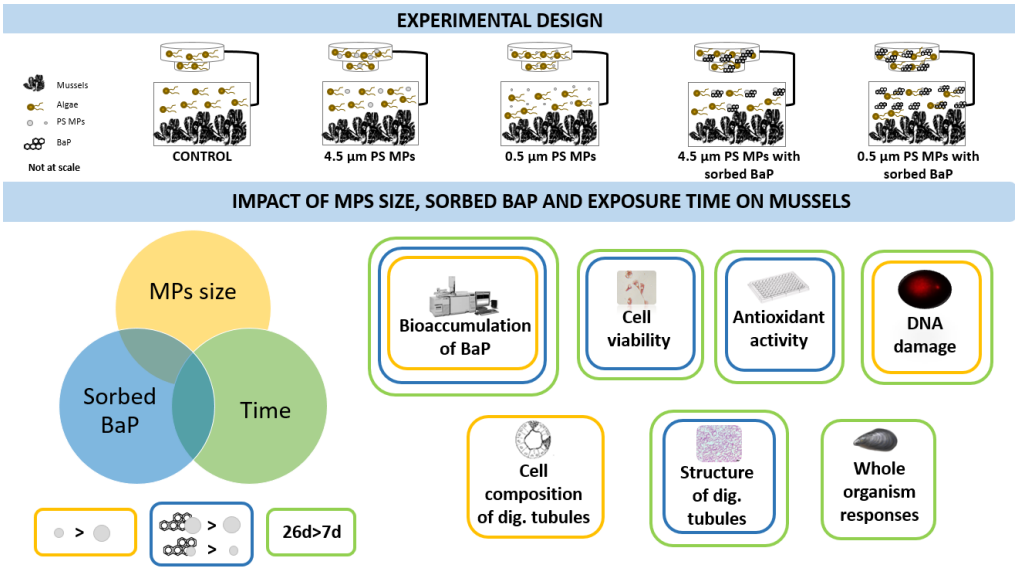

Figure 1. Summary of results obtained in Chapter 1 on the impact of MP size (yellow), sorbed BaP (blue) and exposure time (green) on mussels.

In Chapter 2, the effects of PS MPs of 4.5 µm alone and with sorbed oil compounds from WAF at 25% and 100% dilutions were compared with those caused by exposure to 25% WAF. In this case, PAH accumulation did not occur in mussels exposed to MPs with sorbed oil compounds from WAF (MP25 and MP100). Further, there was a reduced occurrence of MPs in the same two groups compared to mussels exposed to MPs alone, and no effects on mussel physiology and hemocyte functions in the same two groups (Figure 2). Therefore, a carrier effect of MPs for oil compounds from WAF was not observed in Chapter 2.

In Chapter 3, the capacity of GO to act as carrier of sorbed BaP into mussel tissues was observed. However, the extent of BaP bioaccumulation was much higher in mussels exposed to BaP alone compared to those exposed to GO+BaP at equivalent exposure concentrations of BaP. Thus, it appeared that GO nanoplatelets protected mussels against BaP bioaccumulation, as reported in previous studies with other GFNs and BaP in mussels (Barranger et al., 2019a; 2019b; Moore et al., 2021). Regarding the toxicological impact of exposure to GO+BaP in mussels, complex patterns of interaction between GO and BaP emerged which differed depending on the biological endpoint studied. Some responses could be attributted to the effects caused by GO alone but most responses seemed to be due to different types of Trojan horse effects, including 1) effects of BaP carried onto GO nanoplatelets, 2) enhanced toxic effects of GO+BaP compared to GO and/or BaP alone, and 3) synergistic effects of GO+BaP that could not be attributted to either GO or BaP alone (Table 1). No evidence of Trojan horse effect was apparent for other endpoints such as the prevalence of brown cells in the connective tissue of the digestive gland (Table 1). In line with this last result, in Chapter 5 the embryotoxic effects of GO+BaP did not differ significantly in comparison to those of GO or BaP alone at equivalent concentrations, discarding the occurrence of a Trojan horse effect. These results highlight the complexity of the Trojan horse effect of GFNs with sorbed BaP.

Table 1. Summary of results obtained in Chapter 3 comparing the toxicity profile of GO+BaP with respect to controls and to GO or BaP alone. The observed Trojan horse effects are classified as follows: TH1) Carrier effect, toxicity derived from BaP carried onto GO nanoplatelets, TH2) enhanced toxic effects of GO+BaP compared to GO and/or BaP alone, TH3) synergistic effects of GO+BaP that could not be attributted to either GO or BaP alone. BC: brown cell aggregations, CAT: catalase, CT: connective tissue, DG: digestive gland, DT: digestive tract GST: glutathion-S-transferase, SOD: superoxide dismutase.

	Effect of GO+BaP with respect to Controls	Effect of GO+BaP with respect to GO	Effect of GO+BaP with respect to BaP	Same effect with respect to control observed in	Conclusion
BaP bioaccumulation	↑	↑	↓		GO protects against BaP accumulation
Occurrence of GO	↑	=	X	GO	No effect of adsorbed BaP
Hemocyte viability	↓	=	=	BaP	TH1
Genotoxicity	↑	=	=	GO	Nanomaterial toxicity
Neurotoxicity	↓	=	=	BaP	TH1
GST DG	↓	=	=	BaP	TH1
CAT DG	↑	=	=	X	TH3
SOD DG	=	↑	↑	X	TH2
BC in CT of DG	↑	=	=	GO and BaP	No TH
BC in DT of DG	↑ (1R)	↑ (1R)	↑ (1R)	GO and BaP (1R)	TH2
Oocyte atresia	↑	↑	↑	X	TH2 + TH3

4.2. Fate and impact of polystyrene NPs and MPs and GFNs in mussels

In exposed mussels, both MPs (Chapters 1 and 2) and GFNs (Chapters 3 and 4) were mostly observed in the digestive tract and some times between the gill filaments. These results agree with the general idea that nano and micro sized particles get in contact with mussel gill surfaces and they are then transported into the mouth and later to the digestive system through ingestion (Sendra et al., 2021). In addition, the occurrence of GFNs in mussel feces was observed in Chapter 3 and Chapter 4.

Interestingly, a higher occurrence of pristine MPs in comparison to those with sorbed POPs was observed in Chapters 1 and Chapter 2. As in Chapter 3 the amount of GO incorporated in the digestive tract and feces of mussels was not quantified, a quantitative comparison between GO alone and GO with sorbed BaP could not be performed. However, qualitatively no differences were observed in terms of number of animals showing GO and GO+BaP and regarding localization of the two compounds.

As mentioned above, in Chapter 1, 0.5 µm and 4.5 µm PS plastics alone were demonstrated to provoke deleterious effects to marine mussels. Both particles caused genotoxicity in mussel hemocytes and the smaller plastics were able to affect the cell composition of digestive gland and consequently the digestive process in terms of absorption efficiency. In Chapter 2, the impact of 4.5 µm MPs alone on marine mussels was also observed. In addition, after the results observed in Chapter 1, the battery of responses at subcellular level was increased in Chapter 2 by measuring several enzyme activities. For instance, in this second experiment we confirmed that exposure to MPs alone caused genotoxicity in mussel hemocytes and, additionally, we observed changes in aerobic metabolism and catalase activity in digestive gland, induction of phase II biotransformation metabolism (GST) in both digestive gland and gills, and induction of GPx in gills. At a higher biological level, exposure to MPs alone altered the cell composition of digestive tubules of digestive gland, and caused a non-specific inflammatory response and oocyte atresia in mussel gonad and a decrease of absorption efficiency (Figure 2).

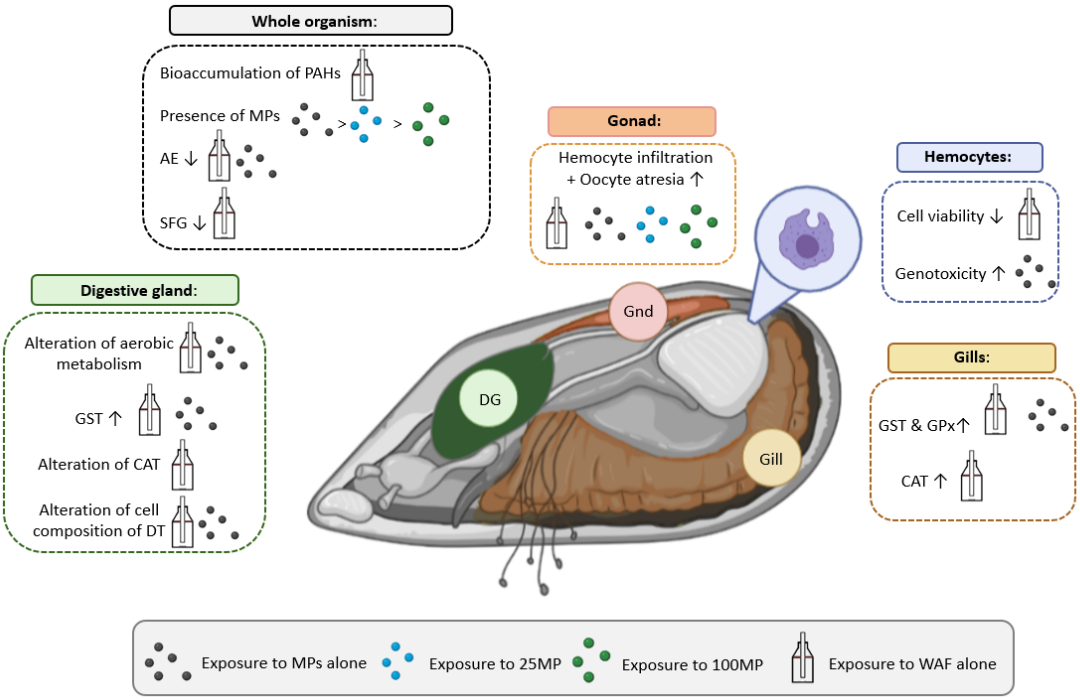

Figure 2. Summary of the results obtained in Chapter 2 on the impacts of 4.5 µm MPs alone or with sorbed oil compounds from WAF at 25% (MP25) and 100% (MP100) dilution and 25% WAF in mussels.

Results from Chapter 3 and 4 showed that all GFNs tested, GO, rGO and rGO-Ag caused deleterious tissue level effects on mussel gonads and digestive gland. In addition, GO (Chapter 3) and rGO (Chapter 4) caused DNA damage in mussel hemocytes, whereas this was not observed in the case of mussels exposed to rGO-Ag (Chapter 4). Differences in the toxicity profiles of GFNs were also observed regarding enzyme activities. While exposure to GO alone did not alter any enzyme activity measured, rGO and rGO-Ag altered the activity of catalase in the digestive gland and rGO-Ag also caused lipid peroxidation in the digestive gland and induction of AChE activity. These differences are probably due to differences in C:O content and surface structure of the GO and rGO nanoplatelets, as discussed in the literature (Malina et al., 2020). On the other hand, in Chapter 4, the comparison between the toxicity of rGO-Ag with that caused by equivalent concentrations of rGO and Ag nanoparticles showed that toxicity of rGO-Ag was mainly due to Ag nanoparticles but, interestingly, toxicity of Ag nanoparticles was lower when combined with rGO than in the form of Ag nanoparticles at equivalent

concentrations. This protective role of rGO on Ag nanoparticle toxicity was also demonstrated in embryos studied in Chapter 5.

4.3. Comparison of responses measured in hemocytes *in vitro* versus *in vivo* responses

In the last decades*, in vitro* approaches have been considered to provide important tools for hazard identification in nanotoxicology due to the large number and diverse types of nanomaterials present in the market (Hristozov & Malsch, 2009). However, *in vitro* assays need to be validated in order to be able to extrapolate *in vitro* results to *in vivo* scenarios.

The hemocytes of bivalves are one of the most widely used cellular model for *in vitro* studies on the impact of pollutants, and especially nano-scale particulate pollutants, in the marine environment (Katsumiti & Cajaraville, 2019). One possible approach is to expose the hemocytes *in vitro* and then measure different responses of cells using *in vitro* assays such as changes in cell viability, phagocytic activity, ROS production, genotoxicity and gene expression, among others (Katsumiti & Cajaraville, 2019). Another approach is to expose mussels *in vivo* and then withdraw the hemolymph to measure responses of hemocytes using the same *in vitro* assays. This second approach is the one that we used in Chapters 1 to 4 of this PhD Thesis and three endpoints were measured in hemocytes: cell viability, catalase activity and genotoxicity (Comet assay or micronuclei frequency). These responses of hemocytes can be compared with responses measured in mussels *in vivo* at different levels of biological organization.

The activity of the antioxidant enzyme catalase was determined in hemocytes and in gills and digestive gland in Chapters 2, Chapter 3 and Chapter 4. In addition, in Chapter 4 gene transcription levels of the same enzyme were assessed in the digestive gland. In all the experiments the outcome was similar: whereas no differences of catalase activity were found in hemocytes, significant differences were observed in all the experiments in different tissues. These results indicate that different cell types and tissues display different sensitivities regarding antioxidant enzyme activities, as shown in the literature (Rocha et al., 2015b; Canesi et al., 2019). Similarly, when mussel hemocytes were exposed *in vitro* to the same polystyrene 4.5 µm MPs (at the same concentration) than

in Chapters 1 and 2, no alterations in ROS production were observed in comparison to the controls (Katsumiti et al., 2021). In addition, no decrease in cell viability was observed in Katsumiti et al. (2017) and (2021) when mussel hemocytes were exposed *in vitro* to the same conditions studied here in Chapters 3 and 1 and 2, respectively. Conversely, the decrease of hemocyte viability observed in mussels exposed to WAF in Chapter 2 agrees well with the results obtained in *in vitro* exposures of hemocytes to the WAF of the same crude oil (Katsumiti et al., 2019).

Overall, this *in vitro/in vivo* comparison suggests that results obtained after *in vitro* exposure of hemocytes could resemble the immunotoxic effects observed after *in vivo* exposures, but further work is needed to extrapolate data obtained in hemocytes to those obtained in other organs after *in vivo* exposures. In this regard, the use of different *in vitro* systems derived from other tissues of mussels could offer a complementary tool to obtain an integrated response more comparable to the *in vivo* situation.

4.4. Comparison of embryo versus adult responses

Early life stages of aquatic organisms are known to be especially sensitive to pollution. In addition, impacts on early life stages can have severe consequences at the population level. Therefore, it would be essential to consider different life stages of a species to establish its sensitivity towards any pollutant and especially towards NMs (Fabbri et al., 2014).

Here the same concentrations of GFNs studied in Chapter 3 and 4 in adults were studied in Chapter 5 in embryos. For all the studied compounds, GO, rGO and rGO-Ag, embryos showed a higher sensitivity than adults. Moreover, the EC_{50}s of GO and rGO-Ag were below the exposure concentration studied with adults in Chapters 3 and 4, respectively and even the smallest concentrations tested caused deleterious effects on mussel embryos for all the compounds.

REFERENCES

Abdel-Shafy H.I., Mansour M.S.M. 2016. A review on polycyclic aromatic hydrocarbons: Source, environmental impact, effect on human health and remediation. Egyptian Journal of Petrolium 25, 107-123

Barranger A., Langan L.M., Sharma V., Rance G.A., Aminot Y., Weston N.J., Akcha F., Moore M.N., Arlt V.M., Khlobystov A.N., Readman J.W., Jha A.N. 2019a. Antagonistic interactions between benzo[a]pyrene and fullerene (C60) in toxicological response of marine mussels. Nanomaterials 9, 87.

Barranger A., Rance G.A., Aminot Y., Dallas L.J., Sforzini S., Weston N.J., Lodge R.W., Banni M., Arlt V.M., Moore M.N., Readman J.W., Viarengo A., Khlobystov A.N., Jha A.N. 2019b. An integrated approach to determine interactive genotoxic and global gene expression effects of multiwalled carbon nanotubes (MWCNTs) and benzo[a]pyrene (BaP) on marine mussels: evidence of reverse 'Trojan Horse' effects. Nanotoxicology, 1, 1324–1343.

Canesi L., Auguste M.; Benianno M.J. 2019. Sublethal effects of nanoparticles on aquatic invertebrates, from molecular to organism level. Ecotoxicology of nanoparticles in aquatic systems, 38-61. ISBN: 978-131515876-1, 978-113806726-4.

Canesi L., Ciacci C., Fabbri R., Marcomini A., Pojana G. and Gallo G. 2012. Bivalve molluscs as a unique target group for nanoparticle toxicity. Marine Environmental Research 76, 16-21.

De Marchi L., Pretti C., Chiellini F., Morelli A., Neto V., Soares A.M.V.M., Figueira E., Freitas R. 2019. The influence of simulated global ocean acidification on the toxic effects of carbon nanoparticles on polychaetes. Science of the Total Environment, 666, 1178–1187.

Deng R., Lin D., Zhu L., Majumdar S., White J.C., Gardea-Torresdey J.L., Xing B. 2017. Nanoparticle interactions with co-existing contaminants: joint toxicity, bioaccumulation and risk. Nanotoxicology, 11, 591–612.

Eriksen M., Maximenko N., Thiel M., Cummins A., Lattin G., Wilson S., Hafner J., Zellers A., Rifman S. 2013. Plastic pollution in the South Pacific subtropical gyre. Marine Pollution Bulletin 68, 71–76.

Ersan G., Apul O. G., Perreault F., Karanfil T. 2017. Adsorption of organic contaminants by graphene nanosheets: A review. Water Research, 126, 385–398.

Fabbri R., Montagna M., Balbi T., Raffo E., Palumbo F., Canesi L. 2014. Adaptation of the bivalve embryotoxicity assay for the high throughput screening of emerging contaminants in *Mytilus galloprovincialis*. Marine Environmental Research 99, 1–8.

Freixa A., Acuña V., Sanchís J., Farré M., Barceló D., Sabater S. 2018. Ecotoxicological effects of carbon based nanomaterials in aquatic organisms. Science of the Total Environment, 619–620, 328–337.

Gottschalk F., Ort C., Scholz R.W., Nowack B., 2011. Engineered nanomaterials in rivers exposure scenarios for Switzerland at high spatial and temporal resolution. Environvental Pollution 159, 3439–3445.

Hartmann N.B., Hüffer T., Thompson R.C., Hassellöv M., Verschoor A., Daugaard A.E., Rist S., Karlsson T., Brennholt N., Cole M., Herrling M.P., Hess M.C., Ivleva N.P., Lusher A.L., Wagner M. 2019. Are We Speaking the Same Language? Recommendations for a Definition and Categorization Framework for Plastic Debris. Environmental Science and Technology 53, 1039–1047.

Heinz H., Pramanik C., Heinz O., Ding Y., Mishra R.K., Marchon D., Flatt R.J., Lopis I.E., Llop J., Moya S., Ziolo R.F. 2017. Nanoparticle decoration with surfactants: molecular interactions, assembly, and applications. Surface Science Reports 72, 1–58.

Hristozov D., Malsch I. 2009. Hazards and risks of engineered nanoparticles for the environment and human health. Sustainability 1: 1161-1194.

Katsumiti A., Cajaraville M.P. 2019. In Vitro Testing: In Vitro Toxicity Testing with Bivalve Mollusc and Fish Cells for the Risk Assessment of Nanoparticles in the Aquatic Environment. In Ecotoxicology of Nanoparticles in Aquatic Systems (pp. 62-98). CRC Press.

Katsumiti A., Losada.Carrillo M.P., Barros M., Cajaraville M.P. 2021 Polystyrene nanoplastics and microplastics can act as Trojan horse carriers of benzo(a)pyrene to mussel hemocytes *in vitro*. Scientific reports 11, 22396.

Katsumiti A., Nicolussi G., Bilbao D., Prieto A., Etxebarria N., Cajaraville M. P. 2019. In vitro toxicity testing in hemocytes of the marine mussel *Mytilus galloprovincialis* (L.) to uncover mechanisms of action of the water accommodated fraction (WAF) of a naphthenic North Sea crude oil without and with dispersant. Science of the Total Environment 670, 1084–1094.

Katsumiti A., Tomovska R., Cajaraville M. 2017. Intracellular localization and toxicity of graphene oxide and reduced graphene oxide nanoplatelets to mussel hemocytes *in vitro*. Aquatic Toxicology 188, 138-147.

Koelmans A.A. 2015. Modeling the role of microplastics in bioaccumulation of organic chemicals to marine aquatic organisms. A critical review. See Bergmann et al. 2015, pp. 309–24.

Kühn S., Rebolledo E.L.B., van Franeker J.A. 2015. Deleterious effects of litter on marine Life. In Marine anthropogenic litter (pp. 75-116). Springer International Publishing

Lechner A., Keckeis H., Lumesberger F., Zens B., Krusch R., Tritthart M., Glas M., Schludermann E. 2014. The Danube so colourful: a potpourri of plastic litter outnumbers fish larvae in Europe's second largest river. Environmental Pollution 188, 177–181.

Li J., Lusher A.L., Rotchell J.M., Deudero S., Turra A., Brate I.L.N., Sun C., Hossain M.S., Li Q., Kolandhasamy P., Shi H. 2019. Using mussel as a global bioindicator of coastal microplastic pollution. Environmental Pollution 244, 522-533.

Malina T., Maršálkova E., Holá K., Zbořil R., Maršálek B. 2020. The environmental fate of graphene oxide in aquatic environment complete mitigation of its acute toxicity to planktonic and benthic crustaceans by algae. Journal of Hazardous Materials 399, 123027.

Meador J.P., Stein J.E., Reichert W.L., Varanasi U. 1995. Bioaccumulation of polycyclic aromatic hydrocarbons by marine organisms. Reviews of Environmental Contamination and Toxicology 143,79-165.

Moore M.N., Sforzini S., Viarengo A., Barranger A., Aminot Y., Readman J.W., Khlobystov A.N., Arlt V.M., Banni M., Jha A.N. 2021. Antagonistic cytoprotective effects of C60 fullerene nanoparticles in simultaneous exposure to benzo[a]pyrene in a molluscan animal model. Science of the Total Environment 755, 142355.

Naasz S., Altenburger R., Kühnel D. 2018. Environmental mixtures of nanomaterials and chemicals: The Trojan-horse phenomenon and its relevance for ecotoxicity. Science of the Total Environment, 635, 1170–1181

Nel A., Xia T., Mädler L., Li N. 2006. Toxic potential of materials at the nanolevel. Science, *311*, 622–627.

Peng Z., Liu X., Zhang W., Zeng Z., Liu Z., Zhang C., Liu Y., Shao B., Liang Q., Tang W., Yuan X. 2020. Advances in the application, toxicity and degradation of carbon nanomaterials in environment: A review. Environment International 134, 105298.

Ren W., Cheng H.M. 2014. The global growth of graphene. Nature Nanotechnology 9, 726–730

Rocha T.L., Gomes T., Mestre N., Cardoso C., Bebianno M.J. 2015b. Tissue specific responses to cadmium-based quantum dots in the marine mussel *Mytilus galloprovincialis*. Aquatic Toxicology 169, 10-18.

Rocha T.L., Gomes T., Sousa V.S., Mestre N.C., Bebianno M.J. 2015a. Ecotoxicological impact of engineered nanomaterials in bivalve molluscs: An overview. Marine Environmental Research 111, 74–88.

Sendra M., Sparaventi E., Novoa B., Figueras A. 2021. An overview of the internalization and effects of microplastics and nanoplastics as pollutants of emerging concern in bivalves. Science of the Total Environment 753, 142024.

Viarengo A., Lowe D., Bolognesi C., Fabbri E., Koehler A. 2007. The use of biomarkers in biomonitoring: a 2-tier approach assessing the level of pollutant-induced stress syndrome in sentinel organisms. Comparative Biochemistry and Physiology Part C: Toxicology & Pharmacology 146, 281-300.

Younis S.A., Maitlo H.A., Lee J., Kim K.H. 2020. Nanotechnology-based sorption and membrane technologies for the treatment of petroleum-based pollutants in natural ecosystems and wastewater streams. Advances in Colloid and Interface Science 275, 102071.

5. CONCLUSIONS AND THESIS

5. CONCLUSIONS AND THESIS

1.- BaP was transferred from PS NPs and MPs to mussels and bioaccumulated in mussel tissues with increased exposure time, with a higher transfer of BaP from smaller NPs (0.5 μm) than from MPs (4.5 μm). NPs and MPs alone and with sorbed BaP caused a range of cellular, tissue and whole organism responses that increased with exposure time, with sorbed BaP or with increased particle size, depending on the response.

2.- MPs did not transfer sorbed oil compounds from the WAF of a naphthenic North Sea crude oil to mussels and effects compatible with a Trojan horse effect were not observed, but exposure to MPs or to WAF alone triggered responses at molecular, cellular, tissue and organism levels.

3.- GO was internalized via ingestion and rapidly excreted in mussels exposed to GO and GO with sorbed BaP at environmentally relevant concentrations and acted as carrier of BaP to mussels even though GO nanoplatelets protected mussels against BaP bioaccumulation. The toxicological impact of exposure to GO with sorbed BaP differed depending on the biological endpoint studied: some responses could be attributted to the effects caused by GO alone but most responses seemed to be due to a variety of Trojan horse effects, including 1) effects of BaP carried onto GO nanoplatelets, 2) enhanced toxic effects of GO+BaP compared to GO and/or BaP alone, and 3) synergistic effects of GO+BaP that could not be attributted to either GO or BaP alone.

4.- The hybrid nanocomposite rGO-Ag as well as rGO were internalized via ingestion and rapidly excreted in mussels whereas Ag bioaccumulation occurred upon exposure to rGO-Ag but at much lower extent than in mussels exposed to equivalent concentrations of Ag nanoparticles. The hybrid material provoked alterations at cell, tissue and organism levels that were comparable in part to those caused by rGO and by Ag

nanoparticles separately but Ag nanoparticles exerted less toxicity when dosed in the form of rGO-Ag than alone.

5.- GO and rGO showed relatively low toxicity to mussel embryos, partly due to their aggregation and sedimentation behaviour in seawater, but they provoked significant embryotoxicity even at the lowest environmentally realistic concentrations tested. GO with sorbed BaP did not pose an additional hazard to mussel embryos, discarding the occurrence of a Trojan horse effect. Ag NPs contributed largely to the embryotoxicity of the rGO-Ag nanocomposite, pointing to the toxic potential of GFN-Ag NP nanocomposites in the marine environment, whereas rGO appeared to exert a protective role against Ag NP toxicity.

THESIS

The **thesis** of this work is that nanoplastics, microplastics and graphene family nanomaterials can act as carriers of the polycyclic aromatic hydrocarbon benzo(a)pyrene, but the role of graphene family nanomaterials in reducing the bioaccumulation and toxicity of associated pollutants must be highlighted. Interactions between nanoplastics, microplastics and graphene-based nanomaterials with sorbed benzo(a)pyrene occur, giving rise to different toxicity patterns depending on the response studied at molecular, cellular, tissue and organism levels. Overall, the Trojan horse effect resulted more complex than previously anticipated and further studies are needed to understand the hazards posed by nanoplastics, microplastics and graphene-based nanomaterials and associated pollutants for marine organisms at both early developmental and adult stages, especially at long-term.